

# Northumbria Research Link

Citation: Reed, Stephen (2010) Synthesis and characterisation of novel glycosidase substrates and evaluation of applications in biomedical science. Doctoral thesis, Northumbria University.

This version was downloaded from Northumbria Research Link:  
<https://nrl.northumbria.ac.uk/id/eprint/1101/>

Northumbria University has developed Northumbria Research Link (NRL) to enable users to access the University's research output. Copyright © and moral rights for items on NRL are retained by the individual author(s) and/or other copyright owners. Single copies of full items can be reproduced, displayed or performed, and given to third parties in any format or medium for personal research or study, educational, or not-for-profit purposes without prior permission or charge, provided the authors, title and full bibliographic details are given, as well as a hyperlink and/or URL to the original metadata page. The content must not be changed in any way. Full items must not be sold commercially in any format or medium without formal permission of the copyright holder. The full policy is available online: <http://nrl.northumbria.ac.uk/policies.html>

Synthesis and Characterisation of Novel  
Glycosidase Substrates and Evaluation of  
Applications in Biomedical Science

Stephen Reed

A thesis submitted in partial fulfilment of the  
requirements of Northumbria University for the  
degree of Doctor of Philosophy.

June 2009



## Abstract

The last fifty years has seen an increase in the production of synthetic or artificial enzyme substrates used to identify and quantify enzymes. These substrates have found applications in a range of biomedical science disciplines. Used in biochemistry and clinical chemistry to identify and measure enzymes, some of these substrates have been adapted for use in microbiology, particularly bacterial diagnosis and, in more recent years, molecular biology.

The use of artificial chromogenic and fluorogenic enzyme substrates to identify certain bacteria is now common place in medical laboratories worldwide. Not all bacteria can be identified with existing and commercially available artificial substrates. Some of these can be slow to yield results, imprecise, expensive or require a technical method too complicated to provide a viable laboratory test. Therefore, the search for new, more efficient, biochemical tests has progressed, with novel substrates and inventive applications being developed continually.

In this study, core compounds were synthesised by various condensation reactions and their characteristics evaluated with respect to colouration/fluorescence and possible enhancement of these properties by metal chelation. Promising candidates were selected for glycosidation, via modified Koenigs-Knorr reactions, in an attempt to synthesise artificial substrates. Several commercially available core molecules were also subjected to glycosidation. The more successful substrates included glycosides of alizarin, nitrosalicylaldehyde and 3-hydroxyflavone.

The galactoside of nitrosalicylaldehyde was evaluated in solid agar media and found to be selective for certain Gram-negative bacteria. When similarly investigated, the 3-hydroxyflavone- $\beta$ -D-glucoside showed the possibility of being used in a procedure for the isolation of the clinically significant pathogens including *Listeria monocytogenes*. The enzyme kinetics of  $\beta$ -glucosidase with this substrate were also determined in a novel fluorescence assay and compared favourably to the well documented 4-methylumbelliferyl- $\beta$ -D-glucopyranoside. Alizarin-2-yl- $\beta$ -D-galactoside and *p*-naphtholbenzein- $\beta$ -D-galactoside were successfully utilized for the screening of recombinant and non-recombinant *Escherichia coli* transformants produced routinely in molecular biology.

Aminopeptidase substrates have been shown to be useful for the detection of enzymes which hydrolyse peptides that are specific to certain bacteria. To allow the evaluation of novel aminopeptidase substrates, that were to be subsequently synthesised, a cost effective, large scale source of recombinant leucyl aminopeptidase enzyme was developed via gene cloning techniques.

Consequently, the products of this study may serve a beneficial purpose in future enzymatic investigations, medical diagnosis and molecular biology.

# Contents

	<b>Page</b>
<b>Table of figures</b>	<b>i</b>
<b>Table of tables</b>	<b>vi</b>
<b>Abbreviations</b>	<b>vii</b>
<b>Declaration</b>	<b>ix</b>
<b>Acknowledgements</b>	<b>x</b>
<b>Dedication</b>	<b>xi</b>
<b>CHAPTER ONE: Introduction</b>	<b>1</b>
<b>1.1 Preface</b>	<b>2</b>
<b>1.2 Nature of enzymes</b>	<b>3</b>
<b>1.3 Enzyme based detection, identification and quantification</b>	<b>5</b>
<b>1.4 Substrates employed in enzymology and enzyme assays</b>	<b>14</b>
<b>1.5 Synthetic substrates</b>	<b>25</b>
<b>1.5.1 Nitrophenols</b>	<b>25</b>
<b>1.5.2 Indoxyls</b>	<b>28</b>
<b>1.5.3 Naphthols</b>	<b>38</b>
<b>1.5.4 <i>p</i>-Nitroanilides</b>	<b>40</b>
<b>1.5.5 Methylumbelliferones</b>	<b>43</b>
<b>1.5.6 7-Amino-4-methylcoumarins</b>	<b>45</b>
<b>1.5.7 Phthaleins</b>	<b>47</b>

1.5.8	Phenoxazines	48
1.5.9	Fluorones	54
1.6	Aims and objectives	61
CHAPTER TWO: Chromogenic core molecules		62
2.1	Introduction	63
2.2	Experimental methods and mechanisms	
2.2.1	Synthesis of 4-nitrovinyl-2-methoxyphenol	64
2.2.2	Synthesis of 4-nitrovinyl-2-methoxy-6-bromophenol	68
2.2.3	2-Hydroxy-1-naphthaldehyde	69
2.2.4	Synthesis of 1-nitrovinyl-2-naphthol	69
2.2.5	Synthesis of 4-hydroxy-3-methoxybenzylidene- 1,3-indandione	70
2.2.6	Synthesis of 4-acetoxy-3-methoxycinnamylidene- 1,3-indandione	72
2.2.7	Synthesis of 4-hydroxy-3-methoxycinnamylidene- 1,3-indandione	74
2.2.8	Synthesis of 4-hydroxy-3-methoxycinnamylidene- 3-phenyl-5-isoxazolone	75
2.2.9	Synthesis of 2-hydroxy-1-naphthaldehyde-4- nitrophenylhydrazone	76
2.2.10	Synthesis of 2-hydroxy-1-naphthaldehyde-2,4- dinitrophenylhydrazone	78

2.2.11	Synthesis of naphthofluorescein	80
2.3	Results	83
2.4	Discussion	86
CHAPTER THREE: Chelating core molecules		87
3.1	Introduction	88
3.2	Experimental methods and mechanisms	
3.2.1	Synthesis of 2-(3,4-dihydroxybenzylidene) -1,3-indandione	94
3.2.2	Synthesis of 3,4-dihydroxybenzylidene benzhydrazide	96
3.2.3	Synthesis of 3,4-dihydroxybenzylidene isonicotinic hydrazide	100
3.2.4	Synthesis of 7,8-dihydroxy-4-methylcoumarin	97
3.2.5	Synthesis of 1-methyl-2-phenyl-3- hydroxy-4(1 <i>H</i> )-quinolone	102
3.2.6	Synthesis of 1-methyl-2-(4'-fluorophenyl)-3- hydroxy-4(1 <i>H</i> )-quinolone	106
3.2.7	5-Nitrosalicylaldehyde	107
3.2.8	Alizarin	107
3.2.9	3-Hydroxyflavone	108
3.2.10	5,7-Dichloro-8-hydroxy-2-methylquinoline	108
3.3	Results	109

3.4	Discussion	114
CHAPTER FOUR: Glycosides and other derivatives		115
4.1	Glycosides introduction	116
4.2	Glycosides experimental methods and mechanisms	
4.2.1	Synthesis of 2-hydroxy-1-naphthaldehyde- $\beta$ -D-galactoside	120
4.2.2	Synthesis of 1-nitrovinyl-2-naphthol- $\beta$ -D-galactoside	122
4.2.3	Synthesis of 4- $\beta$ -D-galactosidoxy- and 4- $\beta$ -D-glucosidoxy- 3-methoxycinnamylidene-1,3-indandione	126
4.2.4	Synthesis of 5-nitrosalicylaldehyde- $\beta$ -D-galactoside	130
4.2.5	Synthesis of 7,8-dihydroxy-4-methylcoumarin- $\beta$ -D-glucoside	131
4.2.6	Synthesis of alizarin-2-yl- $\beta$ -D-glucoside and $\beta$ -D-galactoside	132
4.2.7	Synthesis of 3-hydroxyflavone- $\beta$ -D-glucoside and $\beta$ -D-galactoside	136
4.2.8	Synthesis of 1-methyl-2-(4'-fluorophenyl)-3-hydroxy- 4(1 <i>H</i> )-quinolone- $\beta$ -D-glucoside	138
4.2.9	Synthesis of 5,7-dichloro-8-hydroxy-2-methylquinoline- $\beta$ -D-galactoside	140
4.2.10	Synthesis of naphthofluorescein- $\beta$ -D-glucoside	141
4.2.11	<i>p</i> -Naphtholbenzein- $\beta$ -D-galactoside	142
4.3	Carboxylic esters introduction	143
4.4	Carboxylic esters experimental methods and mechanisms	
4.4.1	Synthesis of alizarin-2-octanoate	144
4.4.2	Synthesis of alizarin-2-palmitate	146

4.4.3	Synthesis of alizarin-2-benzoate	147
4.5	Results	148
4.5.1	Microbiological evaluation	149
4.5.2	Biochemical evaluation	154
4.5.3	Molecular biology application	166
4.6	Discussion	176
4.6.1	Alizarins	176
4.6.2	5-Nitrosalicylaldehyde- $\beta$ -D-galactoside	180
4.6.3	3-Hydroxyflavones and hydroxyquinolones	181
<b>CHAPTER FIVE: Gene cloning and protein expression</b>		<b>186</b>
5.1	Introduction	187
5.2	Experimental Methods	
5.2.1	DNA extraction	189
5.2.2	Gene amplification	190
5.2.3	T4 DNA polymerase reaction	193
5.2.4	Transformation of annealing products	195
5.2.5	Isolation of plasmid	196
5.2.6	Digest	197
5.2.7	Transformation of recombinant plasmid	199
5.2.8	Determination of solubility of protein	199
5.2.9	Purification by nickel affinity chromatography	201
5.2.10	Concentration of protein	203

<b>5.3</b>	<b>Results</b>	<b>204</b>
<b>5.4</b>	<b>Discussion</b>	<b>205</b>
	<b>CHAPTER SIX: Discussion</b>	<b>206</b>
<b>6.1</b>	<b>Conclusions</b>	<b>207</b>
<b>6.2</b>	<b>Future work</b>	<b>208</b>
<b>7</b>	<b>References</b>	<b>215</b>
<b>8</b>	<b>Appendices</b>	
<b>8.1</b>	<b>Appendix A: Chemistry</b>	<b>228</b>
<b>8.2</b>	<b>Appendix B: Biochemistry</b>	<b>230</b>
<b>8.3</b>	<b>Appendix C: Microbiology/molecular biology</b>	<b>244</b>

## Table of figures

1.1	Michaelis-Menten equation.	4
1.2	Fluorescence excitation and emission.	7
1.3	Simplified Jablonski diagram.	8
1.4	Stokes Shift.	9
1.5	4-Methylumbelliferyl- $\beta$ -D-glucuronide.	10
1.6	Luciferin/ luciferase system.	11
1.7	Assay of an esterase enzyme.	12
1.8	Urease catalyses the hydrolysis of urea $(\text{NH}_2)_2\text{CO}$ to $\text{NH}_3$ and $\text{CO}_2$ .	15
1.9	Action of aspartate aminotransferase.	16
1.10	The reversible oxidoreduction of ethanol.	17
1.11	Equilibrium of NAD/NADH.	18
1.12	General formula for a tetrazolium salt.	18
1.13	Iodonitrotetrazolium chloride (INT).	19
1.14	Reduction of a tetrazolium salt by NADH.	19
1.15	Transamination of alanine coupled to an LDH reaction.	21
1.16	Creatine kinase assay.	22
1.17	Structure of nitrophenyl- $\beta$ -D-galactoside.	25
1.18	The two resonance structures of nitrophenol.	26
1.19	<i>p</i> -Nitrophenyl- $\beta$ -D-glucuronide.	27
1.20	<i>p</i> -Nitrophenyl phosphate ( $\text{K}^+$ salt).	28
1.21	3-Hydroxyindole.	28
1.22	Indigo dye.	29
1.23	Plant indican.	29
1.24	Histochemical use of Blue gal.	31
1.25	Structure of blue nonanoate.	31
1.26	Structure of 6-chloro-3-indolyl- $\beta$ -D-glucopyranoside.	32
1.27	6-chloro-3-indolyl- $\beta$ -D-glucopyranoside hydrolysed by <i>Yersina pseudotuberculosis</i> .	32
1.28	Magenta-caprylate hydrolysed by <i>Salmonella</i> spp.	33
1.29	Structure of 5-bromo-6-chloro-3-indolyl- $\beta$ -D-glucopyranoside.	34
1.30	Structure of 5-bromo-4-chloro-3-indolyl- $\beta$ -D-galactopyranoside.	34
1.31	Blue/white screening. <i>E. coli</i> on LB agar containing X-gal.	35
1.32	Trypsin Bile agar containing X-gluc (TBX agar).	36
1.33	Alpha-beta chromogenic medium.	37
1.34	Structures of naphthol AS-BI and naphthol AS-D.	38
1.35	Esterase activity for naphthol AS-D chloroacetate substrate.	39

1.36	Indophenol blue formed by coupling 1-naphthol and DMpPD.	40
1.37	Structure of 4-nitroaniline.	41
1.38	Structure of L-alanyl- <i>p</i> -nitroanilide.	41
1.39	L- $\gamma$ -glutamyl nitroanilide.	42
1.40	Structure of 4-methylumbelliferone.	43
1.41	Fluorescence of 4-methylumbelliferone.	44
1.42	Structure of <i>N</i> -acetyl- $\beta$ -D-glucosaminide.	44
1.43	Structure of 7AMC.	45
1.44	7AMC <i>p</i> -dimethylaminocinnamaldehyde	46
1.45	Structure of L-alanyl 7-amido-4-methylcoumarin.	46
1.46	Phenolphthalein pH effect.	47
1.47	Structure of phenoxazine.	48
1.48	Cresyl violet stained neurons in the cerebellum.	49
1.49	Reduction of resazurin to resorufin to dihydroxyresorufin.	50
1.50	Colour contrast of resazurin and resorufin.	51
1.51	Structure of resorufin acetate.	51
1.52	Structure of 7-benzyloxyresorufin.	52
1.53	Structure of Amplex Red.	52
1.54	Amplex Red coupled to an assay for glucose.	53
1.55	Fluorone ring structure	54
1.56	Fluorescein pH effect.	54
1.57	Corneal staining with fluorescein sodium.	55
1.58	Structure of eosin Y.	55
1.59	An example of haematoxylin and eosin staining.	56
1.60	Structure of eosin diacetate.	56
1.61	Conjugation reaction of fluorescein isothiocyanate.	57
1.62	<i>Pasteurella tularensis</i> stained with anti-tularensis serum labeled with FITC.	57
1.63	Structure of rhodamine B.	58
1.64	Oocysts of <i>Cryptosporidium parvum</i> stained with the fluorescent stain auramine-rhodamine	58
1.65	<i>Bacillus anthracis</i> stained with anti-rabbit serum labeled with rhodamine B ITC.	59
1.66	Two stage removal of amino acids or peptides to produce highly fluorescent rhodamine 110.	60
2.1	Acid catalysed formation of 4-nitrovinyl-2-methoxyphenol	65
2.2	Base catalysed formation of 4-nitrovinyl-2-methoxyphenol.	67
2.3	Formation of 4-nitrovinyl-2-methoxy-6-bromophenol.	68
2.4	Structure of 2-hydroxy-1-naphthaldehyde.	69
2.5	Formation of 1-nitrovinyl-2-naphthol.	69
2.6	Formation of 4-hydroxy-3-methoxybenzylidene 1,3-indandione.	71

2.7	Formation of 4-acetoxy-3-methoxycinnamylidene-1,3-indandione.	73
2.8	Formation of 4-hydroxy-3-methoxycinnamylidene-1,3-indandione.	74
2.9	Formation of 4-hydroxy-3-methoxycinnamylidene-3-phenyl-5-isoxazolone.	75
2.10	Formation of 2-hydroxy-1-naphthaldehyde-4-nitrophenylhydrazone.	77
2.11	Formation of 2-hydroxy-1-naphthaldehyde-2,4-dinitrophenylhydrazone.	79
2.12	Formation of naphthofluorescein.	81
2.13	Spectrum scan of 4-hydroxy-3-methoxycinnamylidene-1,3-indandione.	85
2.14	Spectrum scan of naphthofluorescein.	85
3.1	Hydrolysis of CHE-Gal by <i>E. coli</i> in the presence of iron (II).	89
3.2	Colonies of <i>E. coli</i> showing hydrolysis of alizarin- $\beta$ -D-galactoside in the presence of ferric ions and aluminium.	89
3.3	Aliz-gal with lanthanum nitrate spreading.	90
3.4	Possible chelation of alizarin and aluminium through two adjacent hydroxyl groups.	91
3.5	Formation of 2(3,4-dihydroxybenzylidene)-1,3-indandione.	95
3.6	Formation of 3,4-dihydroxybenzylidene benzhydrazide.	97
3.7	Formation of 3,4-dihydroxybenzylidene isonicotinic hydrazide.	99
3.8	Formation of 7,8-dihydroxy-4-methylcoumarin.	101
3.9	Formation of 1-methyl-2-phenyl-3-hydroxy-4(1 <i>H</i> )-quinolone.	104
3.10	Formation of 1-methyl-2-(4'-fluorophenyl)-3-hydroxy-4(1 <i>H</i> )-quinolone.	106
3.11	Structure of 5-nitrosalicylaldehyde.	107
3.12	Structure of alizarin.	107
3.13	Structure of 3-hydroxyflavone.	108
3.14	Structure of 5,7-dichloro-8-hydroxy-2-methylquinoline.	108
3.15	Spectrum scan of 2(3,4-dihydroxybenzylidene)-1,3-indandione.	112
3.16	Spectrum scan of 5-nitrosalicylaldehyde.	112
3.17	Spectrum scan of alizarin.	113
4.1	Structure of acetobromo- $\alpha$ -D-galactose.	117
4.2	Formation of tetraacetyl 2-hydroxy-1-naphthaldehyde- $\beta$ -D-galactoside.	121
4.3	Formation of 1-nitrovinyl-2-naphthol- $\beta$ -D-galactoside.	123
4.4	Formation of 4- $\beta$ -D-galactosidoxy-3-methoxycinnamylidene-1,3-indandione.	127
4.5	Structure of 4- $\beta$ -D-glucosidoxy-3-methoxycinnamylidene-1,3-indandione.	129
4.6	Structure of 5-nitrosalicylaldehyde- $\beta$ -D-galactoside.	130
4.7	Structure of 7,8-dihydroxy-4-methylcoumarin- $\beta$ -D-glucoside.	131
4.8	Formation of alizarin-2-yl- $\beta$ -D-glucoside.	133
4.9	Structure of alizarin-2-yl- $\beta$ -D-galactoside.	135
4.10	Structure of 3-hydroxyflavone- $\beta$ -D-glucoside.	136
4.11	Structure of 3-hydroxyflavone- $\beta$ -D-galactoside.	137
4.12	Structure of 1-methyl-2-(4'-fluorophenyl)-3-hydroxy-4(1 <i>H</i> )-quinolone- $\beta$ -D-glucoside.	139
4.13	Structure of 5,7-dichloro-8-hydroxy-2-methylquinolone- $\beta$ -D-galactoside.	140

4.14	Structure of <i>p</i> -naphtholbenzein- $\beta$ -D-galactoside.	142
4.15	Formation of alizarin-2-octanoate.	145
4.16	Formation of alizarin-2-palmitate.	146
4.17	Formation of alizarin-2-benzoate.	147
4.18	Pattern of multi-point inoculation.	150
4.19	Multi-point inoculation of Aliz-gal, 3HF-gluc, NSA-gal, PNB-gal and PNB-gal exposed to NaOH.	152
4.20	Hydrolysis of 3HF-gluc by <i>Serratia marcescens</i> NCTC 10211 as seen under U.V. light.	153
4.21	Structure of 3-hydroxyflavone (3HF).	154
4.22	Fluorescence of 3HF.	154
4.23	3HF chelation with zinc.	155
4.24	Fluorescence measurements of 3HF + varying amounts of zinc compared to the effects of the same quantities of 3HF and zinc separately.	156
4.25	Rate of reactions of 3HF-gluc and $\beta$ -glucosidase at pH 4-8.	158
4.26	Rate of reactions of 3HF-gluc and $\beta$ -glucosidase at substrate concentrations 0.01-1 mmol/L.	159
4.27	Linear standard curve for 3HF complex.	160
4.28	Lineweaver-Burk plot for 3HF-gluc.	161
4.29	Alizarin-2-octanoate and when reacted with lipase R.	163
4.30	Production of alizarin when alizarin-2-octanoate is acted upon by lipase R.	163
4.31	Increasing concentrations of alizarin-2-octanoate and then reacted with lipase C and lipase R.	164
4.32	Variation of alizarin-2-octanoate concentration.	164
4.33	Hydrolysis of alizarin-2-octanoate by <i>Salmonella typhimurium</i> NCTC 74 to produce a purple iron chelate.	165
4.34	Transformed recombinant and non-recombinant XL1 Blue cells.	167
4.35	Aliz-gal concentration (0.001 - 0.03 g/100ml Agar).	169
4.36	The effect of different metal chelators with Aliz-gal in LB/ampicillin agar.	171
4.37	The effect of different aluminium salts with Aliz-gal in LB/ampicillin agar.	173
4.38	PNB-gal incorporated into solid agar media for use in the screening of recombinant and non-recombinant transformants and after exposure to ammonia fumes.	174
4.39	pH effect of <i>p</i> -naphtholbenzein.	175
4.40	Structure of alizarin-2-yl- $\beta$ -D-glucoside.	177
4.41	A comparison of four galactoside substrates separately incorporated into solid agar media for use in the screening of recombinant and non-recombinant transformants.	178
4.42	Structure of alizarin-2-octanoate.	179
4.43	Structures of 5-nitrosalicylaldehyde and <i>p</i> -nitrophenol.	180
4.44	Structure of 3-hydroxyflavone.	181

4.45	<i>Listeria</i> isolation with Harlequin™ <i>Listeria</i> Medium.	183
4.46	Structure of 1-methyl-2-(4'-fluorophenyl)-3-hydroxy-4(1 <i>H</i> )-quinolone.	185
5.1	Action of <i>E. coli</i> K12 cell suspension on dilutions of L-leucine-7-amido-4-methyl-coumarin hydrochloride in 0.1 M tris buffer pH 7.4.	188
5.2	Elutions of purified genomic DNA from <i>E. coli</i> K12.	189
5.3	Amplified PCR product. Gene of interest is approximately 1.5 Kbp.	191
5.4	Extracted and purified PCR product.	192
5.5	Purified pET-YSBLIC vector.	193
5.6	Undigested and digested plasmid.	198
5.7	Undigested and digested plasmid.	198
5.8	Total protein sample.	200
5.9	Soluble protein sample.	200
5.10	Purification of protein by nickel affinity chromatography.	202
5.11	Purified protein.	203
5.12	Leucyl aminopeptidase activity.	204
6.1	Structure of 4-nitroalizarin.	209
6.2	Possible cyclisation of 4-aminoalizarin to form alizarin green via the Skraup reaction.	210
6.3	Structure of alizarin Red S-2-octanoate.	211
6.4	Possible synthesis of 5-nitrosalicylidene-aniline.	212
6.5	Chelation of 5-nitrosalicylidene-aniline with Fe <sup>2+</sup> .	213
6.6	Formation of 1-methyl-2(4'-diethylaminophenyl)-3-hydroxy-4(1 <i>H</i> )-quinolone.	214
B1	Structure of 4-methylumbelliferone.	238
B2	Fluorescence of 4-MU.	238
B3	Rate of reactions of MUD and β-glucosidase at pH 4-9.	239
B4	Rate of reactions of MUD and β-glucosidase at substrate concentrations 0.003-3 mmol/L.	240
B5	Linear standard curve for 4-MU.	241
B6	Lineweaver-Burk plot for MUD.	242
C1	Agarose gel size standards. Bioline Hyperladder I.	250

## Table of tables

2.1	Colour change of synthesised core compounds due to varying pH.	84
3.1a	pH effect and metal interaction of chelating core compounds.	110
3.1b	pH effect and metal interaction of chelating core compounds continued.	111
4.1	Substrate quantity and media selection.	149
4.2	Microbiological evaluation of selected substrates.	151
4.3	Fluorescence of 3HF metal complexes.	155
4.4	Summary of the effects of various metal chelators with Aliz-gal.	170
4.5	Effects of various aluminium salts with Aliz-gal.	172
4.6	Comparison of Lineweaver-Burk enzyme kinetic data for MUD and 3HF-gluc.	184
5.1	Contents of PCR reaction mixture.	190
5.2	Conditions of PCR reaction.	191
5.3	T4pol reaction with vector and thymidine triphosphate.	194
5.4	T4pol reaction with insert and adenosine triphosphate.	194
5.5	Annealing reaction.	195
5.6	Contents of digestion reaction mixture.	197

# Abbreviations

ATP	Adenosine triphosphate
bp	Base pair(s)
°C	Degree Celsius
Da	Dalton
DNA	Deoxyribonucleic acid
dNTP	deoxynucleotide triphosphate
DTT	Dithiothreitol
g	Gram(s)
HEPES	N-[2-hydroxyethyl]piperazine-N'-[2-ethanesulphonic acid]
His <sub>6</sub> tag	Hexahistidine tag
IMAC	Immobilised metal affinity chromatography
IPTG	Isopropyl-β-D-thiogalactopyranoside
kb	Kilobase pair(s)
k <sub>cat</sub>	Turnover number
kDa	Kilodalton
K <sub>M</sub>	Michaelis-Menten constant
l	Litre(s)
LB	Luria-Bertani medium
M	Molar
mA	Milliamps
min	Minute(s)
MW	Molecular weight
PAGE	Polyacrylamide gel electrophoresis
PCR	Polymerase chain reaction
rpm	revolutions per minute
s	second(s)
SDS	Sodium dodecyl sulphate
TAE	Tris-Acetate-EDTA
TEMED	N,N,N',N'-tetramethylethylene diamine
Tris	tris(hydroxymethyl)aminomethane
U.V.	Ultraviolet
V	Volts
V <sub>max</sub>	maximum velocity
v/v	volume per volume
w/v	weight per volume
x g	times gravity
ε	molar absorptivity coefficient
α	Alpha
β	Beta
K	Kilo
λ	Lambda
m	milli
μ	micro
1°	Primary
2°	Secondary
3'	Three prime

### Proton Nuclear Magnetic Resonance Spectroscopy ( $^1\text{H}$ -NMR) data

Where possible NMR data were obtained for the products of each synthesis using a JEOL Eclipse NMR spectrophotometer.

Multiplicity key:

s	singlet
d	doublet
dd	double doublet
t	triplet
q	quartet
p	pentet
m	multiplet
om	overlapping multiplet
ArH	aromatic hydrogen
AlH	aliphatic hydrogen
?H	unknown hydrogen intergral

Carbon Nuclear Magnetic Resonance Spectroscopy ( $^{13}\text{C}$ -NMR) data were obtained using a JEOL Eclipse NMR spectrophotometer.

Electron Spray Ionisation Mass Spectroscopy (ESI-MS) data were obtained using a ThermoFinnigan LCQ Advantage Ion Trap ESI.

Fourier Transform Infrared Spectroscopy (FTIR) data were obtained using a Perkin Elmer Spectrum RX1 FTIR spectrophotometer.

High Resolution Mass Spectroscopy (HRMS) data were obtained using the EPSRC mass spectrometry service centre (Swansea, England).

## **Declaration**

I declare that the work contained in this thesis has not been submitted for any other award and that it is all my own work.

Name: Stephen Reed

Signature:

Date: 04/06/09

## **Acknowledgements**

I would like to thank Professors Arthur James and Gary Black for their guidance and encouragement throughout the research and the writing of this thesis.

I would also like to thank Professor Stephen Stanforth, Dr Justin Perry, Dr Jonathon Bookham, Dr Meng Zhang, Dr Annette Rigby and Dr Anna Lindsay for their advice at various stages of this study.

Thanks also go to Professor John Perry of the Freeman Hospital, Newcastle.

## **Dedication**

For my parents, Leonard and Shirley, for teaching me to pick myself up when I fall down.

# **CHAPTER ONE**

## **Introduction**

## 1.1 Preface

Over the last fifty years the production of synthetic or artificial enzyme substrates to identify and quantify enzymes has increased (Manafi et al., 1991; Dealler, 1993).

Used primarily in biochemistry to study enzyme kinetics, clinical chemistry to quantify enzymes and to a lesser extent cellular pathology to mark the locality of enzymes in tissue. Some of these substrates have been adapted for use in microbiology, particularly bacterial diagnosis.

In other areas such as in industry and research the ability to detect and quantify enzyme activity is also of interest (Pettipher et al., 1980; Ley et al., 1988).

In the field of medical diagnostics the need to identify bacteria rapidly and precisely is of the utmost importance. This can be achieved by a variety of methods including the utilization of the sometimes highly specific enzymes produced by bacteria during their normal existence (Goodfellow et al., 1987; Bascomb and Manafi, 1998).

Traditional methods of identifying bacteria in pathological laboratories can be time consuming. They can involve many sequential tests that require handling time to set up and long incubations (Hugh and Leifson, 1953; Edberg et al., 1988). Procedures were revolutionised by the development of biochemical methodologies for the detection of specific bacterial enzymes (Le Minor, 1962), since the 'natural' enzyme substrates that are sometimes employed in these tests can be less than perfect as they have a low enzyme affinity or are not easily detected (MacFaddin, 2000).

These flaws have led to the creation of artificial substrates, the properties of which, ideally, include high enzyme reactivity and sensitivity (James and Yeoman, 1988; Perry et al., 1999).

The use of artificial chromogenic and fluorogenic enzyme substrates to identify certain bacteria is now common place in medical laboratories worldwide (Manafi, 1996). By incorporating a colour producing (chromogenic) or fluorescence producing (fluorogenic) agent into a specific substrate a 'novel' enzyme substrate is

produced. When acted upon by the relevant enzyme the substrate is cleaved, the agent is released and can then be detected.

Not all bacteria can be identified with existing and commercially available artificial substrates and even some of these can be slow to yield results, imprecise, expensive or require a technical method too complicated to provide a viable laboratory test. Therefore, the search for new, more ideal, biochemical tests has progressed with novel substrates and inventive applications being developed continually.

## **1.2 Nature of Enzymes**

All proteins are composed of linked amino acids to create polypeptide chains. These usually show secondary and tertiary structure (folding and three dimensional arrangement) and often exhibit high levels of organisation (quaternary) with association of subunits, e.g. lactose dehydrogenase. Frequently, other groups are present to create conjugated proteins by post-translational modification to give, for example, glycoproteins, haemoproteins, etc. Nevertheless, they are all fundamentally formed from 20 amino acids, but are arranged in totally different sequences.

The biological activity of enzymes depends on their catalytic function. They effectively lower the activation energy for the reaction which they catalyse. This requires an intimate association of the enzyme with its substrate. This association is not random, but occurs at specific points of the enzyme's structure known as active sites, e.g. acetyl cholinesterase operating on its normal substrate acetylcholine, where histidine and serine residues have been implicated.

In addition to the catalytic nature of enzymes, the specific nature of the enzyme-substrate interaction needs consideration. For example, D-amino acid oxidase accepts and transforms D-alanine, D-valine, etc., but not the corresponding L-amino acids. In contrast, the L-amino acid oxidase of snake venom converts only L-amino

acids into the corresponding ketoacids and not into their D-series counterparts. Likewise, *Escherichia coli*  $\beta$ -galactosidase catalyses the hydrolysis of  $\beta$ -galactosides, e.g. lactose methyl- $\beta$ -galactoside, etc., but not the corresponding  $\alpha$ -galactosides.

The majority of enzyme catalysed reactions can be described by the Michaelis-Menten equation (Figure 1.1).

$$V_0 = \frac{V_{\max} [S]}{K_m + [S]}$$

where:

$V_0$  is the initial rate of reaction

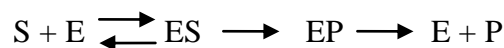
$V_{\max}$  is the maximum rate

$[S]$  is the substrate concentration

and  $K_M$  the Michaelis constant (substrate concentration at half the maximum rate i.e.  $V_{\max} \div 2$ )

**Figure 1.1:** Michaelis-Menten equation.

This equation relates to:



Where:

S is the substrate

E is the enzyme

and P is the product

Michaelis-Menten kinetics (Michaelis, 1913) are used in the description of the rate of enzyme mediated reactions. These kinetics parameters are only valid if the substrate concentration is higher than that of the enzyme,

To determine the maximum rate of an enzyme catalysed reaction, the substrate concentration ( $[S]$ ) is increased until a constant rate of product formation is achieved.

This is the *maximum velocity* ( $V_{\max}$ ) of the enzyme. In this state, all enzyme active sites are saturated with substrate.

With increasing substrate concentration [S], the enzyme is approaching its maximum speed  $V_{\max}$ , but never actually reaching it. Because of that, no substrate concentration for  $V_{\max}$  can be given. Instead, the characteristic value for the enzyme is defined by the substrate concentration at its half-maximum speed ( $V_{\max}/2$ ). This  $K_M$  value is also called the Michaelis-Menten constant.  $K_M$  is a good measure of the binding strength within the ES complex or a measure of the affinity between the enzyme and substrate. A high  $K_M$  would indicate a weak affinity, whilst a low  $K_M$  would indicate a strong affinity.

### **1.3 Enzyme based detection, identification and quantification**

Several methods exist for the above processes:-

In microbiology, visualisation of potential or actual pathogens frequently involves growing the organism on a nutrient agar plate to produce discrete colonies. A specific enzyme substrate is incorporated into the agar and is enzymatically transformed to yield a coloured product which, ideally, is localised on the colonies possessing the correct enzyme. This is frequently in contrast to negative or 'self-coloured' colonies. Alternatively, a large number of enzymatic substrates each defining a single reaction are incorporated into a plastic card in discrete microwells. Microorganisms introduced into the wells produce a characteristic and individual pattern of reactivity evidenced by coloured products. The wells are interrogated by a light beam of appropriate wavelength and results recorded as positive or negative signals leading to a computerised identification of the organism.

In cell pathology, the use of specific substrates for the detection/visualisation of sites of enzymatic activity has great value in distinguishing normal cells and tissues from abnormal forms. This forms the basis of enzyme histochemistry and cytochemistry.

There are numerous examples and the subject is discussed throughout this introduction. It is important to state however that it was in this area (histochemistry) that the application of chemistry to the detection of localised regions of specific enzyme activity in cells and tissues was first demonstrated. This led to the much wider use of localising enzyme substrates in other areas of cell biology. In histochemistry/cytochemistry, microscopes are commonly used with a U.V. light source (fluorescence), e.g. molecular probes.

In the field of immunology, detection of the specific antigen-antibody reaction does not necessarily require an enzymatic involvement. Older procedures involved eliciting a precipitation reaction, haemolysis or other effects. The technique of enzyme labelling however changed this dramatically. A specific antibody labelled with an enzyme is used to determine the presence or concentration of a particular antigen. The method requires a substrate which is transformed, usually by hydrolysis, to give a coloured or fluorescent product, the concentration of which may then be determined by, for example, Enzyme-Linked ImmunoSorbent Assay (ELISA) (Lequin, 2005).

Many other examples can be drawn from the field of genetics and molecular biology e.g. *lac Z* gene in bacterial transformation, hybridisation, blotting techniques, etc (Brown, 2006).

In clinical chemistry visual and spectrophotometric methods are employed. In its simplest sense, the colour of the product of the enzymatic process is observed or, for quantification, the colour intensity is measured either by a colorimeter, U.V./visible spectrophotometer or spectrofluorimeter. Such instruments either utilise diffraction grating monochromators or interference filters where specific wavelengths are required. The applications of colour observation or measurement are numerous in biomedical science

Types of Spectrophotometric Methodologies:

- a) U.V./Visible Spectrophotometry. Techniques may vary from simple colorimeters to dual beam spectrophotometry and highly automated optical

systems such as the automatic analysers found in clinical chemistry laboratories.

- b) Fluorescence Spectrophotometry. An atom or molecule fluoresces when it has been electrically excited by the absorption of a photon then returned to its ground state by the emission of a photon with a longer (less energetic) wavelength (Figure 1.2).



Where:-  $h\nu$  is photon energy ( $h$  = Planck's constant,  $\nu$  = frequency of light),  $S_0$  = ground state and  $S_1$  = 1<sup>st</sup> excited state.

**Figure 1.2:** Fluorescence excitation and emission.

Fluorescence was a term first used by George Gabriel Stokes in 1852 when studying the mineral Fluorite which he discovered will emit light in the visible region of the electromagnetic spectrum when excited by ultraviolet light.

The processes involved during fluorescence can be shown with the Jablonski diagram (Figure 1.3), first devised by Professor Alexander Jablonski in 1933 to describe absorption and emission of light.

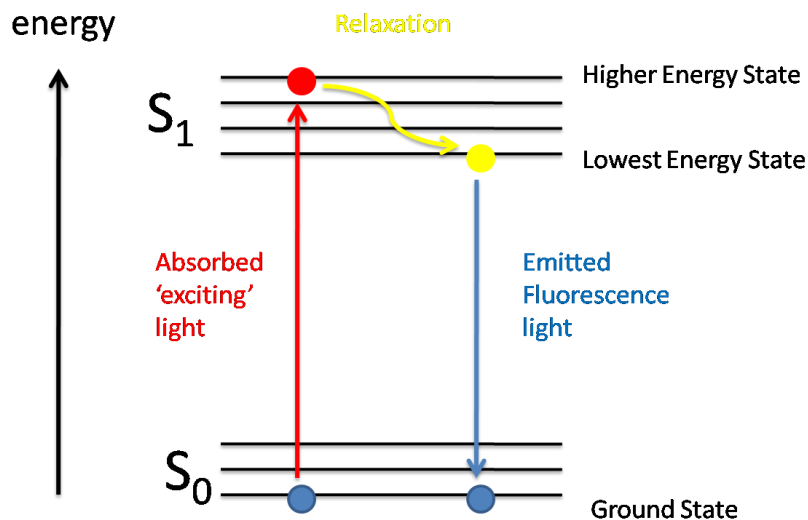
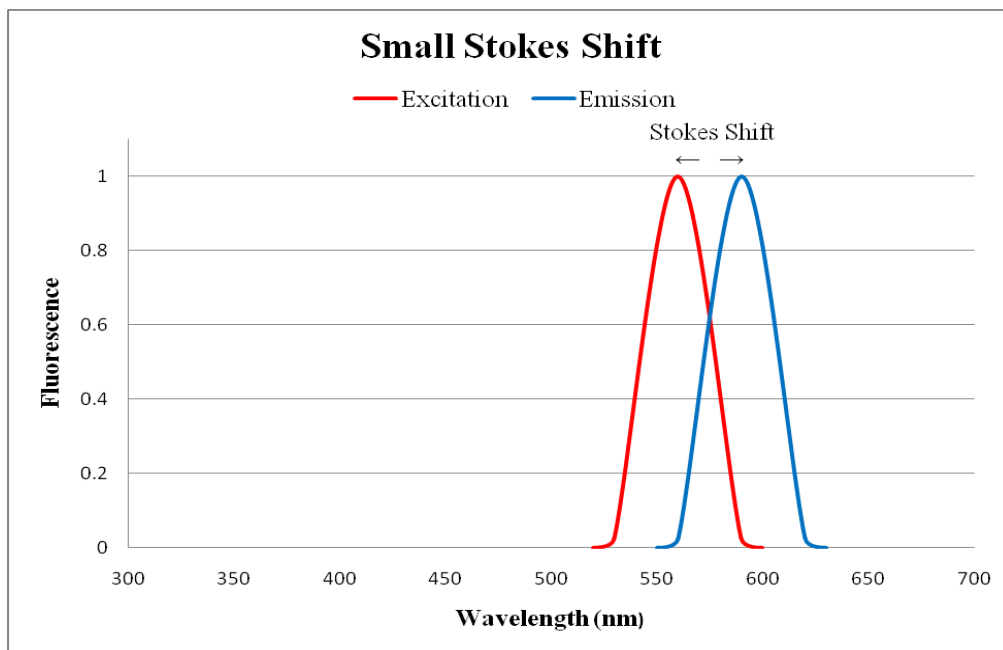


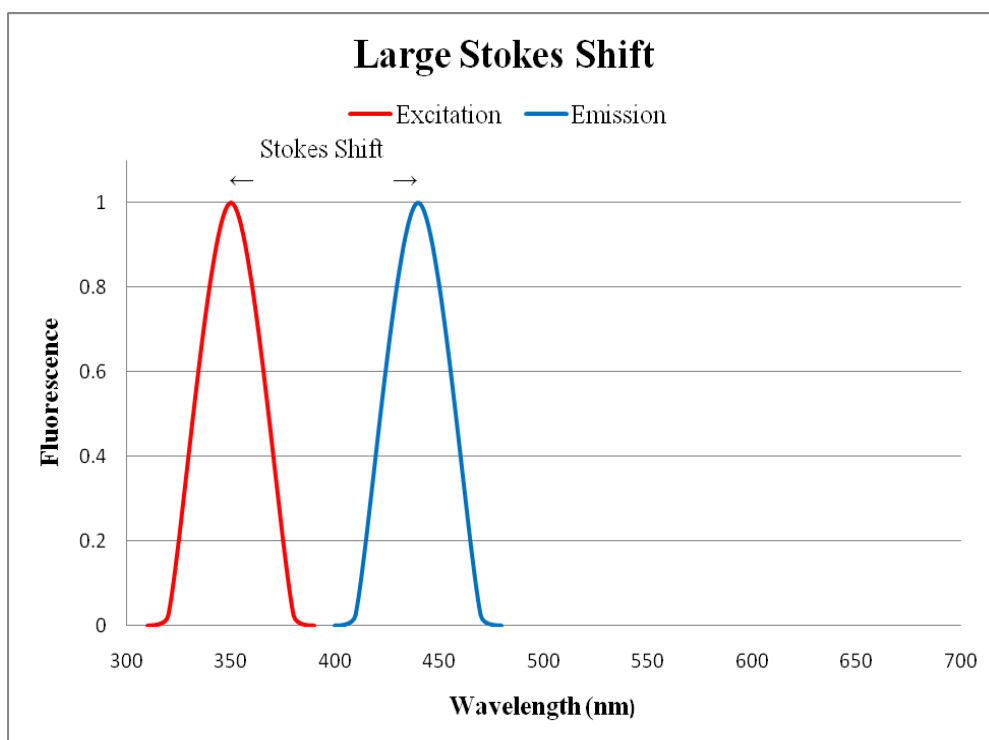
**Figure 1.3:** Simplified Jablonski diagram.

During fluorescence, electrons are elevated to a higher energy state by the absorption of electromagnetic radiation (usually light). This higher state is unstable and some of the energy is lost to the surroundings as heat (non-radiant energy). The remaining energy is emitted as light as the electrons return to their stable ground state. As there is a loss of energy during the relaxation step, the light emitted is lower in energy (of a longer wavelength) than the light absorbed. As demonstrated by the Einstein-Planck equation  $e=hc/\lambda$ . Therefore, a fluorescent molecule has an absorption and emission spectrum. The distance between the  $\lambda_{\max}$  of these two spectra can be measured in nanometres and is known as 'Stokes Shift'. (Figure 1.4)

A large Stokes Shift is desirable because less of the two spectra overlap meaning less interference and a greater area can be used to make a measurement. This also has the benefit of increasing the sensitivity of the measurement resulting in detection at lower concentrations or in a smaller time frame.



resorufin spectra (Ex 560nm, Em 590nm)



7-amino-4-methylcoumarin spectra (Ex 350nm, Em 440nm)

**Figure 1.4:** Stokes Shift. Examples of large and small Stokes Shift.

Where fluorometric substrates are used in an enzyme assay, the fluorescent molecule (fluorophore) released can be measured using a fluorimeter. Here again, there is a considerable variation in the type of instrumentation available. In the simplest case direct observation under a U.V. source can demonstrate areas or zones of fluorescence colour. This is common practice in diagnostic microbiology, e.g. substrates based on 4-methylumbelliferone (4-MU) or the more recently developed cyclohexenoescluletin (CHE) to locate specific organisms. 4-MU glucuronide has been used to differentiate *E. coli* from other enterobacteria (Szabo et al., 1986) and CHE- $\beta$ -glucoside to visualise *Listeria* spp. (James, 2001; Smith et al., 2001). As 4-MU glucuronide colonies of organisms possessing the relevant enzyme show as bright sky-blue areas on a weakly purple agar back ground (Figure 1.5).



**Figure 1.5:** 4-Methylumbelliferyl- $\beta$ -D-glucuronide. Used in agar to differentiate *E. coli* (fluorescent blue) from other enterobacteria. Picture courtesy of Merck.

Fluorometric measurement can be made using a spectrofluorimeter. Design and construction may vary, but essentially a source of U.V. radiation is generated (mercury, deuterium, xenon lamp, etc.). Monochromation is achieved by use of a diffraction grating or interference filter. The latter is used when a broader bandwidth is acceptable. Sophistication of this

technique can be extensive as illustrated by the Fluorescence Activated Cell Sorter (FACS) a device which can identify and measure specific fluorophores on a cell's surface and then separate cells based on their charge (Herzenberg et al., 2002).

- c) Luminescence Spectrophotometry. This includes chemiluminescence and bioluminescence. The latter is more commonly employed as it is, in theory, applicable to all reactions involving adenosine triphosphate (ATP) and nicotinamide dinucleotides (NAD and NADH). Visible light is generated through the activation of the luciferin/luciferase system (firefly enzyme) (Figure 1.6) or other light generating system, e.g. Green Fluorescent Protein.

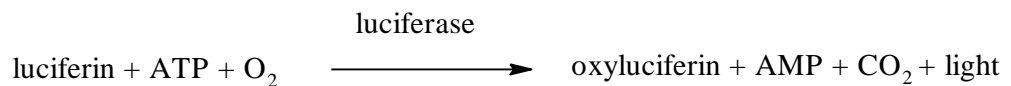
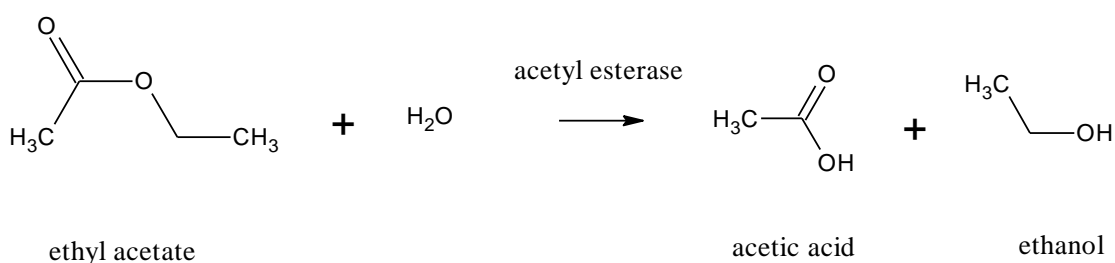


**Figure 1.6:** Luciferin/ luciferase system.

One of the significant advantages of the system is its extreme sensitivity since, in contrast to other spectrophotometric procedures; no prior light interaction is needed. As a result there is no extraneous light and the luminescence generated can be greatly amplified and detected using photodiodes or photomultiplier devices. An interesting example of an application of luminometry is the use of the bioluminescence photoprotein aequorin (*Aequorea victoria* jellyfish) to measure very low levels of calcium ions (Shimomura et al., 1990). Non-fluorescent aequorin interacts with  $\text{Ca}^{2+}$  ions undergoing a structural change. This new form is in an excited state which then emits a blue light when returning to its ground state.

Other methods of enzyme assay:-

- d) Electrometric. The enzyme catalysed reaction may be associated with changes in electrical/ionic variables, e.g. pH, conductivity, redox potential etc. All have been used to monitor enzymatic reactions and to determine activity. A specific example would be the assay of an esterase enzyme (Figure 1.7). In its simplest form the substrate, ethyl acetate, when hydrolysed in the presence of acetyl esterase (from wheat germ) produces acetic acid and ethanol.



But

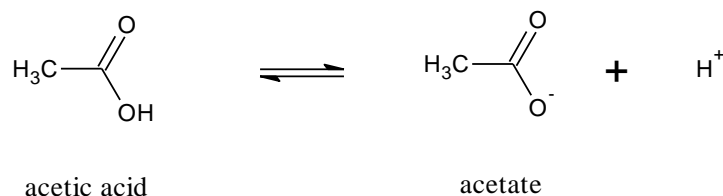


**Figure 1.7:** Assay of an esterase enzyme.

As hydrogen ions are generated in the reaction there is a decrease in pH which can be monitored using a pH meter. A disadvantage of this is the possible variation in enzyme activity caused by this change in pH (pH optimum effect). Therefore, it is common practice to use a pH-stat device which ensures the constancy of pH during the reaction in absence of buffers by the addition of alkali. The rate of alkali consumption becomes a measure of enzyme activity. In the example above, ethyl acetate is not an ideal substrate due to its volatility. Consequently, other substrates,

such as glyceryl triacetate (triacetin), can be used. Alternatively, if the esterase has a broad enough specificity then ethyl butyrate could be used. For the lipase assay, esters of even longer carbon chains, e.g. palmitate are used, but a surfactant is required to cause emulsification and hence give a greater surface area. This type of approach is also applicable to urease and other enzyme systems where the pH increases due to release of a base, e.g. amino and decarboxylases, but is usually reserved for assays where no satisfactory spectrophotometric alternative exists.

- e) Conductimetric. These methods are usually employed in a similar manner to electrometric, since released hydrogen and hydroxide ions have a much higher ionic mobility than other ions and contribute strongly to the observed conductivity and signal generated. Another case in point is that of polymer hydrolysis, e.g. peptidase or nuclease hydrolysis, where the released amino acids or nucleotides give a much higher conductimetric signal than the initial polymeric substrate (Besson et al., 1994).
  
- f) Redox Potential. Changes in redox potential are accompanied by a change in observed electromagnetic field (EMF) and, while this could be measured, it is more common to link the change to a spectrophotometric method using a chromogenic redox indicator, such as triphenyl tetrazolium chloride (TTC) or another member of the tetrazolium family (Bieniarz et al., 1992).
  
- g) Radiometric. Although not commonly used nowadays, radiometric methods have played a significant part in enzyme assays, as well as in immunological assay (RIA), and in the understanding of the mechanisms of enzyme action and metabolic sequences (Yalow and Berson, 1995). In general, the substrate is synthesised in a radiolabelled form ( $^{14}\text{C}$ ,  $^3\text{H}$ ,  $^{15}\text{N}$ , etc.) and preferably of high specific activity. During the reaction, the substrate is transformed into its products, one of which will contain the radioactive label. In many cases this product must then be separated before they can be measured, e.g. by a

scintillation counter. Problems concerning availability of labelled substrates, difficulty of synthesis and the need for a separation stage led to alternative methods being used where possible. Also, the inherent risks associated with the use of radioisotopes compounded this.

- h) Calorimetric. Isothermal titration calorimetry (ITC) is becoming a popular method to investigate enzyme kinetics as it can be employed with enzyme types that have no traditional direct assays. The thermal energy produced or taken up when an enzyme converts substrate to product is proportional to the rate of reaction and can be measured using ITC. Measurements are based on the amount of power needed to maintain equal temperatures between two cells, reference and sample. The reference cell can be considered to be a 'blank', as generally it will only contain buffer or reaction medium, while enzyme and substrate are injected in known amounts into the sample cell. If the reaction is exothermic the temperature will increase in the sample cell, therefore less power will have to be applied to maintain equilibrium. If, on the other hand, the reaction is endothermic, then more power is needed to keep the temperature of the two cells balanced (Todd and Gomez, 2001).

#### **1.4 Substrates employed in enzymology and enzyme assays**

In the determination of enzyme activity, it is better in the great majority of cases to measure the rate of formation of product rather than the rate of disappearance of the substrate. There are many reasons for this but mainly, at the early stage of the process, the substrate concentration is changing only slightly, whereas that of the product goes from zero to progressively higher and higher values, thus permitting more sensitive and accurate determination.

Several general procedures for determination of enzyme activity may be identified;

- a) Natural substrates
- b) Coenzymes or other cofactors
- c) Coupled systems
- d) Artificial substrates

- a) Natural substrates

In many cases, it is fairly obvious what the principle compound (or sometimes the only compound) being transformed by a particular enzyme is, e.g. urea and urease (Figure 1.8).

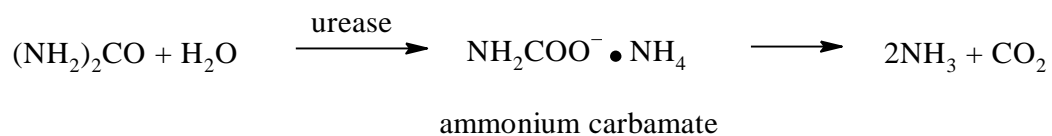


**Figure 1.8:** Urease catalyses the hydrolysis of urea (NH<sub>2</sub>)<sub>2</sub>CO to NH<sub>3</sub> and CO<sub>2</sub>.

Urea is a very simple molecule and few, if any other, molecules are capable of being hydrolysed by the enzyme urease. The term absolute specificity is often used for this effect. Thus, related compounds, such as thiourea, hydrazine and semicarbazide, are inert; however, there is evidence that they bind to the active site of the urease enzyme and act as competitive inhibitors. Urea is therefore used as the substrate for urease assay, utilising the change in pH or conductivity or alternatively determining the amount of ammonia formed colorimetrically, e.g. by reaction with phenol hypochlorite or diacetyl monoxime. Other examples of situations where the natural substrate is preferred or necessary include:-

Creatine phosphokinase (CPK) – the natural substrate of which is creatine phosphate.

Aminotransferases – although many such enzymes exist, two are of prime importance in the area of clinical chemistry:

Aspartate aminotransferase (AST), synonym glutamic oxalacetic transaminase (GOT), and alanine aminotransferase (ALT), synonym glutamic pyruvic transaminase (GPT). Both enzymes individually catalyse the transfer of the amino group from L-aspartate and L-alanine respectively to the acceptor keto acid  $\alpha$ -ketoglutarate (Figure 1.9).

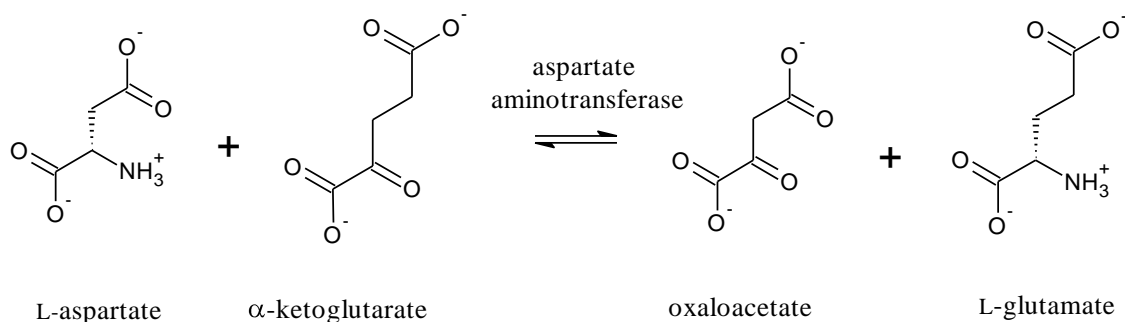


**Figure 1.9:** Action of aspartate aminotransferase.

In both reactions there is an absolute requirement for  $\alpha$ -ketoglutarate (1.5) and for either of the two amino acids individually. In the equilibrium, there are two amino acids and two  $\alpha$ -keto acids, so that following the progress of reaction is not straight forward. In practice, advantage may be taken of the technique of enzyme coupling, where a second enzyme specific to one of the products is added. This is usually an  $\text{NAD}^+$  or  $\text{NADP}^+$  dependent dehydrogenase. Enzyme coupled reactions are dealt with later in this section.

#### b) Coenzymes/cofactors

By far the most widely used coenzymes for determination of enzyme activity are NADH and the related NADPH. These are the reduced forms of the nicotinamide nucleotides  $\text{NAD}^+$  and  $\text{NADP}^+$ . Together with the reduced forms, they constitute redox pairs and are obligatory participants in many dehydrogenase reactions. They include:-

- i. Alcohol dehydrogenase
- ii. Lactate dehydrogenase
- iii. Pyruvate dehydrogenase
- iv. Malate dehydrogenase
- v. Isocitrate dehydrogenase
- vi.  $\alpha$ -Ketoglutarate dehydrogenase

Many of these reactions are central to the metabolism of the cell. Others are more central to amino acid metabolism and include:-

- vii. Glutamate dehydrogenase
- viii. Glutathione reductase

For example, alcohol dehydrogenase enzyme (ADH) catalyses the reversible oxidoreduction of ethanol and certain other alcohols/hydroxyl compounds to the corresponding aldehydes (Figure 1.10).

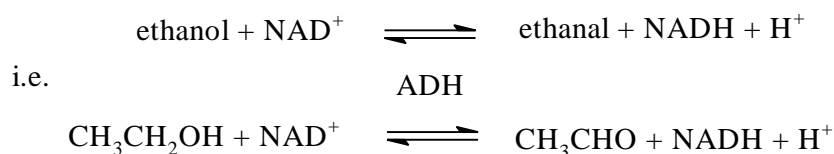


**Figure 1.10:** The reversible oxidoreduction of ethanol.

There are at least two possibilities for monitoring this reaction. One is to determine the ethanal (acetaldehyde) formed by a specific chemical reaction e.g. with 2,4-dinitrophenylhydrazine (DNPH); however this would require addition of an auxiliary reagent post-incubation, i.e. a fixed time assay.

Alternatively, the rate of formation of NADH may be monitored kinetically due to its spectroscopic characteristics, which are different to the oxidised forms. Only the reduced forms, e.g. NADH, exhibit emitted fluorescence at  $\lambda_F = 450 \text{ nm}$ , when excited at  $\lambda_x = 340 \text{ nm}$ .

It follows that dehydrogenase reactions involving the formation of NADH or NADPH can be followed kinetically either by absorption at 340 nm or by the appearance of fluorescence at  $\lambda_F$  max.

Since most dehydrogenase reactions are reversible, it is often possible to measure the decrease in  $A_{340}$  and use this as a measure of the consumption of NADH. In certain cases, the position of equilibrium can be adjusted in order to 'drive' the reaction in one direction. This may involve the addition of a carbonyl trapping reagent such as semicarbazide or adjustment of the buffer pH, since hydrogen ions are involved in the reaction (Figure 1.11)

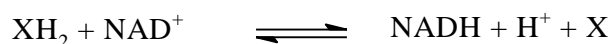


**Figure 1.11:** Equilibrium of NAD/NADH.

While the U.V. absorbing and fluorescing properties of NADH/NADPH are very useful in measuring enzyme activity, it is often desirable to have a coloured product produced and measured by the dehydrogenase system. This can be illustrated by the use of tetrazolium salts, which may be regarded as dye precursors since they are readily reduced to highly coloured derivatives called formazans. Many tetrazolium salts have been synthesised and are commercially available (Altman, 1976). The general formula for the simpler salts is shown in Figure 1.12

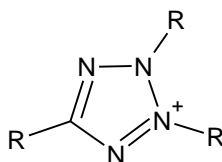


**Fig 1.12** General formula for a tetrazolium salt.

The simplest example still used in diagnostic microbiology to detect growth of living cells is the reduction of 2,3,5-triphenyltetrazolium chloride. This is somewhat inhibitory to many enzymes, so that others, e.g. iodonitrotetrazolium chloride (INT) (Figure 1.13) or neotetrazolium chloride, are more widely used in a 'linked' assay (Gong, 1996).

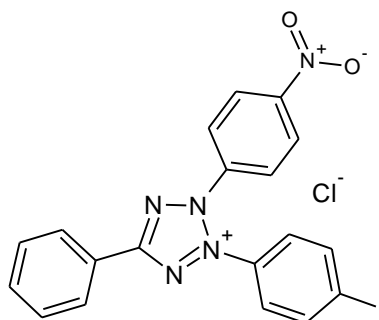


**Figure 1.13:** Iodonitrotetrazolium chloride (INT).

The reduction of such a tetrazolium salt by NADH can be represented as shown in Figure 1.14.

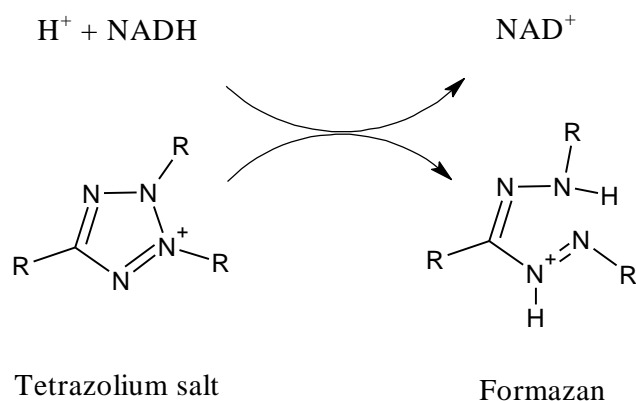


**Figure 1.14:** Reduction of a tetrazolium salt by NADH.

Tetrazolium salts have a number of advantages, including a very substantial increase in colour and at longer  $\lambda$  on reduction.

Monotetrazolium compounds become deep red while ditetrazolium salts become deep purple or blue. The reduction is irreversible and the products are non-autoxidisable unlike, for example, methylene blue. Additionally, the molar absorptivities of tetrazolium products (formazans) are about 3 or 4 times higher than that of NADH and at longer and, therefore more accessible wavelengths. This commonly lowers the detection limits for dehydrogenase enzyme by several fold and makes the system more applicable to the automated methodologies, e.g. centrifugal analysers.

### c) Coupled systems

The coupling of NADH or NADPH production to the reduction of a tetrazolium salt to produce a coloured formazan is one example of a coupled system. However, it is also possible to employ a second enzyme to cause one of the products to be further transformed. If the second reaction is catalysed by an NAD dependent dehydrogenase, then the NADH formed will be related to the overall enzymatic activity. Provided that the second enzyme is in considerable excess over the initial enzyme to be measured, then this former enzymatic activity will be rate limiting. A good example of the use of a dehydrogenase as the second enzyme is in the assay of the clinically important enzyme alanine aminotransferase (ALT) shown in Figure 1.15. In this reaction, the product, pyruvate, can be used to form  $\text{NAD}^+$  via NADH using lactate dehydrogenase (LDH).

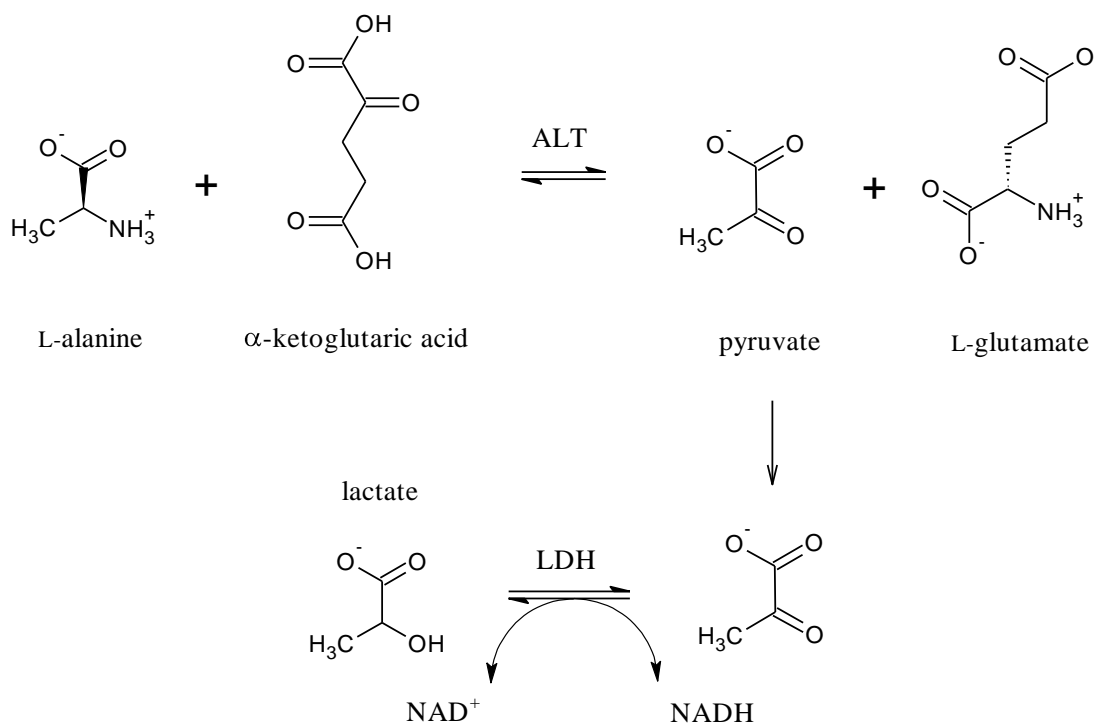
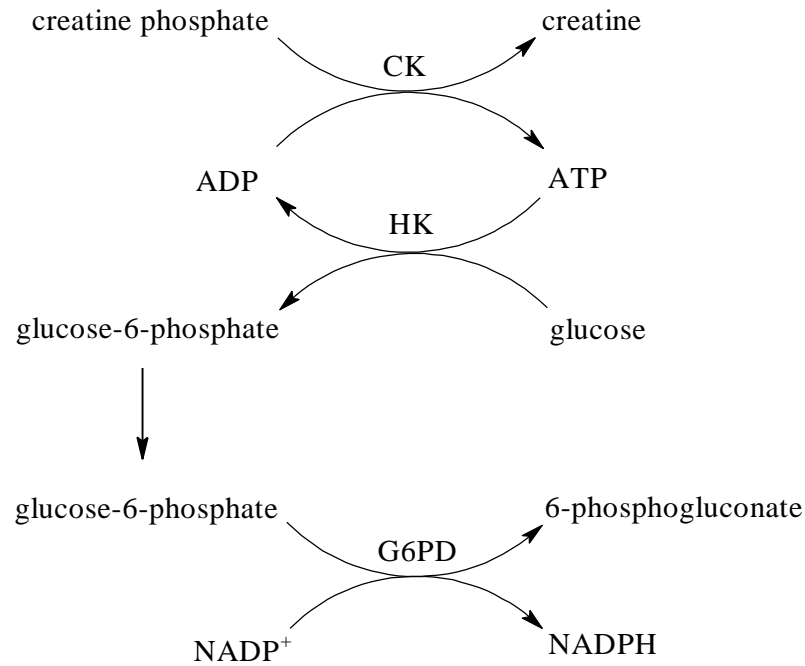


**Figure 1.15:** Transamination of L-alanine coupled to an LDH reaction.

The decrease in absorbance at 340 nm, as NADH is oxidised, reflects the amount of pyruvate available to the enzyme lactate dehydrogenase (LDH), which in turn depends on the activity of the ALT in the original reaction. In practice, the experimental reagent contains α-ketoglutaric acid, L-alanine, NADH and LDH so that the first and second reactions can proceed. Sometimes, the enzymatic coupling can be more complex, e.g. in the assay of creatine kinase (CK) there are two sequentially linked derivatising reactions (Figure 1.16).



CK = creatine kinase

HK = hexokinase

G6PD = glucose-6-phosphate dehydrogenase

**Figure 1.16:** Creatine kinase assay.

In this case there will be an increase in absorbance at 340 nm, reflecting the activity of CK, provided that this is rate limiting. For this reason, it is general practice to make the activity of the derivatising enzymes ten times the activity of the first enzyme. It is also possible to link the production of NADPH to the reduction of a tetrazolium salt, as previously discussed.

#### d) Artificial substrates

Perhaps the greatest advance in diagnostic enzymology over the last 50 years has been the synthesis of derivatives of biomolecules, e.g. sugars, fatty acids, amino acids, peptides, to give substrates which are transformable, usually by hydrolysis, to

release highly coloured or fluorescent molecules. The terms chromogenic and fluorogenic substrate, respectively, are used to describe these. Even where natural substrates are available, it is often preferable to use a synthetic analogue, provided that the enzyme in question exhibits group specificity. This term is used to denote enzymes which will accept a range of related compounds. The feature is commonly shown by hydrolases (where  $H_2O$  is the hydrolytic agent and is always present in excess), a very large group of enzymes which include glycosidases, lipases, peptidases, nucleases and phosphatases, etc. (James, 1993). It is often found that a very considerable increase in sensitivity can be achieved by the use of synthetic analogues. This may be in part due to better kinetic parameters, i.e. lower  $K_M$  (affinity of enzyme and substrate) caused by a greater affinity of the substrate for the active site of the enzyme and higher  $V_{max}$  (a measure of the limiting rate of transformation of the substrate). These two catalytic constants are often expressed together as the  $k_{cat}/K_M$  ratio ( $k_{cat}$  being the rate constant related to  $V_{max}$ ). Equally important for sensitivity is the mode of measurement of the product from a synthetic substrate. If the product molecule from a synthetic substrate is highly coloured, e.g. resorufin, or fluorescent, e.g. 4-methylumbelliferone (4-MU), then the spectrophotometric method used to measure product formation can greatly increase sensitivity and hence lower detection limits, e.g. acid phosphatase. This enzyme occurs in human semen, being derived from the prostate gland. It also has wider distribution in animal prostate tissue. Determination of acid phosphatase activity is important in the diagnosis of metastatic spread of prostate cancer, particularly to bony tissue. In general, acid phosphatase may be determined using a variety of 'natural' substrates, e.g. glycerol phosphate or glucose-6-phosphate, by measurement of the release of inorganic phosphate, such as the method of (Fiske and Subbarow, 1925), or it can be measured by the formation of glycerol or glucose by colorimetric methods. However, these methods are relatively insensitive and do not lend themselves to a kinetic assay. One exception would be the coupling of glucose oxidation by adding glucose oxidase to generate hydrogen peroxide.  $H_2O_2$  in the presence of peroxidase can then oxidise a pro-chromogen such as *o*-dianisidine or diaminobenzidine to yield a coloured product end point.

In place of such natural substrates, it is possible to use a variety of synthetic (artificial) substrates, since the phosphatase exhibits group specificity. Examples include:-

- i. Phenolphthalein diphosphate
- ii. Thymolphthalein phosphate
- iii. Fluorescein diphosphate
- iv. *p*-nitrophenol phosphate
- v. Indoxyl phosphate
- vi. X-phosphate
- vii. 4-Methylumbelliferyl phosphate

The high molar absorptivities of the released chromogens give a sensitive assay. Similarly with  $\beta$ -galactosidase, the natural substrate for which is lactose, the synthetic substrate *o*-nitrophenyl- $\beta$ -D-galactoside (ONPG) was shown to be thirty times more effective as a substrate. Additionally the *o*-nitrophenol produced is readily detected and measured by the yellow colour ( $\lambda_{\text{max}} = 410 \text{ nm}$ ) (Lederberg, 1950).

The vast majority of these artificial substrates are synthetic, made explicitly for the detection of enzymes in specific circumstances and therefore warrant a more indepth section in this introduction.

## 1.5 Synthetic substrates

A wide variety of synthetic substrates targeting a similarly wide range of enzymatic activities are currently available. Many of these are used routinely in hospital laboratories, food technology and in research. Most of these generate either a strong colour or fluorescence when hydrolysed or otherwise transformed. A few produce bio or chemiluminescence. The various groups may be categorised for convenience as follows.

- Nitrophenols
- Indoxyls
- Naphthols
- *p*-Nitranilides
- Methylumbelliferones
- 7-Amino-4-methylcoumarins
- Phthaleins
- Phenoxazines
- Fluorones

In addition, there are many recently developed substrates outside of the above list.

### 1.5.1 Nitrophenols

One of the earliest synthetic enzyme substrates to be developed was *o*-nitrophenyl- $\beta$ -D-galactoside (ONPG) (Seiderman and Link, 1950) shown below in Figure 1.17.

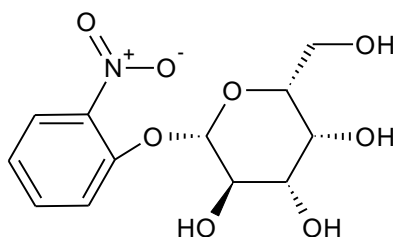


**Figure 1.17:** Structure of nitrophenyl- $\beta$ -D-galactoside.

It was shown to be a good substrate for  $\beta$ -galactosidase having good characteristics and yielding a strong yellow colouration at pH 7.5 (Lederberg, 1950).

The reason for the rapid transformation/hydrolysis of ONPG is due largely to the ability of nitrophenol to act as a good leaving group. The phenoxide ion produced is stabilised by resonance and consequently of lower energy than the nitrophenolic substrate (Figure 1.18). Since systems tend to a state of minimum energy, the rate of cleavage of the glycosidic bond is enhanced.

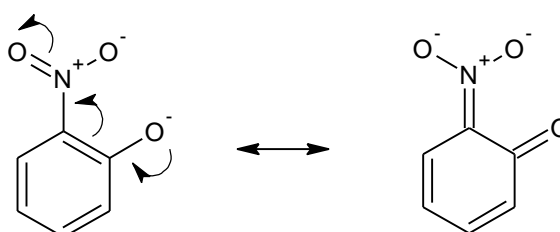


**Figure 1.18:** The two resonance structures of nitrophenol.

ONPG has been used in the detection and enumeration of coliforms in water by a membrane filtration technique (Apte et al., 1995) and also in a medium for screening for *Salmonella* spp. (Berlutti et al., 1986).

*o*-Nitrophenyl- $\beta$ -D-glucoside was similarly developed as a substrate for  $\beta$ -glucosidase (Jermyn, 1955) and has been used as a reagent in the investigation of immunologically based separations in capillary electrophoresis (Ljungberg et al., 1998). The corresponding *p*-isomer has been employed in plant biotechnology (Marcinowski and Grisebach, 1978) and in the identification of members of the genus *Bacillus* (Mizuno et al., 1998).

The enzyme  $\beta$ -glucuronidase occurs in the great majority of naturally occurring *E. coli*, but excluding the enteropathogenic 0157 strain. Other coliforms, in the main, do not produce  $\beta$ -glucuronidase and thus differentiation is achievable (Kilian and Bulow, 1976).

A very important substrate in this group was developed and used to identify and demonstrate *E. coli*: *p*-nitrophenyl- $\beta$ -D-glucuronide (Kilian and Bulow, 1979) (Figure 1.19).

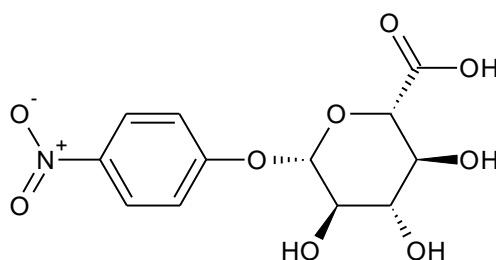


**Figure 1.19:** *p*-Nitrophenyl- $\beta$ -D-glucuronide.

The above substrates are all hydrolysed by the relevant  $\beta$ -glycosidase enzyme. Nitrophenolic substrates targeting  $\alpha$ -glycosidase are also commercially available, including *p*-nitrophenyl- $\alpha$ -D-glucoside, which has been used clinically in a urine screening test for Pompe disease (Schram et al., 1979). Pompe disease is a metabolic disorder caused by a lack of  $\alpha$ -glycosidase, which is required to metabolise glycogen. An excessive amount of glycogen in the body results in myopathy, particularly of the heart.

The use of nitrophenolic substrates is not limited to the glycosidases. Phosphatase and lipase substrates have also been developed. An example of the former, *p*-nitrophenyl phosphate (Figure 1.20), has been used extensively to assay both acid and alkaline phosphatase in human serum (Lowry, 1957; Breaudiere et al., 1977). This substrate has also been involved in studies to identify rapidly *E. coli* (Husson et al., 1989) and makes up part of the BD (Becton, Dickinson and Company) ‘BBL Crystal<sup>TM</sup> Enteric/Non-fermentor Identification System, a micro-method test kit for the identification of aerobic Gram-negative bacteria that belong to the *Enterobacteriaceae* family, as well as some of the more commonly isolated fermenting and non-fermenting Gram-negative bacilli.

*p*-Nitrophenyl acetate has been used to determine lipase activity in milk (Wang, 1981).

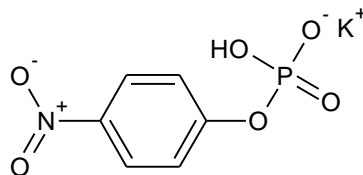


**Figure 1.20:** *p*-Nitrophenyl phosphate ( $K^+$  salt).

### 1.5.2 Indoxyls

Indoxyl substrates are probably the most widely used chromogenic substrates, particularly in microbiological culture media. When they were first introduced, it was not into microbiology, but into histochemistry for histochemical applications in the 1950's (Pearson, 1957).

Their great value is that they can produce insoluble deposits, which are highly coloured, and therefore specifically located at the site of the enzyme action. When an indoxyl substrate is cleaved by enzyme action, it produces free indoxyl, i.e. 3-hydroxyindole (Figure 1.21).

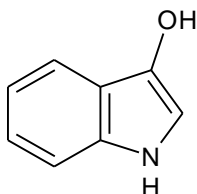


**Figure 1.21:** 3-Hydroxyindole.

Under oxidative conditions, two molecules of indoxyl dimerise to form a molecule of a highly coloured indigo dye (Figure 1.22). This has considerable application in diagnostic microbiology because the indigo dye is capable of binding strongly to the bacterial colonies. This means that the colour is generated in a highly localised manner on those colonies which contain the enzyme responsible for the cleavage of the substrate. Thus, it allows a very clear differentiation of the organisms that are to be targeted within a mixed culture. The other advantage of indoxylic substrates is that they exhibit a very low toxicity towards most microorganisms

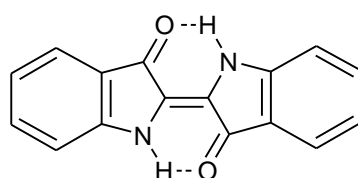


**Figure 1.22:** Indigo dye.

The molecule indoxyl does not occur itself as free indoxyl, but is very widely distributed as the  $\beta$ -glucoside in a variety of plants. It was commonly referred to as plant indican (Figure 1.23) and was the source of indigo for centuries for the process of indigo dyeing. The plant was macerated to release the  $\beta$ -glucosidase enzyme, which then cleaved the  $\beta$ -glucoside to give free indoxyl. The cloth was then impregnated with this to give a deposit of indigo by atmospheric oxidation.

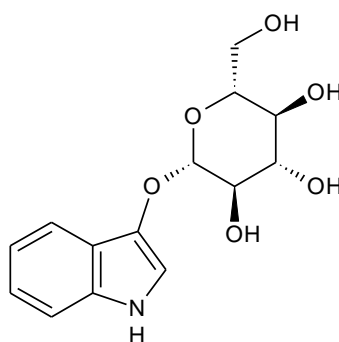


**Figure 1.23:** Plant indican.

Whilst substrates based on indoxyl itself have been very useful in the past to identify  $\beta$ -glucosidase or bacteria that produce this enzyme, e.g. *E. coli* (Ley et al., 1988; Delisle and Ley, 1989), they do not give very bright colours; they tend to give rather grey-blue shades. However, it is possible, by halogenation of the core indole nucleus at specific positions in the benzenoid ring to give much brighter colours and also to increase the intensity of colouration. The halogens involved may be any of the four normal ones – fluorine, chlorine, bromine or, more recently, iodine, and more than one position may be halogenated. This usually does not affect the specificity of the substrate, but does alter the sensitivity and the ease of reading, which is important when one is dealing with, for example, a bacterial plate.

The introduction of a bromine atom at position 5 of the indole nucleus produces 5-bromoindole and substrates have been developed based on this. First synthesised for histochemical localization of glycosidases (Anderson and Leback, 1961), then employed in bacterial identification, examples of these include Blue glucoside (5-bromo-3-indolyl- $\beta$ -D-glucoside) so named because of the intense dark blue colour that is generated by positive bacterial colonies which possess  $\beta$ -glucosidase.

Additionally, 5-bromo-3-indolyl- $\beta$ -D-galactoside, otherwise known as Blue gal, has been used as a histochemical substrate for the *lac Z* gene (Weis et al., 1991), shown in Figure 1.24.



**Figure 1.24:** Histochemical use of Blue gal. Intercostal muscle of mouse stained with Blue gal (Weis et al., 1991).

Blue nonanoate (5-bromo-3-indolyl nonanoate) is an esterase substrate (Figure 1.25) and has been used in investigations of *Salmonella* esterase and in the visualisation of *Salmonella* colonies (Agban et al., 1990; Orenge, 2009).

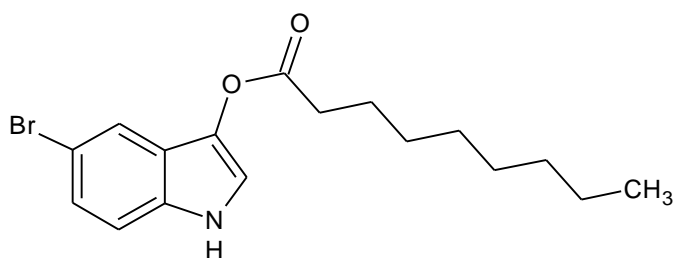


**Figure 1.25:** Structure of blue nonanoate.

Introduction of a chlorine atom at position 6 of the indole nucleus produces 6-chloroindoxyl and this is the basis of many substrates of the Rose/Salmon series, so called because the red-pink colour of the colonies is very evident. The same is true of its applications in histochemistry. Thus, for example, Salmon glucopyranoside (6-

chloro-3-indolyl- $\beta$ -D-glucopyranoside) has been synthesised and its use was reported in the year 2000 (de Silloniz et al., 2000) (Figures 1.26 and 1.27).

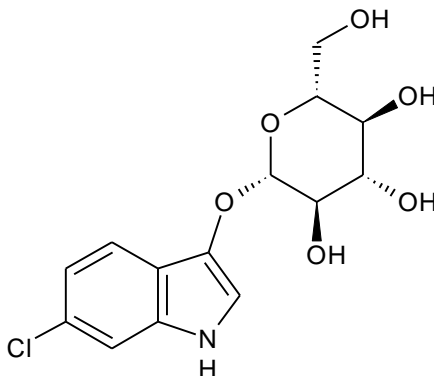


**Figure 1.26:** Structure of 6-chloro-3-indolyl- $\beta$ -D-glucopyranoside.



**Figure 1.27:** 6-chloro-3-indolyl- $\beta$ -D-glucopyranoside hydrolysed by *Yersinia pseudotuberculosis*.  
Picture courtesy of Glycosynth.

Rose acetylglucosaminide (6-chloro-3-indolyl-n-acetyl- $\beta$ -D-glucosaminide) is a substrate for  $\beta$ -N-acetylglucosaminidase and has been reported to have value in the differentiation of the *Candida* spp. (Gilbert, 2002).

A combination of halogen atoms with 5-bromo and 6-chloro substituents in the indole nucleus produces 5-bromo-6-chloroindoxyl and this forms a magenta precipitate when released from appropriate substrates. Consequently, the substrates

are usually referred to as Magenta substrates. An example is 5-bromo-6-chloro-3-indolyl- $\beta$ -D-galactopyranoside and this has been used as a substrate for gene expression studies (Mohler and Blau, 1996).

Magenta-caprylate is used to visualise *Salmonella* spp. (Cassar and Cuschieri, 2003) (Figure 1.28).

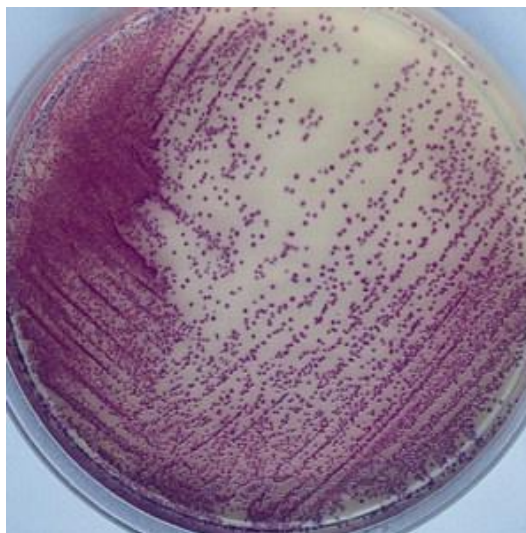


**Figure 1.28** Magenta-caprylate hydrolysed by *Salmonella* spp. results in magenta coloured colonies. Picture courtesy of Carlroth Ltd.

The corresponding *N*-acetyl- $\beta$ -D-glucosaminide (5-bromo-6-chloro-3-indoxyl *N*-acetyl-beta-D-glucosaminide) has been used as a histochemical substrate for demonstration of *N*-acetyl- $\beta$ -D-glucosaminidase (hexosaminidase) and this produces a magenta precipitate localised at the site of the hexosaminidase (Wolf et al., 1965).

The corresponding  $\beta$ -D-glucopyranoside (5-bromo-6-chloro-3-indolyl- $\beta$ -D-glucopyranoside) (Figure 1.29), has shown value in the detection and differentiation of *Vibrio* spp. (Rambach, 2007).

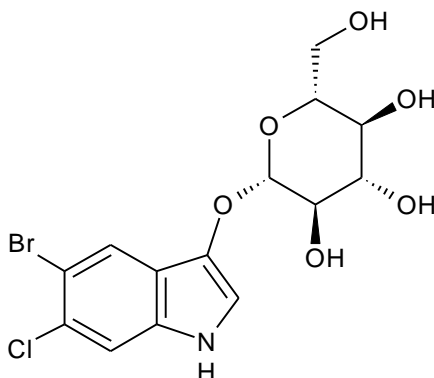


**Figure 1.29:** Structure of 5-bromo-6-chloro-3-indolyl- $\beta$ -D-glucopyranoside.

Even more widely used indoxyl substrates have the bromine atom substituted at position 5 and chlorine at position 4. The change in colouration becomes quite striking. The 5-bromo-4-chloroindoxyl when released produces blue colouration on appropriate colonies or in histochemical applications. It is commonly referred to as X and the best known derivative of this is certainly X-gal (Figure 1.30).

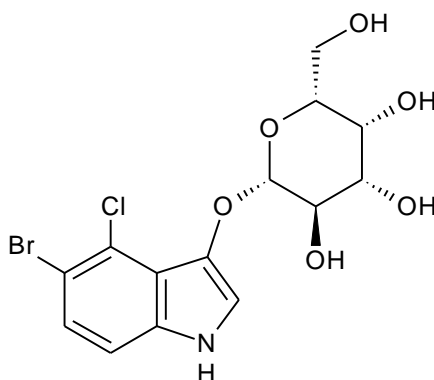


**Figure 1.30:** Structure of 5-bromo-4-chloro-3-indolyl- $\beta$ -D-galactopyranoside.

X-gal or 5-bromo-4-chloro-3-indolyl- $\beta$ -D-galactoside is a chromogenic substrate and is used to distinguish recombinant transformants (white) from non-recombinant transformants (blue) when using plasmids carrying the *lac Z* gene associated with  $\beta$ -galactosidase production (Blue/white screening) in molecular biology (Figure 1.31).

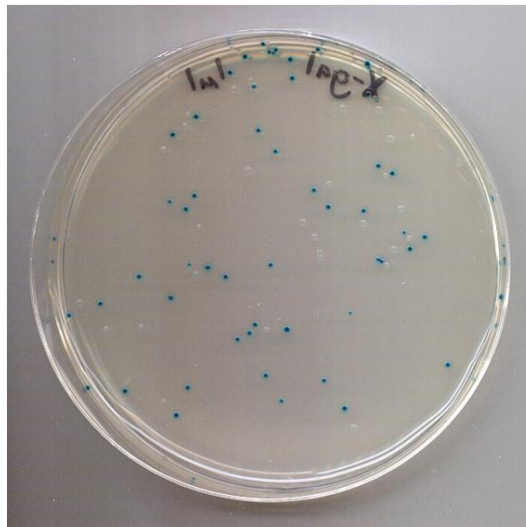


**Figure 1.31:** Blue/white screening. *E. coli* on LB agar containing X-gal.

It has also been used as a substrate for the detection of coliforms in water (Ley et al., 1993), urine (Kodaka et al., 1995) and food (Manafi and Rotter, 1991).

The corresponding glucoside (X-gluc) has been used in an assay for the identification of enterococci, which are  $\beta$ -glucosidase positive (Manafi and Sommer, 1993; Manafi, 1997).

X-glucuronide has been used in a medium for direct plating of *E. coli* (Frampton et al., 1988; Ogden and Watt, 1991) then for membrane filtration for the enumeration of *E. coli* and coliforms from drinking water (Sartory and Howard, 1992). In this case, the X-glucuronide only picks out the *E. coli*, where as a second substrate is necessary to evaluate the coliforms (Figure 1.32).

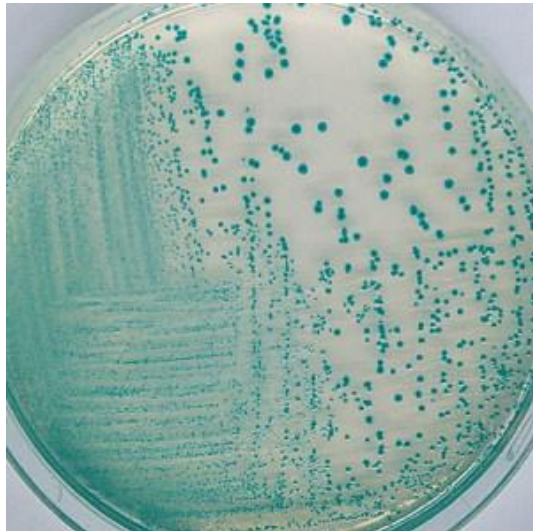


**Figure 1.32:** Trypsin Bile agar containing X-gluc (TBX agar). *E. coli* are coloured blue/green by reaction of  $\beta$ -D-glucuronidase. Other *Enterobacteriaceae* (e.g., *Salmonella*, *Streptococcus*, *Klebsiella*) are clear or inhibited. Picture courtesy of Carlotro Ltd.

In the detection and demonstration of salmonella X- $\alpha$ -gal has proved to be very useful, producing green or green-blue colonies with this substrate (Perry et al., 1999).

One important feature of indoxylic substrates is that it is possible to combine more than one with a different enzymatic specificity targeted and thereby demonstrate at least two different bacterial species on the same plate provided that the contrast between the two colours is great enough, for example the Alpha-beta chromogenic medium (ABC medium) (Perry et al., 1999). ABC medium contains X- $\alpha$ -gal as described above and also 3,4-cyclohexenoesculetin- $\beta$ -D-galactoside (CHE-gal). CHE-gal produces brown/black colonies from non-*Salmonella Enterobacteriaceae* (Figure 1.33).

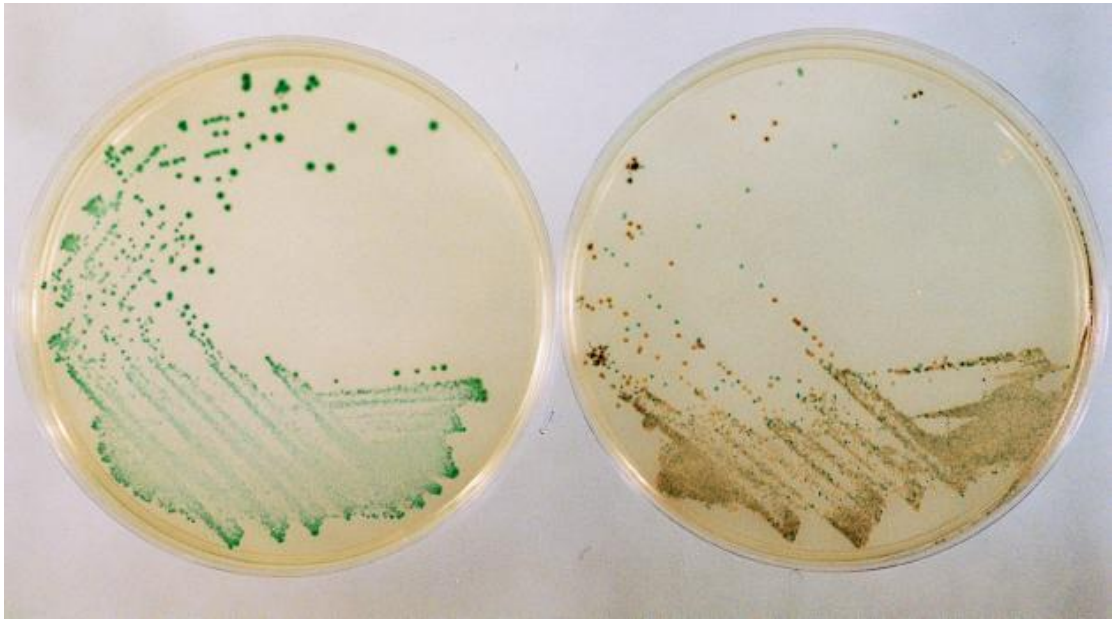


**Figure 1.33:** Alpha-beta chromogenic medium. Typical colonies produced by *S. typhi* on ABC medium (left) and a wild strain of *S. napoli* isolated in mixed culture from a stool sample (right) (Perry et al., 1999).

Alternatively, it is possible to use an esterase substrate based on X-nonanoate or X-octanoate for the detection of this particular class of bacterium.

Further modifications of the indoxyl molecule are possible to create further variations in colour of the colonies produced. Thus, for example, substitution of a fluorine atom into position 6 will give the 6-fluoroindolyl derivative which produces bright red colonies. Glycosides of this core molecule include, for example, Rougegal. Substitution of iodine into position 5 produces the corresponding iodo compound. Colonies exhibited here are violet.

An important modification is to methylate the nitrogen atom of the indole ring to produce *N*-methyl compounds such as 1-methyl-3-indolyl- $\beta$ -D-galactoside (green- $\beta$ -D-gal, so called because it produces green colonies). These galactoside substrates of fluoro, iodo and methyl indoxyls have demonstrated applications in the screening of recombinant transformants as they produce brightly coloured, vivid and, therefore easily identifiable colonies (Sambrook, 1989).

### 1.5.3 Naphthols

These are mainly derived from the two isomers, 1-naphthol and 2-naphthol, or derivatives of these, particularly 6-bromo-2-naphthol. It is well known that 1- and 2-naphthols are capable of generating highly coloured dyes by linkage to diazonium salts. This, of course, produces azo dyes. Consequently, a variety of substrates based particularly on 2-naphthol, have been developed. Furthermore, derivatives of 2-naphthol with a substituent in the 3 position have been prepared many years ago, particularly by German chemists for use in the dye industry, and are named according to the German language as, e.g. naphthol AS-BI and naphthol AS-D (Figure 1.34). The purpose of these was to extend the conjugation and give brighter colours with higher molar extinction coefficients.

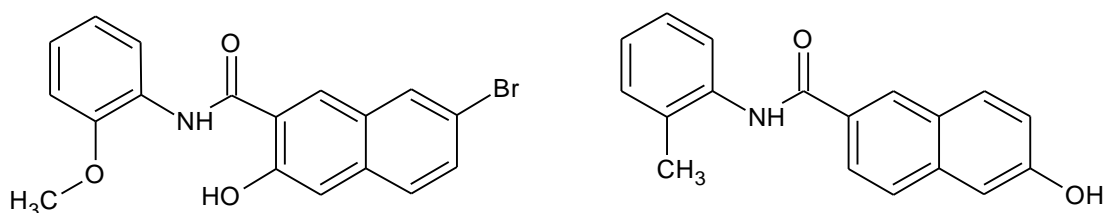


**Figure 1.34:** Structures of naphthol AS-BI (left) and naphthol AS-D (right).

The simpler substrates are usually based either on 2-naphthol or 6-bromo-2-naphthol. More complex substrates which have a greater degree of application, particularly in histochemistry, are derived from naphthol AS-BI and AS-D. For example, naphthyl AS-BI- $\beta$ -D-glucuronide has been used as a biochemical and histochemical substrate for the determination of  $\beta$ -D-glucuronidase. The coupling reagent employed is a stabilised diazonium salt such as hexazonium pararosanilin, which gives a precipitate at the site of the glucuronidase within the cell (Fishman, 1964; Hayashi et al., 1964).

Likewise, naphthyl AS-D-chloroacetate is a substrate for esterase activity and has been used in a similar manner to the glucuronide for localisation studies. In particular, myeloid cancer cells of leukaemia have shown a high level of esterase

activity which can be demonstrated histochemically (Figure 1.35) (Moloney et al., 1960; Leder, 1970).

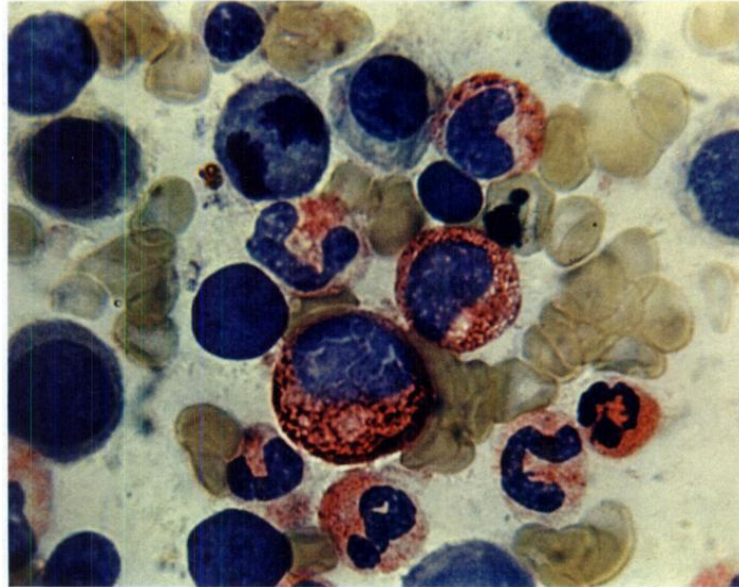


**Figure 1.35:** Esterase activity for naphthol AS-D chloroacetate substrate. Shown in the bone marrow smear of a patient with pernicious anemia. The mature and immature neutrophilic leukocytes demonstrate a strongly positive cytoplasmic red staining in contrast to the completely negative megoblasts (Moloney et al., 1960).

2-Naphthyl- $\alpha$ -D-glucopyranoside is interesting in the sense that it has been used as a substrate for glycogen synthetase (Meezan et al., 1997). It is usually rather difficult to use such substrates for biosynthetic enzymes, but the nature of the glycogen synthetic scheme is that glucose units are added via progressive  $\alpha$ -glycosidic links onto the growing chain and, as this happens, the molecule of naphthol is released which can be visualised by the addition of a stabilised diazonium salt, as has been indicated.

Substrates based on 1-naphthol are less common but have received a degree of interest within the last 10 years due to the development of the twin substrate protocol (Pemberton et al., 1999; Burestedt et al., 2000).

In this, a substrate such as 1-naphthol- $\beta$ -D-galactoside is incorporated simultaneously into a growing medium with a peptidase substrate based on an aromatic amine such as dimethyl-*p*-phenylene diamine (DM*p*PD) or 2,6-dichloro-4-aminophenol (DCAP). The simultaneous release of these core molecules from the peptidase and glycosidase substrates involved leads to a coupling in the presence of the enzyme cytochrome oxidase, which is present in the majority of *Enterobacteriaceae* to some degree (Figure 1.36). This produces a blue colouration thereby increasing the selectivity of the system, since two enzymatic activities are necessary to generate the colour. This system is used by bioMerieux to a substantial degree in the automated identification protocol inherent in the Vitek cards (Bascomb and Manafi, 1998).

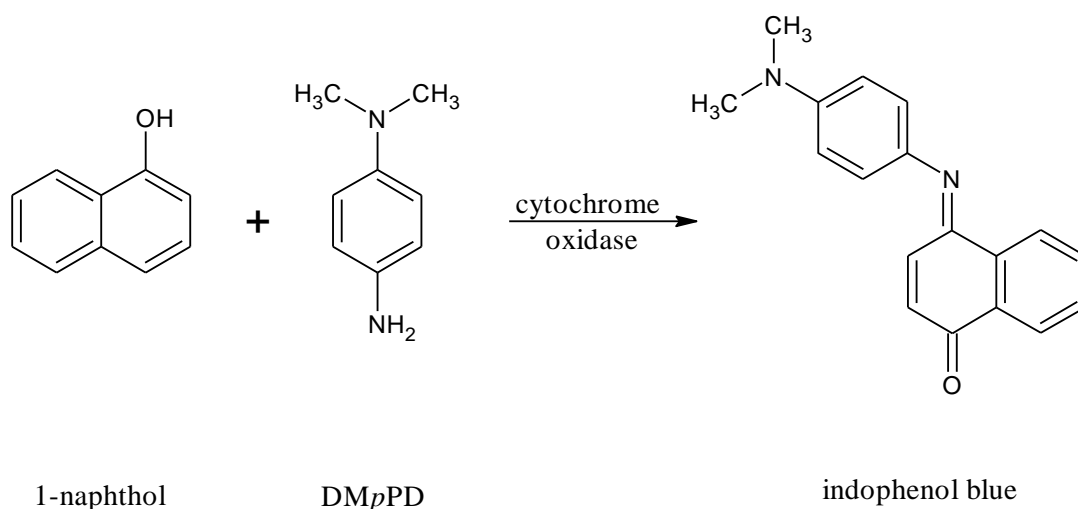


**Figure 1.36:** Indophenol blue formed by coupling 1-naphthol and DM*p*PD.

#### 1.5.4 *p*-Nitroanilides

The molecule of *p*-nitroaniline or 4-nitroaniline may be regarded as an analogue of *p*-nitrophenol. This has already been discussed as a core molecule for the creation of substrates for glycosidases, phosphatases, lipases, etc. The molecule of 4-

nitroaniline has an amino group conjugated through to a nitro group at the other end of the molecule (Figure 1.37). Consequently, the amino group can be substituted by peptide groupings to give substrates for peptidases of various types.

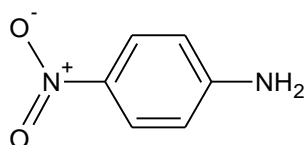


**Figure 1.37:** Structure of 4-nitroaniline.

For example, L-alanyl-*p*-nitroanilide (Figure 1.38) is a substrate for alanine aminopeptidase, which is widely distributed in Gram-negative bacteria, but not so in those that are Gram-variable or Gram-positive bacteria. When the peptide bond is hydrolysed, the products are obviously alanine and 4-nitroaniline. The 4-nitroaniline is recognised by the intense yellow colour which it exhibits at 405-410 nm (Redondo et al., 1986).

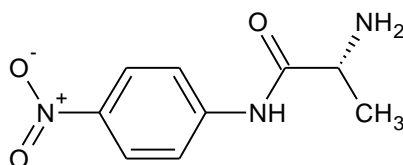


**Figure 1.38:** Structure of L-alanyl-*p*-nitroanilide.

Substrates, such as alanyl-*p*-nitroanilide, are good substrates, in the sense of having good kinetic constants. The  $k_{\text{cat}}/K_M$  ratio is high, in fact considerably higher than many other aminopeptidase core molecules, such as, 7AMC.

Whilst the yellow colour of *p*-nitroaniline is quite strong, there is often a problem in biological systems where there is a yellow background colour anyway. This makes it quite difficult to differentiate the yellow colour due to *p*-nitroaniline from the

background. In these cases, it is possible to add a second reagent to couple with the *p*-nitroaniline released.

Two possibilities exist. Firstly, the *p*-nitroaniline may be coupled with a stable diazonium salt, such as Fast Blue RR salt or some analogue. Alternatively, the reagent *p*-dimethylaminocinnamaldehyde has been used. This usually gives a much stronger colour in the red-purple region with a much higher molar absorptivity. However, in all these cases, the released *p*-nitroaniline tends to diffuse away from the site of production and hence these substrates are not ideally suitable for bacterial identification or for histochemical applications. They are more suited to detection of the enzyme in liquid culture.

A typical example of the use of such substrates in the biological sciences is the detection of  $\gamma$ -glutamyl transpeptidase or  $\gamma$ -glutamyl transferase ( $\gamma$ -GT), which is an important enzyme in the detection of liver disease. Since the levels of  $\gamma$ -GT vary over a very wide range depending on the severity of the condition, various substrates have been used to detect this enzyme in blood. Certainly,  $\gamma$ -glutamyl nitroanilide is one such substrate (Figure 1.39) and  $\gamma$ -glutamyl AMC has also been used to measure levels in human serum (Prusak et al., 1980). It is necessary in this reaction to have an acceptor peptide to ensure that the enzyme being detected is the transferase and not merely a hydrolase. For this purpose, glycylglycine is usually used as the acceptor.

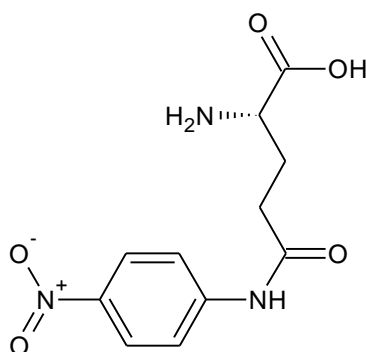


**Figure 1.39:** L- $\gamma$ -glutamyl nitroanilide.

Another example of the application of peptidase substrates based on *p*-nitroaniline is the use of pyroglutamyl-*p*-nitroanilide for the detection of Group A *Streptococci* and also enterococci and their differentiation from other *Streptococci* (Manafi et al., 1991) . In this case, it is necessary to detect the *p*-nitroaniline released using reagents such as dimethylaminocinnamaldehyde (Doronin et al., 2004).

### 1.5.5 Methylumbelliferones

4-Methylumbelliferone (4-MU), (Figure 1.40) is a trivial name for 7-hydroxy-4-methylcoumarin. The possession of the coumarin ring, with suitable substitution of hydroxyl or amino groups confers highly fluorescent properties upon the molecule and this is exploited of in the creation of enzymatic substrates.

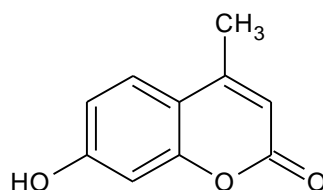


**Figure 1.40:** Structure of 4-methylumbelliferone.

When the hydroxyl group at position 7 is free, e.g. in the molecule of methylumbelliferone, there is a strong fluorescence due to electron release from the hydroxyl group conjugated through to the carbonyl group in position 2 over a planar structure. There is a very high degree of fluorescence with excitation at 360 nm and fluorescence at approximately 440 nm giving a bright sky-blue fluorescence which is easily detectable and measurable. This fluorescence is, however, pH dependent reaching a maximum at pH ~ 9-10, although a strong fluorescent is still exhibited at pH ~ 7-8 (Figure 1.41).

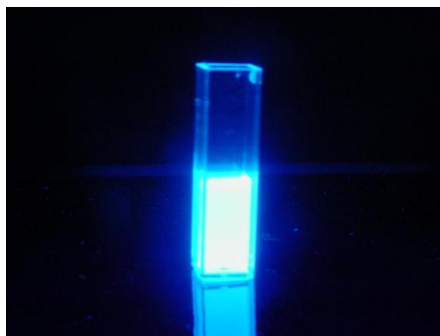


**Figure 1.41:** Fluorescence of 4-methylumbelliferone.

Many examples of methylumbelliferone substrates exist. For example, the  $\beta$ -D-galactoside, 4MU- $\beta$ -D-gal has been used for fluorimetric assay of lectin binding to yeast cells (Oda et al., 1997) and for the detection of faecal coliforms (Berg and Fiksdal, 1988). Similarly, the  $\alpha$ -D-galactoside has been used in a medium for detecting faecal *Streptococci* (Littel and Hartman, 1983). The  $\alpha$ -D-glucoside has had histochemical applications (Gossrau, 1977) and also in clinical chemistry in the detection of Pompe's disease (Fensom et al., 1976).

The *N*-acetyl- $\beta$ -D-glucosaminide (Figure 1.42) is a fluorogenic substrate for the enzyme *N*-acetyl- $\beta$ -glucosaminidase and this substrate has been used to assess the presence of fungi in soil (Miller et al., 1998) and also to measure the biomass of heterotrophic nanoplankton (Zubkov and Sleight, 1998).

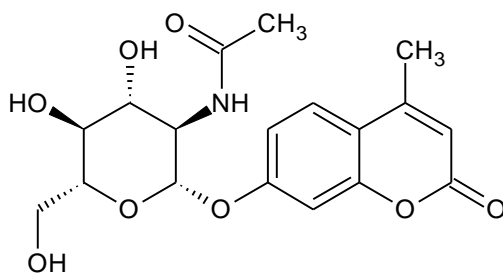


**Figure 1.42:** Structure of *N*-acetyl- $\beta$ -D-glucosaminide.

More complex substrates based on 4MU are known and quite widely available. For example, the  $\alpha$ -L-fucoside has been used for the identification of slow growing mycobacteria (Grange and McIntyre, 1979).

4MU phosphate has been used in many applications. Particularly important was the differentiation of mycobacterial strains by Grange (Grange, 1978). In fact, very many of the 4MU substrates have found application in the differentiation of groups of microorganisms and have been of great value in the taxonomic evaluation of these groups (Goodfellow et al., 1990).

### 1.5.6 7-Amino-4-methylcoumarins

Like the 4MU substrates, those based on 7-amino-4-methylcoumarins (7AMC) contain the coumarin nucleus and in fact 7AMC may be regarded as the amino analogue of 4MU (Figure 1.43). Due to the possession of the amino group it may give rise to substrates for a wide variety of peptidases, in particular aminopeptidases.

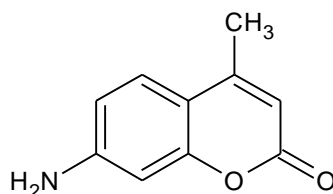


**Figure 1.43:** Structure of 7AMC

When hydrolysed, the 7AMC released gives a strong blue fluorescence similar to that of 4MU. Unlike 4MU, however, the fluorescence of the released 7AMC is not pH dependent, since the amino group is only ionised at very low pH outside of the physiological range. The fluorescence is strong and the substrate may be converted into a chromogenic form by addition of a reagent such as *p*-dimethylaminocinnamaldehyde to detect the released amine (Figure 1.44). This

gives a strong blue-violet colour and this has been applied to identify certain peptidases (Clark and McLauchlin, 1997).

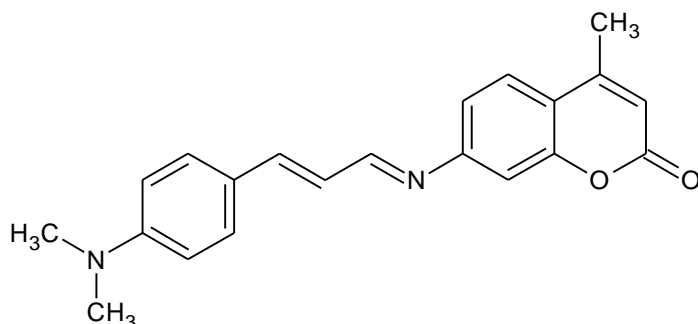


**Figure 1.44:** 7AMC *p*-dimethylaminocinnamaldehyde.

Both 7AMC and 4MU based substrates are well designed for use in microtitre wells. The use of these substrates is applicable to the scanning of a wide range of organisms as is necessary in taxonomic evaluations (Goodfellow, 1991 ).

Specific examples of the use of 7AMC based substrates include that of L-alanyl 7-amido-4-methylcoumarin (AAMC) (Figure 1.45), which is a fluorogenic substrate for aminopeptidase M, i.e. microsomal alanyl aminopeptidase. It is shown to be the major aminopeptidase from human skeletal muscle showing the highest activity with this substrate (Mantle et al., 1983).

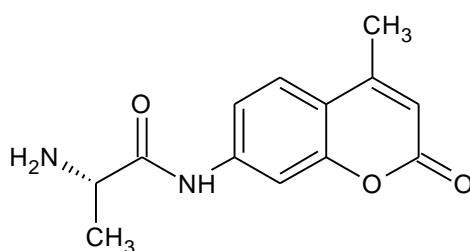


**Figure 1.45:** Structure of L-alanyl 7-amido-4-methylcoumarin.

AAMC has proved to be a reliable method to differentiate between Gram-positive and Gram-negative bacteria (Manafi and Kneifel, 1990). Only Gram-negative

bacteria have the necessary enzyme to cleave this substrate and therefore produce fluorescence.

More complex substrates based on AMC include <sup>1</sup>BOC-val-pro-arg-7-AMC, which is an effective substrate for thrombin, and this has been used haematologically in the evaluation of certain coagulation abnormalities (Enyedy and Kovach, 2004).

### 1.5.7 Phthaleins

Phthaleins are used as pH indicators, especially in titrations, as they can give dramatic colour changes. Phenolphthalein is colourless in acid or neutral conditions below pH 8.2 and bright pink to purple in basic conditions (Figure 1.46).

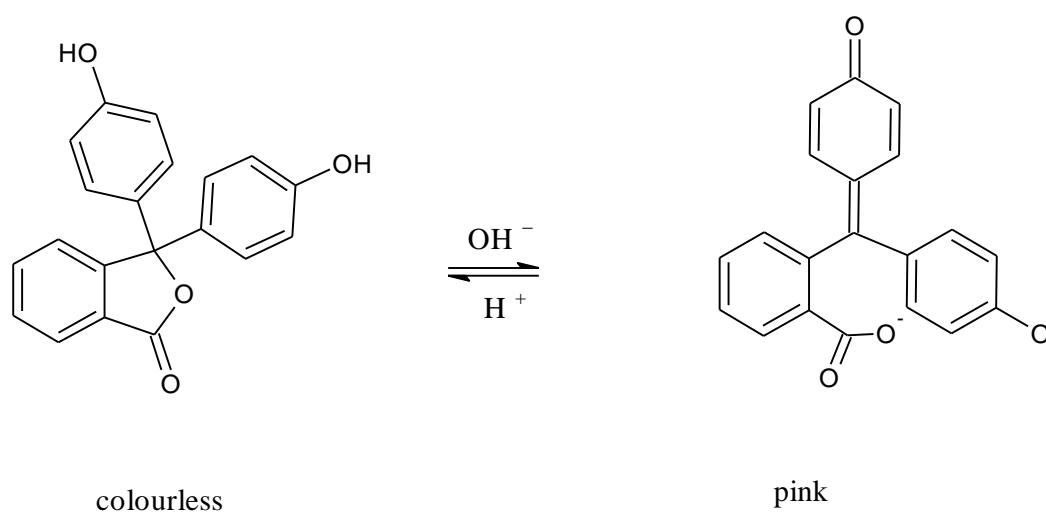


**Figure 1.46:** Phenolphthalein pH effect.

Phenolphthalein is used in the Kastle-Meyer forensic presumptive blood test. The test involves reducing phenolphthalein, by boiling in zinc powder, to phenolphthalin.

This colourless form is oxidised by the peroxidase-like activity of haemoglobin reacting with hydrogen peroxide to the pink form (Tobe et al., 2007).

Phenolphthalein is a core molecule for substrates such as  $\beta$ -D-glucuronide (Marsh and Reid, 1965; Tsukada and Yoshino, 1987) and phosphates (Babson et al., 1966). In humans, raised levels of  $\beta$ -glucuronidase has clinical significance as an indicator of such diseases as diabetes and pancreatic cancer (Schrecker and Chirigos, 1978). Phenolphthalein phosphates have been successfully used in automated procedures for serum alkaline phosphatase quantification (Comfort and Campbell, 1966) and in agar for the detection of phosphatase positive colonies of *Staphylococcus aureus* (MacFaddin, 2000).

Thymolphthalein has similar properties but differs by changing from colourless to blue at pHs above 9.5. This compound has also been used as a core molecule to determine phosphatase activity (Dalal et al., 1971).

### 1.5.8 Phenoxazines

Phenoxazines are highly coloured polycyclic ring structures (Figure 1.47).



**Figure 1.47:** Structure of phenoxazine.

Phenoxazines occur naturally in the polypeptide antibiotic actinomycins. These groups are rarely used as antibiotics nowadays due to their high toxicity and their ability to bind to and damage genetic material. Due to this affinity, actinomycin D,

and in particular a fluorescent variation known as 7-aminoactinomycin D, can be used as stains for DNA in the fields of flow cytometry and fluorescent microscopy (Rabinovitch et al., 1986).

Other compounds, such as cresyl violet (Figure 1.48) and Nile blue, contain a phenoxazine ring and are used as biological stains and textile dyes.

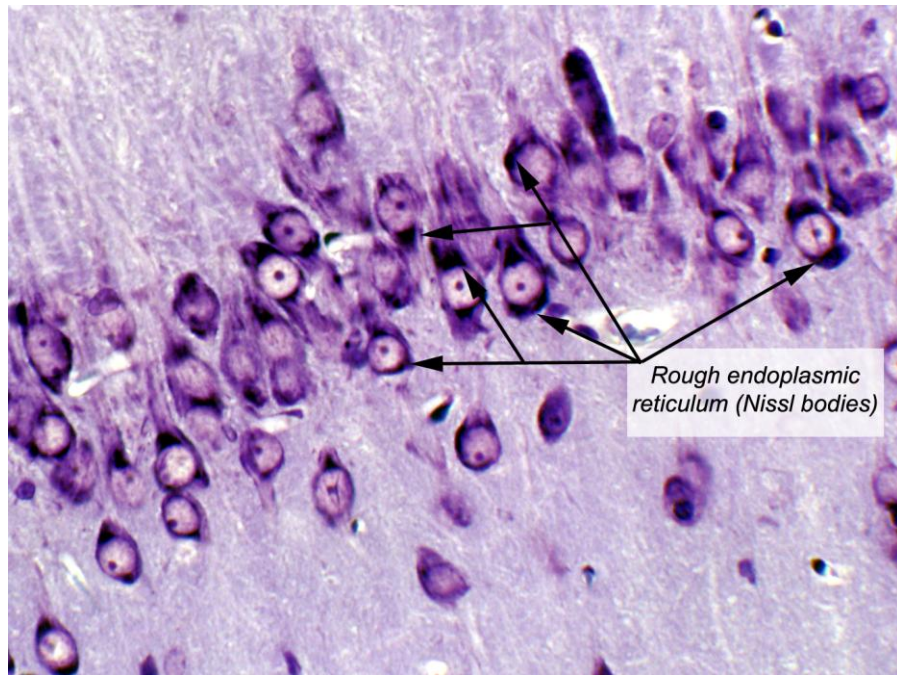


**Figure 1.48:** Cresyl violet stained neurons in the cerebellum. A basic stain commonly used to visualise nervous system tissues as it has a strong affinity for the acidic components of the neurons, especially those of rough endoplasmic reticulum. Picture courtesy of VetMed Resource.

A widely used phenoxazine system involves resazurin and two derivatives. Resazurin can be irreversibly reduced to resorufin which in turn can be reversibly reduced to dihydroresorufin (Figure 1.49).

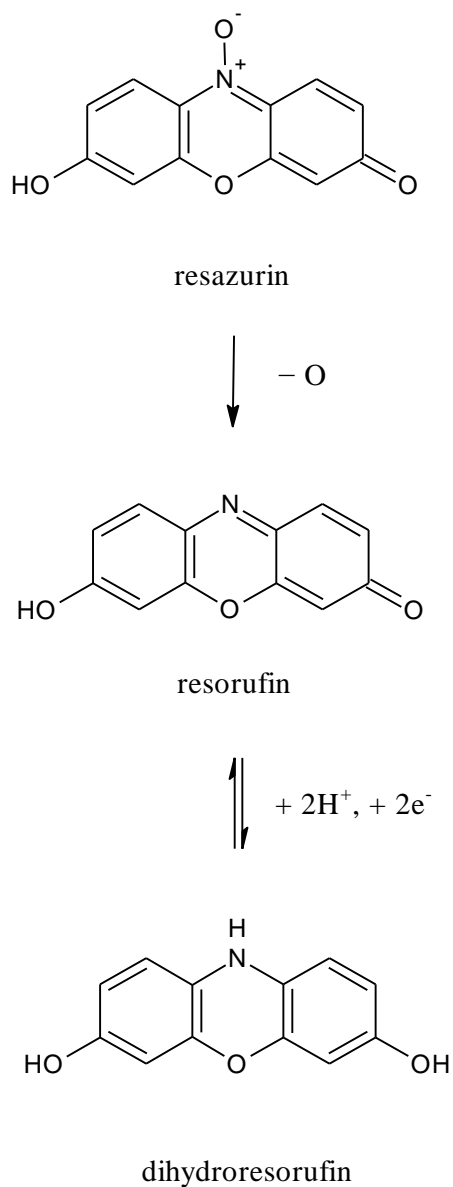


**Figure 1.49:** Reduction of resazurin to resorufin to dihydroxyresorufin.

Resazurin is purple in colour, resorufin is bright pink and fluorescent. Dihydroresorufin is colourless (Figure 1.50).



**Figure 1.50:** Colour contrast of resazurin (top) and resorufin (bottom).

Bacterial contamination in raw milk has been characterised by the reduction of resazurin (decrease in purple colour) by viable, metabolically active cells (reduction by microbial dehydrogenase enzymes generating NADH). The oxidation of dihydroresorufin (colourless→pink) is used as an indicator of oxygen contamination when culturing anaerobic bacteria. These colour differences also give scope for chromo and fluorogenic substrates.

Resorufin- $\beta$ -D-galactopyranoside (Wittrup and Bailey, 1988) and glucopyranoside (Hays et al., 1998) are both commercially available and have been used to assay their respective enzymes.

Resorufin acetate (Figure 1.51) has been used in studies of esterase activity (Kitson and Kitson, 1997).

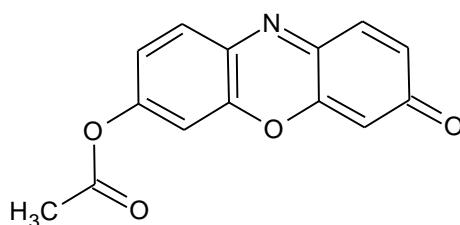


**Figure 1.51:** Structure of resorufin acetate.

There is also a series of ethoxyphenoxazine substrates (ethyl, pentyl and benzyl) that have been developed to investigate the mixed function oxidase, cytochrome P450, a prolific enzyme associated with metabolism and the breakdown of toxins (Figure 1.52) (Burke et al., 1985).

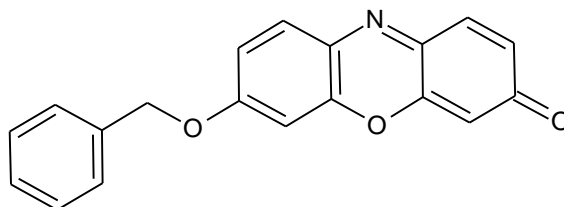


**Figure 1.52:** Structure of 7-benzyloxyresorufin.

Amplex Red (10-acetyl-3,7-dihydroxyphenoxazine) (Figure 1.53) is produced by Invitrogen as a phenoxazine substrate for oxidases. Oxidases are commonly tested for in microbiology as they are a natural by-product of oxygen metabolism. The purpose of the test is to differentiate bacteria that contain cytochrome c oxidase and can, via an electron transport chain, use oxygen for energy production.

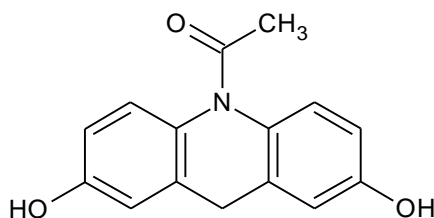


**Figure 1.53:** Structure of Amplex Red

Amplex Red was initially developed as a substrate to measure hydrogen peroxide (Zhou et al., 1997). During the reaction, the acetyl group is removed by the peroxidase in the presence of hydrogen peroxide leaving fluorescent resorfin. Amplex Red has been coupled to other enzyme reactions that produce hydrogen peroxide allowing sensitive assays for glucose (Kitazawa et al., 2007), galactose, cholesterol and phosphate. The mechanism for the coupled glucose assay is shown below (Figure 1.54), where the action of glucose oxidase produces hydrogen

peroxide which is then utilized by peroxidase in the creation of resorufin. The resulting oxygen by-product is then incorporated and the reaction cycle continues on.

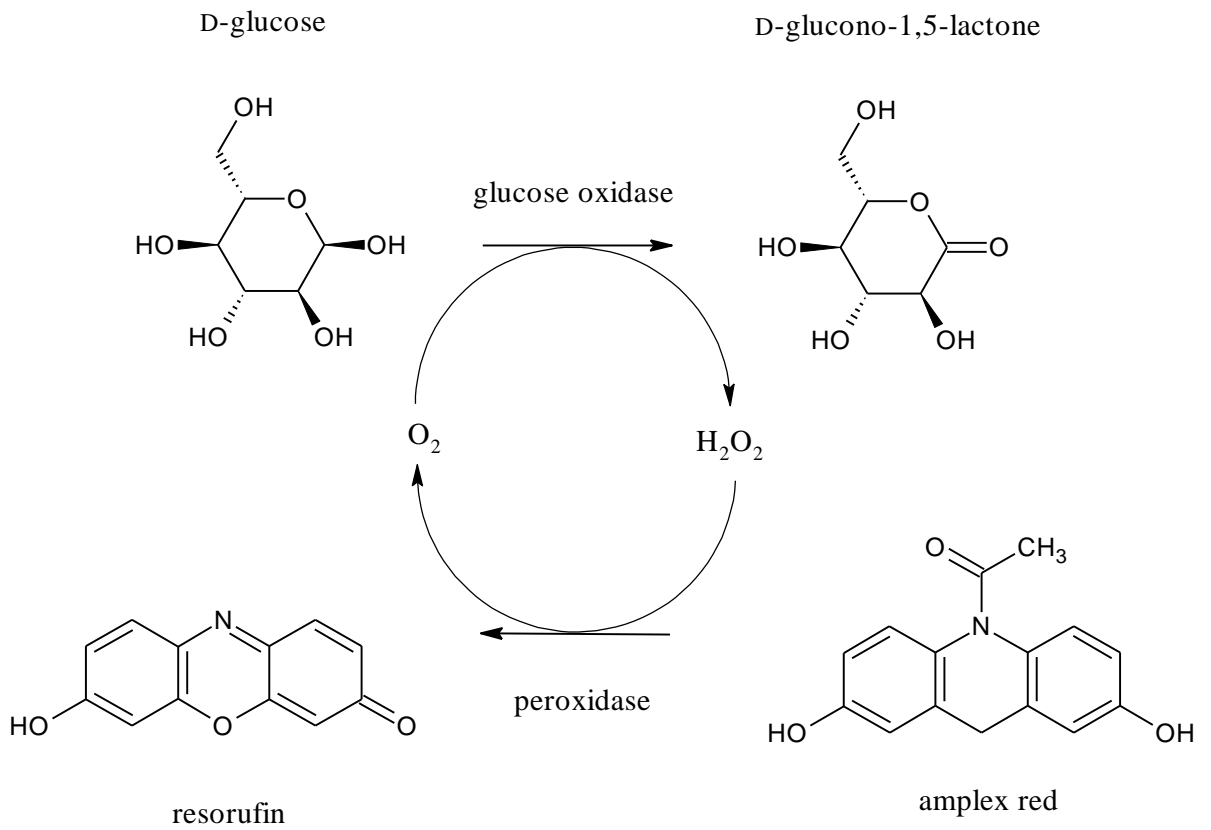
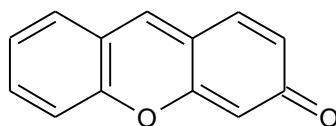


**Figure 1.54:** Amplex Red coupled to an assay for glucose.

### 1.5.9 Fluorones

Fluoresceins and rhodamines belong to a group of fluorescent compounds whose basic arrangement comprises of a fluorone ring structure (Figure 1.55).



fluorone

**Figure 1.55:** Fluorone ring structure.

Fluorescein or resorcinolphthalein, as it is also known, has a pka of 6.9 in acidic conditions, the lactone ring is closed but in alkaline conditions the lactone ring is open (Figure 1.56), pka changes to 6.4. In even higher alkalinity the carboxyl and hydroxyl groups are de-protonated resulting in greater fluorescence due to increased free electron movement.

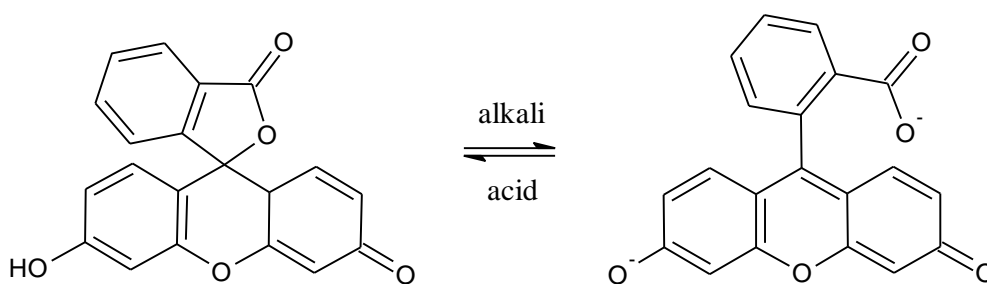
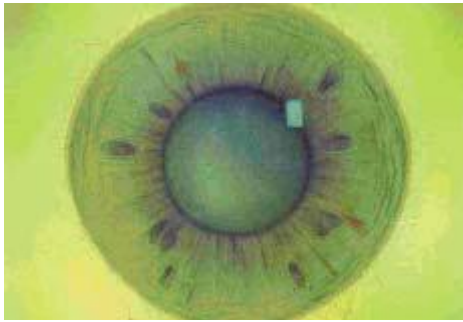
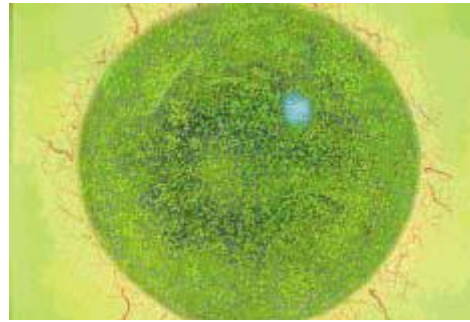


**Figure 1.56:** Fluorescein pH effect.

Fluorescein sodium dye is a standard ophthalmic test for corneal abrasions. A drop of dye solution is placed on the eye and fills any defects while the excess liquid is blinked away. The eye is then exposed to blue light at 490 nm which excites the dye causing it to fluoresce at 530 nm, revealing any imperfections (Figure 1.57) (Snyder, 2005).



No staining, not clinically significant



Severe staining, treatment required.

**Figure 1.57:** Corneal staining with fluorescein sodium (Snyder, 2005).

Eosin Y is a tetrabromo derivative of fluorescein (Figure 1.58) and is used in a number of histological staining techniques, the most commonly used being haematoxylin and eosin (H & E).

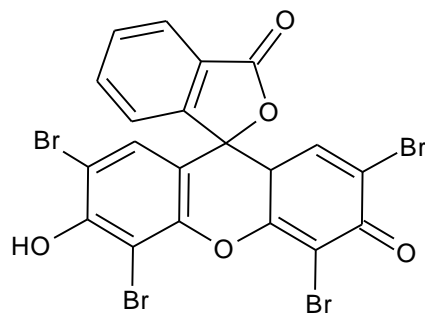


**Figure 1.58:** Structure of eosin Y.

Eosin is an acidic dye that binds to basic cell structures (usually proteins) such as cytoplasm. Haematoxylin is the opposite, being a basic dye that binds to acidic structures, e.g. nucleic acids (Figure 1.59).

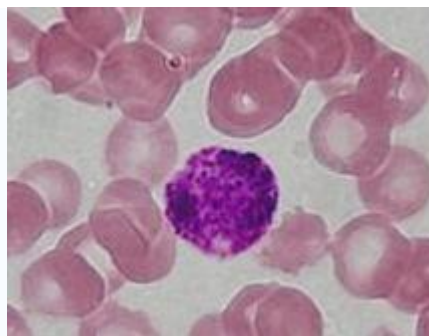


**Figure 1.59:** An example of haematoxylin and eosin staining. A basophil granulocyte surrounded by lightly staining eosinophilic erythrocytes in an H&E staining. Picture courtesy of the Department of Histology, Jagiellonian University Medical College.

Eosin diacetate (Figure 1.60), a fluorogenic substrate for lipases and esterases has been produced (Guilbault, 1966).

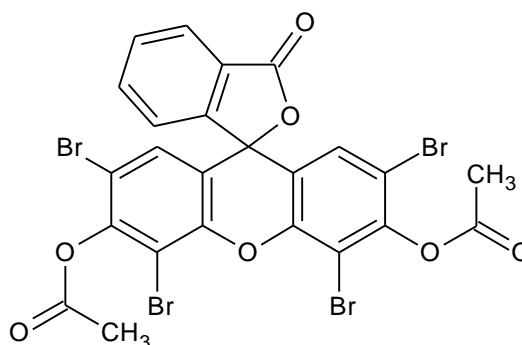
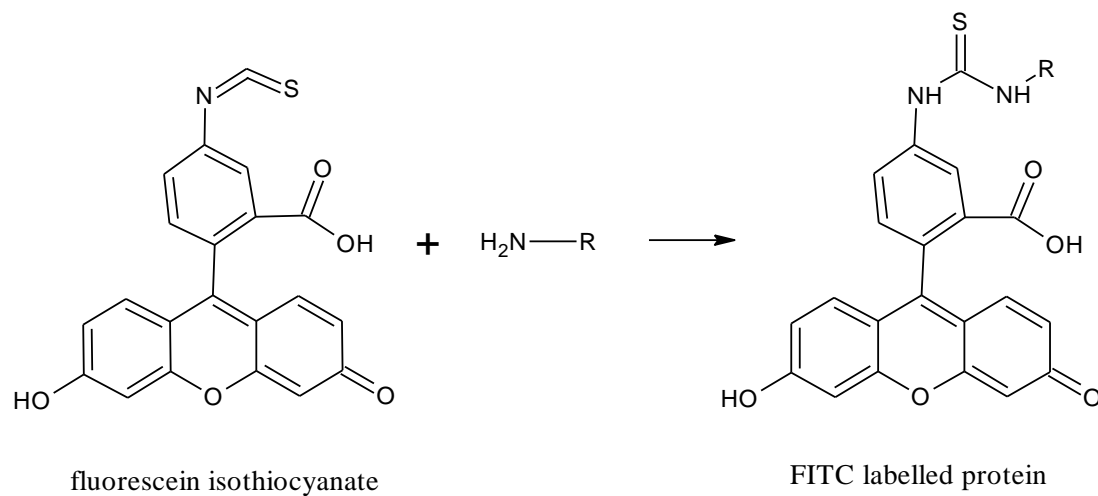


**Figure 1.60:** Structure of eosin diacetate.

Fluorescein isothiocyanate (FITC) is employed in techniques such as flow cytometry and immunofluorescence to label proteins, mainly antibodies. Its ability to bind to proteins is due to the isothiocyanate group which readily reacts with nucleophilic

amino groups on proteins to form a stable thiourea bond, known as a conjugation reaction (Figure 1.61 and 1.62) (Riggs et al., 1958).



where R = a protein

**Figure 1.61:** Conjugation reaction of fluorescein isothiocyanate.

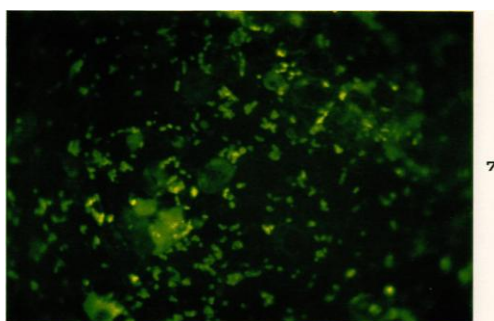


**Figure 1.62:** *Pasteurella tularensis* stained with anti-tularensis serum labeled with FITC (Riggs et al., 1958).

A number of substrates have been synthesised using fluorescein to measure enzyme activity. These include a galactopyranoside and a phosphate (Rotman et al., 1963). Also, lipases have been studied in soil using fluorescein diacetate (Green et al., 2006). Other fluorescein lipase substrates have been evaluated, e.g. dibutyrate and dilaurate (Ge et al., 2007).

Like fluorescein there are several rhodamine derivatives. Rhodamine B (Figure 1.63) is used as part of a staining technique in fluorescence microscopy for mycobacterium and other acid-fast bacteria. This auramine-rhodamine stain can also detect parasite oocysts, which would otherwise be difficult to identify using more traditional stains (Figure 1.64).

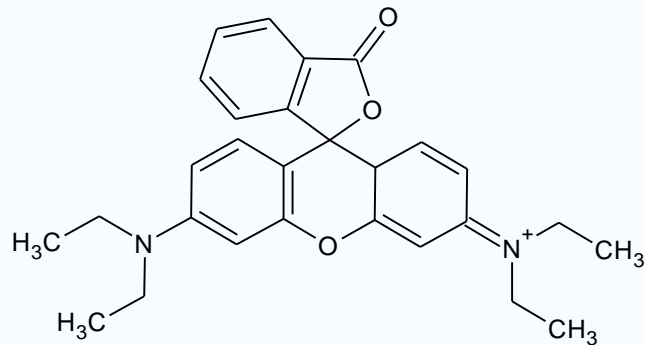


**Figure 1.63:** Structure of rhodamine B.

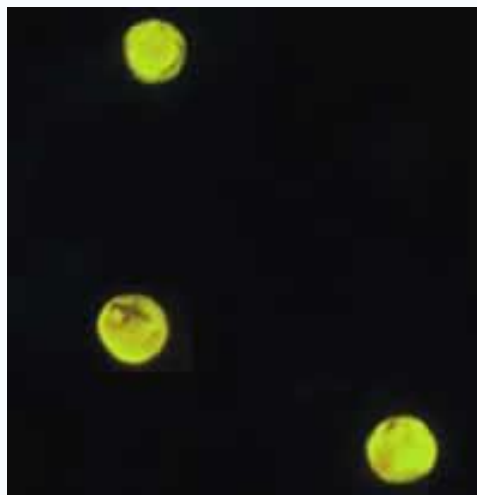


**Figure 1.64:** Oocysts of *Cryptosporidium parvum* stained with the fluorescent stain auramine-rhodamine. Picture courtesy of Centers for Disease Control, Division of Parasitic Diseases, U.S.A.

Like FITC, rhodamine isothiocyanate has been employed to label antibodies (Figure 1.65) (Riggs et al., 1958; Smith et al., 1962).

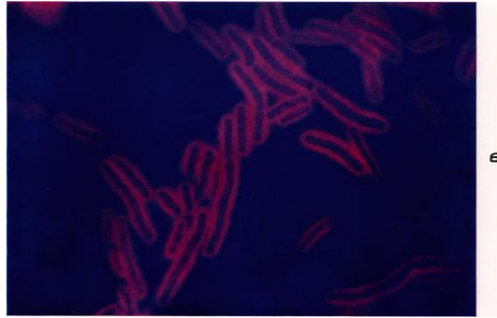
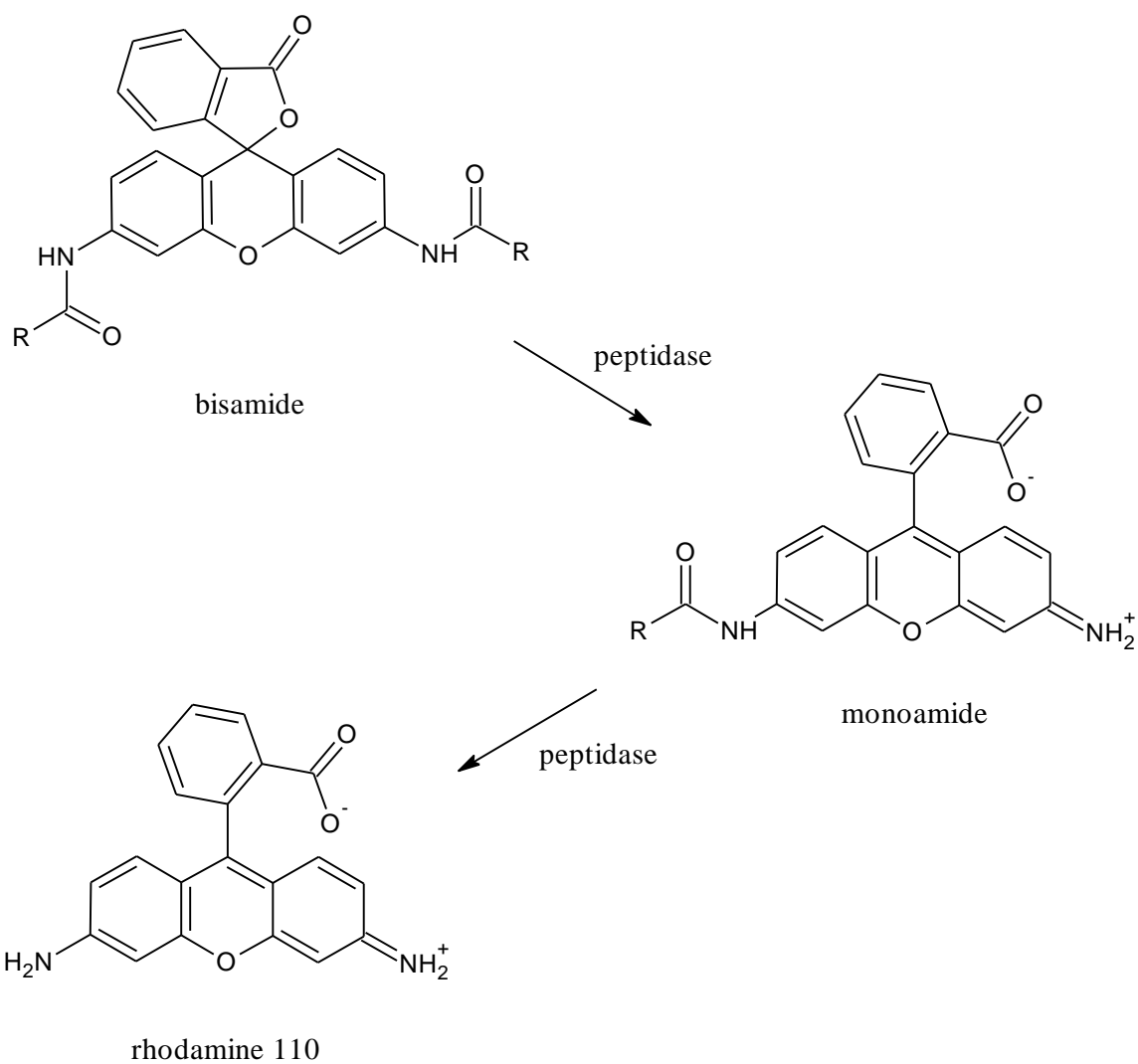


**Figure 1.65:** *Bacillus anthracis* stained with anti-rabbit serum labeled with rhodamine B ITC (Riggs et al., 1958).

A rhodamine 110 substrate has been developed by Invitrogen as a way to quantify specific peptidases (Leytus et al., 1983a; Leytus et al., 1983b). An amino acid or peptide is covalently bound to both of the amino groups on the rhodamine 110 molecule. This complex is known as a bisamide and, in this form, colour and fluorescence are subdued. The relevant peptidase enzyme removes the amino acids or peptides in two stages. The first converts the substrate into a monoamide, which is fluorescent. The second stage releases the highly fluorescent rhodamine 110 (Figure 1.66).



where R = an amino acid or peptide

**Figure 1.66:** Two stage removal of amino acids or peptides to produce highly fluorescent rhodamine 110.

## 1.6 Aims and objectives

The specific aim of this study was to produce novel glycosidase enzyme substrates and apply them to uses in biomedical science.

The specific objectives of this study are as follows:

- 1) To synthesise a range of chromogenic and fluorogenic core compounds.
- 2) To evaluate their suitability as chromophores and fluorophores and as metal chelators.
- 3) Attempt to glycosidate suitable core compounds.
- 4) Evaluate successful substrates with respect to applications in biomedical science.

## **CHAPTER TWO**

### **Chromogenic core molecules**

## 2.1 Introduction

Two classes of chromogenic core molecules can be distinguished. These are firstly, those prepared by the Knoevenagel condensation method and secondly, those prepared by a cyclisation reaction.

The Knoevenagel reaction, so named after the Russian chemist, Emil Knoevenagel, involves the condensation of a carbonyl compound, usually an aromatic aldehyde with a compound possessing an activated methylene group.

This methylene or CH<sub>2</sub> group is usually activated by one or two electron withdrawing groups, e.g. nitro, trifluoromethyl, carbonyl, etc. The effect of these electron withdrawing groups is to make it more likely for the CH<sub>2</sub> group to lose a proton and produce a carbanion, which then reacts with the electron deficient centre of the aromatic aldehyde thus generating a C=C double bond and creating, essentially, a styryl compound. This will be illustrated with the examples below.

- 4-nitrovinyl-2-methoxyphenol
- 4-nitrovinyl-2-methoxy-6-bromophenol
- 2-hydroxy-1-naphthaldehyde (commercial sample from Sigma)
- 1-nitrovinyl-2-naphthol
- 4-hydroxy-3-methoxybenzylidene-1,3-indandione
- 4-hydroxy-3-methoxycinnamylidene-1,3-indandione
- 4-acetoxy-3-methoxycinnamylidene-1,3-indandione
- 4-hydroxy-3-methoxycinnamylidene-3-phenyl-5-isoxazolone

In all of these reactions, to form the carbanion from the activated methylene group, it is necessary to add a base and the nature of the base will become apparent in a subsequent description of the methodology.

These next two examples did not involve a Knoevenagel condensation, but made use of the formation of a hydrazone group derived by condensation of the aldehyde with

a substituted phenylhydrazine. Such hydrazones can have intense colours and are used to identify aldehydes and ketones (Bartos and Pesez, 1979); they could therefore, in this particular case, act as core molecules for subsequent derivatisation.

- 2-hydroxy-1-naphthaldehyde-4-nitrophenylhydrazone
- 2-hydroxy-1-naphthaldehyde-2,4-dinitrophenylhydrazone

The final core molecule was synthesised by condensation of 1,6-dihydroxynaphthalene with phthalic anhydride using zinc chloride as condensing agent.

- Naphthofluorescein

### 2.2.1 Synthesis of 4-nitrovinyl-2-methoxyphenol

This compound had already been prepared several years ago (Milhazes et al., 2006), but its synthesis was undertaken again to gain experience in this type of Knoevenagel reaction.

This compound was made as a model for future Knoevenagel condensations.

Ammonium acetate (1.5 g, 20 mmol) and absolute ethanol (25 ml) were placed in a 100 ml conical flask and stirred until dissolved. Glacial acetic acid (1 ml) then 4-hydroxy-3-methoxybenzaldehyde (vanillin) (**2.2**), (1.52 g, 10 mmol) were added. After dissolving, nitromethane (**2.1**) (1.22 g, 20 mmol) was added and the solution left stirring at room temperature for 24 h. The reaction mixture was subject to vacuum filtration and the residue washed with ethanol chilled to 4 °C (30 ml). The residue was then dissolved in boiling ethanol and allowed to recrystallise by cooling on ice for 1 h. TLC in ethyl acetate showed a single spot. The 4-nitrovinyl-2-

methoxyphenol (**2.3**) crystals were dried in a vacuum desiccator (1.37 g, 70.2 % yield) (Figure 2.1).

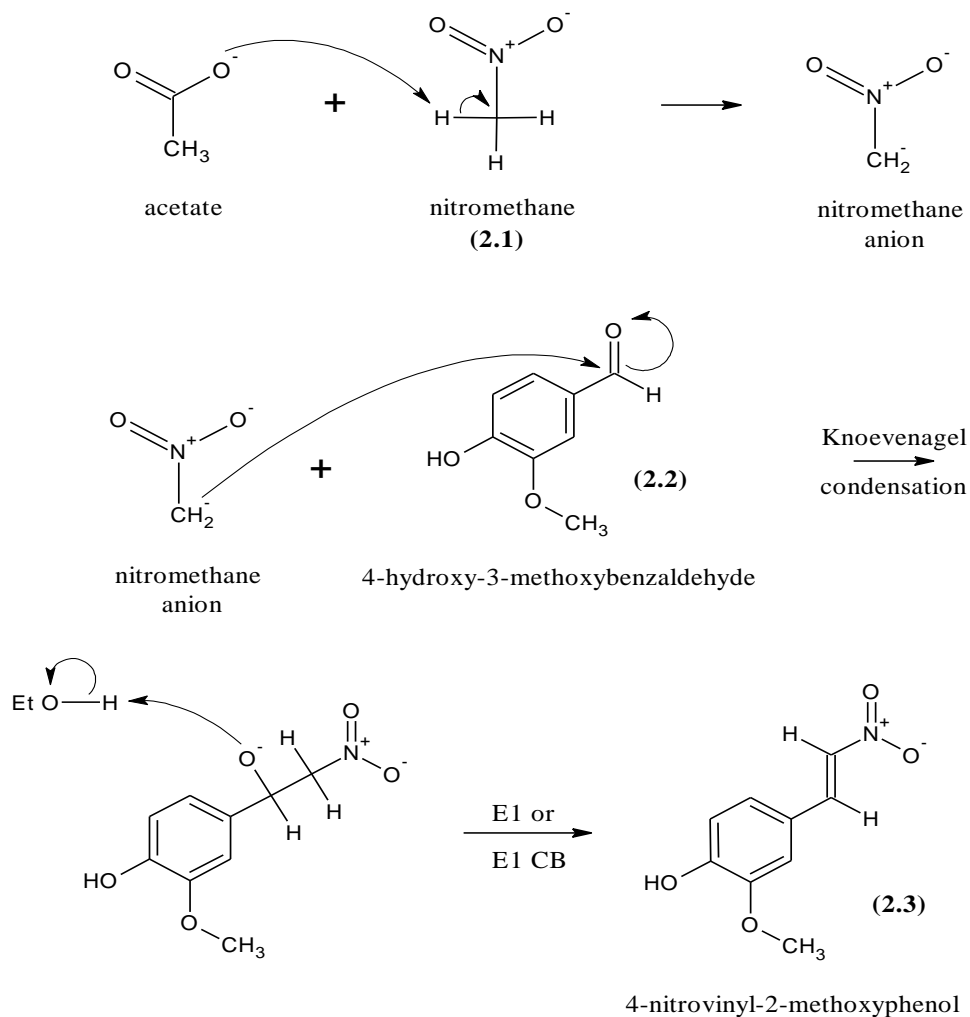


**Figure 2.1:** Acid catalysed formation of 4-nitrovinyl-2-methoxyphenol.

### Analytical data

Mp 169-171 °C (lit. 168-171 °C).

IR  $\nu_{\max}$   $\text{cm}^{-1}$ , 3464 (O-H), 1485, 1353 (N-O<sub>2</sub>).

<sup>1</sup>H-NMR (d<sub>6</sub>-DMSO, 270 MHz)  $\delta$  8.1(1H, d,  $J=13.6$  Hz, vinylicH), 8.0 (1H, d,  $J=13.4$  Hz, vinylicH), 7.5 (1H, d,  $J=2.0$  Hz, ArH), 7.3 (1H, d,  $J=8.2$  Hz, ArH), 6.8 (1H, d,  $J=8.2$  Hz, ArH), 3.8 (3H, om, CH<sub>3</sub>).

<sup>13</sup>C-NMR (d<sub>6</sub>-DMSO, 270 MHz)  $\delta$  152, 149, 141, 136, 127, 122, 116, 113, 56.

ESI-MS (M-H)<sup>-</sup> calculated/found; 194.17/194.12.

### Alternative method for 4-nitrovinyl-2-methoxyphenol

Piperidine (**2.4**) (0.85 g, 10 mmol) and 4-hydroxy-3-methoxybenzaldehyde (**2.2**) (1.52 g, 10 mmol) were placed in a 100 ml conical flask and stirred until dissolved. Nitromethane (**2.1**) (1.22 g, 20 mmol) was then added and the solution left stirring at room temperature for 24 h. The 4-nitrovinyl-2-methoxyphenol (**2.3**) was then purified as in the previous method (0.77 g, 39.5 % yield) (Figure 2.2).

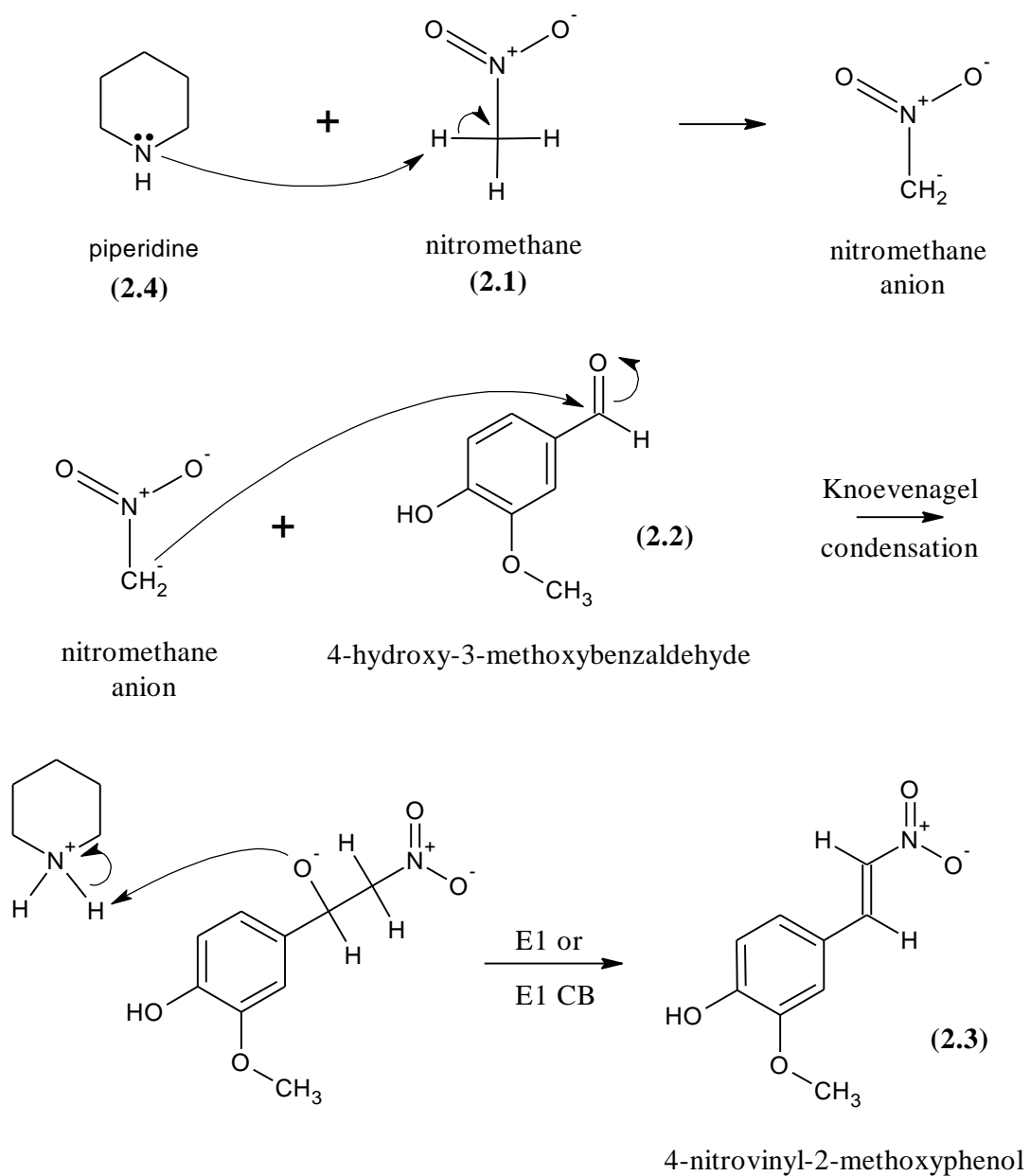


**Figure 2.2:** Base catalysed formation of 4-nitrovinyl-2-methoxyphenol.

## 2.2.2 Synthesis of 4-nitrovinyl-2-methoxy-6-bromophenol

This compound had been previously synthesised (Raiford, 1944) but repeated to illustrate the effect of a halogen atom suitably disposed in the aromatic nucleus and to study its effect on the colour and the pH dependence of this type of molecule.

It was synthesised as for 2.2.1, except 5-bromo-4-hydroxy-3-methoxybenzaldehyde (**2.4**) (2.31 g, 10 mmol) was used instead of 4-hydroxy-3-methoxybenzaldehyde. Yielded 2.29 g, 83.6 % of 4-nitrovinyl-2-methoxy-6-bromophenol (**2.6**) (Figure 2.3).

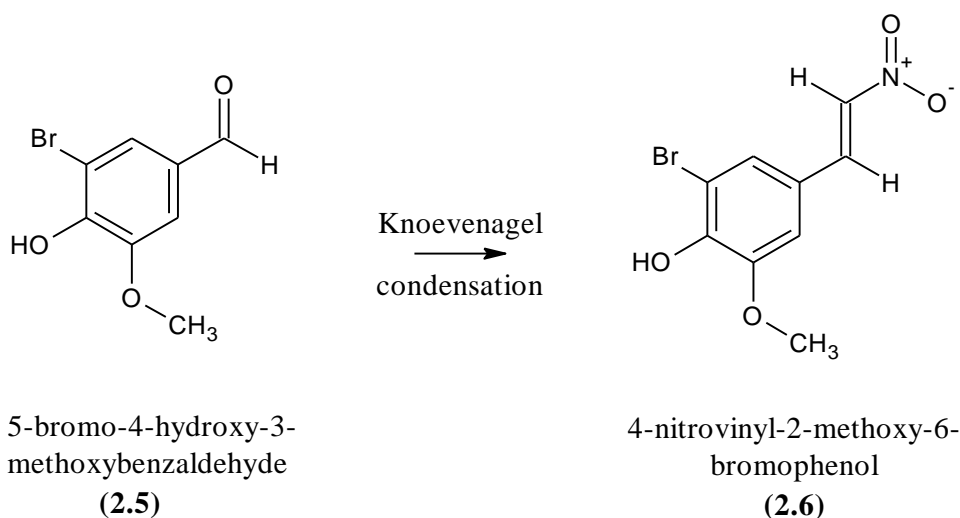


**Figure 2.3:** Formation of 4-nitrovinyl-2-methoxy-6-bromophenol.

### Analytical data

Mp 187-189 °C (lit. 190-191 °C).

IR  $\nu_{\max}$   $\text{cm}^{-1}$ , 3465 (O-H), 1488, 1350 (N-O<sub>2</sub>), 679 (C-Br).

<sup>1</sup>H-NMR (d<sub>6</sub>-DMSO, 270 MHz)  $\delta$  8.1(1H, d,  $J=13.6$  Hz, vinylicH), 8.0 (1H, d,  $J=13.4$  Hz, vinylicH), 7.6 (1H, d,  $J=7.9$  Hz, ArH), 7.2 (1H, d,  $J=6.4$  Hz, ArH), 3.8 (3H, om,CH<sub>3</sub>).

<sup>13</sup>C-NMR (d<sub>6</sub>-DMSO, 270 MHz)  $\delta$  151, 149, 140, 138, 129, 123, 116, 110, 57.

ESI-MS (M-H)<sup>-</sup> calculated/found; 273.07/274.16.

### 2.2.3 2-Hydroxy-1-naphthaldehyde

This core compound was investigated but was commercially available from Sigma.

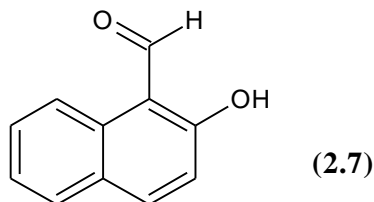


**Figure 2.4:** Structure of 2-hydroxy-1-naphthaldehyde.

### 2.2.4 Synthesis of 1-nitrovinyl-2-naphthol

This compound had been previously synthesised (Dauzonne and Royer, 1984). 1-nitrovinyl-2-naphthol (**2.8**) was synthesised as for 2.2.1 4-nitrovinyl-2-methoxyphenol, except the scale was doubled in size and 4-hydroxy-3-methoxybenzaldehyde was replaced with 2-hydroxy-1-naphthaldehyde (**2.7**) (3.44 g, 20 mmol). Yielded 3.6 g, 83.7 % of 1-nitrovinyl-2-naphthol (**2.8**) (Figure 2.5).

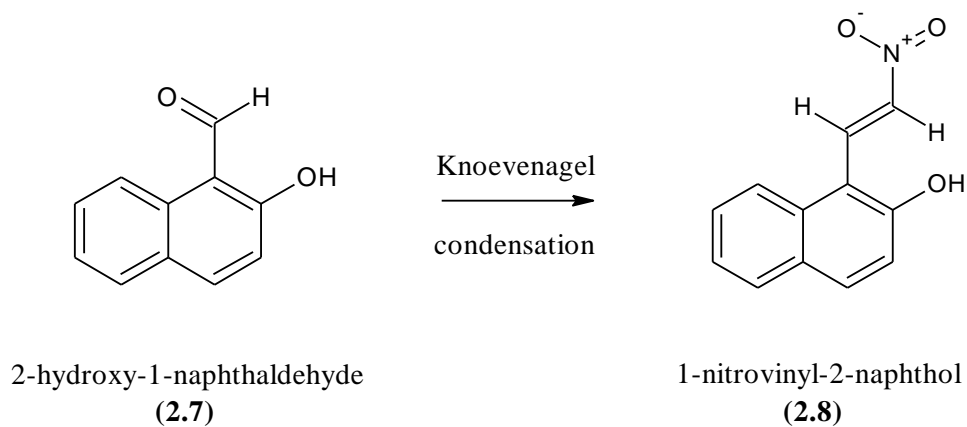


**Figure 2.5:** Formation of 1-nitrovinyl-2-naphthol.

### Analytical data

Mp 220-222 °C (lit. 224 °C).

IR  $\nu_{\max}$   $\text{cm}^{-1}$ , 3332 (O-H), 1510, 1355 (N-O<sub>2</sub>).

<sup>1</sup>H-NMR (d<sub>6</sub>-DMSO, 270 MHz)  $\delta$  8.2 (1H, d,  $J=8.4$  Hz, ArH), 7.8 (3H, t,  $J=9.4$  Hz, ArH), 7.6 (1H, t,  $J=7.5$  Hz, ArH), 7.4 (1H, t,  $J=7.5$  Hz, ArH), 7.0 (1H, d,  $J=8.9$  Hz, ArH), 6.7 (1H, d,  $J=3.0$  Hz, ArH).

### 2.2.5 Synthesis of 4-hydroxy-3-methoxybenzylidene-1,3-indandione

The indandione compounds were prepared by the Knoevenagel condensation since indandione contains an activated CH<sub>2</sub> group activated by two flanking carbonyl groups and this was considered to be a good choice for reaction. 4-hydroxy-3-methoxybenzylidene 1,3-indandione had been previously synthesised (Inayama et al., 1976).

4-Hydroxy-3-methoxybenzaldehyde (**2.2**) (0.76 g, 5 mmol) was dissolved in methanol (10 ml) in a 50 ml conical flask and stirred. To this 1,3-indandione (**2.9**) (0.73 g, 5 mmol) was added. After 5 min ammonium acetate (0.6 g, 8 mmol) dissolved in methanol (5 ml) with glacial acetic acid (1 ml). The solution was allowed to stand at room temperature for 1 h during which time precipitation occurred. The crystals were filtered under pressure then washed with 5 ml chilled (4 °C) methanol.

TLC in ethyl acetate showed only a single spot near the solvent front. The 4-hydroxy-3-methoxybenzylidene-1,3-indandione (**2.10**) crystals were dried in a vacuum desiccator (0.83 g, 59.3 % yield) (Figure 2.6).

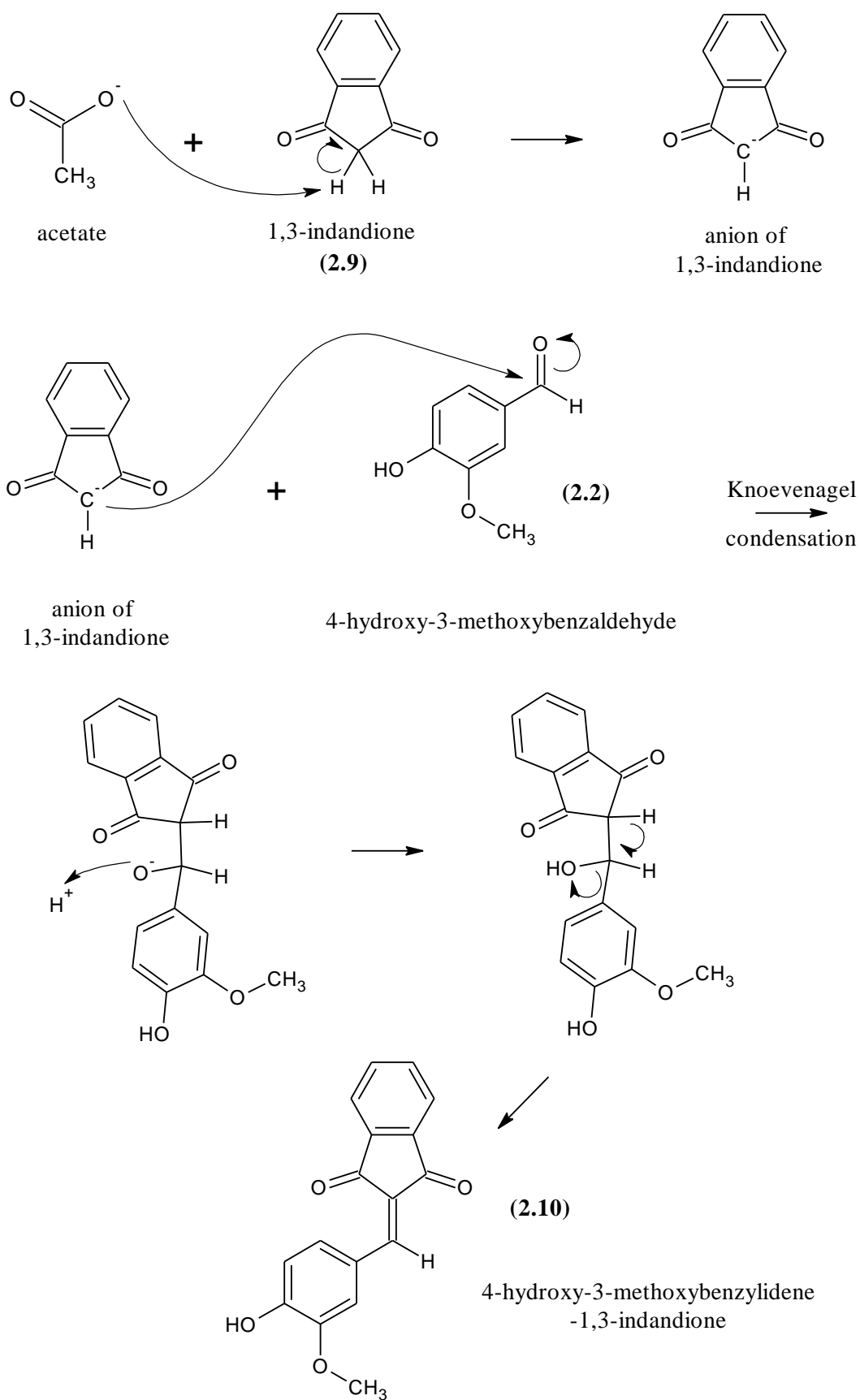


**Figure 2.6:** Formation of 4-hydroxy-3-methoxybenzylidene 1,3-indandione.

### Analytical data

Mp 211-213 °C (lit. 213-215 °C).

<sup>1</sup>H-NMR (d<sub>6</sub>-DMSO, 270 MHz) δ 8.7 (1H, s, ArH), 7.9-8.0 (4H, om, ArH), 7.8 (1H, s, ArH), 6.9 (1H, d, *J*=8.2 Hz, ArH), 3.9 (3H, s, CH<sub>3</sub>).

### **2.2.6 Synthesis of 4-acetoxy-3-methoxycinnamylidene-1,3-indandione**

This compound was synthesised as for 2.2.5 using 4-acetoxy-3-methoxycinnamaldehyde (**2.11**) (6.61 g, 30 mmol) and 1,3-indandione (**2.9**) (4.38 g, 30 mmol).

The product was purified by adding the crystals to stirred, boiling methanol (300 ml) in 500 ml conical flask. The solution was poured into a new flask, leaving any undissolved material behind and allowed to re-crystallize by cooling the flask on ice (0 °C) for 1 h. TLC in showed only a single spot near the solvent front. The 4-acetoxy-3-methoxycinnamylidene-1,3-indandione (**2.12**) crystals were dried in a vacuum desiccator (3.0 g, 48.4 % yield) (Figure 2.7).

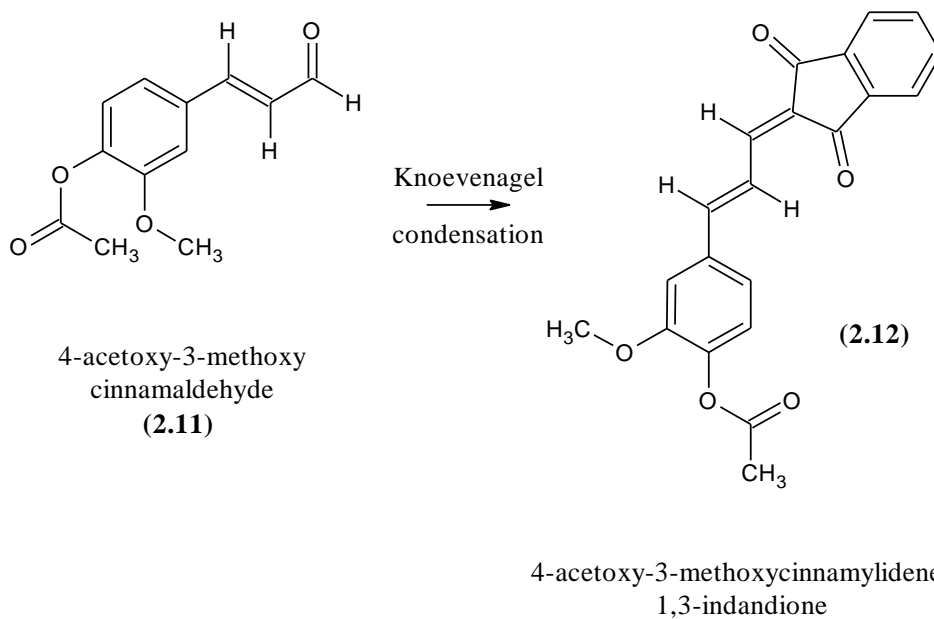


**Figure 2.7:** Formation of 4-acetoxy-3-methoxycinnamylidene-1,3-indandione.

#### Analytical data

Mp 180-182 °C.

IR  $\nu_{\max}$   $\text{cm}^{-1}$ , 1760, 1678 (C=O).

$^1\text{H-NMR}$  ( $d_6$ -DMSO, 270 MHz)  $\delta$  7.9 (5H, om, ArH), 7.6-7.8 (2H, dd,  $J_1=9.5$  Hz,  $J_2=8.0$  Hz, ArH), 7.4-7.5 (2H, om, ArH), 7.2-7.3 (2H, d,  $J=8.0$  Hz, ArH), 3.9 (4H, om, ArH + CH<sub>3</sub>).

$^{13}\text{C-NMR}$  ( $d_6$ -DMSO, 270 MHz)  $\delta$  195, 190, 189, 168, 153, 152, 151, 144, 142, 141, 136, 134, 133, 129, 128, 125, 124, 122, 113, 56, 21.

ESI-MS (M-H) calculated/found; 347.35/348.92.

HRMS (M+NH<sub>4</sub>) calculated/found; 366.3866/366.1341.

### 2.2.7 Synthesis of 4-hydroxy-3-methoxycinnamylidene-1,3-indandione

This compound had been previously synthesised (Inayama et al., 1976). 4-Hydroxy-3-methoxycinnamylidene-1,3-indandione (**2.14**) and was synthesised as for 2.2.5 except 4-hydroxy-3-methoxybenzaldehyde was replaced with 4-hydroxy-3-methoxycinnamaldehyde (**2.13**) (0.89g, 5mmol). Yielded 0.92 g, 60.1 % (Figure 2.8).

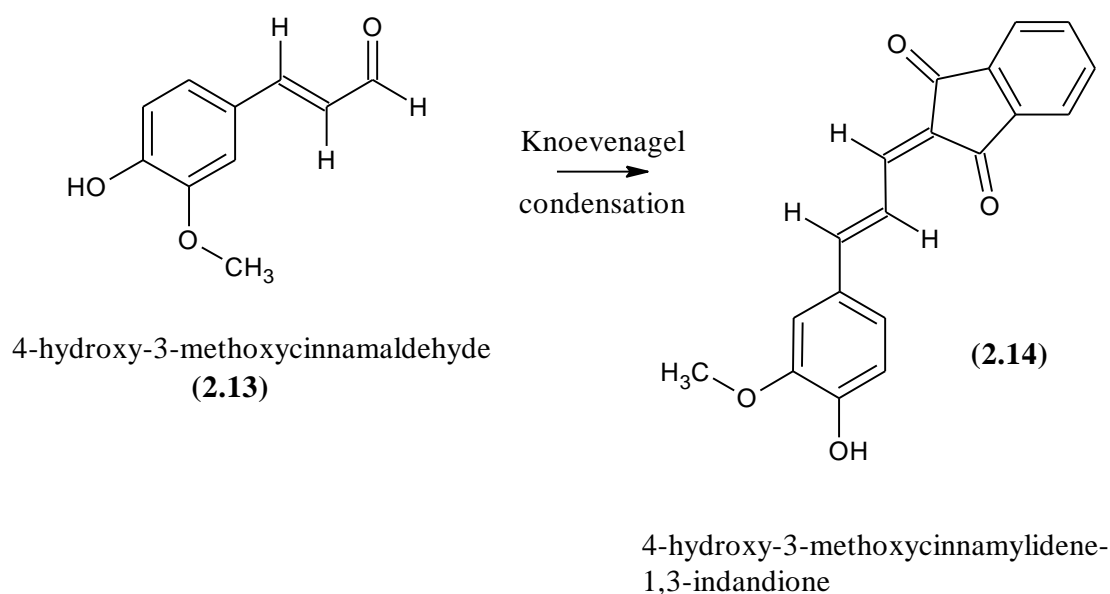


**Figure 2.8:** Formation of 4-hydroxy-3-methoxycinnamylidene-1,3-indandione.

#### Analytical data

Mp 225-227 °C (lit. 224-226 °C).

IR  $\nu_{\max}$   $\text{cm}^{-1}$ , 3216 (O-H), 1713, 1658 (C=O).

$^1\text{H-NMR}$  ( $\text{d}_6$ -DMSO, 270 MHz)  $\delta$  10.1 (1H, s, OH), 8.2 (1H, dd,  $J=11.9$  Hz,  $J=11.6$  Hz, ArH), 7.9 (4H, s, ArH), 7.6 (2H, om, ArH), 7.3 (2H, s + d,  $J=8.2$  Hz, ArH), 6.9 (1H, d,  $J=7.9$  Hz, ArH), 3.9 (3H, s,  $\text{CH}_3$ ).

$^{13}\text{C}$ -NMR ( $d_6$ -DMSO, 270 MHz)  $\delta$  191, 190, 154, 151, 149, 146, 142, 141, 136 (x2), 128, 126, 124, 123 (x2), 121, 117, 112, 56.

ESI-MS ( $\text{M-H}^-$ ) calculated/found; 305.31/305.16.

### 2.2.8 Synthesis of 4-hydroxy-3-methoxycinnamylidene-3-phenyl-5-isoxazolone

This is an analogous compound to the previously mentioned indandione but using 3-phenyl-5-isoxazolone (**2.15**) as the compound bearing the activated methylene group.

4-Hydroxy-3-methoxycinnamylidene-3-phenyl-5-isoxazolone (**2.16**) was synthesised as for 2.2.5 using 4-hydroxy-3-methoxycinnamaldehyde (**2.13**) (0.89 g, 5 mmol) and 3-phenyl-5-isoxazolone (0.80 g, 5 mmol). Yielded 1.2 g, 74.8 % (Figure 2.9).

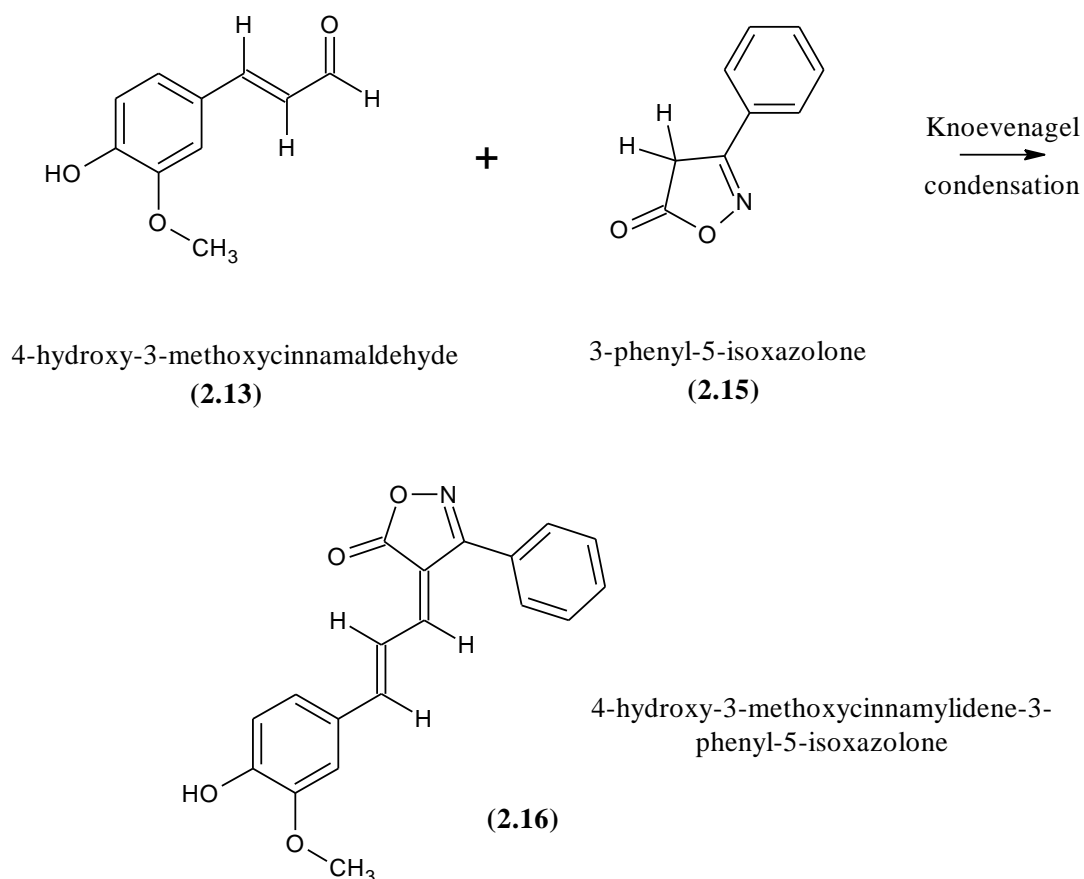


**Figure 2.9:** Formation of 4-hydroxy-3-methoxycinnamylidene-3-phenyl-5-isoxazolone.

### Analytical data

Mp 186-188°C

IR  $\nu_{\max}$   $\text{cm}^{-1}$ , 3407 (O-H), 1739, 1613 (C=O).

$^1\text{H-NMR}$  ( $\text{d}_6\text{-DMSO}$ , 270 MHz)  $\delta$  10.3 (1H, Broad s, OH), 8.1 (1H, dd,  $J_1=11.6$  Hz,  $J_2=11.4$  Hz, ArH), 7.2 + 7.5-7.8 (9H, om, ArH), 6.9 (1H, d,  $J=7.8$  Hz, ArH), 3.8 (3H, s,  $\text{CH}_3$ ).

$^{13}\text{C-NMR}$  ( $\text{d}_6\text{-DMSO}$ , 270 MHz)  $\delta$  171, 163, 156, 153, 152, 149, 131, 130 (x2), 129 (x2), 128, 127, 126, 120, 117, 113, 112, 56.

ESI-MS (M-H) calculated/found; 320.33/320.11.

HRMS (M-H) calculated/found; 320.3267/320.0922.

### **2.2.9 Synthesis of 2-hydroxy-1-naphthaldehyde-4-nitrophenylhydrazone**

2-Hydroxy-1-naphthaldehyde (**2.7**) (0.86 g, 5 mmol) was dissolved in ethanol (20 ml). 4-Nitrophenylhydrazine (**2.17**) (0.77 g, 5 mmol) was dissolved in ethanol (10 ml) with concentrated hydrochloric acid (5 ml) and water (10 ml). The two solutions were mixed and stirred for 10 min. The precipitate was filtered, washed with a 50% (v/v) mixture of ethanol and water (50 ml) then dried. 2-hydroxy-1-naphthaldehyde-4-nitrophenylhydrazone (**2.18**) was recrystallised from hot ethanol (20ml). Yield 0.8 g, 52.1 % (Figure 2.10).

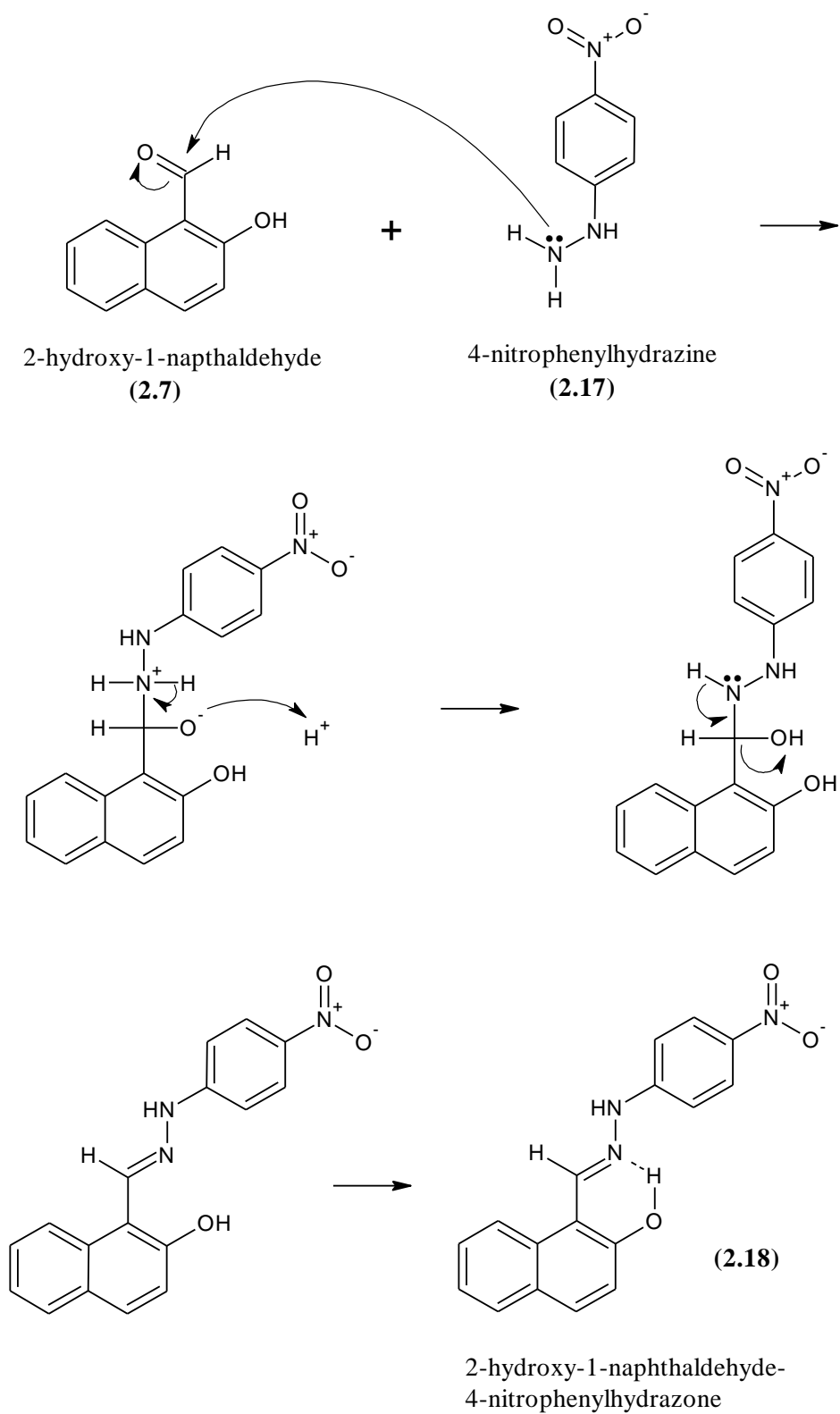


**Figure 2.10:** Formation of 2-hydroxy-1-naphthaldehyde-4-nitrophenylhydrazone.

### Analytical data

Mp 249-251 °C.

IR  $\nu_{\max}$   $\text{cm}^{-1}$ , 3290 (O-H), 1590 (C=N), 1476, 1300 (N-O<sub>2</sub>).

<sup>1</sup>H-NMR (d<sub>6</sub>-DMSO, 270 MHz)  $\delta$  11.4 (1H, s, ArH), 11.2 (1H, s, ArH), 9.0 (1H, s, ArH), 8.8 (1H, d,  $J=8.2$  Hz, ArH), 8.2 (2H, d,  $J=9.4$  Hz, ArH), 7.9 (2H, d,  $J=8.7$  Hz, ArH), 7.6 (1H, t,  $J=7.8$  Hz, ArH), 7.4 (1H, t,  $J=7.4$  Hz, ArH), 7.2 (1H, d,  $J=8.9$  Hz, ArH), 7.1 (2H, d,  $J=9.2$  Hz, ArH).

<sup>13</sup>C-NMR (d<sub>6</sub>-DMSO, 270 MHz)  $\delta$  157, 151, 142, 139, 133, 132, 130, 129, 128, 127 (x2), 124, 123, 119, 112 (x2), 111.

ESI-MS (M-H)<sup>-</sup> calculated/found; 306.30/306.11.

HRMS (M+H) calculated/found; 308.3034/308.1034.

#### **2.2.10 Synthesis of 2-hydroxy-1-naphthaldehyde-2,4-dinitrophenylhydrazone**

This compound had been previously synthesised (Ibanez et al., 2002). 2-hydroxy-1-naphthaldehyde-2,4-dinitrophenylhydrazone (**2.20**) was synthesised as for 2-hydroxy-1-naphthaldehyde-4-nitrophenylhydrazone but 4-nitrophenylhydrazine was replaced with 2,4-dinitrophenylhydrazine (**2.19**) (0.99 g, 5 mmol). Yield 1.42 g, 80.7 % (Figure 2.11).

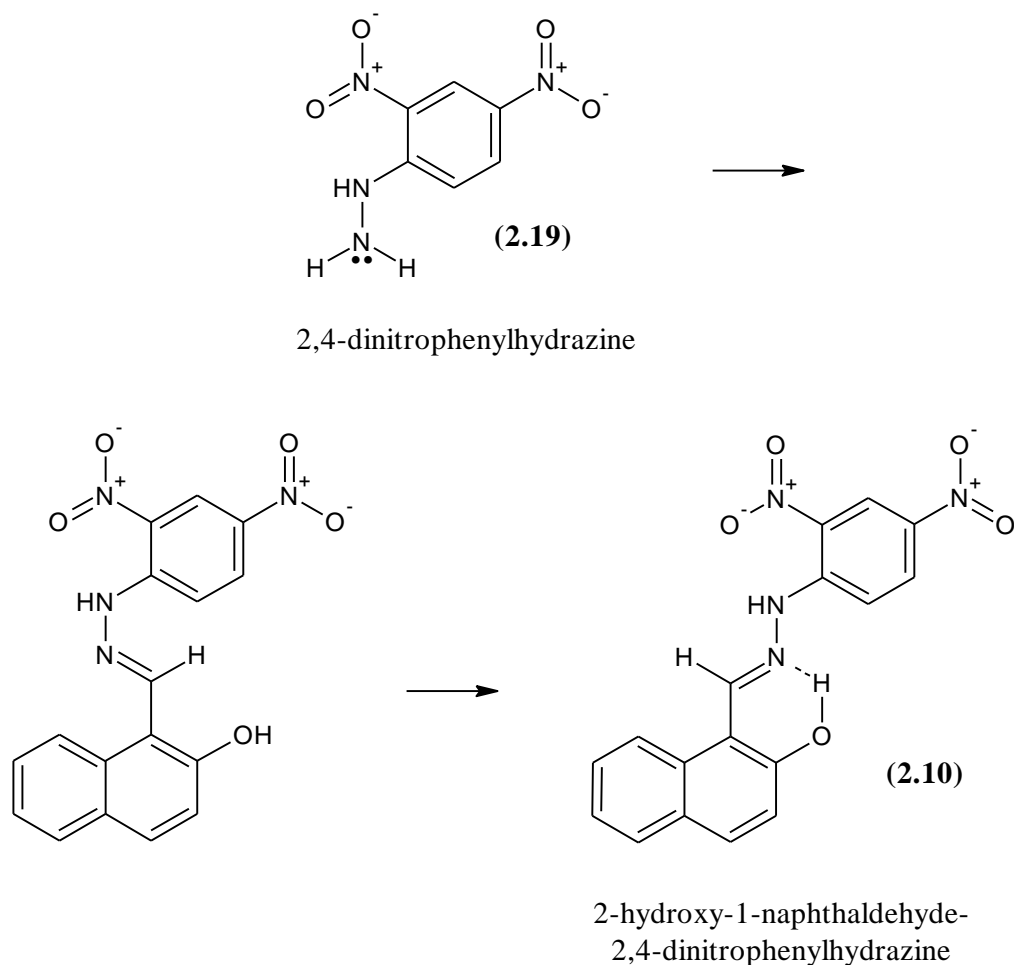


**Figure 2.11:** Formation of 2-hydroxy-1-naphthaldehyde-2,4-dinitrophenylhydrazone.

#### Analytical data

Mp 290-292 °C (lit. not stated)

IR  $\nu_{\max}$   $\text{cm}^{-1}$ , 3274 (O-H), 1586 (C=N), 1511, 1322 (N-O<sub>2</sub>), 1498, 1266 (N-O<sub>2</sub>).

<sup>1</sup>H-NMR (d<sub>6</sub>-DMSO, 270 MHz)  $\delta$  11.6 (1H, s, ArH), 11.3 (1H, s, ArH), 9.5 (1H, s, ArH), 8.8 (1H, d,  $J=8.1$  Hz, ArH), 8.3 (2H, d,  $J=9.1$  Hz, ArH), 7.9 (2H, d,  $J=8.4$  Hz, ArH), 7.6-7.7 (1H, om, ArH), 7.4 (1H, t,  $J=7.0$  Hz, ArH), 7.2 (1H, d,  $J=9.1$  Hz, ArH).

<sup>13</sup>C-NMR (d<sub>6</sub>-DMSO, 270 MHz) – Spectrum too weak for analysis.

ESI-MS (M-H) calculated/found; 351.30/351.11.

HRMS (M-H) calculated/found; 351.3010/351.0725.

### 2.2.11 Synthesis of naphthofluorescein

This molecule, although already known (Fischer, 1914), appeared to have desirable characteristics both to act as a pH indicator and to form enzyme substrates e.g. glycosides. The core molecule was synthesised by condensation of 1,6-dihydroxynaphthalene (**2.21**) with phthalic anhydride using zinc chloride as condensing agent.

1,6-dihydroxynaphthalene (3.2 g, 20 mmol) and phthalic anhydride (**2.22**) (1.5 g, 10 mmol) were intimately mixed with fused zinc chloride (2.7 g, 20 mmol) and heated in a hard glass boiling tube in an oil bath at 120 °C for 3 h with occasional stirring using a glass rod. After cooling, the solid melt was removed by breaking the tube and subsequently ground in a pestle and mortar. The powder was extracted by stirring with excess warm sodium hydroxide (2 M). The deep blue solution was filtered and the stirred solution was acidified to ~ pH 3 using HCl (2 M). The flocculent red precipitate of undissociated naphthofluorescein (**2.23**) was removed by suction filtration and washed with more HCl (2 M) and then with distilled water. The dried product was difficult to recrystallise and hence was purified by redissolving in alkali followed by acidification as previously described. Yield 2.8 g, 32.4 % (Figure 2.12).

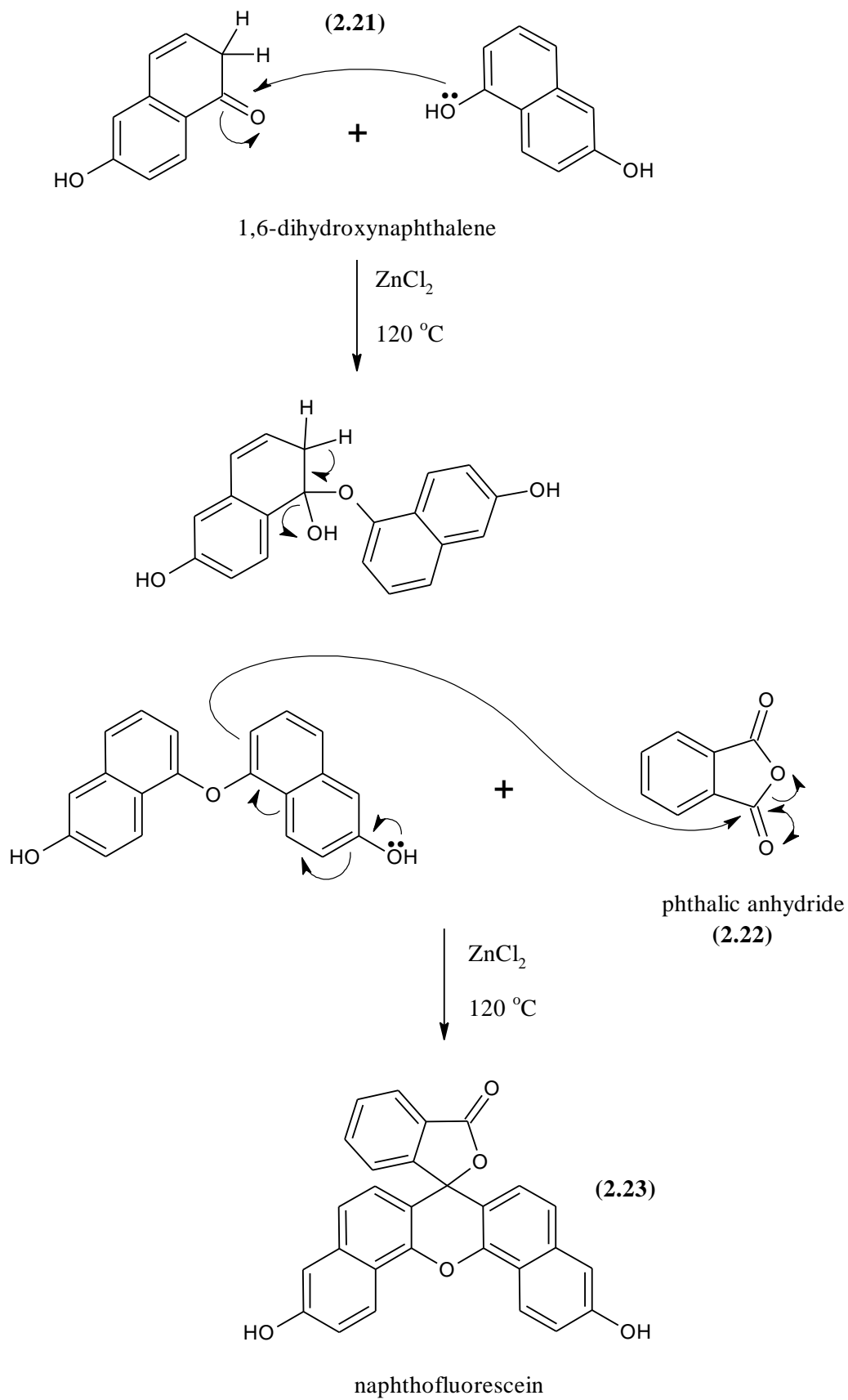


**Figure 2.12:** Formation of naphthofluorescein.

Analytical data

Mp 190-192 °C (lit. 189 °C)

<sup>1</sup>H-NMR (d<sub>6</sub>-DMSO, 270 MHz) δ 10.2 (2H, s, OH), 8.7 (2H, d, *J*=8.9 Hz, ArH), 7.8 (2H, om, ArH), 7.4 (2H, d, *J*=8.7 Hz, ArH), 7.3 (2H, d, *J*=9.4 Hz, ArH), 7.2 (2H, s, ArH), 6.7 (2H, d, *J*=8.9 Hz, ArH).

### 2.3 Results

The majority of compounds synthesised showed strong colouration especially on the alkaline side of neutrality. This is, of course, not surprising, since a hydroxy group is present in them all and the hydroxyl group is capable of ionisation. Consequently, colours were recorded across the pH range and absorption spectra were measured.

The core compounds (100 mg/L) were dissolved in 50% (v/v) ethanol/water and the pH adjusted with either HCl (0.2 M) or NaOH (0.2 M). When appropriate, the compounds were observed under U.V. light (~350 nm) and any fluorescence was recorded (Table 2.1).

**Table 2.1:** Colour change of synthesised core compounds due to varying pH.

Core compound	pH					
	3	5	7	9	11	13
4-nitrovinyl-2-methoxyphenol						
4-nitrovinyl-2-methoxy-6-bromophenol						
1-nitrovinyl-2-naphthol						
2-hydroxy-1-naphthaldehyde						
4-hydroxy-3-methoxybenzylidene-1,3-indandione						
4-hydroxy-3-methoxycinnamylidene-1,3-indandione						
4-acetoxy-3-methoxycinnamylidene-1,3-indandione						
4-hydroxy-3-methoxycinnamylidene-3-phenyl-5-isoxazolone						
2-hydroxy-1-naphthaldehyde-4-nitrophenylhydrazone						
2-hydroxy-1-naphthaldehyde-2,4-dinitrophenylhydrazone						
naphthofluorescein						
naphthofluorescein under U.V.						
<i>p</i> -naphtholbenzein						

Spectrum scans from 300 to 700 nm were recorded at each pH using a Biotek Synergy multi-detection microplate reader. A representative sample of these can be seen below in Figures 2.13 and 2.14 (others appear in Appendix B).

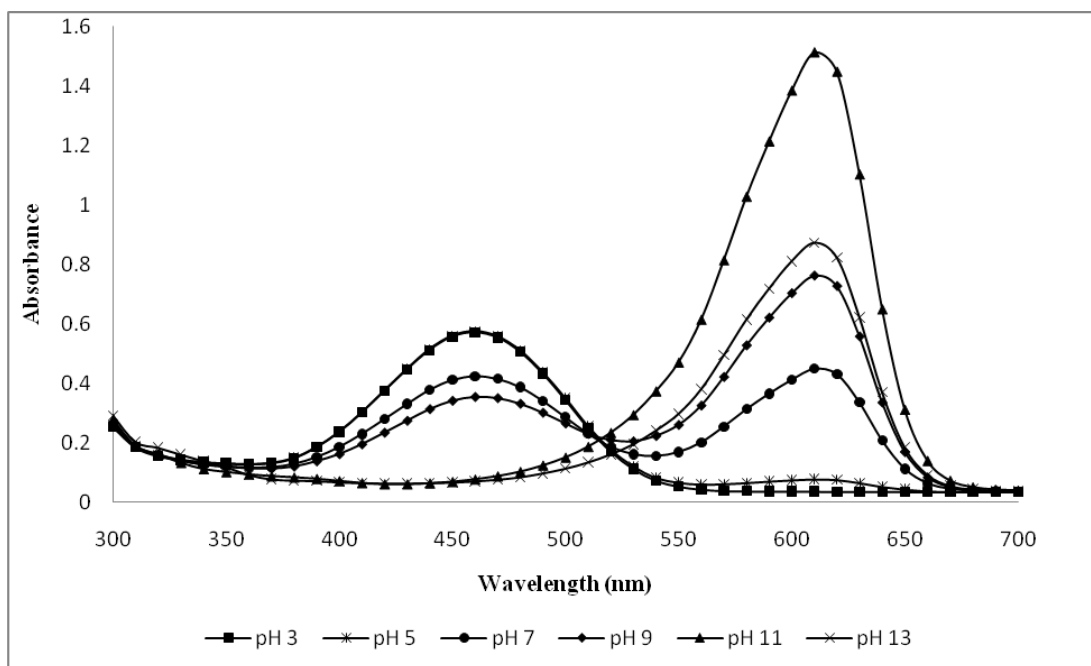


**Figure 2.13:** Spectrum scan of 4-hydroxy-3-methoxycinnamylidene-1,3-indandione.

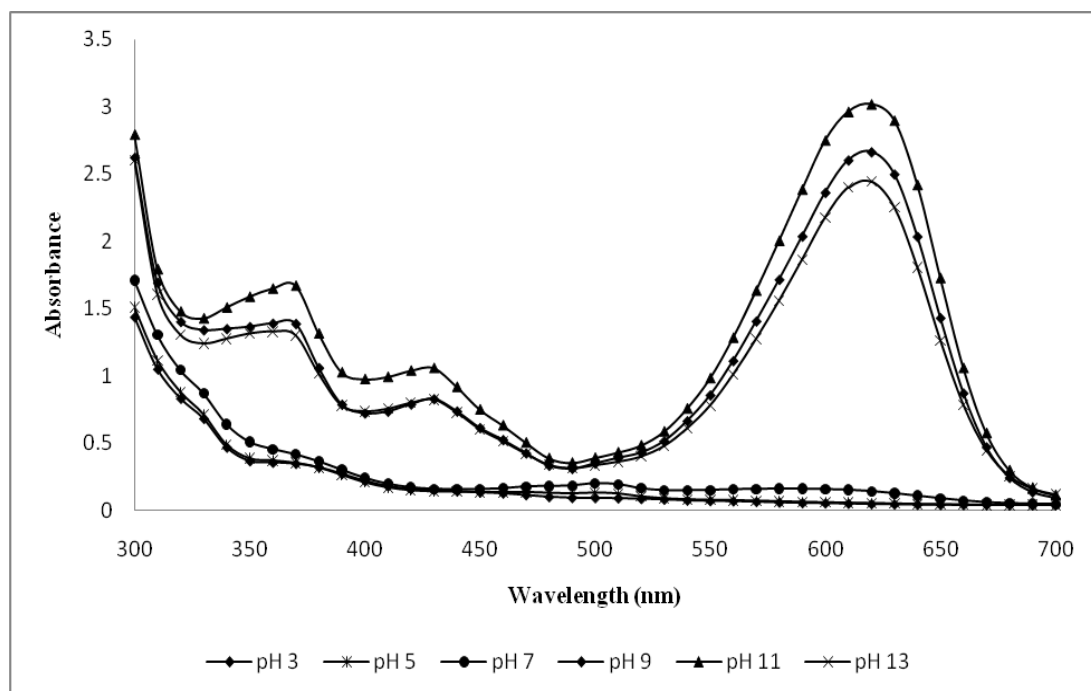


**Figure 2.14:** Spectrum scan of naphthofluorescein.

## 2.4 Discussion

The results indicate that many of these compounds have the capacity to be used as pH indicators, e.g. in bacterial identification by alkalisiation reactions, such as decarboxylase or urease activity.

A more complete analysis, however, would be necessary before this could be applied in a practical microbiological situation. The change in coloration and spectra, which is dependent on pH, also indicated that if the hydroxyl group was protected, as in fact would be the case in glycosidation, then the colour could be markedly reduced and such glycosides should therefore be capable of acting as substrates for the appropriate glycosidase, since cleavage of the glycoside group would restore the hydroxyl function and restore the colour of the original chromogen.

Consequently, several of these compounds were subject to glycosidation and the results of this are given later, in the appropriate section.

## **CHAPTER THREE**

### **Chelating core molecules**

### 3.1 Introduction

In this section, as well as the novel compounds synthesised, several commercially available chelators, such as alizarin, have been included for subsequent glycosidation or other method of derivatisation.

The term chelation is used to describe the process by which structures possessing certain groups, which usually are electron rich and spatially adjacent or proximate, react with metal ions, thereby giving stable complexes. The types of ions involved are usually those of the transition elements i.e. iron, cobalt, nickel, zinc, manganese, copper, etc, and also the rare earth metals, such as lanthanum, cerium and europium. However, other multivalent ions may also chelate, especially if these are highly electron deficient and have a strong multivalent positive charge, e.g.  $\text{Al}^{3+}$ , where an appropriate ion affinity exists. Even ions like  $\text{Mg}^{2+}$  can chelate under appropriate circumstances. An example would be 8-hydroxyquinoline (8HQ) which forms a stable and highly fluorescent magnesium complex involving two molecules of 8HQ. 8-Hydroxyquinoline-5-sulphonic acid has been proposed as a reagent for the determination of low concentrations of magnesium in serum by fluorescence (Zhu and Kok, 1998).

The chelates so formed are frequently highly coloured due to electronic transitions. This is particularly so with the transition elements. In addition, the chelates are often insoluble in aqueous media due to the association of two or more chelating molecules with one metal ion, e.g.  $\text{Fe}^{2+} \cdot 2\text{CHE}$  (Figure 3.1). This has considerable importance in the creation and design of chelating substrates for use in agar plate methodology for use in microbial identification protocols (James et al., 1996).

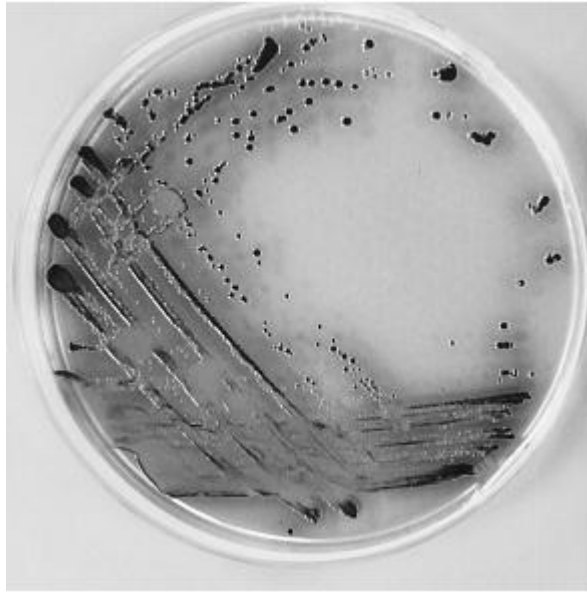


**Figure 3.1:** Hydrolysis of CHE-Gal by *E. coli* in the presence of iron (II) (James et al., 1996).

Often a metal chelate exhibits a dark coloration (black or dark brown) which can be observed in the colonies above. However, some chelating agents give rise to highly coloured metal chelates and the colour frequently depends on the metal ion which is present. A suitable example would be alizarin, which gives a deep purple iron chelate, a deep red aluminium chelate (James et al., 2000b) and also various colours with other metals, such as chromium and tin, etc (Figure 3.2).

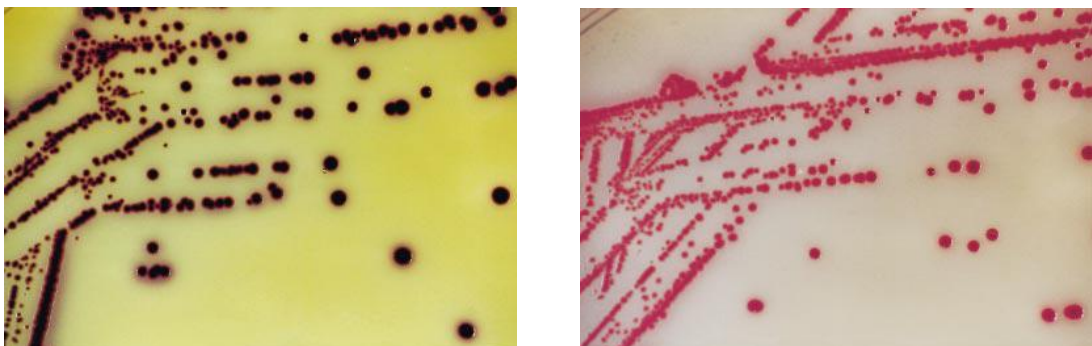
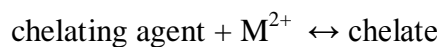


**Figure 3.2:** Colonies of *E. coli* showing hydrolysis of alizarin- $\beta$ -D-galactoside in the presence of ferric ions (left) and aluminium ions (right) (James et al., 2000b).

One important feature of metal chelates is the stability constant. This defines the tendency of the chelate to dissociate into its component parts. The general formula would be:



If the chelate is very stable, the dissociation constant will be very low, for example frequently in the order of  $10^{-20}$ ,  $10^{-30} \text{ M}^{-1}$ .

For microbiological identification purposes it is desirable to have a very stable chelate because if the chelate tends to dissociate and produce more of the free chelating agent then spreading of the colour is likely to be observed on the agar plate (Figure 3.3).



**Figure 3.3:** Aliz-gal with lanthanum nitrate spreading.

This same order of magnitude of the dissociation constant, i.e.  $10^{-30} \text{ M}^{-1}$ , or even lower, is observed with some of the naturally occurring chelating molecules which are present in bacteria, such as, enterobactin or enterochelin, where their function in the wild state is to access particularly iron, as  $\text{Fe}^{2+}$  and  $\text{Fe}^{3+}$ , into the bacteria.

Enterobactin is a siderophore, which is a peptide produced and released by Gram-negative bacteria, such as *E. coli* and *Salmonella* spp. It binds to  $\text{Fe}^{3+}$  with the

affinity  $10^{52} \text{ M}^{-1}$  which is then taken up by the cell via active transport (Raymond et al., 2003) where, it is proposed,  $\text{Fe}^{3+}$  is reduced to  $\text{Fe}^{2+}$  with ferrienterobactin esterase (Ward et al., 1999). Due to this strong affinity, enterobactin can chelate when  $\text{Fe}^{3+}$  concentrations are low, e.g. in living organisms. Pathogens can utilize this to commandeer iron from other organisms.

Some chelating agents are used therapeutically (chelation therapy), e.g. to eliminate excess or unwanted ions from the body. Such an example would be the compound desferrioxamine, which has a very high affinity for iron and can actually remove iron from temporary deposits in the body, such as ferritin and haemosiderin, by making it more easily excreted in urine, therefore preventing any liver damage the toxic iron would have caused. However, it is not strong enough to dissociate haem and therefore intact red cells are not destroyed. This is used in the treatment of a hereditary condition, known as haemochromatosis or sideraphilia, characterised by excess absorption of iron, which is fairly common in Africa (Gordeuk et al., 2004)

Several groups or types of group may be involved in the formation of a metal chelate. One of the most common is probably what is termed *O-O* coordination, where two adjacent hydroxyl groups serve to anchor the metal ion to the organic structure. Again, this is seen very well in alizarin (Figure 3.4) and also in the molecule of cyclohexenoesuletin (CHE). This will be alluded to later.

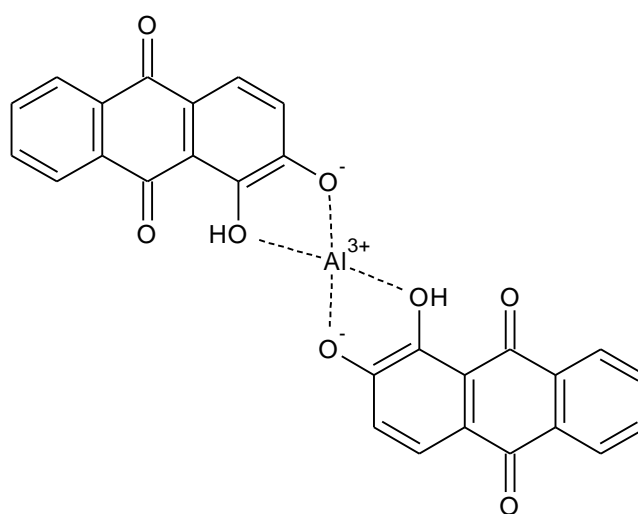


**Figure 3.4:** Possible chelation of alizarin and aluminium through two adjacent hydroxyl groups.

Derivatives of alizarin, and also CHE, have been synthesised, largely in these laboratories, over the last several years and have found application in microbial identification protocols, particularly those of bioMérieux and also Lab M.

A similar compound, 3,4-dihydroxyflavone has been synthesised and is marketed by Glycosynth. Here again, this may have certain applications as the glycoside or riboside (Butterworth et al., 2004), where it may be useful in the differentiation and identification of Gram-negative bacteria.

A rather different form of *O-O* coordination is where a hydroxy group is adjacent to a carbonyl group in a suitable orientation. Again, this will be described later since several of the compounds synthesised in this particular exercise bear that structure.

*O-N* coordination is also seen, where there is a hydroxyl group adjacent to an amino group or some other nitrogen function. Frequently that nitrogen function represents a ring nitrogen atom of, say, pyridine or a quinoline ring and here again, one can refer back to 8-hydroxyquinoline which is the archetypal compound of this type (James and Yeoman, 1987; James and Yeoman, 1988).

*N-N* coordination is also observed with molecules such as *o*-phenanthroline and 2,2'-bipyridyl. However, these compounds do not have any great application in terms of microbial identification or creation of enzyme substrates, since they have no derivatisable groupings. They are, however, used in the colorimetric, and sometimes fluorimetric, determination of metal ions, such as iron (Heaney and Davison, 1977; Wright, 1983).

One further possibility is *N-S* coordination. This is rather more limited in the acceptance of a metal ion. Not all metals will chelate with such structures and those which do frequently require conditions of pH which are inimicable to growth and to physiological conditions. Also, these metals which are involved are usually of the heavy metal type, i.e. lead, mercury, cadmium, etc, and, consequently, because of the toxicity of these metals, they have very little application in the design of enzyme substrates.

In the present study, several potential chelating core molecules were synthesised, these being:

- 2-(3,4-dihydroxybenzylidene)-1,3-indandione
- 3,4-dihydroxybenzylidene benzhydrazide
- 3,4-dihydroxybenzylidene isonicotinic hydrazide
- 7,8-dihydroxy-4-methylcoumarin (otherwise known as daphnetin)
- 1-methyl-2-phenyl-3-hydroxy-4(1*H*)-quinolone
- 1-methyl-2-(4-fluorophenyl)-3-hydroxy-4(1*H*)-quinolone

For comparative purposes and in order to create a wider range of glycosides eventually, several existing chelating agents were also investigated for their metal binding capacity. These included:

- 5-nitrosalicylaldehyde
- alizarin (1,2-dihydroxyanthraquinone)
- 3-hydroxyflavone
- 5,7-dichloro-8-hydroxy-2-methylquinoline

### 3.2.1 Synthesis of 2-(3,4-dihydroxybenzylidene)-1,3-indandione.

Previously synthesised (Artico et al., 1998), this compound was produced by a type of Knoevenagel reaction by condensation of 3,4-dihydroxybenzaldehyde (**3.1**) with indandione (**2.9**) according to standard conditions, as previously described earlier when synthesising chromogenic core compounds.

3,4-Dihydroxybenzaldehyde (0.69 g, 5 mmol) was dissolved in methanol (10 ml) in a 50 ml conical flask and stirred. To this, 1,3-indandione (0.73 g, 5 mmol) was added. After 5 min, ammonium acetate (0.6 g, 8 mmol) dissolved in methanol (5 ml) with glacial acetic acid (1 ml) were added. The solution was allowed to stand at room temperature for 1 h, during which time precipitation occurred. The crystals were filtered, then washed with methanol (5 ml) chilled to 4 °C.

TLC in ethyl acetate showed only a single spot near the solvent front. The 2-(3,4-dihydroxybenzylidene)-1,3-indandione (**3.2**) crystals were dried in a vacuum desiccator (0.72 g, 54.1 % yield) (Figure 3.5).

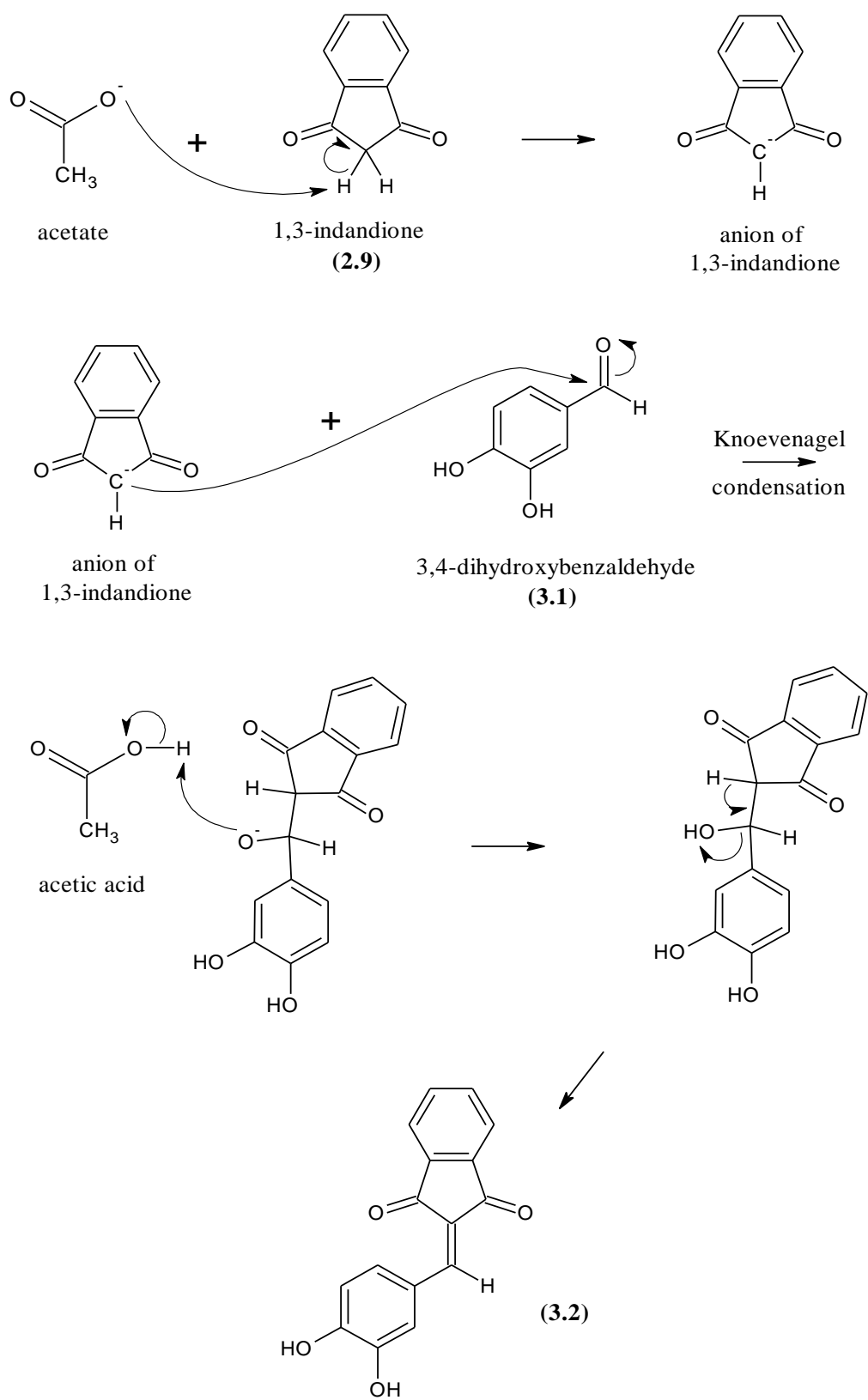


**Figure 3.5:** Formation of 2-(3,4-dihydroxybenzylidene)-1,3-indandione.

### Analytical data

Mp 260-262 °C (lit. 262-264 °C).

<sup>1</sup>H-NMR (d<sub>6</sub> DMSO, 270 MHz) δ 10.5 (1H, s, OH), 9.6 (1H, s, OH), 8.4 (1H, s, ArH), 7.8-8.1 (5H, om, ArH), 7.2 (1H, s, ArH), 6.9 (1H, d, J=8.4 Hz, ArH).

### **3.2.2 Synthesis of 3,4-dihydroxybenzylidene benzhydrazide**

This was synthesised by condensation of the previously mentioned dihydroxybenzaldehyde (**3.1**), but with benzhydrazide (**3.3**) (1 g, 7 mmol) in place of 1,3-indandione. Yielded 0.75 g, 41.9 % 3,4-dihydroxybenzylidene benzhydrazide (**3.4**) (Figure 3.6).

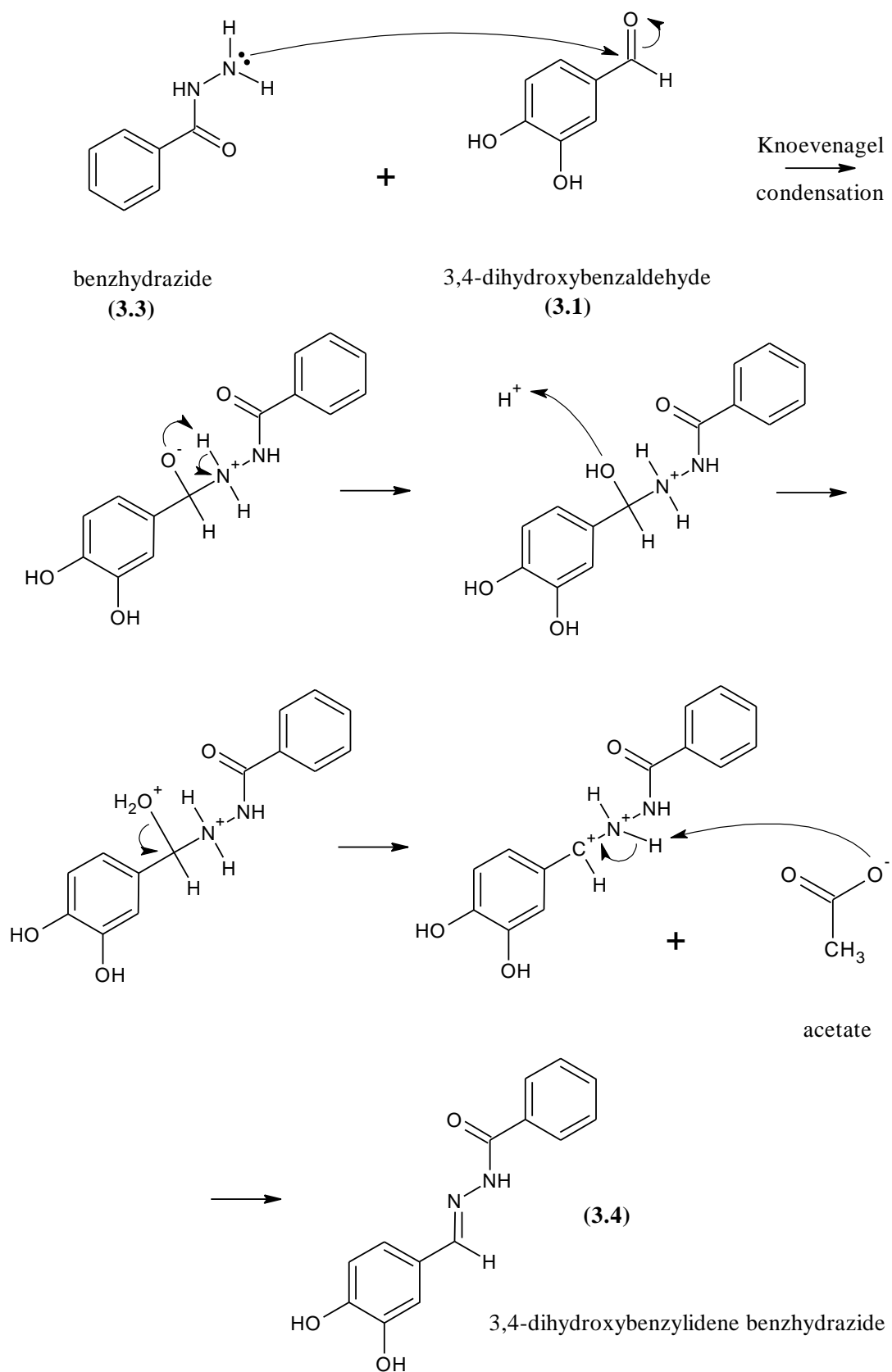


**Figure 3.6:** Formation of 3,4-dihydroxybenzylidene benzhydrazide.

### Analytical data

Mp 219-221 °C.

IR  $\nu_{\max}$   $\text{cm}^{-1}$ , 3302, 3180 (O-H), 1649 (C=O), 1578 (C=N).

$^1\text{H-NMR}$  ( $d_6$  DMSO, 270 MHz)  $\delta$  9.4 (2H, Broad s, OH), 8.3 (1H, s, ArH), 7.9 (2H, d,  $J=6.7$  Hz, ArH), 7.5 (3H, om, ArH), 7.3 (1H, s, ArH), 6.8-6.9 (2H, dd,  $J_1=8.1$  Hz,  $J_2=8.2$  Hz, ArH).

$^{13}\text{C-NMR}$  ( $d_6$ -DMSO, 270 MHz)  $\delta$  163, 149, 148, 146, 134, 132, 129 (x2), 128 (x2), 126, 121, 116, 113.

ESI-MS (M-H) calculated/found; 255.26/255.17.

HRMS (M-H) calculated/found; 255.2567/255.0771.

### **3.2.3 Synthesis of 3,4-dihydroxybenzylidene isonicotinic hydrazide**

3,4-dihydroxybenzylidene isonicotinic hydrazide (**3.6**) had been previously synthesised (Luedy-Tenger, 1956). This compound was synthesised as for 3,4-dihydroxybenzylidene benzhydrazide, but with isonicotinic hydrazide (**3.5**) (1g, 7 mmol) instead of benzhydrazide (0.8 g, 44.5% yield) (Figure 3.7).

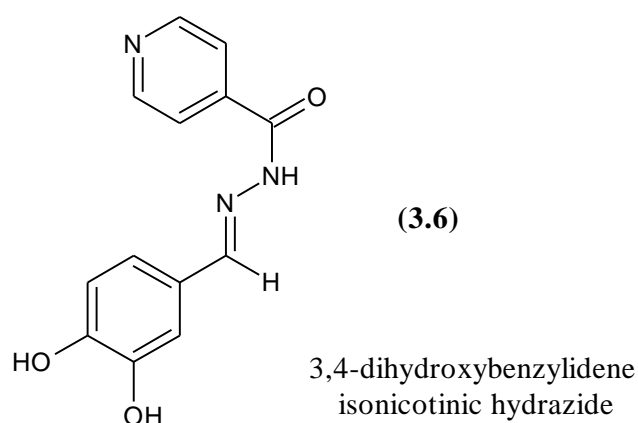
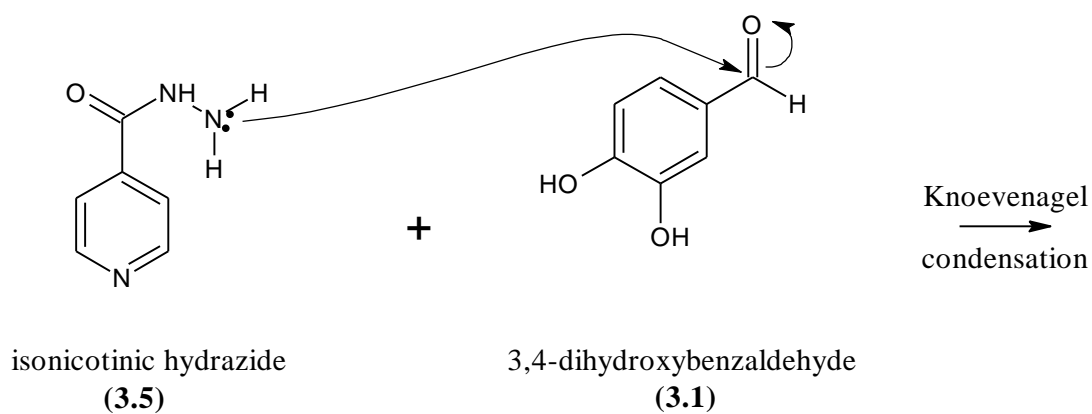


**Figure 3.7:** Formation of 3,4-dihydroxybenzylidene isonicotinic hydrazide.

#### Analytical data

Mp 260-262 °C (lit. 259-261.5 °C).

IR  $\nu_{\text{max}}$   $\text{cm}^{-1}$ , 3241, 3088 (O-H), 1644 (C=O), 1588 (C=N).

$^1\text{H-NMR}$  ( $d_6$  DMSO, 270 MHz)  $\delta$  9.5 (1H, s, OH), 9.4 (1H, s, OH), 8.8 (2H, d,  $J=5.9$  Hz, ArH), 8.3 (1H, s, ArH), 7.8 (2H, d,  $J=4.5$  Hz, ArH), 7.3 (1H, s, ArH), 6.8-7.0 (2H, dd,  $J_1=8.2$  Hz,  $J_2=7.9$  Hz, ArH).

$^{13}\text{C-NMR}$  ( $d_6$ -DMSO, 270 MHz)  $\delta$  162, 151 (x2), 150, 149, 146, 141, 126, 122 (x2), 121, 116, 113.

ESI-MS (M-H) calculated/found; 256.24/256.16.

### 3.2.4 Synthesis of 7,8-dihydroxy-4-methylcoumarin

7,8-dihydroxy-4-methylcoumarin (**3.9**) was synthesised by the Pechmann condensation (Pechmann, 1883) of pyrogallol (**3.7**) and ethyl acetoacetate (**3.8**) with sulphuric acid as a proton donor (De and Gibbs, 2005; Kumar et al., 2005).

Pyrogallol (1,2,3-trihydroxybenzene) (3.78 g, 30mmol) was melted into ethyl acetoacetate (4.29 g 33mmol) in a 250 ml conical flask by gentle warming. The melt was rapidly cooled to room temperature and stirred with 75% (w/w) sulphuric acid/distilled water (100 ml) while being cooled in a water bath (10 °C). The reaction mixture was inspected after several hours to observe a precipitate and then left stirring overnight (total time 24 h). The reaction mix, which initially became very viscous, formed a slurry containing the suspected coumarin. The reaction mix was then poured into well stirred iced water (500 ml total volume) in a thin stream. The precipitate which formed was removed by suction filtration under reduced pressure and washed well with ice cold distilled water and dried. The residue was dried in air at room temperature and recrystallised by initially dissolving in the minimum quantity of hot ethanol, followed by addition of water until the formation of crystals was apparent. After cooling in the fridge for 3 h, the solid product was removed by suction filtration and air dried as before (3 g, 52.1 % yield) (Figure 3.8).

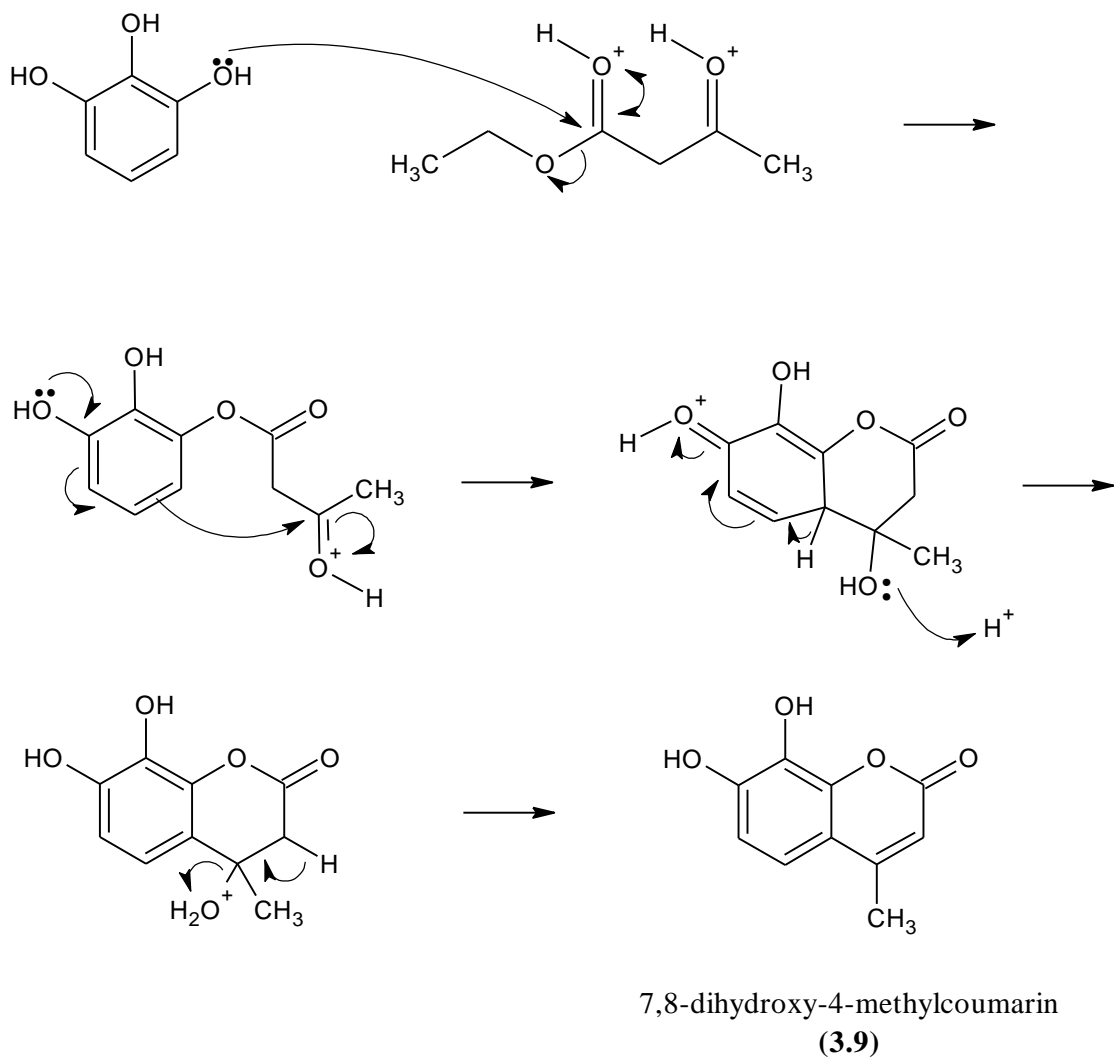
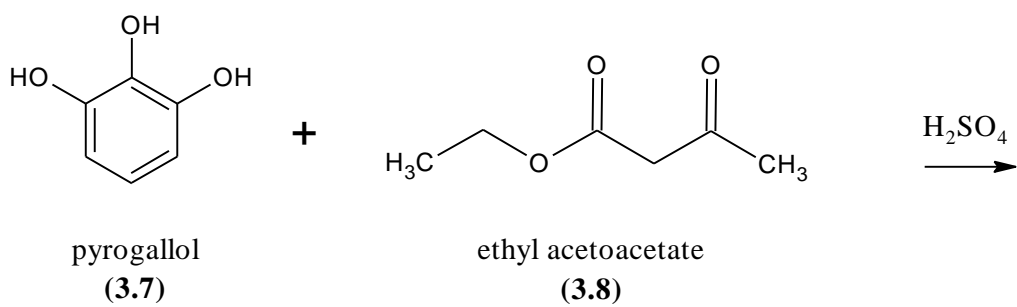


**Figure 3.8:** Formation of 7,8-dihydroxy-4-methylcoumarin.

### Analytical data

Mp 230-232°C (lit. 235°C).

<sup>1</sup>H-NMR (d<sub>6</sub> DMSO, 270 MHz) δ 9.5-10.0 (2H, Broad, OH), 7.1 (1H, d, *J*=8.7 Hz, Ar*H*), 6.8 (1H, d, *J*=8.7 Hz, Ar*H*), 6.1 (1H, s, alkene*H*), 2.3 (3H, s, CH<sub>3</sub>).

### 3.2.5 Synthesis of 1-methyl-2-phenyl-3-hydroxy-4(1*H*)-quinolone

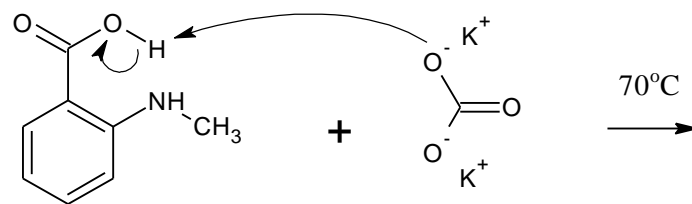
Similar in structure to 3-hydroxyflavone, a series of hydroxyquinolone compounds were first synthesised by Yushchenko (Yushchenko et al., 2006a) who reported their fluorescence properties. This, along with the compounds having a hydroxyl group necessary for glycosidation or attachment of other groups to create potential substrates (e.g. by esterification), would make them suitable candidates as fluorophores. The position of a hydroxy group adjacent to a carbonyl group also adds the possibility of metal chelation. Both of these attributes were thought worthy of further investigation.

The hydroxyquinolone compound was synthesised by condensation of anthranilic acid or its *N*-methyl derivative with the appropriate substituted phenacyl halide.

*N*-Methylantranilic acid (**3.10**) (3.2 g, 20 mmol) was suspended in dimethylformamide (10 ml) with potassium carbonate (3 g, 20 mmol). The mixture was stirred and heated at 70 °C for 1 h then allowed to cool to room temperature. Phenacyl bromide (2-bromoacetophenone) (**3.11**) (2.4 g, 20 mmol) was added. The mixture was stirred and heated to 50 °C for 1 h then poured into stirring distilled water (100 ml). A precipitate was formed, which was filtered, washed with distilled water (100 ml), then dried in a vacuum desiccator (yield 3.6 g, 71.7%, of phenacyl-*N*-methylantranilate).

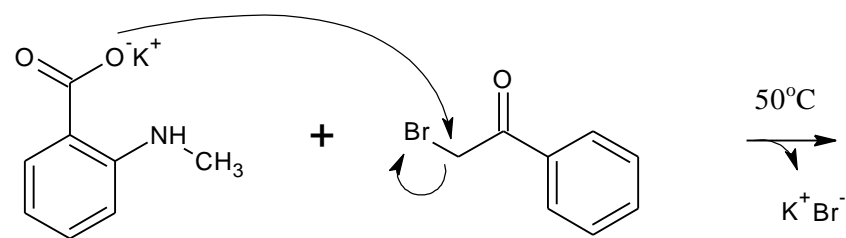
Phenacyl-*N*-methylantranilate (**3.12**) (2 g, 7.5 mmol) was suspended in polyphosphoric acid (PPA) (13.2 g, 7.5 mmol), heated at 120 °C for 2 h, then poured into stirring ice water (80 ml) to produce a black oil. After stirring for 1 h, the oil

became a grey solid (yield 1.2 g). The solid was filtered then allowed to dry before being recrystallised from warm DMF (20 ml). Yield 0.5 g, 26.5%, of 1-methyl-2-phenyl-3-hydroxyquinolone (**3.13**) (Figure 3.9).



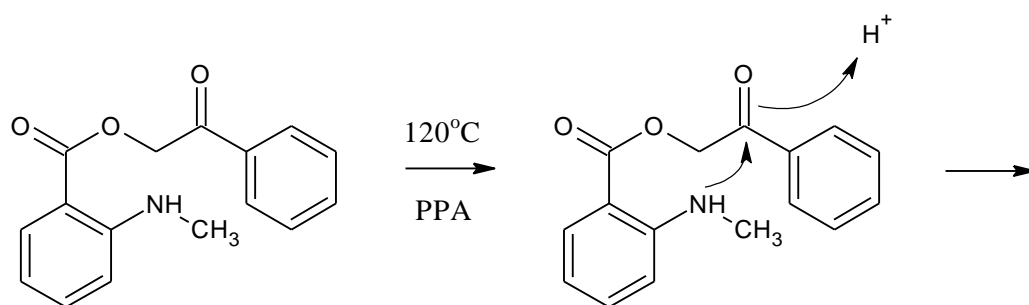
*N*-methylantranilic acid  
(3.10)

potassium carbonate

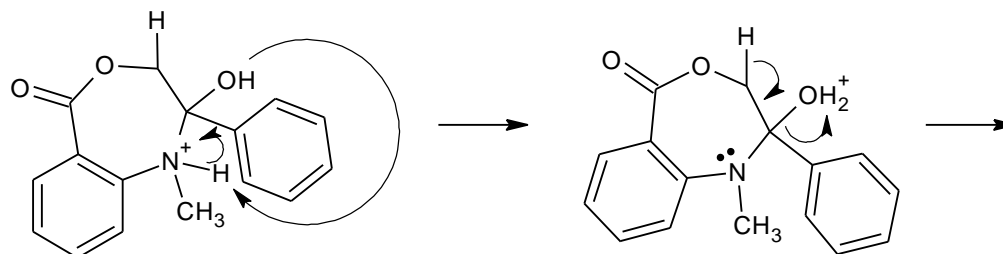


anion of *N*-methylantranilic acid (potassium salt)

2-bromoacetophenone  
(3.11)



phenacyl-*N*-methylantranilate  
(3.12)



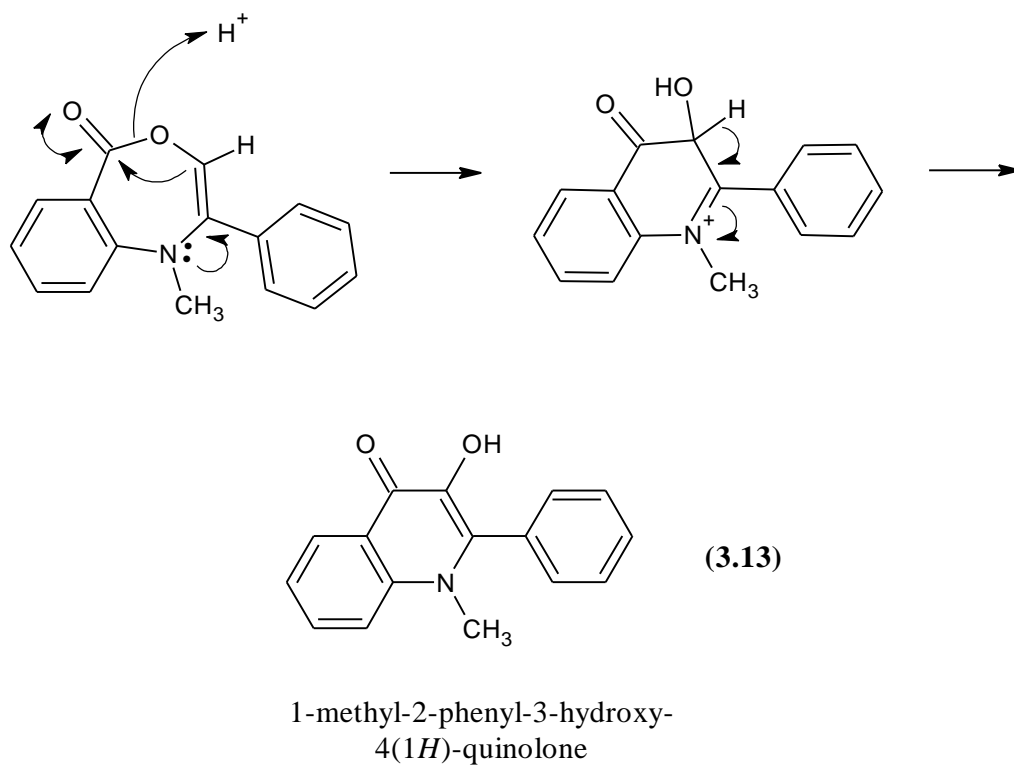


**Figure 3.9:** Formation of 1-methyl-2-phenyl-3-hydroxy-4(1*H*)-quinolone.

Analytical data

Mp 265-266°C (lit. 262 °C).

$^1H$ -NMR ( $d_6$  DMSO, 270 MHz)  $\delta$  8.3 (1H, d,  $J=7.9$  Hz, Ar*H*), 7.3-7.9 (8H, om, Ar*H*), 3.5 (3H, s, CH<sub>3</sub>).

### 3.2.6 Synthesis of 1-methyl-2-(4'-fluorophenyl)-3-hydroxy-4(1*H*)-quinolone

An analogue of the previous compound, again synthesised by (Yushchenko et al., 2006a), with the addition of a fluorine atom on the aryl ring was synthesised.

*N*-Methylantranilic acid (**3.10**) (12.8 g, 80 mmol) was reacted in a similar manner to 3.2.5 except 4'-Fluorophenacyl bromide (**3.14**) (17.2 g, 80 mmol) was used instead of 2-bromoacetophenone (yield 20 g, 87.0%, of 4'-fluorophenacylanthranilate).

4'-Fluorophenacylanthranilate (2 g, 7 mmol) was suspended in polyphosphoric acid (13.2 g, 7.5 mmol) and again treated as for 3.2.5. Yield 1.2 g, 63.7%, of 1-methyl-2-(4'-fluorophenyl)-3-hydroxy-4(1*H*)-quinolone (**3.15**) (Figure 3.10).

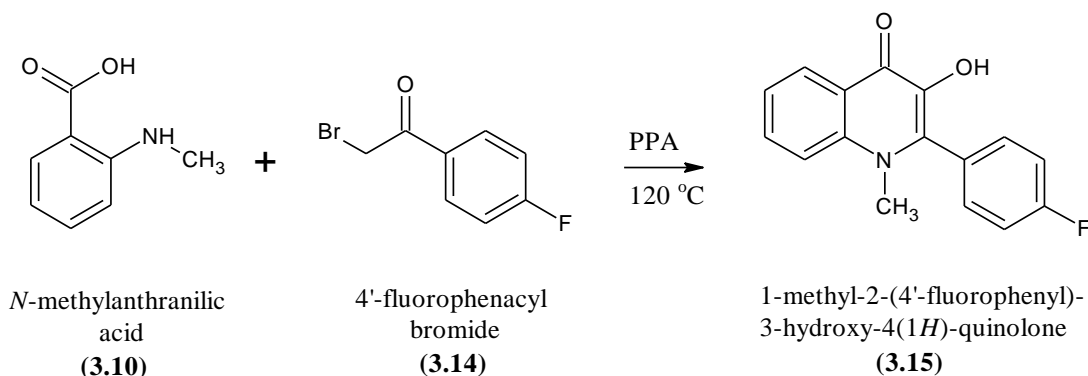


**Figure 3.10:** Formation of 1-methyl-2-(4'-fluorophenyl)-3-hydroxy-4(1*H*)-quinolone.

#### Analytical data

Mp 241-243°C (lit. 238 °C)

<sup>1</sup>H-NMR (d<sub>6</sub> DMSO, 270 MHz) δ 8.3 (1H, d, *J*=8.2 Hz, Ar*H*), 7.4-8.1 (7H, om, Ar*H*), 3.7 (3H, s, CH<sub>3</sub>).

The following possible chelating agents were investigated but were already commercially available (Figures 3.11, 3.12, 3.13, 3.14).

### 3.2.7 5-Nitrosalicylaldehyde

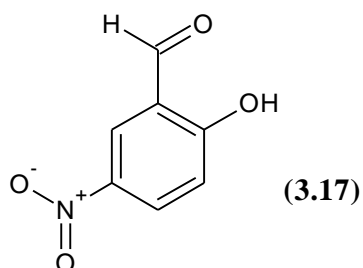


**Figure 3.11:** Structure of 5-nitrosalicylaldehyde.

$^1\text{H-NMR}$  ( $d_6$  DMSO, 270 MHz)  $\delta$  10.3 (1H, s, CHO), 8.4 (1H, d,  $J=12.1$  Hz, ArH), 8.3 (1H, d,  $J=8.9$  Hz, ArH), 7.2 (1H, d,  $J=9.1$  Hz, ArH).

### 3.2.8 Alizarin

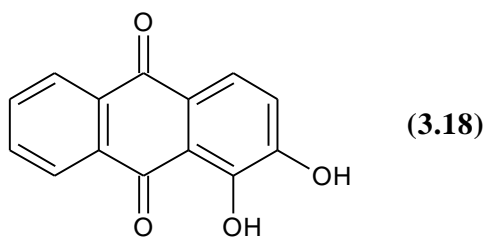


**Figure 3.12:** Structure of alizarin.

### 3.2.9 3-Hydroxyflavone

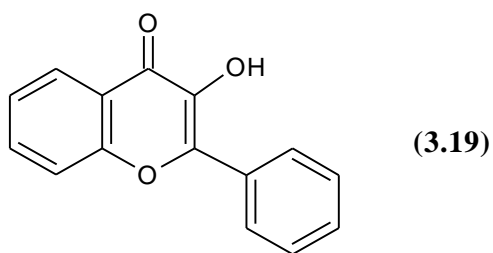


Figure 3.13: Structure of 3-hydroxyflavone.

### 3.2.10 5,7-Dichloro-8-hydroxy-2-methylquinoline

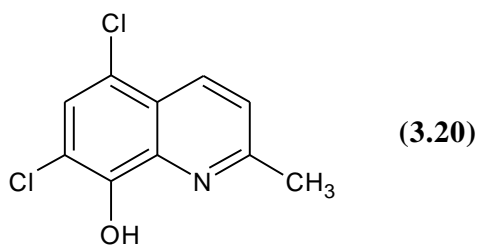


Figure 3.14: Structure of 5,7-dichloro-8-hydroxy-2-methylquinoline.

### 3.3 Results

As for the chromogenic compounds, the majority of the potential chelating compounds showed some coloration, especially in highly alkali conditions. Again, this is probably due to the presence of hydroxyl groups capable of ionisation. Colours were recorded across the pH range, the absorption spectra measured and any fluorescence observed under U.V. light (~350 nm) was also recorded.

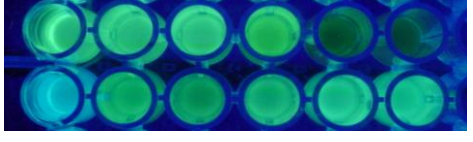
The core compounds (100 mg/L) were dissolved in 50% (v/v) ethanol water and the pH adjusted with either HCl (0.2 M) or NaOH (0.2 M).

To investigate any chelation effects, samples of these compounds at pH 7, as described above, were mixed with a selection of metal sulfate salts, i.e. aluminium, cobalt, ferrous, ferric ammonium, magnesium and zinc sulphates (500 mg/L), the results of which were recorded in Tables 3.1a and 3.1b.

**Table 3.1a:** pH effect and metal interaction of chelating core compounds. Colour change due to varying pH, (top row); possible chelation with different metal ions (bottom row).

Chelating compound	pH					
	3 Al	5 Co	7 Fe <sup>2+</sup>	9 Fe <sup>3+</sup>	11 Mg	13 Zn
2(3,4-dihydroxybenzylidene)-1,3-indandione						
3,4-dihydroxybenzylidene benzhydrazide						
3,4-dihydroxybenzylidene isonicotinic hydrazide						
7,8-dihydroxy-4-methylcoumarin						
7,8-dihydroxy-4-methylcoumarin under U.V.						
1-methyl-2-phenyl-3-hydroxy-4(1H)-quinolone						
1-methyl-2-phenyl-3-hydroxy-4(1H)-quinolone under U.V.						
1-methyl-2-(4-fluorophenyl)-3-hydroxy-4(1H)-quinolone						
1-methyl-2-(4-fluorophenyl)-3-hydroxy-4(1H)-quinolone under U.V.						

**Table 3.1b:** pH effect and metal interaction of chelating core compounds continued.

Chelating compound	pH					
	3 Al	5 Co	7 Fe <sup>2+</sup>	9 Fe <sup>3+</sup>	11 Mg	13 Zn
5-nitrosalicylaldehyde						
alizarin						
3-hydroxyflavone						
3-hydroxyflavone						
5,7-dichloro-8-hydroxy-2-methylquinoline						

Spectrum scans from 300 to 700 nm were recorded at each pH using a Biotek Synergy multi-detection microplate reader. A representative sample of these can be seen below in Figures 3.15, 3.16 and 3.17 (others appear in Appendix B).

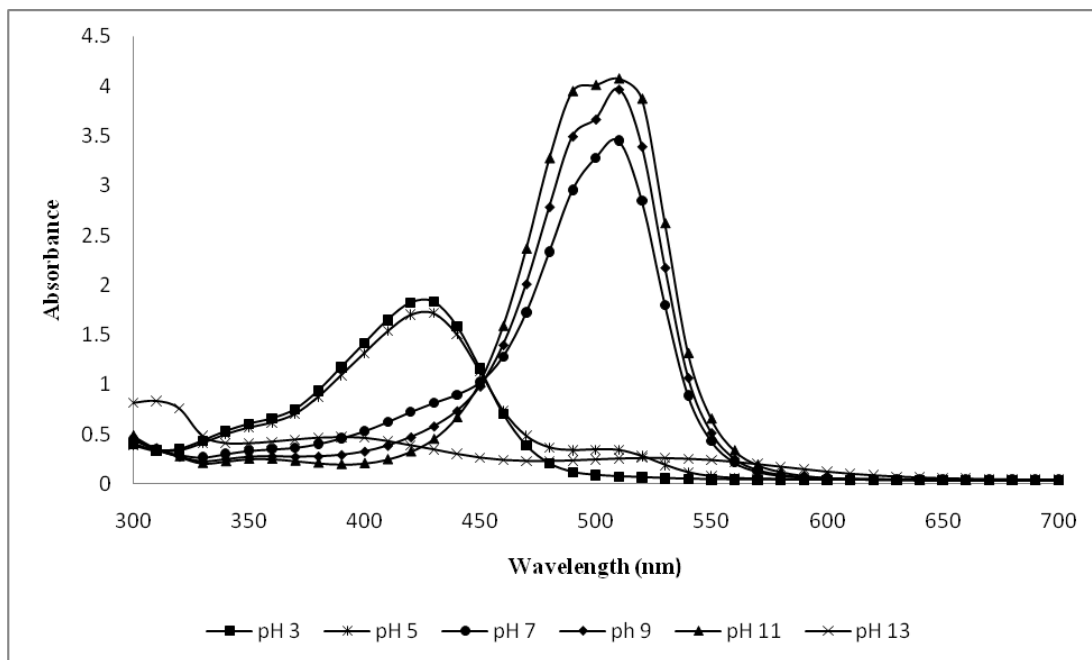


**Figure 3.15:** Spectrum scan of 2(3,4-dihydroxybenzylidene)-1,3-indandione.

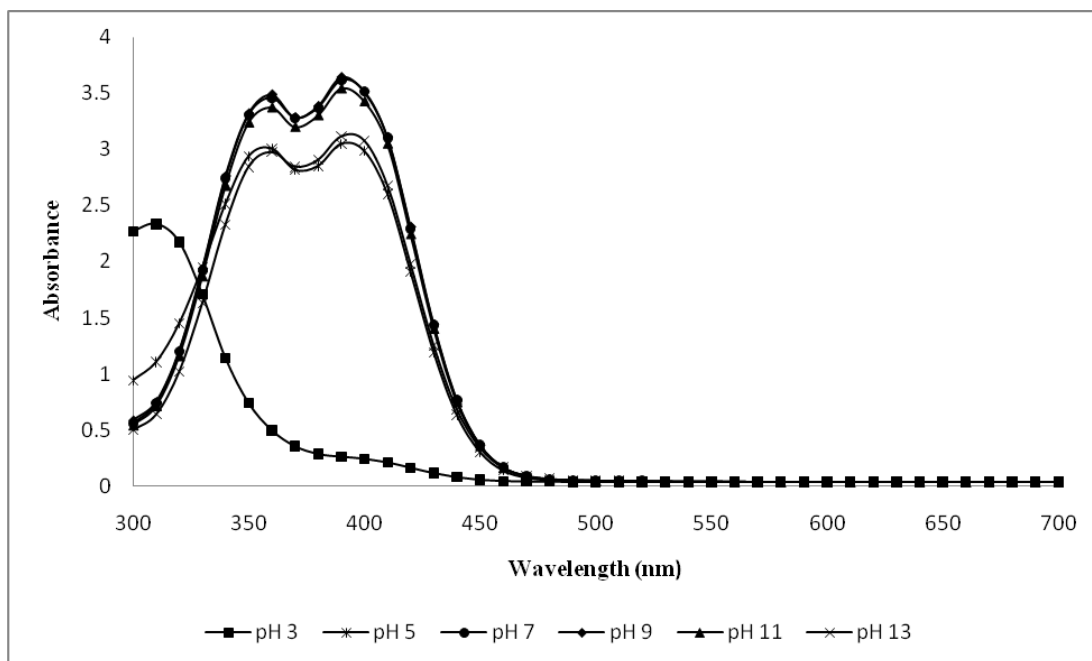


**Figure 3.16:** Spectrum scan of 5-nitrosalicylaldehyde.

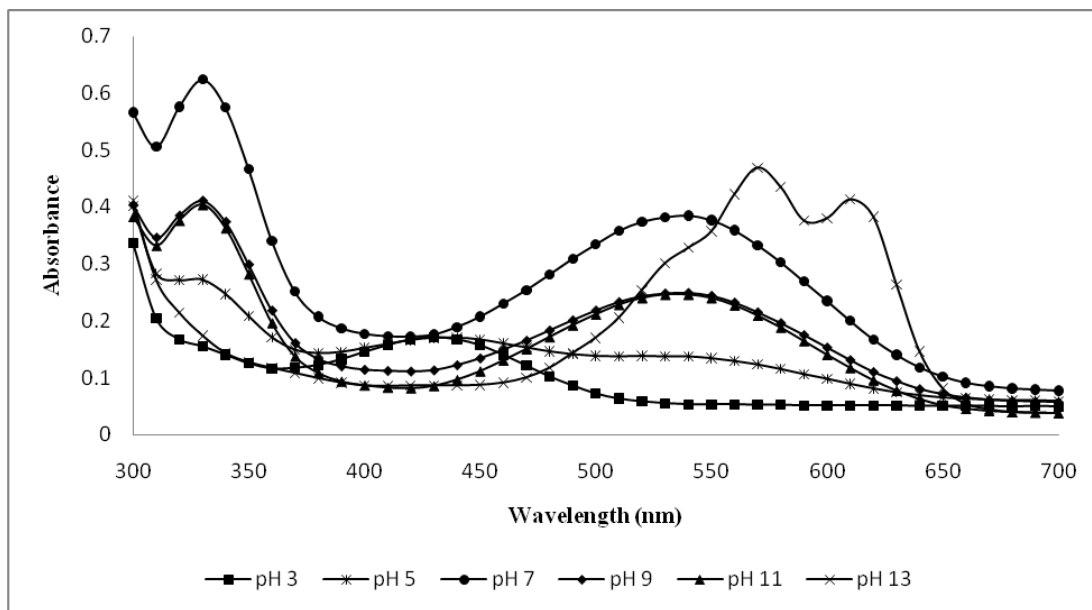


Figure 3.17: Spectrum scan of alizarin.

### 3.4 Discussion

Again these results showed compounds such as 2-(3,4-dihydroxybenzylidene)-1,3-indandione and alizarin had possible uses as pH indicators due to their variation in colour across the pH range. Both of these also produced a range of colours when chelated with metal ions. It was also noted that some alizarin chelates, such as those with iron and magnesium, precipitated out of solution.

Other compounds of interest included 5-nitrosalicylaldehyde, which gave a strong yellow coloration even at pHs on the acidic side of neutral. With the addition of ferrous iron, this coloration was darkened making it more intense.

3-Hydroxyflavone gave some coloration just above neutrality but its most striking characteristics were its fluorescence and its ability to form chelates, which altered or enhanced this fluorescence.

1-Methyl-2-phenyl-3-hydroxy-4(1*H*)-quinolone and its fluoro analogue were also highly fluorescent and again this could be altered or enhanced with metal chelation.

Other compounds that showed no or little coloration darkened when chelated to ferrous iron and it was thought even this trait could be exploited.

As with the chromogenic core compounds, several of these chelating compounds were subject to glycosidation and the results of this are given later in the appropriate section.

## **CHAPTER FOUR**

### **Glycosides and other derivatives**

## 4.1 Glycosides introduction

Most of the derivatives of the molecules mentioned have been of the glycoside class; although certain esters have been synthesised, targeting the glycosidase and esterase enzymes, which are widely distributed across a variety of bacteria and also in both the animal and plant kingdoms.

In microbial identification systems, glycosidases are widely targeted. This has previously been described in the introduction section related to indoxyllic and other glycosidic substrates.

The synthesis of glycosides depends largely on whether the attempted glycoside is of the  $\alpha$  or  $\beta$  type. In the main, the  $\beta$ -glycosidases have been examined predominantly. These are widely distributed and have been useful in the identification of coliforms, *E. coli* and many other organisms. More recently, the  $\alpha$ -glycosides have assumed prominence, particularly with respect to such organisms as *Staphylococcus aureus* and *Salmonella* spp, where  $\alpha$ -glucosidase and  $\alpha$ -galactosidase have been specifically targeted for identification purposes.

Several methods of synthesis of  $\beta$ -glucosides have been used dating back to the work of Koenigs and Knorr in the late 19<sup>th</sup> Century and, in fact, the Koenigs-Knorr method is still widely used today, although often substantially modified. Essentially, the Koenigs-Knorr method uses an activated form of the sugar which is to be attached to the aglycone. This activation is usually through the possession of a halogen atom, very frequently bromine, at the anomeric position, i.e. position 1 of the sugar molecule. The other hydroxyl groups require protection and this is usually done by acetylation, although, in some cases, where extra stability is required or alternatively there is a need for removal by hydrogenolysis rather than hydrolysis, the benzyl group is employed. Most commonly, however, compounds such as 1-bromo-2,3,4,6-tetraacetyl galactopyranose (Figure 4.1) are used. This compound is frequently referred to as acetobromogalactose and has the  $\alpha$ -configuration as normally made. The possession of the  $\alpha$ -configuration is not unusual, since the  $\alpha$  form is usually the most stable and, in the course of transfer of the sugar unit to an aglycone, there is an

inversion of configuration such that the use of the  $\alpha$ -bromo compound produces the  $\beta$ -glycoside.

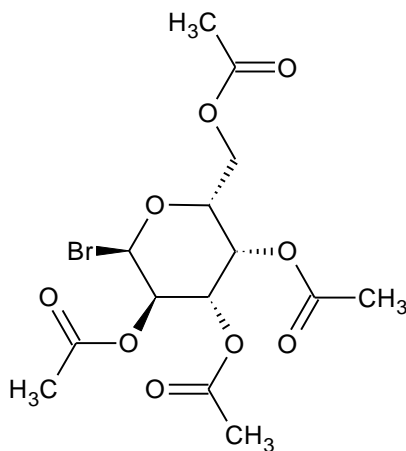


**Figure 4.1:** Structure of acetobromo- $\alpha$ -D-galactose.

Certain of these activated sugar units are commercially available, in particular, so-called  $\alpha$ -acetobromoglucose and  $\alpha$ -acetobromogalactose (Sigma). The others can be made by relatively straightforward means involving the use of acetic anhydride and bromine plus red phosphorus to generate the hydrogen bromide necessary for bromination at the anomeric position. In a typical method, the aglycone is reacted with e.g.  $\alpha$ -acetobromoglucose in a mixture of water and acetone, necessary to obtain homogeneity in the presence of a base such as sodium hydroxide or potassium hydroxide. As the reaction proceeds, a substitution occurs leading to the elimination of the  $\text{Br}^-$  ion which is taken up by the alkali. It is necessary in such reactions to check the pH periodically because, as the pH falls, the reaction tends to slow down and precipitation of the aglycone frequently occurs. It is common practice therefore to add small quantities of alkali during the Koenigs-Knorr reaction.

The protected glycoside can be isolated by standard means and the acetyl group subsequently removed by using alkali, either sodium hydroxide or, if the molecule tends to be unstable, sodium methoxide in absolute methanol is more frequently employed. This method has been commonly used in the present work.

A modification of this method involves dissolving the aglycone as the sodium or potassium salt in anhydrous dimethylformamide and adding the  $\alpha$ -acetobromo sugar. This has the advantage of avoiding aqueous conditions which can lead to degradation of the glycosidating agent.

A third procedure which also involves non-aqueous conditions is reported by Haughland (Haughland, 2002). In this, the aglycone is dissolved in dichloromethane with the aid of a base. Generally, a pyridine based compound is used: 2,6-lutidine or 2,4,6-collidine. The silver carbonate is added and, after the addition of the  $\alpha$ -acetobromo sugar, the reaction proceeds at room temperature. Glycosidation is accompanied by release of the bromide ion, which is trapped by the silver carbonate to form insoluble silver bromide. This tends to drive the reaction towards completion. It is possible to get considerably higher yields by this method than by the standard Koenigs-Knorr procedure. However, it is not suitable for all aglycones. For example, where a vicinal dihydroxy system exists, it has been found that complexation with silver ions can occur which inhibits the glycosidation.

Consequently, a variety of methods have been attempted in this particular project, depending upon the nature of the aglycone.

The following core molecules have been subject to glycosidation:

- 2-hydroxy-1-naphthaldehyde
- 1-nitrovinyl-2-naphthol
- 4-hydroxy-3-methoxycinnamylidene-1,3-indandione
- 4-hydroxy-3-methoxycinnamylidene-5-phenylisoxazolone
- 5-nitrosalicylaldehyde
- 7,8-dihydroxy-4-methylcoumarin
- alizarin
- 3-hydroxyflavone
- 1-methyl-2-(4'-fluorophenyl)-3-hydroxy-4(1*H*)-quinolone

- 5,7-dichloro-8-hydroxy-2-methylquinoline
- naphthofluorescein
- *p*-naphtholbenzein

## 4.2 Glycosides experimental methods and mechanisms

### 4.2.1 Synthesis of 2-hydroxy-1-naphthaldehyde- $\beta$ -D-galactoside

A Koenigs-Knorr reaction using 2,6-lutidine and silver carbonate was performed.

2-Hydroxy-1-naphthaldehyde (**2.7**) (1.72 g, 10 mmol) was dissolved in dry DCM (20 ml), and 2,6 lutidine (**4.1**) (2 ml, 20 mmol) was added. The solution was then stirred for 15 min. Silver carbonate (2.75 g, 10 mmol) was added and then stirred for 10 min. Acetobromo- $\alpha$ -D-galactose (**4.2**) (4.1 g, 10 mmol) was added and then stirred for a further 24 h. A sample was taken for TLC using ethyl acetate as a solvent. The TLC plate was flooded with Brady's reagent (see Appendix A). A red spot at the solvent front indicated unreacted 2-hydroxy-1-naphthaldehyde. The TLC plate was then flooded with charring reagent (see Appendix A) and gently heated on a hot plate. A black or charred spot on the baseline showed unreacted acetobromo- $\alpha$ -D-galactose and a black spot on the solvent front showed acetylated 2-hydroxy-1-naphthaldehyde- $\beta$ -D-galactoside (**4.3**). The reaction was allowed to progress for another 24 h at which time TLC showed only a small red spot at the solvent front when flooded with Brady's reagent and a small black or charred spot on the baseline and a large black spot at the solvent front when charred.

A bed of silica gel 2 cm deep was made in a sintered-glass funnel and primed with DCM (20 ml). The solution was then poured into the funnel and the filtrate collected. More DCM (20 ml) was poured into the funnel and also collected. TLC of the filtrate showed no free 2-hydroxy-1-naphthaldehyde as no red spot was observed with the addition of Brady's reagent. The filtrate was placed in a 250 ml separating funnel and washed with sodium bicarbonate (50 ml, 0.2 M), then three times with hydrochloric acid (50 ml, 0.2 M) and finally with distilled H<sub>2</sub>O (50 ml). The DCM solution was then placed in a 250 ml conical flask with excess dry magnesium sulphate and stirred for 1 h, then filtered. The solution was evaporated under reduced pressure at 40 °C using a rotary evaporator, then dried in a vacuum

desiccator to give a 3.0 g, 59.7%, yield of acetylated 2-hydroxy-1-naphthaldehyde- $\beta$ -D-galactoside (Figure 4.2).

Removal of the acetyl groups from the protected galactoside (de-protection) was attempted with sodium methoxide (2 ml, 200 mmol) (see Appendix A) but failed to give rise to a product from which a successful compound could be isolated.

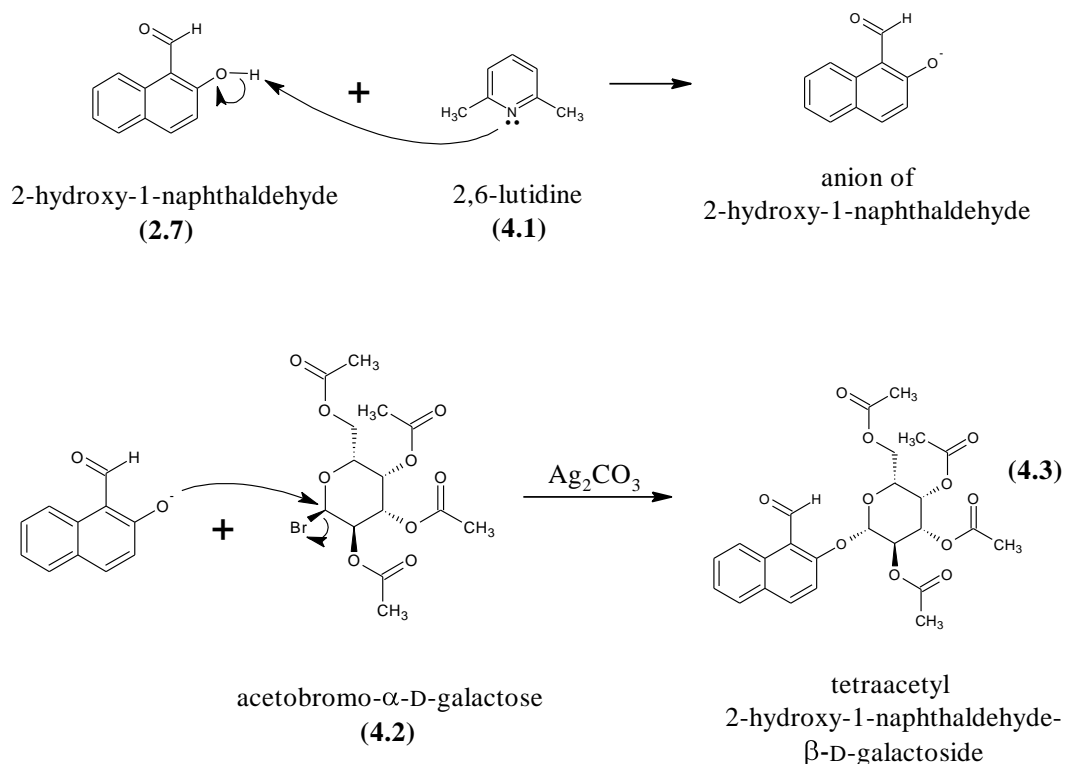


**Figure 4.2:** Formation of tetraacetyl 2-hydroxy-1-naphthaldehyde- $\beta$ -D-galactoside. Glycosidation via Koenigs-Knorr lutidine/silver carbonate method, deprotection using sodium methoxide failed.

#### Analytical data

$^1\text{H-NMR}$  ( $d_6$ -DMSO, 270 MHz)  $\delta$  10.5 (1H, s, CHO) 9.1 (1H, d,  $J=8.2$  Hz, ArH), 7.2-8.5 (difficult to interpret ArH), 4.0-6.0 (7H, difficult to interpret AlH) 1.9-2.2 (12H, 4s, AlH). Impure.

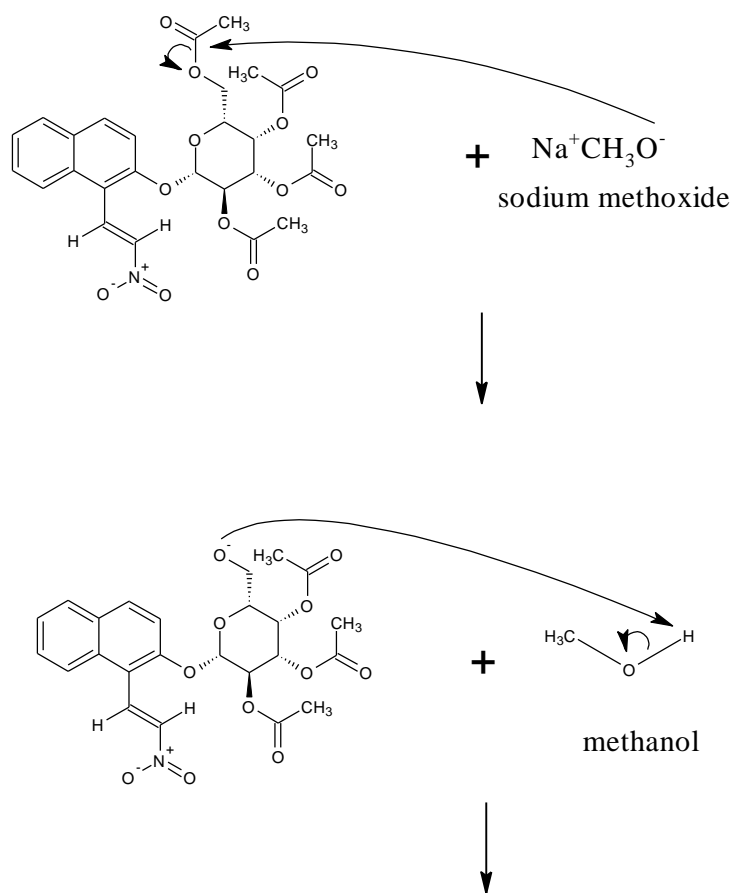
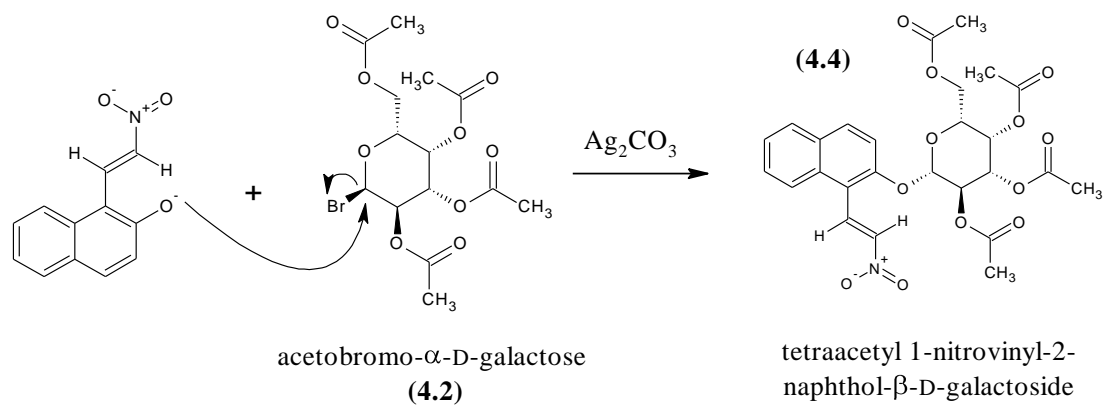
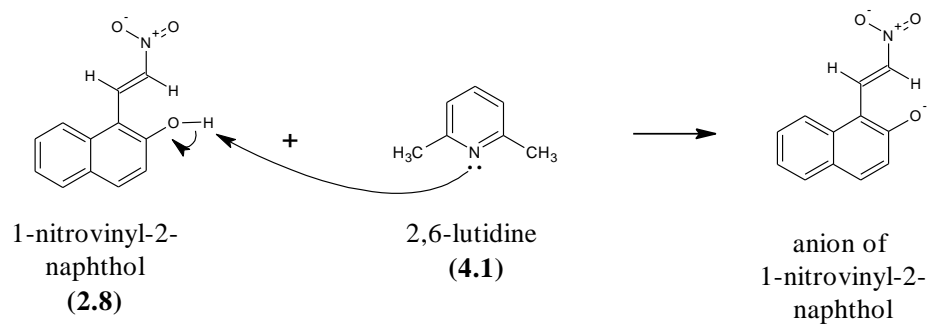
### 4.2.2 Synthesis of 1-nitrovinyl-2-naphthol- $\beta$ -D-galactoside

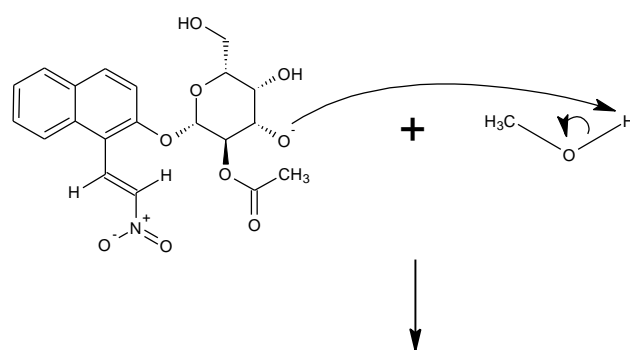
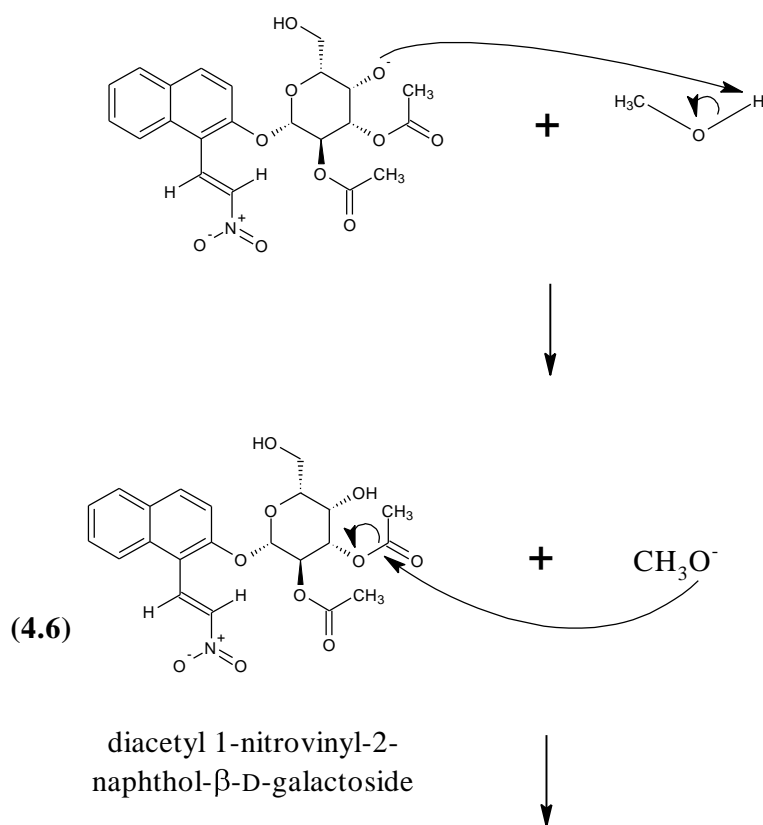
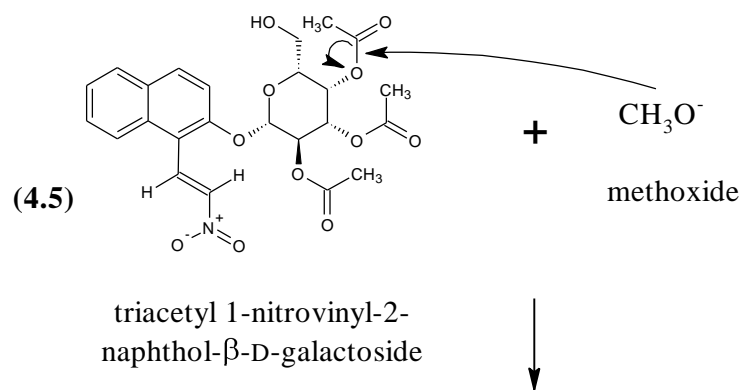
A Koenigs-Knorr method using 2,6-lutidine and silver carbonate was performed.

1-nitrovinyl-2-naphthol (**2.8**) (2 g, 10 mmol) was placed in a 100 ml conical flask with 30ml DCM and stirred. 2,6 Lutidine (**4.1**) (2 ml, 20 mmol) was then added and stirred for 15 min. Silver carbonate (2.75 g, 10 mmol) (see Appendix A) was added and then stirred for 10 min. Acetobromo- $\alpha$ -D-galactose (**4.2**) (4.1 g, 10 mmol) was added and then stirred for a further 24 h. A sample was taken for TLC using ethyl acetate as a solvent showed two spots, one on the solvent front and another trailing. On exposure to ammonia the front spot gave a purple colour (1-nitrovinyl-2-naphthyl) and when flooded with charring reagent (see Appendix A) and gently heated on a hot plate the trailing spot blackened (acetylated 1-nitrovinyl-2-naphthyl- $\beta$ -D-galactoside (**4.4**)).

A bed of silica gel 2 cm deep was made in a sintered-glass funnel and primed with DCM (20 ml). The solution was then poured into the funnel and the filtrate collected. More DCM (20 ml) was poured into the funnel and also collected. TLC of the filtrate showed no free 1-nitrovinyl-2-naphthol as a purple spot when exposed to ammonia, but there was still a charred spot. The filtrate was placed in a 250 ml separating funnel and washed with sodium bicarbonate (50 ml, 0.2 M), then three times with hydrochloric acid (50 ml, 0.2 M) and finally with H<sub>2</sub>O (50 ml). The DCM solution was then placed in a 250 ml conical flask with excess dry magnesium sulphate and stirred for 1 h, then filtered. The solution was evaporated under reduced pressure at 40 °C using a rotary evaporator, then dried in a vacuum desiccator (1.35 g yield, 24.7%). The foam was dissolved in methanol (20 ml).

Sodium methoxide (2 ml, 200 mmol) (see Appendix A) was added to the methanol solution, stirred briefly then chilled at 4 °C for 24 h to allow de-protection (**4.5-4.8**). The solution was evaporated under reduced pressure to ~25 ml at 60 °C then allowed to recrystallise by cooling the flask on ice (0 °C) for 1 h. The sand coloured 1-nitrovinyl-2-naphthol- $\beta$ -D-galactoside (**4.8**) crystals were filtered under pressure then dried in a vacuum desiccator (1 g yield, 74.0%), (Figure 4.3).





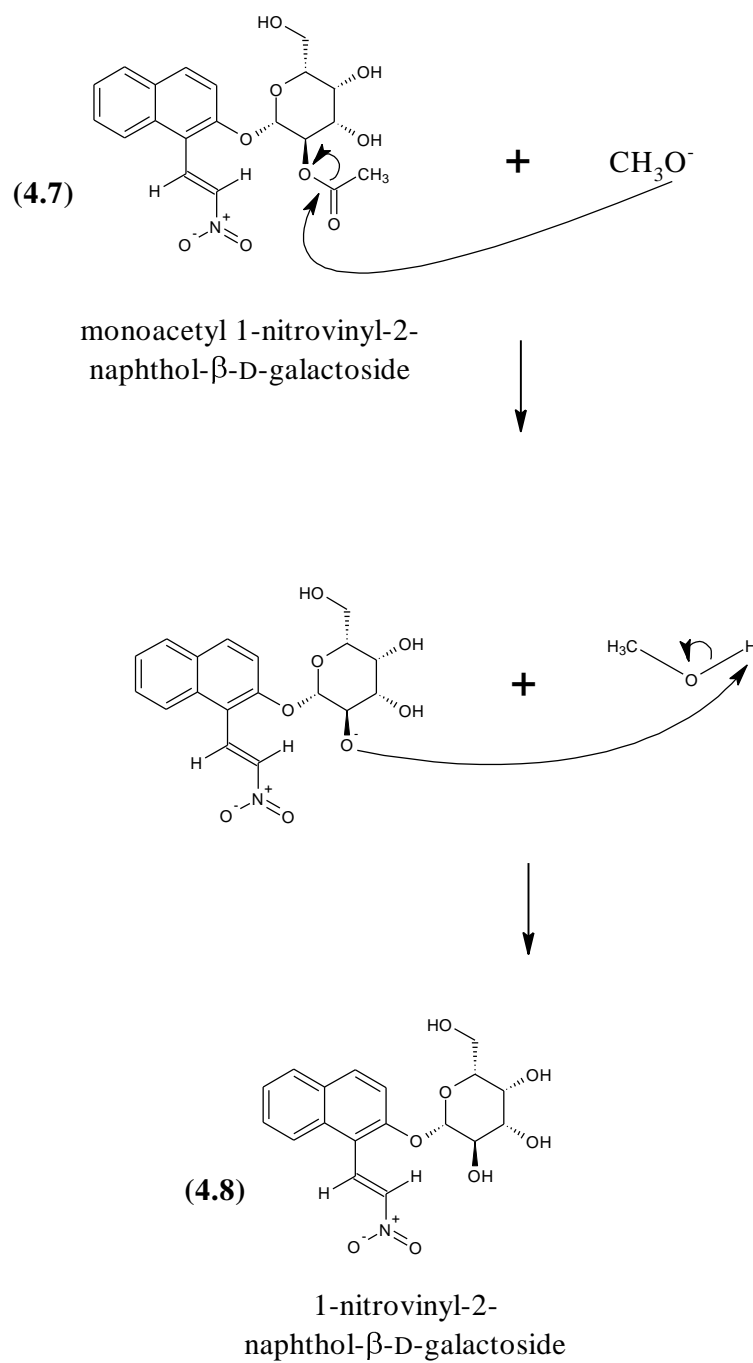


**Figure 4.3:** Formation of 1-nitrovinyl-2-naphthol- $\beta$ -D-galactoside. Glycosidation via Koenigs-Knorr lutidine/silver carbonate method; deprotection using sodium methoxide.

NMR in  $d_6$ -DMSO not possible due to the insolubility of the compound.

### 4.2.3 Synthesis of 4- $\beta$ -D-galactosidoxy- and 4- $\beta$ -D-glucosidoxy-3-methoxycinnamylidene-1,3-indandione

#### 4- $\beta$ -D-Galactosidoxy-3-methoxycinnamylidene-1,3-indandione

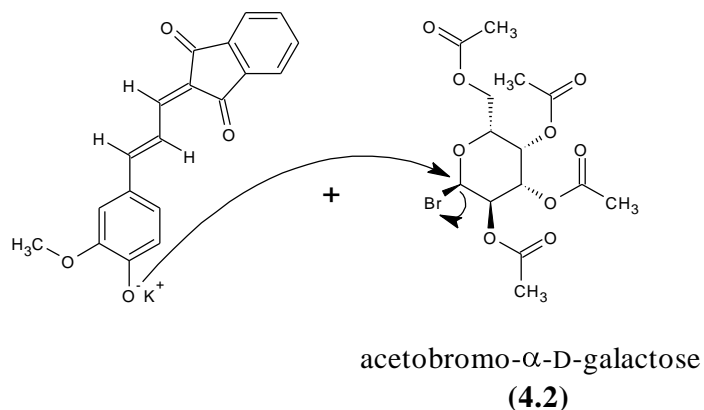
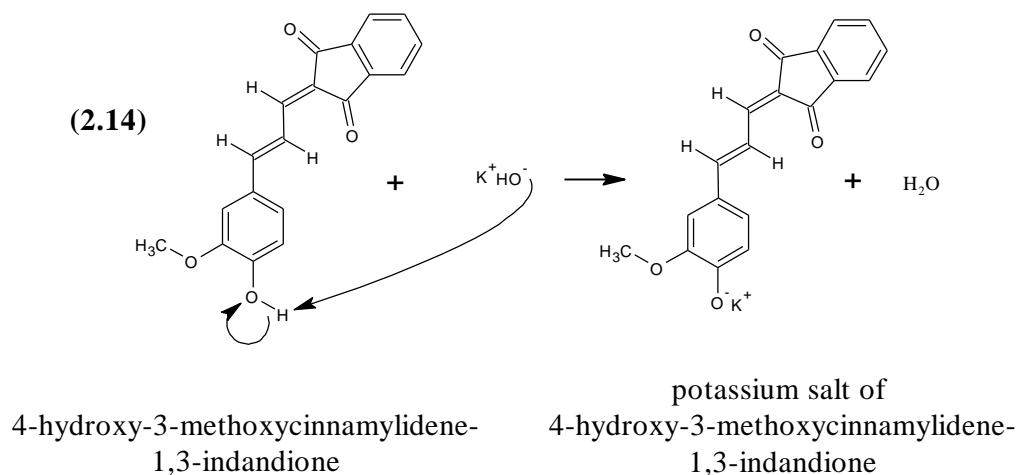
A Koenigs-Knorr reaction using potassium hydroxide as a base was performed.

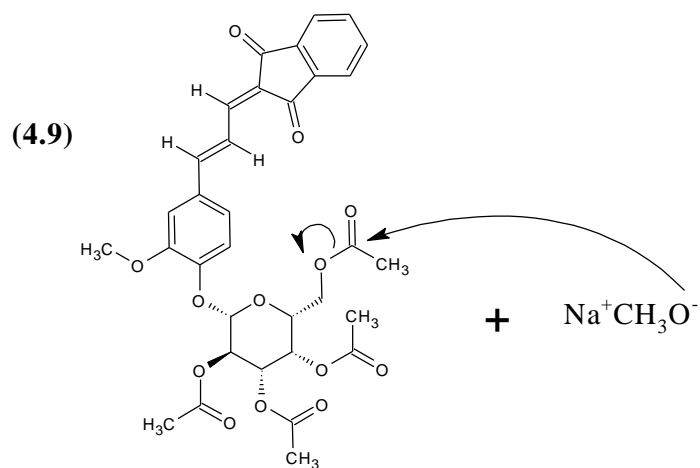
4-Acetoxy-3-methoxycinnamylidene-1,3-indandione (**2.12**) was hydrolysed via the following method: 4-acetoxy-3-methoxycinnamylidene-1,3-indandione (2.6 g, 7.5 mmol) and methanol (75 ml) were added to a 250 ml conical flask and stirred at 0 °C in an ice bath. Potassium hydroxide (1.1 g, 20 mmol) was dissolved in distilled H<sub>2</sub>O, (5 ml) added to the above suspension and stirred for 2 h. Ice (100 g) was then added and the pH adjusted to pH 3 using 2 M hydrochloric acid. The resulting precipitate was filtered under pressure then dried in a vacuum desiccator (2.2 g yield, 95.8%).

4-Hydroxy-3-methoxycinnamylidene-1,3-indandione (**2.14**) (1.53 g, 5 mmol) and acetone (15 ml) were placed in a 50 ml conical flask and stirred. Potassium hydroxide (0.28 g, 5 mmol) was dissolved in distilled H<sub>2</sub>O (2 ml) and then added to the above suspension. The pH was measured with Whatman Universal Indicator papers and found to be pH 12 then stirred for 30 min. Acetobromo- $\alpha$ -D-galactose (**4.2**) (2.46 g, 6 mmol) was dissolved in acetone (2 ml) and added and stirring continued for 24 h. The pH was regularly adjusted to pH 12 using potassium hydroxide (0.28 g, 5 mmol). TLC using ethyl acetate as a solvent showed a yellow band (product) at the solvent front and a blue spot on the base line (starting material) when exposed to ammonia fumes. The reaction was allowed to continue for a further 24 h, after which TLC showed the yellow band and a smaller blue spot with exposure to ammonia fumes. The solution was then evaporated at 40 °C using a rotary evaporator. Dichloromethane (50 ml) was used to re-dissolve the product which was then transferred to a 250 ml conical flask. Anhydrous magnesium sulphate (1 g) was added and stirred for 1 h to remove any water. The magnesium sulphate was removed by filtration and then discarded. Alumina (1 g) was added to the solution and stirred for 1 h to remove any unreacted starting material. The alumina was removed by filtration and discarded. TLC using ethyl acetate as a solvent showed

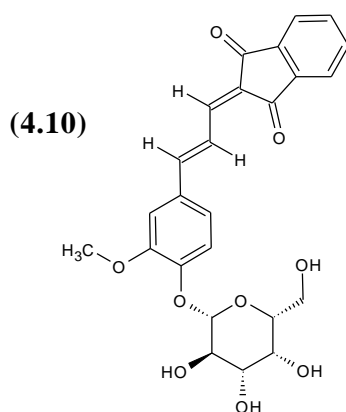
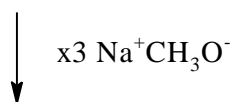
only a yellow band at the solvent front and a no blue spot on the base line when exposed to ammonia fumes. The solution was transferred to a 100 ml round bottom flask then evaporated under reduced pressure to a 'foam' at 40 °C (yield 1.5 g, 47.1% of acetylated 4-β-D-galactosidoxy-3-methoxycinnamylidene-1,3-indandione (**4.9**)). The foam was dissolved in methanol (50 ml).

De-protection was performed with sodium methoxide as in previous glycosidations. The 4-β-D-galactosidoxy-3-methoxycinnamylidene-1,3-indandione (**4.10**) crystals were filtered under pressure then dried in a vacuum desiccator (0.7 g yield, 63.3%) (Figure 4.4).





tetraacetyl  
4-β-D-galactosidoxy-3-methoxycinnamylidene-  
1,3-indandione



4-β-D-galactosidoxy-3-methoxycinnamylidene-  
1,3-indandione

**Figure 4.4:** Formation of 4-β-D-galactosidoxy-3-methoxycinnamylidene-1,3-indandione.  
Glycosidation via Koenigs-Knorr potassium hydroxide method, deprotection using sodium methoxide.

NMR in d<sub>6</sub>-DMSO - Spectrum too weak for analysis.

4-β-D-Glucosidoxy-3-methoxycinnamylidene-1,3-indandione

4-β-D-glucosidoxy-3-methoxycinnamylidene-1,3-indandione (**4.11**) was synthesised as for 4-β-D-galactosidoxy-3-methoxycinnamylidene-indandione but acetobromo-α-D-galactose was replaced with acetobromo-α-D-glucose (**4.15**) (yield 0.75 g, 67.8%) (Figure 4.5).

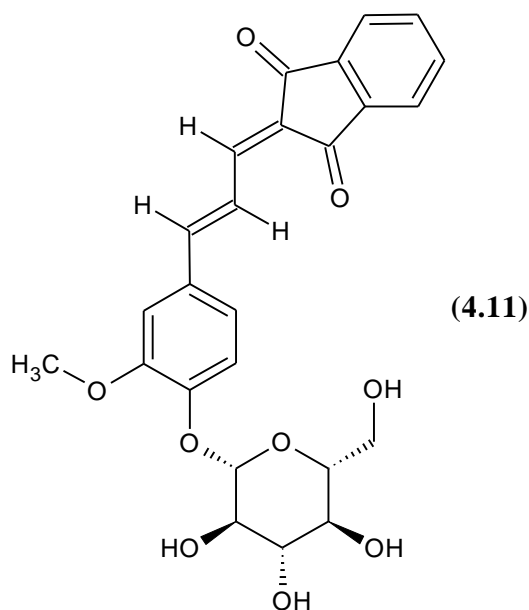


**Figure 4.5:** Structure of 4-β-D-glucosidoxy-3-methoxycinnamylidene-1,3-indandione.

NMR in  $d_6$ -DMSO - Spectrum too weak for analysis.

#### 4.2.4 Synthesis of 5-nitrosalicylaldehyde- $\beta$ -D-galactoside

This compound had previously been synthesised (Kroger and Thiem, 2007) but its biomedical properties had not been evaluated in great detail.

A Koenigs-Knorr reaction using 2,6-lutidine and silver carbonate was performed as for 4.2.2. 5-Nitrosalicylaldehyde (**3.17**) (1.67 g, 10 mmol) and acetobromo- $\alpha$ -D-galactose (**4.2**) (4.1 g, 10 mmol) were reacted to give acetylated nitrosalicylaldehyde- $\beta$ -D-galactoside (3.1 g, 62.3%, yield).

De-protection was performed with sodium methoxide as in previous glycosidations. The 5-nitrosalicylaldehyde- $\beta$ -D-galactoside crystals (**4.13**) were filtered under pressure then dried in a vacuum desiccator (1.72 g, 83.8% yield) (Figure 4.6).

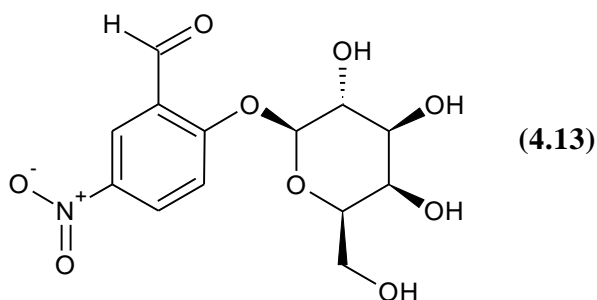


**Figure 4.6:** Structure of 5-nitrosalicylaldehyde- $\beta$ -D-galactoside.

#### Analytical data

Mp 198-201 °C (lit. 203 °C).

$^1\text{H-NMR}$  ( $d_6$ -DMSO, 270 MHz)  $\delta$  10.3 (1H, s, CHO), 8.5 (1H, d,  $J=8.0$  Hz, ArH), 8.3 (1H, d,  $J=6.4$  Hz, ArH), 7.1 (1H, d,  $J=8.9$  Hz, ArH), 4.7 (1H, d,  $J=15.1$  Hz, AlH), 3.2-3.8 (?H, om, AlH).

#### 4.2.5 Synthesis of 7,8-dihydroxy-4-methylcoumarin- $\beta$ -D-glucoside

A Koenigs-Knorr reaction using potassium hydroxide as a base was performed as for 4.2.3. 7,8-Dihydroxy-4-methylcoumarin (**3.9**) (0.96 g, 5 mmol) and acetobromoglucose (**4.15**) (3.1 g, 7.5 mmol) were reacted but, due to poor yield (<50 mg), the Koenigs-Knorr method using 2,6-lutidine and silver carbonate was attempted.

##### Alternative method for 7,8-dihydroxy-4-methylcoumarin- $\beta$ -D-glucoside

A Koenigs-Knorr reaction using 2,6-lutidine and silver carbonate was performed as for 4.2.2. 7,8-Dihydroxy-4-methylcoumarin (**3.9**) (0.96 g, 5 mmol) and acetobromoglucose (**4.15**) (2.1 g, 5 mmol) were reacted to give acetylated 7,8-Dihydroxy-4-methylcoumarin.

De-protection was performed with sodium methoxide as in previous glycosidations. The solid was recrystallised from hot ethanol. TLC showed a single spot on the baseline that charred. The 7,8-dihydroxy-4-methylcoumarin- $\beta$ -D-glucoside (**4.14**) crystals were filtered then dried in a vacuum desiccator (0.8 g, 45.2%, yield) (Figure 4.7).

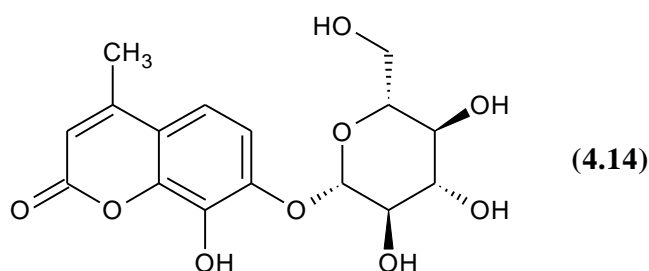


**Figure 4.7:** Structure of 7,8-dihydroxy-4-methylcoumarin- $\beta$ -D-glucoside.

NMR in  $d_6$ -DMSO - Spectrum too weak for analysis.

#### 4.2.6 Synthesis of alizarin-2-yl- $\beta$ -D-glucoside and $\beta$ -D-galactoside

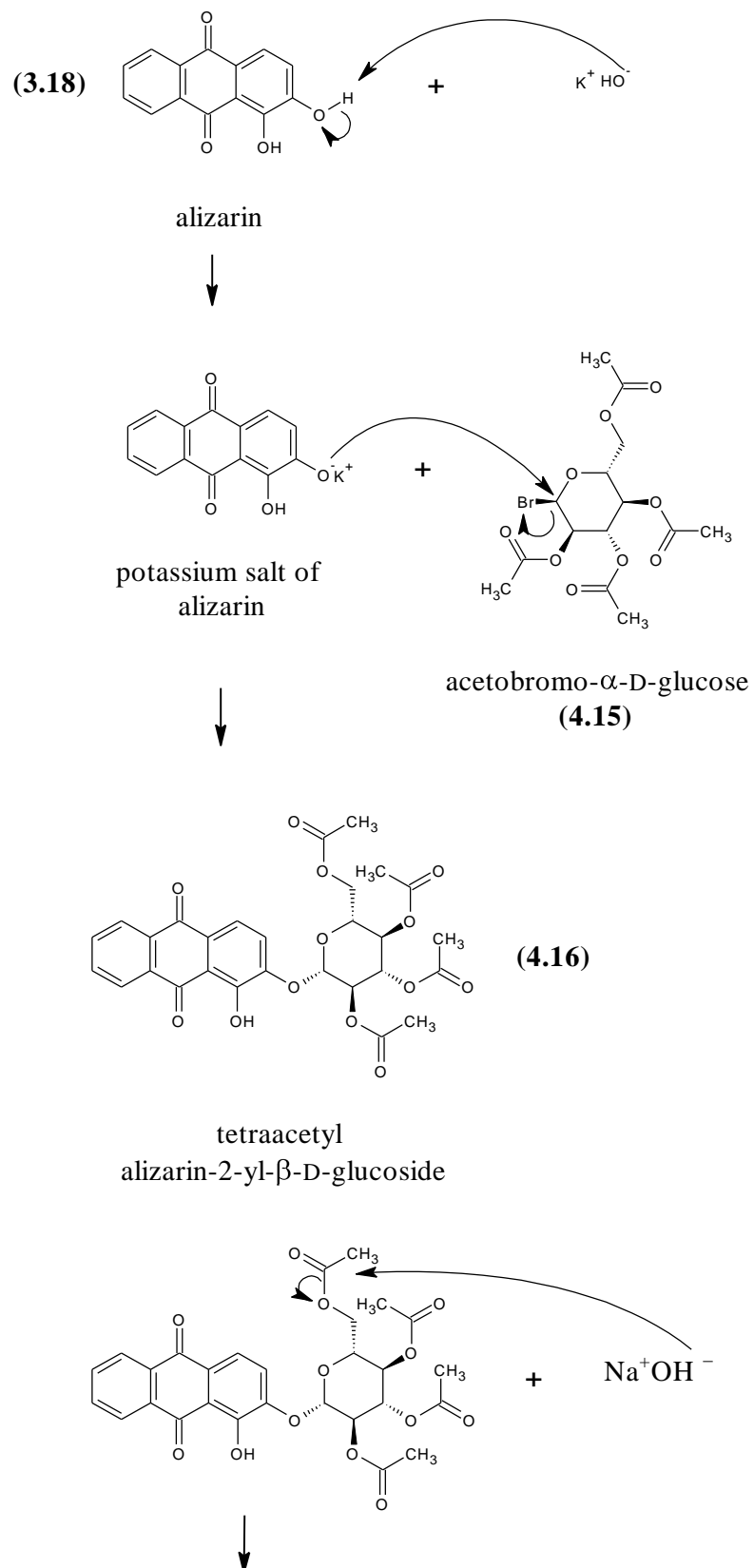
##### Synthesis of alizarin-2-yl- $\beta$ -D-glucoside

The galactoside analogue of this compound had previously been synthesised (James et al., 2000b) and a modified method was followed to produce the glucoside.

A Koenigs-Knorr reaction using potassium hydroxide as a base was performed.

Alizarin (**3.18**) (6 g, 25 mmol) was placed in a 250 ml conical flask and suspended in acetone (70 ml). To this, aqueous potassium hydroxide (70 ml, 0.3 M) was added and stirred. Acetobromo- $\alpha$ -D-glucose (**4.15**) (10.3 g, 25 mmol) was dissolved in acetone (10 ml) then added to the above solution and stirred for 12 h. More aqueous potassium hydroxide (10 ml, 1.25 M) was added, followed by acetobromo- $\alpha$ -D-glucose (4.1 g, 10 mmol) dissolved in acetone (5 ml). The solution was stirred for a further 12 h. The acetone was then removed by rotary evaporation at 40 °C. The pH of the solution was lowered to pH 5 by the addition of glacial acetic acid. The resulting precipitate was filtered and washed with cold H<sub>2</sub>O (50 ml). TLC, using ethyl acetate as a solvent, showed free alizarin as a red spot near the solvent front and also tetraacetyl-alizarin-glucoside as a pale yellow spot trailing that charred. The solid was dried in a vacuum dessicator then dissolved in DCM (200 ml) and triethylamine (2 ml, 20 mmol) added. Basic alumina was added until TLC showed no free alizarin remained in solution by the lack of a red spot near the solvent front. The solution was filtered and the filtrate was rotary evaporated at 40 °C to dryness. A yellow solid was produced (4.9 g, 34.4%, yield).

Tetraacetyl alizarin-2-yl- $\beta$ -D-glucoside (**4.16**) (1.1 g, 2 mmol) was added to methanol (60 ml) and stirred. Aqueous sodium hydroxide (30 ml, 0.125 M) was added to deprotect and gave a red solution. The solution was heated at 65 °C for 15 min, then cooled to 0 °C. The resulting precipitate (sodium salt of alizarin-2-yl- $\beta$ -D-glucoside (**4.17**)) was filtered and washed with ether (30 ml) then dried in a vacuum dessicator (0.5 g, 62.1% yield) (Figure 4.8)



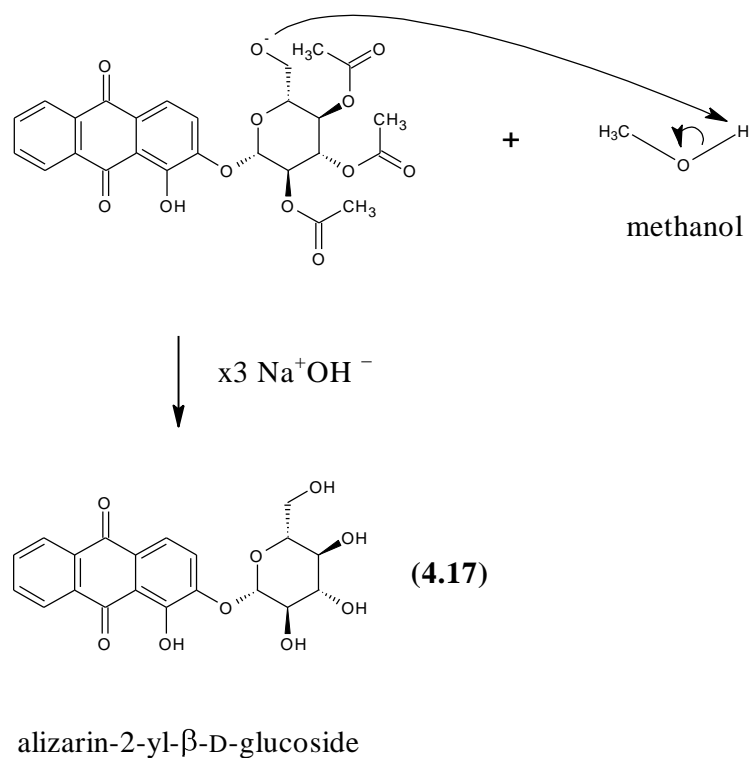


**Figure 4.8:** Formation of alizarin-2-yl- $\beta$ -D-glucoside. Glycosidation via Koenigs-Knorr potassium hydroxide method, deprotection using sodium hydroxide.

#### Analytical data

Mp 240-242 (lit. 237°C).

$^1\text{H-NMR}$  ( $\text{d}_6$ -DMSO, 270 MHz)  $\delta$  8.2 (1H, d,  $J=7.6$  Hz, ArH), 8.1 (1H, d,  $J=7.6$  Hz, ArH), 7.8 (1H, t,  $J=7.1$  Hz, ArH), 7.7 (1H, t,  $J=7.6$  Hz, ArH), 7.0 (2H, d,  $J=8.3$  Hz, ArH), 4.7 (1H, d,  $J=7.8$  Hz, AlH), 3.0-4.0 (?H, om, AlH).

### Synthesis of alizarin-2-yl- $\beta$ -D-galactoside

Alizarin-2-yl- $\beta$ -D-galactoside (**4.18**) had previously been synthesised and evaluated as a substrate to differentiate bacteria (James et al., 2000b), but the synthesis was repeated as the application of this substrate as a molecular biology tool was investigated later in this study.

The synthesis was as for alizarin-2-yl- $\beta$ -D-glucoside but acetobromo- $\alpha$ -D-galactose (**4.2**) (10.3 g, 25mmol) was substituted for acetobromo- $\alpha$ -D-glucose (yield 0.55 g, 68.3%) (Figure 4.9).

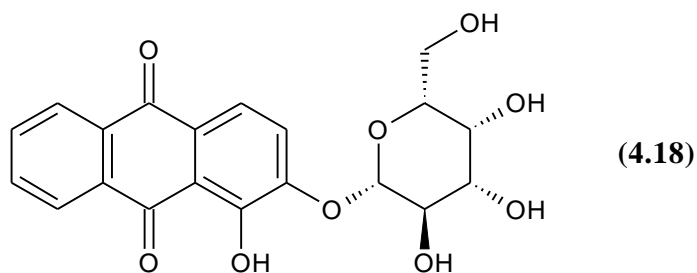


**Figure 4.9:** Structure of alizarin-2-yl- $\beta$ -D-galactoside.

### Analytical data

Mp 242°C (lit. 237°C).

$^1\text{H-NMR}$  ( $d_6$ -DMSO, 270 MHz)  $\delta$  8.3 (1H, d,  $J=7.4$  Hz, ArH), 8.1 (1H, d,  $J=7.4$  Hz, ArH), 7.8 (1H, t,  $J=7.2$  Hz, ArH), 7.7 (1H, t,  $J=7.3$  Hz, ArH), 7.1 (2H, d,  $J=8.2$  Hz, ArH), 4.7 (1H, d,  $J=7.7$  Hz, AlH), 3.0-4.0 (?H, om, AlH).

## 4.2.7 Synthesis of 3-hydroxyflavone- $\beta$ -D-glucoside and $\beta$ -D-galactoside

### Synthesis of 3-hydroxyflavone- $\beta$ -D-glucoside

A Koenigs-Knorr reaction using potassium hydroxide as a base was performed as for 4.2.3. 3-Hydroxyflavone (3HF) (**3.19**) (4.76 g, 20 mmol) and acetobromo- $\alpha$ -D-glucose (**4.15**) (8.2 g, 20 mmol) were reacted. When deprotected yielded 4.5 g, 56.2%, (Figure 4.10) 3-hydroxyflavone- $\beta$ -D-glucoside (**4.19**).

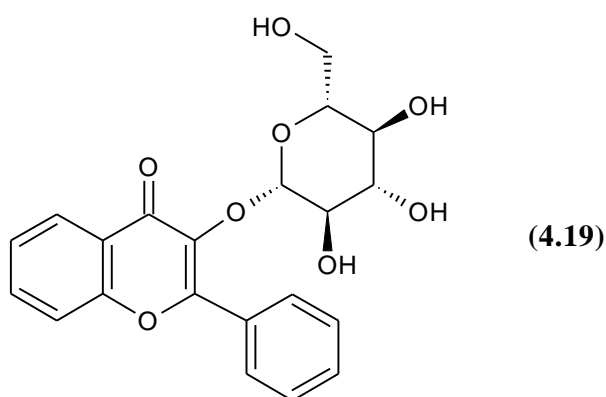


**Figure 4.10:** Structure of 3-hydroxyflavone- $\beta$ -D-glucoside.

### Analytical data

Mp 178-180 °C.

$^1\text{H-NMR}$  ( $d_6$ -DMSO, 270 MHz)  $\delta$  8.2 (2H, t,  $J=4.9$  Hz, ArH), 7.7-7.9 (3H, t,  $J=7.8$  Hz, ArH), 7.4 (4H, om, ArH), 3.0-5.5 (11H, om, AlH).

### Alternative method for the synthesis of 3-hydroxyflavone- $\beta$ -D-glucoside

A Koenigs-Knorr reaction using 2,6-lutidine and silver carbonate was performed as for 4.2.2. 3-Hydroxyflavone (**3.19**) (0.28 g, 5 mmol) and acetobromo- $\alpha$ -D-glucose (**4.15**) (3 g, 7.5 mmol) were reacted and when deprotected gave 0.1 g, 6.1 % yield of 3-hydroxyflavone- $\beta$ -D-glucoside (**4.19**).

### Synthesis of 3-hydroxyflavone- $\beta$ -D-galactoside

This compound had been previously synthesised (Chen et al., 2006). 3-Hydroxyflavone- $\beta$ -D-galactoside (**4.20**) was prepared as for 3-hydroxyflavone- $\beta$ -D-glucoside (Koenigs-Knorr method using potassium hydroxide), but acetobromo- $\alpha$ -D-galactose (**4.2**) (8.2 g, 20 mmol) was substituted for acetobromo- $\alpha$ -D-glucose (yield 4.0 g, 50.0%), (Figure 4.11).

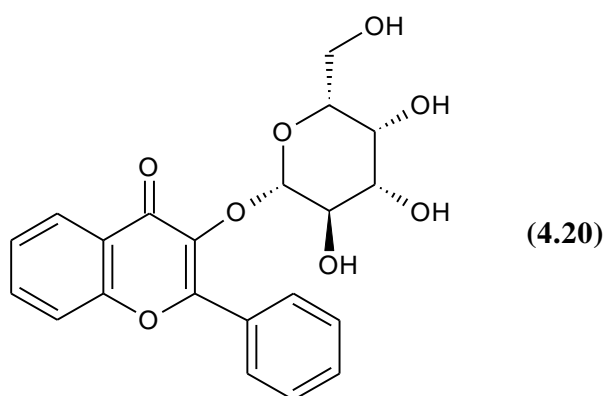


**Figure 4.11:** Structure of 3-hydroxyflavone- $\beta$ -D-galactoside.

### Analytical data

Mp 180-181 °C (lit. 175-177 °C).

$^1\text{H-NMR}$  ( $d_6$ -DMSO, 270 MHz)  $\delta$  8.2 (2H, t,  $J=4.9$  Hz, ArH), 8.1 (1H, t,  $J=7.9$  Hz, ArH), 7.9 (1H, t,  $J=7.8$  Hz, ArH), 7.8 (1H, t,  $J=4.2$  Hz, ArH) 7.5 (4H, om, ArH), 3.0-5.5 (11H, om, AlH).

#### 4.2.8 Synthesis of 1-methyl-2-(4'-fluorophenyl)-3-hydroxy-4(1*H*)-quinolone- $\beta$ -D-glucoside

A Koenigs-Knorr reaction using potassium tert-butoxide as a base was performed.

1-Methyl-2-(4'-fluorophenyl)-3-hydroxyquinolone (**3.15**) (1.35 g, 5 mmol) was suspended in dimethylformamide (10ml) with potassium tert-butoxide (0.56 g, 5 mmol) to form a potassium salt. The suspension was stirred until dissolved, then acetobromoglucose (**4.15**) (1.03 g, 2.5 mmol) was added. After 4 h, more acetobromoglucose (1.03 g, 2.5 mmol) was added and the solution was stirred for a further 24 h. TLC, using ethyl acetate as a solvent, showed a large spot above the base line which fluoresced green under U.V. light (1-methyl-2-(4'-fluorophenyl)-3-hydroxyquinolone) and a small spot near the solvent front which fluoresced blue under U.V. light and charred (acetylated 1-methyl-2-(4'-fluorophenyl)-3-hydroxyquinolone- $\beta$ -D-glucoside). To increase conversion to the tetraacetyl form, 18-crown-6 (0.13 g, 0.5 mmol) was added and the reaction stirred for another 24 h. TLC showed the reaction had not progressed therefore this method was abandoned.

#### Alternative method for 1-methyl-2-(4'-fluorophenyl)-3-hydroxy-4(1*H*)-quinolone- $\beta$ -D-glucoside

A Koenigs-Knorr reaction using 2,6-lutidine and silver carbonate was performed as for 4.2.2. 1-Methyl-2-(4'-fluorophenyl)-3-hydroxyquinolone (**3.15**) (1.35 g, 5 mmol) and acetobromoglucose (**4.15**) (2.9 g, 7 mmol) were reacted to produce acetylated 1-methyl-2-(4-fluorophenyl)-3-hydroxyquinolone- $\beta$ -D-glucoside (1.5 g, 50.0%, yield).

De-protection was performed with sodium methoxide as in previous glycosidations (0.92 g, 85.3%, yield 1-methyl-2-(4'-fluorophenyl)-3-hydroxy-4(1*H*)-quinolone- $\beta$ -D-glucoside (**4.21**)) (Figure 4.12).

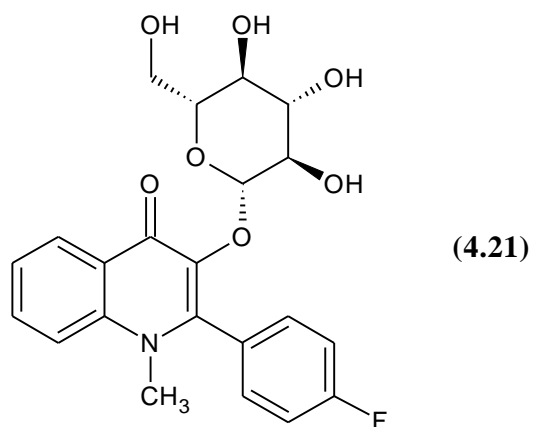


**Figure 4.12:** Structure of 1-methyl-2-(4'-fluorophenyl)-3-hydroxy-4(1*H*)-quinolone- $\beta$ -D-glucoside.

Analytical data

$^1\text{H-NMR}$  ( $\text{d}_6\text{-DMSO}$ , 270 MHz)  $\delta$  7.0-8.3 (8H, om, Ar*H*), 4.9(1H, d,  $J=3.5$  Hz, Ar*H*), 2.3 (3H, s,  $\text{CH}_3$ ), 2.8-4.3 (?H, om, Al*H*). Impure.

#### 4.2.9 Synthesis of 5,7-dichloro-8-hydroxy-2-methylquinoline- $\beta$ -D-galactoside

A Koenigs-Knorr reaction using potassium hydroxide as a base was performed as for 4.2.3. 5,7-Dichloro-8-hydroxy-2-methylquinoline (Sigma) (**3.20**) (1.14 g, 5 mmol) and acetobromo- $\alpha$ -D-galactose (**4.2**) (2 g, 5 mmol) were reacted to give acetylated 5,7-dichloro-8-hydroxy-2-methylquinoline- $\beta$ -D-galactoside (1.6 g, 57.3%, yield). The solid was dissolved in methanol (20ml).

De-protection was performed with sodium methoxide as in previous glycosidations (0.95 g, 85.0% yield of 5,7-dichloro-8-hydroxy-2-methylquinoline- $\beta$ -D-galactoside (**4.22**)) (Figure 4.13).

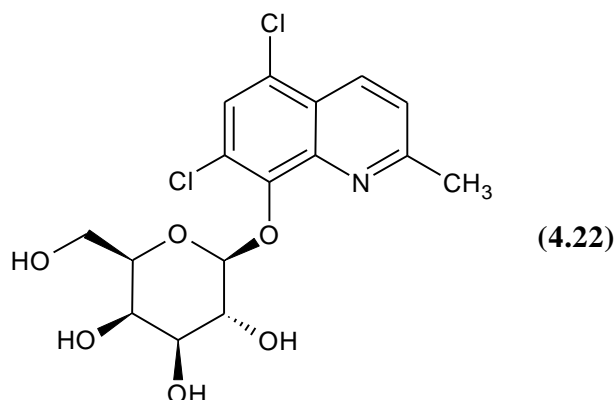


**Figure 4.13:** Structure of 5,7-dichloro-8-hydroxy-2-methylquinolone- $\beta$ -D-galactoside.

#### Analytical data

Mp 242 °C.

$^1\text{H-NMR}$  ( $d_6$ -DMSO, 270 MHz)  $\delta$  8.5 (1H, d,  $J=8.6$  Hz, ArH), 7.9 (1H, s, ArH), 7.7 (1H, d,  $J=8.6$  Hz, ArH), 6.4 (1H, om, ArH), 5.1-5.2 (2H, dd,  $J_1=7.6$  Hz,  $J_2=6.0$  Hz, ArH), 4.5-4.7 (2H, dd,  $J_1=4.5$  Hz,  $J_2=4.4$  Hz, AlH), 3.3-3.8 (?H, om AlH), 2.7 (3H, s,  $\text{CH}_3$ ).

#### 4.2.10 Synthesis of naphthofluorescein- $\beta$ -D-glucoside

A Koenigs-Knorr reaction using potassium hydroxide as a base was performed as for 4.2.3. Naphthofluorescein (**2.23**) (1.3 g, 3 mmol) and acetobromo- $\alpha$ -D-glucose (**4.15**) (2.06 g, 5 mmol) were reacted but, it was not possible to dry the naphthofluorescein-tetraacetyl-glucoside therefore the deprotection was not attempted.

##### Alternative method for the synthesis of naphthofluorescein- $\beta$ -D-glucoside

A Koenigs-Knorr reaction using 2,6-lutidine and silver carbonate was performed as for 4.2.2. Naphthofluorescein (**2.23**) (1.3 g, 3 mmol) and acetobromoglucose (**4.15**) (2.5 g, 6 mmol) were reacted to give acetylated naphthofluorescein- $\beta$ -D-glucoside (1.42 g, 62.1%, yield).

Removal of the acetyl groups from the protected galactoside (de-protection) was attempted with sodium methoxide (2 ml, 200 mmol) (see Appendix A) but failed to give rise to a product from which a compound could be isolated successfully.

NMR in  $d_6$ -DMSO not possible due to the insolubility of the compound.

#### 4.2.11 *p*-Naphtholbenzein- $\beta$ -D-galactoside

This synthesis was not attempted, since a galactoside sample of *p*-naphtholbenzein (4.23) had already been prepared (James et al., 2000a) (Figure 4.14) via the Koenigs-Knorr method using potassium hydroxide as a base and had been evaluated by Prof. J. Perry at Freeman Hospital. However, the application of this substrate as a molecular biology tool was investigated later in this study. Also the microbiological results of this substrate were included for comparative purposes.

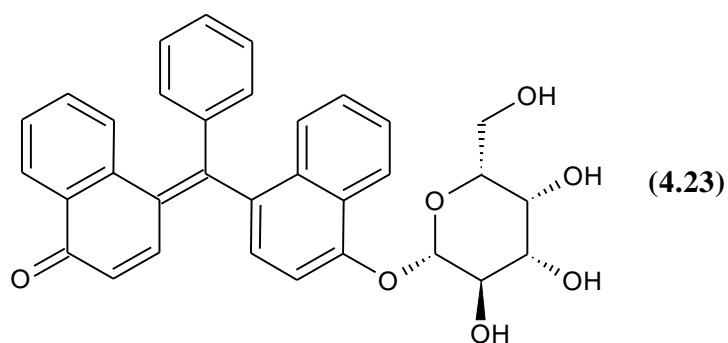


**Figure 4.14:** Structure of *p*-naphtholbenzein- $\beta$ -D-galactoside.

### 4.3 Carboxylic esters introduction

It was decided to concentrate mainly on the esters since these have value in microbiological identification of *Salmonella* spp. (Manafi and Sommer, 1992; Cooke et al., 1999; Perez et al., 2003).

Because esters are frequently relatively unstable, the synthesis of esters was confined to the molecule of alizarin, since it had been found previously that the esters of this dihydroxy compound are relatively stable in comparison to other phenolic esters.

The following esters were synthesised:

- Alizarin-2-octanoate
- Alizain-2-palmitate
- Alizarin benzoate

These were prepared by a standard technique involving the particular acid chloride. It was necessary to use an acyl chloride or an acyl halide or an acyl anhydride in this procedure to form the particular ester.

## 4.4 Carboxylic esters experimental methods and mechanisms

### 4.4.1 Synthesis of alizarin-2-octanoate

This compound had been previously synthesised (Mellidis and Papageorgiou, 1986), but its biological properties had not been evaluated.

Alizarin (**3.18**) (4.8 g, 20 mmol) and dry dichloromethane (150 ml) were added to a 500 ml round bottomed flask and stirred until dissolved. Triethylamine (**4.24**) (4.1 g, 40 mmol) was then added and stirred.

Octanoyl chloride (**4.25**) (3.25 g, 20 mmol) was dissolved in dry dichloromethane (10 ml) then dripped into the above alizarin solution and stirred for 1 h. The solution went from purple to an orange/yellow colour. Thin layer chromatography (TLC), performed in ethyl acetate, showed a leading yellow spot (alizarin-2-octanoate) with a purple trail (alizarin). To remove some of the unreacted alizarin, aluminium oxide (25 g) was added and stirred for 15 min then the mixture was filtered.

The pH of the solution was then neutralized by the addition of acetic acid. As the pH decreased the colour changed from orange/yellow to yellow. The solution was then evaporated under reduced pressure at 40 °C. Dryness was achieved by increasing the temperature to 70 °C to evaporate the last of the liquid. Yellow crystals were formed. TLC showed a leading yellow spot (alizarin-2-octanoate) with a slight purple trail (alizarin).

The crystals were dissolved in acetone (50 ml), transferred to a 100 ml round bottomed flask and rotary evaporated until ~20 ml remained. 60-80 Light petroleum (1 ml) was added which caused the alizarin-2-octanoate (**4.26**) to precipitate, leaving the unreacted alizarin in the acetone. The solution was cooled to -20 °C for 30 min to maximise crystallisation then filtered. TLC showed a single yellow spot with no purple trail. The crystals were dried in a vacuum desiccator (4.3 g, 58.7%, yield) (Figure 4.15).

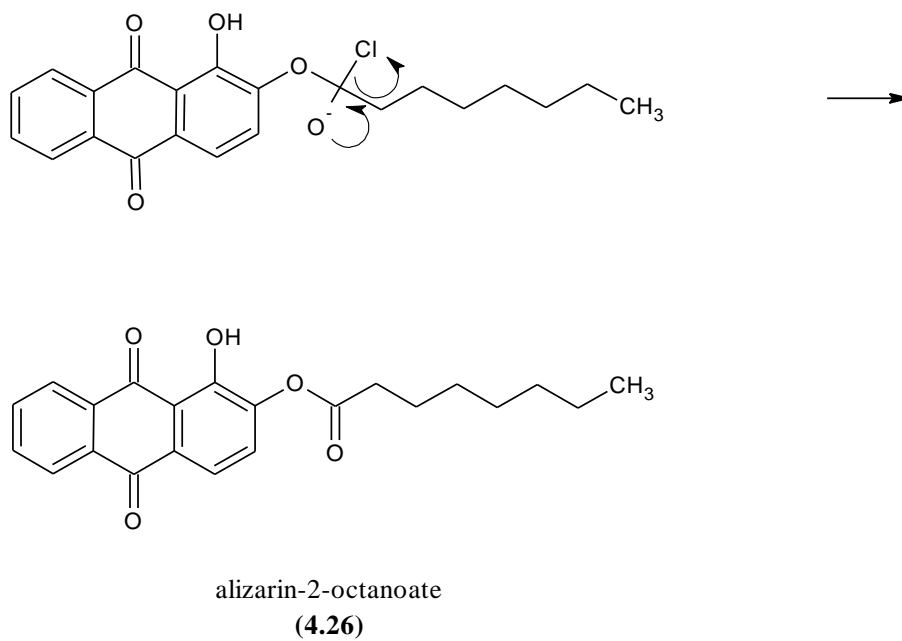
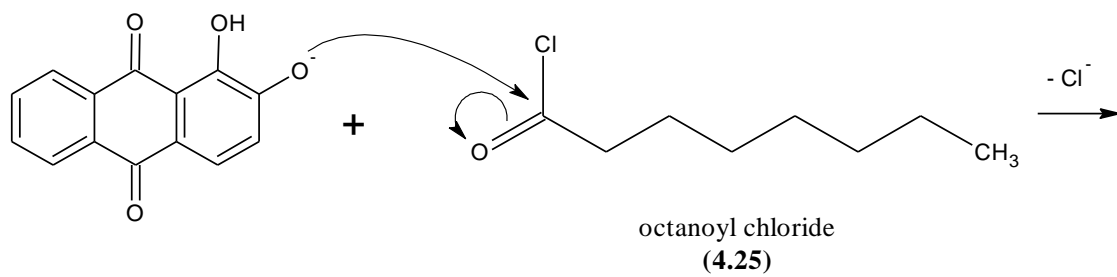
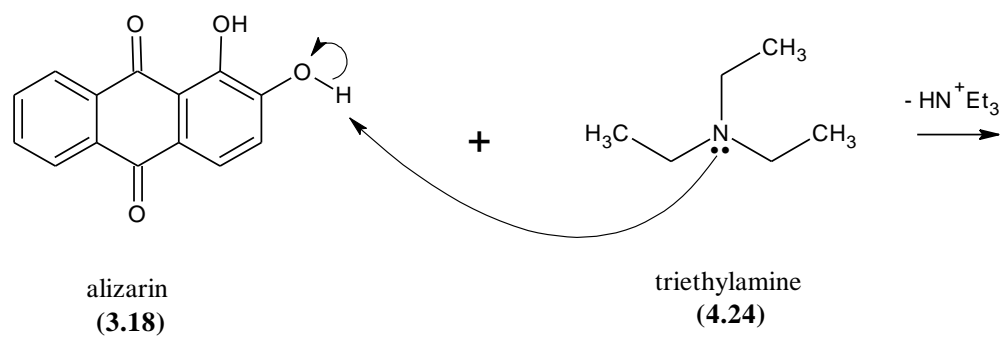


**Figure 4.15:** Formation of alizarin-2-octanoate.

### Analytical data

Mp 122-124 °C (lit. 121-123 °C).

<sup>1</sup>H-NMR (d<sub>6</sub>-DMSO, 270 MHz) δ 7.5-8.3 (3H, t, *J*=7.8 Hz, ArH), 2.7 (2H, t, *J*=7.3 Hz, CH<sub>2</sub>), 1.6 (2H, p, *J*=6.3 Hz, ArH), 1.2 (8H, om, ArH) 0.8 (3H, s, CH<sub>3</sub>).

### 4.4.2 Synthesis of alizarin-2-palmitate

The procedure for the preparation of 4.4.1 alizarin-2-octanoate was followed substituting palmitoyl chloride (**4.27**) (5.5 g, 20 mmol) for octanoyl chloride. Crystallisation was achieved by dissolving the crude material in hot methanol (50 ml), and cooling to -20 °C (5.3 g, 55.4%, yield of alizarin-2-palmitate (**4.28**)) (Figure 4.16).

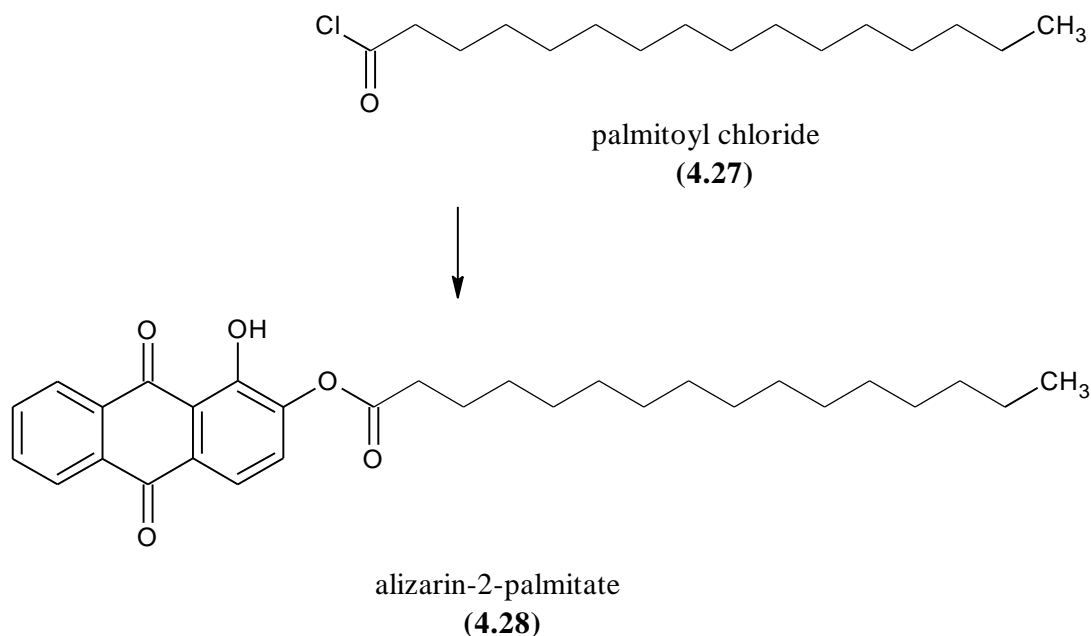


**Figure 4.16:** Formation of alizarin-2-palmitate.

### 4.4.3 Synthesis of alizarin-2-benzoate

Alizarin-2-benzoate (**4.30**) had been previously synthesised (Green, 1927). The procedure for the preparation of 4.4.1 alizarin-2-octanoate was followed substituting benzoyl chloride (**4.29**) (2.8 g, 20 mmol) for octanoyl chloride. Crystallisation was achieved by dissolving the crude material in hot methanol (50 ml) and cooling to -20 °C (6.0 g, 87.1% yield) (Figure 4.17).

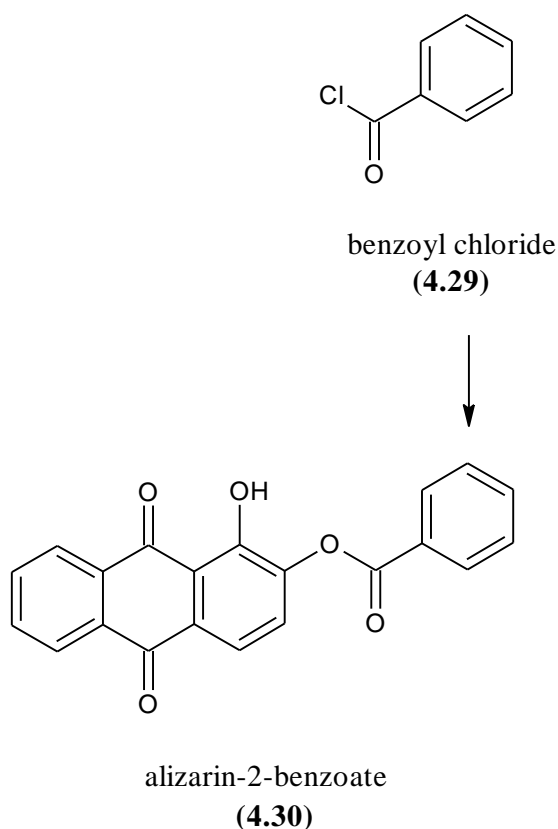


**Figure 4.17:** Formation of alizarin-2-benzoate.

#### Analytical data

Mp 213-214 °C (lit. 208-210 °C).

## 4.5 Results

Examination of the properties of selected glycosides which were synthesised fall into three broad categories:

- a) Examination in a microbiological situation, usually as a plate method to assess their capability to differentiate between different spp of bacteria.
- b) Molecular biology application as device for the screening of recombinant and non-recombinant transformants.
- c) Biochemical characteristics, enzyme assay, kinetics.

### 4.5.1 Microbiological evaluation

The microbiological work was mainly carried out by Professor John Perry at Freeman Hospital, Department of Microbiology and the author is indebted to him for the information and the related photographs which appear subsequently.

In this section, the results are presented in comparison to various known glycosidase substrates which are being used in bacterial identification such as those based on Alizarin and *p*-naphtholbenzein.

All substrates were dissolved in 1-methyl-2-pyrrolidone (1 ml) then incorporated into either Columbia agar (4.06 g/99 ml distilled water) which had previously been sterilised, then cooled to 50 °C or, in the case of possible chelators, the same agar, but containing 500 mg/L ferric ammonium citrate (FAC) (Table 4.1). Control plates with no substrates, only Columbia agar or Columbia agar containing FAC were also prepared.

**Table 4.1:** Substrate quantity and media selection.

Substrate	Amount (mg)	Columbia agar	Columbia agar + FAC
alizarin-2-yl-β-D-galactoside	5	×	✓
4-β-D-glucosidoxy-3-methoxycinnamylidene-1,3-indandione	20	✓	×
3-hydroxyflavone-β-D-glucoside	30	×	✓
<i>p</i> -naphtholbenzein-β-D-galactoside	10	✓	×
5-nitrosalicylaldehyde-β-D-galactoside	30	×	✓

The substrates were tested against a range Gram-negative and positive-bacteria and also yeasts. Inocula for each type of microorganism were prepared in physiological saline to give a suspension equivalent to 0.5 McFarland units (approximately

100,000 colony forming units/ $\mu\text{l}$ ). The inocula (1  $\mu\text{l}$ ) were applied to the agar plate using multi-point inoculation (Denley), the pattern of which can be seen in Figure 4.18. The plates were then incubated at 37 °C for 24 h, the results of which can be seen in Table 4.2. Images of the more successful plates can be seen in Figure 4.19.

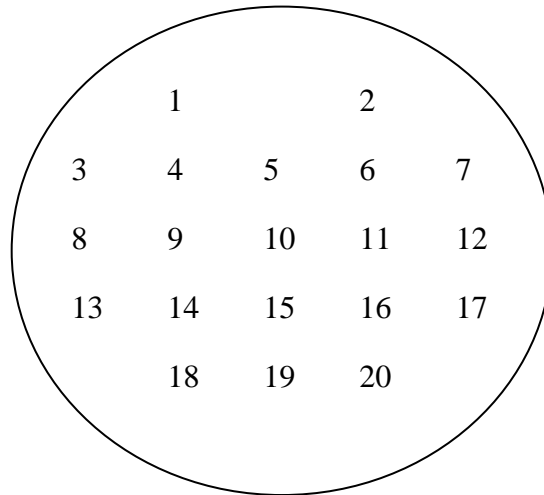


**Figure 4.18:** Pattern of multi-point inoculation. Numbers correspond to the microorganisms in Table 4.2

**Table 4.2:** Microbiological evaluation of selected substrates.

Bacteria	Control Growth	Control* Growth	Aliz-gal Growth	Aliz-gal Colour	MCI-gluc Growth	MCI-gluc Colour	3HF-gluc Growth	3HF-gluc Colour	PNB-gal Growth	PNB-gal Colour	NSA-gal Growth	NSA-gal Colour
<b>Gram negatives</b>												
1 <i>E. coli</i> NCTC 10418	+	+	+	++Purple	+	-	+	Tr.brown	+	+orange	+	+orange(D)
2 <i>S. marcescens</i> NCTC 10211	+	+	+	++Purple	+	-	+	-	+	+orange	+	+orange(D)
3 <i>Ps. Aeruginosa</i> NCTC 10662	+	+	+	-	+	-	+	-	+	-	+	-
4 <i>B. cepacia</i> LMG 1222	+	+	+	-	+	-	+	-	+	-	+	-
5 <i>Y. enterocolitica</i> NCTC 11176	+	+	+	-	+	-	+	-	+	-	+	-
6 <i>S. typhimurium</i> NCTC 74	+	++	+	-	+	-	+	-	+	-	+	-
7 <i>C. freundii</i> 46262 (wild)	+	+	+	++Purple	+	-	+	-	+	+orange	+	+orange(D)
8 <i>M. morgani</i> 462403 (wild)	+	++	+	-	+	-	+	-	+	-	+	-
9 <i>E. cloacae</i> NCTC 11936	+	++	+	++Purple	+	-	+	-	+	+orange	+	+orange(D)
10 <i>P. rettgeri</i> NCTC7475	+/-	++	Tr.	-	Tr.	-	+/-	-	+/-	-	+/-	-
<b>Gram Positives</b>												
11 <i>B. subtilis</i> NCTC 6372	+	+	+	-	+	-	+	+brown	+/-	-	+	-
12 <i>E. faecalis</i> NCTC 775	+	+	+	++Purple	+	-	+	+brown	-	-	+	-
13 <i>E. faecium</i> NCTC 7171	+	+	+	++Purple	+	-	+	+brown	+	-	+	-
14 <i>St. epidermidis</i> NCTC 11047	+	+	+	-	+	-	+	-	-	-	+	-
15 <i>St. aureus</i> NCTC 6571	+	+	+	++Purple	+	-	+	-	+	-	+	-
16 <i>M.R.S.A.</i> NCTC 11939	+	+	+	++Purple	+	-	+	Tr.brown	+	-	+	-
17 <i>S. pyogenes</i> NCTC 8306	+	+	+	-	+	-	+	-	-	-	+	-
18 <i>L. monocytogenes</i> NCTC 11994	+	+	+	-	+	-	+	++brown	+	-	+	-
<b>Yeasts</b>												
19 <i>C. albicans</i> ATCC 90028	+	+	+	-	+	-	+	-	+	-	+	-
20 <i>C. glabrata</i> NCPF 3943	+/-	+/-	+/-	-	+/-	-	+/-	-	+/-	-	+/-	-

Growth code: + good,  
+/- weak,  
Tr. trace,  
- none.

Colouration code: ++ strong  
+ moderate  
Tr. trace  
- none

\* Control containing ferric ammonium citrate

(D) diffusion of colour

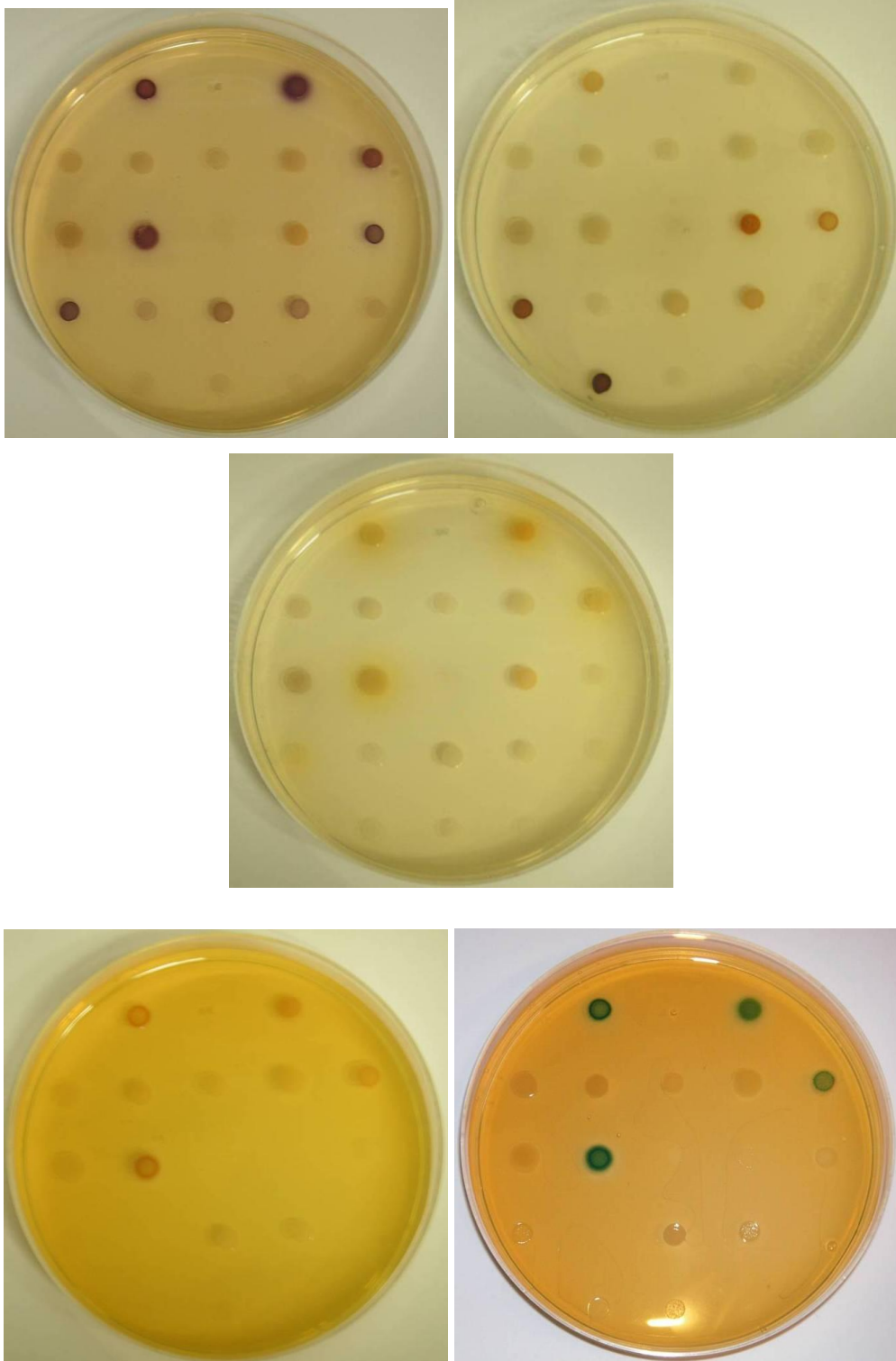


**Figure 4.19:** Multi-point inoculation of (from top left) Aliz-gal, 3HF-gluc, NSA-gal, PNB-gal and PNB-gal exposed to NaOH (1 M).

The fluorescence properties of 3HF-gluc were evaluated by incorporating the substrate in agar as described in Table 4.1, except for replacing ferrous ammonium citrate with zinc acetate (500 mg/L). The agar plate was inoculated with *Serratia marcescens* NCTC 10211 and incubated at 37 °C for 17 h.

*Serratia marcescens* NCTC 10211, a  $\beta$ -glucosidase producing Gram-negative bacterium, showed no or little activity with the same substrate when tested under the conditions described previously. When exposed to U.V. light, evidence of enzyme activity could be seen in the form of fluorescent colonies (Figure 4.20), indicating that the fluorescence properties of this substrate were highly sensitive when compared to its chromogenic properties.

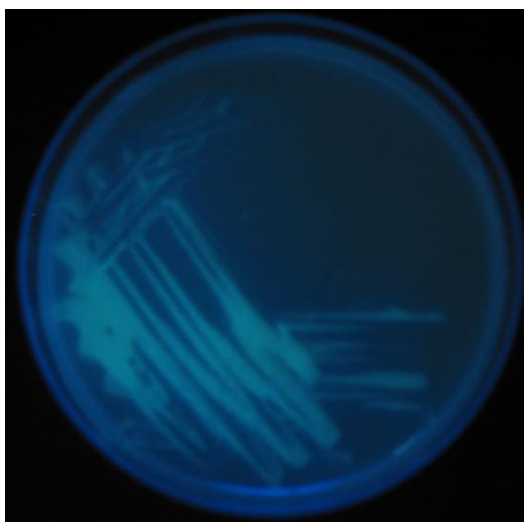


**Figure 4.20:** Hydrolysis of 3HF-gluc by *Serratia marcescens* NCTC 10211 as seen under U.V. light.

#### 4.5.2 Biochemical evaluation

To further evaluate 3-hydroxyflavone- $\beta$ -D-glucoside, an assay with  $\beta$ -glucosidase was devised and its reaction kinetics determined.

##### Enzyme kinetics of 3-hydroxyflavone- $\beta$ -D-glucoside

1 mmol of 3-hydroxyflavone (3HF) (Sigma) (Figure 4.21) was dissolved in the minimum amount of ethanol and made to one litre with distilled water. The fluorescence maximum ( $\lambda_F$ ) of this core compound (Figure 4.22) was determined using a Hitachi F-4000 fluorescence spectrophotometer and found to be Ex 380, Em 530 nm.

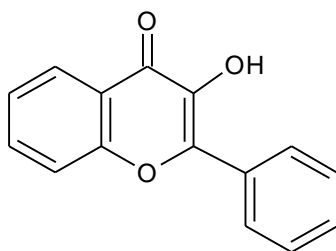


**Figure 4.21:** Structure of 3-hydroxyflavone (3HF).

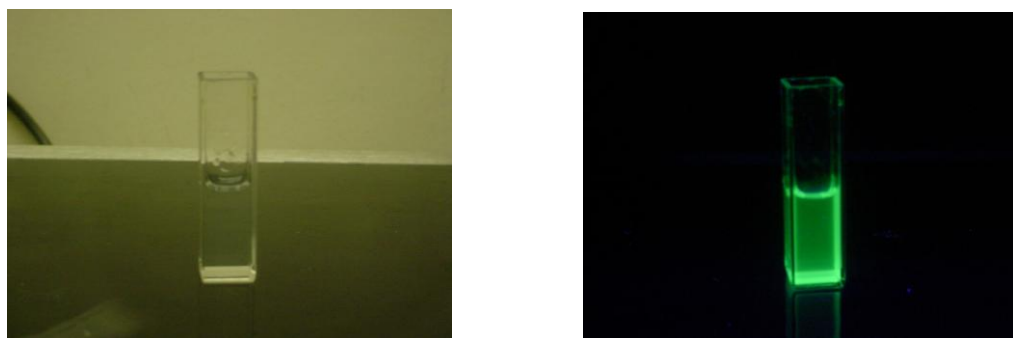


**Figure 4.22:** Fluorescence of 3HF.

It has been documented that 3HF can chelate with certain metal ions (Cornard and Merlin, 2003; Valente et al., 2007) (Figure 4.23) and the products of these chelations or complexes have different  $\lambda_F$  (Boudet et al., 2000; Protti et al., 2008). These changes in  $\lambda_F$  can be explained by the complexes forming different structures, i.e. their shape.

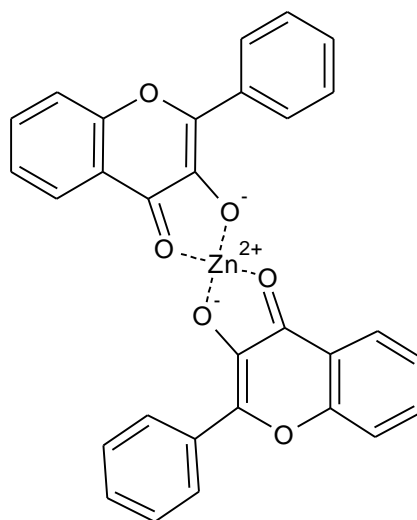


**Figure 4.23:** 3HF chelation with zinc.

The effects of three possible metal chelations were investigated; aluminium, magnesium and zinc (Table 4.3). From these preliminary measurements, zinc was selected for further study as it gave the greatest increase in fluorescence.

**Table 4.3:** Fluorescence of 3HF metal complexes. 1 mmol/L 3HF was dissolved in 50% (v/v) ethanol and varying amounts of metal (2, 10 and 100  $\mu$ moles) were added.

Metal	$\lambda_F$	2 $\mu$ moles	10 $\mu$ moles	100 $\mu$ moles
Aluminium	390 <sub>Ex</sub> 460 <sub>Em</sub>	55	60	25
Magnesium	418 <sub>Ex</sub> 480 <sub>Em</sub>	522	248	26
Zinc	408 <sub>Ex</sub> 475 <sub>Em</sub>	1048	522	37

A more in depth study was made of the effect zinc concentration had on fluorescence (Figure 4.24).

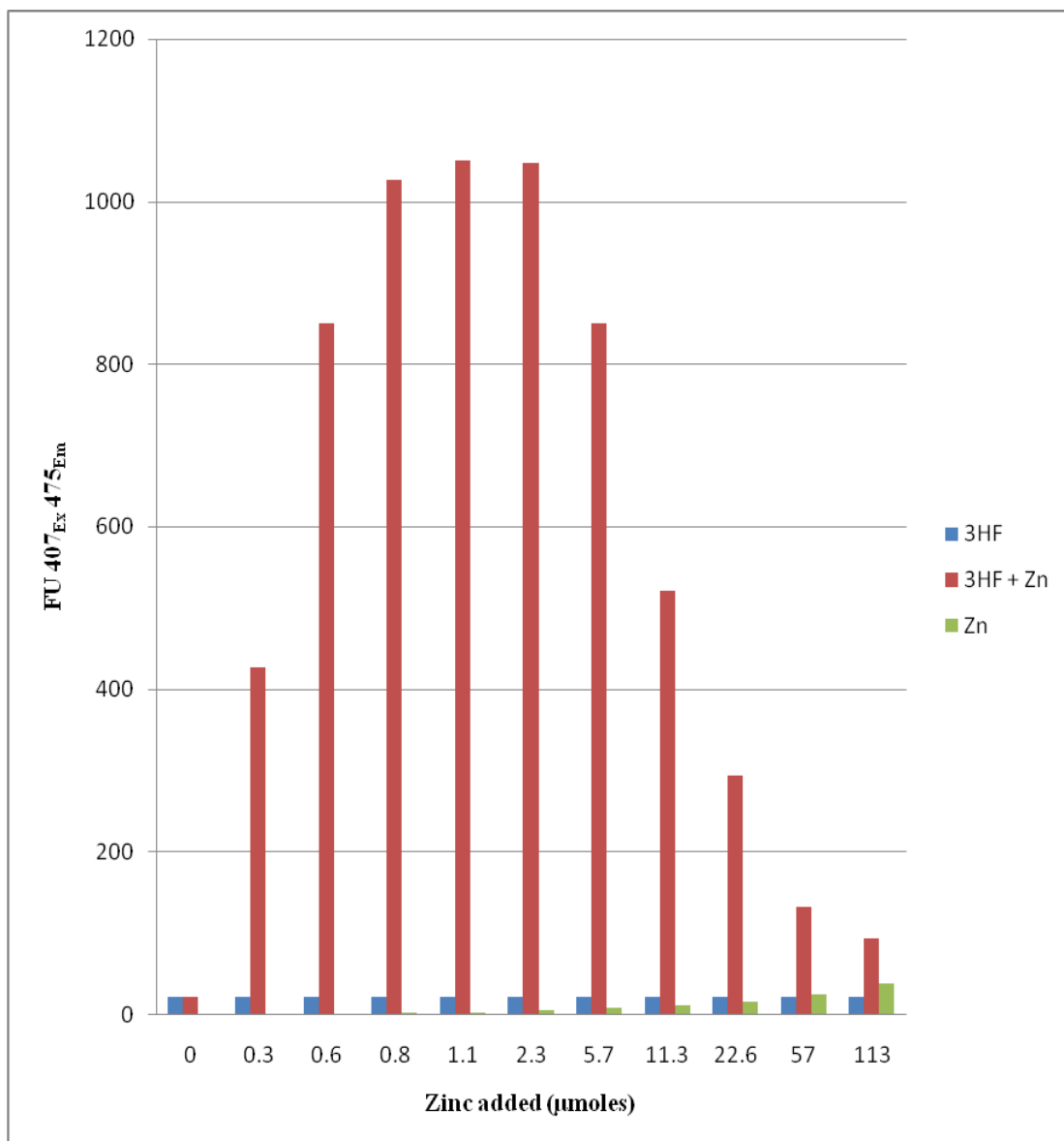


**Figure 4.24:** Fluorescence measurements of 3HF + varying amounts of zinc compared to the effects of the same quantities of 3HF and zinc separately.

From this data it was determined that optimum fluorescence was achieved when 1.1 µmoles of zinc were added to a sample containing 2 µmoles (2 ml of 1 mmol/L) of 3HF. This corresponded to the theory that if the complex formed has the same

structure as previous studies have ascertained (Cornard and Merlin, 2003; Valente et al., 2007) (Figure 4.23 above), two molecules of 3HF are bound to one molecule of zinc, and if 2 ml of 1 mmol/L 3HF contains 2  $\mu$ moles then the greatest fluorescence should be obtained when 1  $\mu$ mole of zinc was added.

The complex has increased in size and planarity compared to a free 3HF molecule. This may explain the dramatic increase in fluorescence found with the complex. It can also be noted, that as the excess amount of zinc increased, a quenching effect took place decreasing the amount of fluorescence.

The glucoside of 3HF (3HF-gluc) was then reacted with  $\beta$ -glucosidase enzyme (Sigma) at varying pH using the following reaction mixture.

2 ml 0.05 M sodium acetate/acetic acid buffer containing:-

1 mmol/L 3HF-gluc

1  $\mu$ l 5 M zinc sulphate

0.05 ml 10 g/L  $\beta$ -glucosidase

So as not to affect the concentrations and pH of the reactants, zinc was to be delivered in a small volume and therefore of high concentration (i.e. 1  $\mu$ l of 5 M ZnSO<sub>4</sub> which contains 1.132  $\mu$ moles Zn). The reactions were monitored for 30 min, at 37 °C, at pH 5-8 and the rates of the reaction are shown (Figure 4.25).

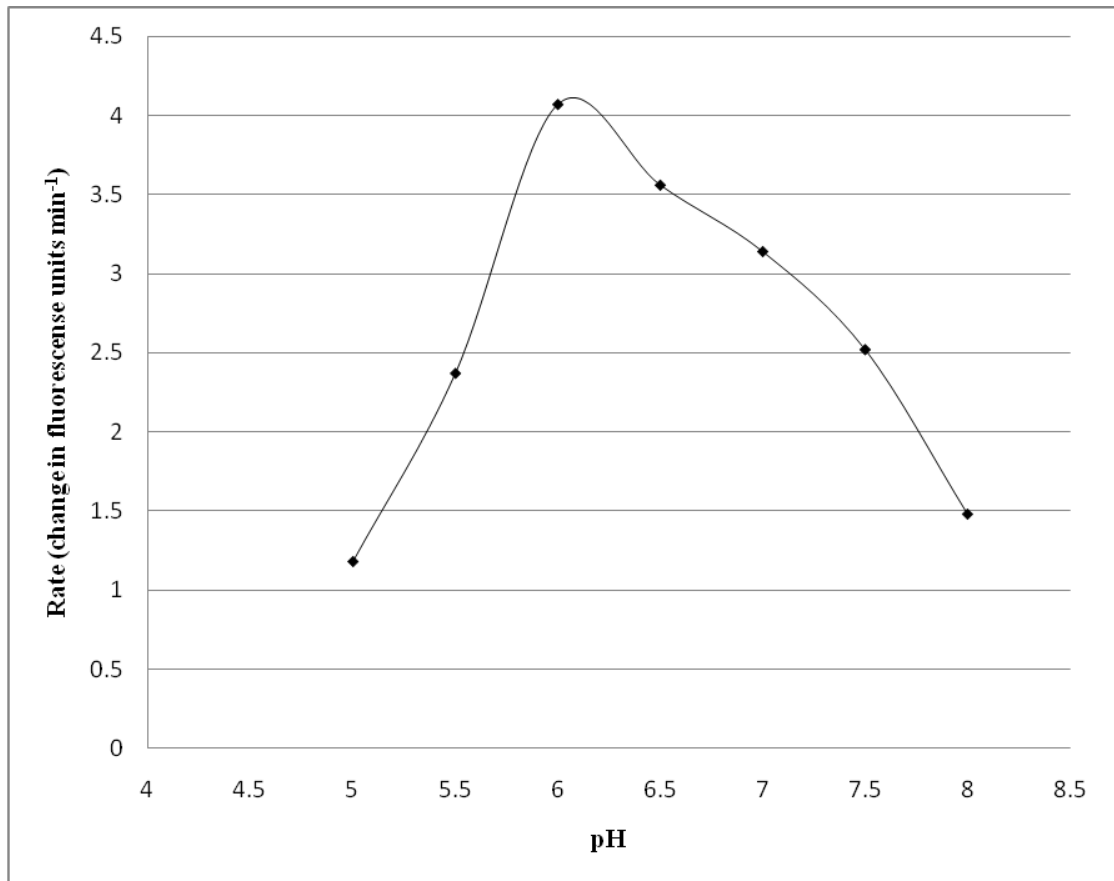


**Figure 4.25:** Rate of reactions of 3HF-gluc and  $\beta$ -glucosidase at pH 4-8.

The pH optimum for this enzyme system was determined to be pH 6.

Using the same reaction mixture at pH 6, the substrate concentration was varied (Figure 4.26).

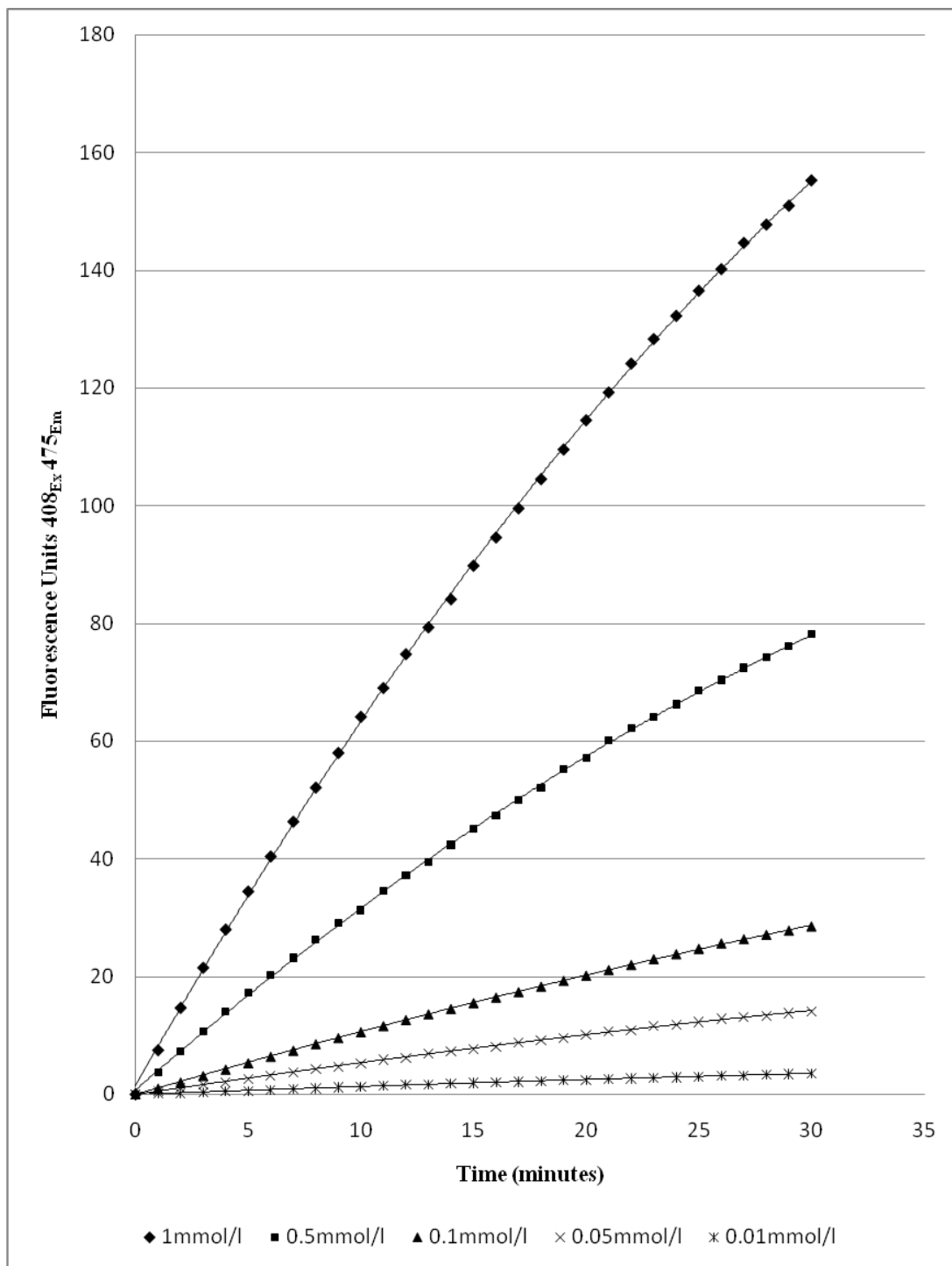


**Figure 4.26:** Rate of reactions of 3HF-gluc and  $\beta$ -glucosidase at substrate concentrations 0.01-1 mmol/L.

To convert FU into concentrations (mmol/L) of 3HF complex, a standard curve was prepared and measured. A linear relationship between FU and 3HF concentration was found to exist up to 0.75 mmol/L (Figure 4.27).

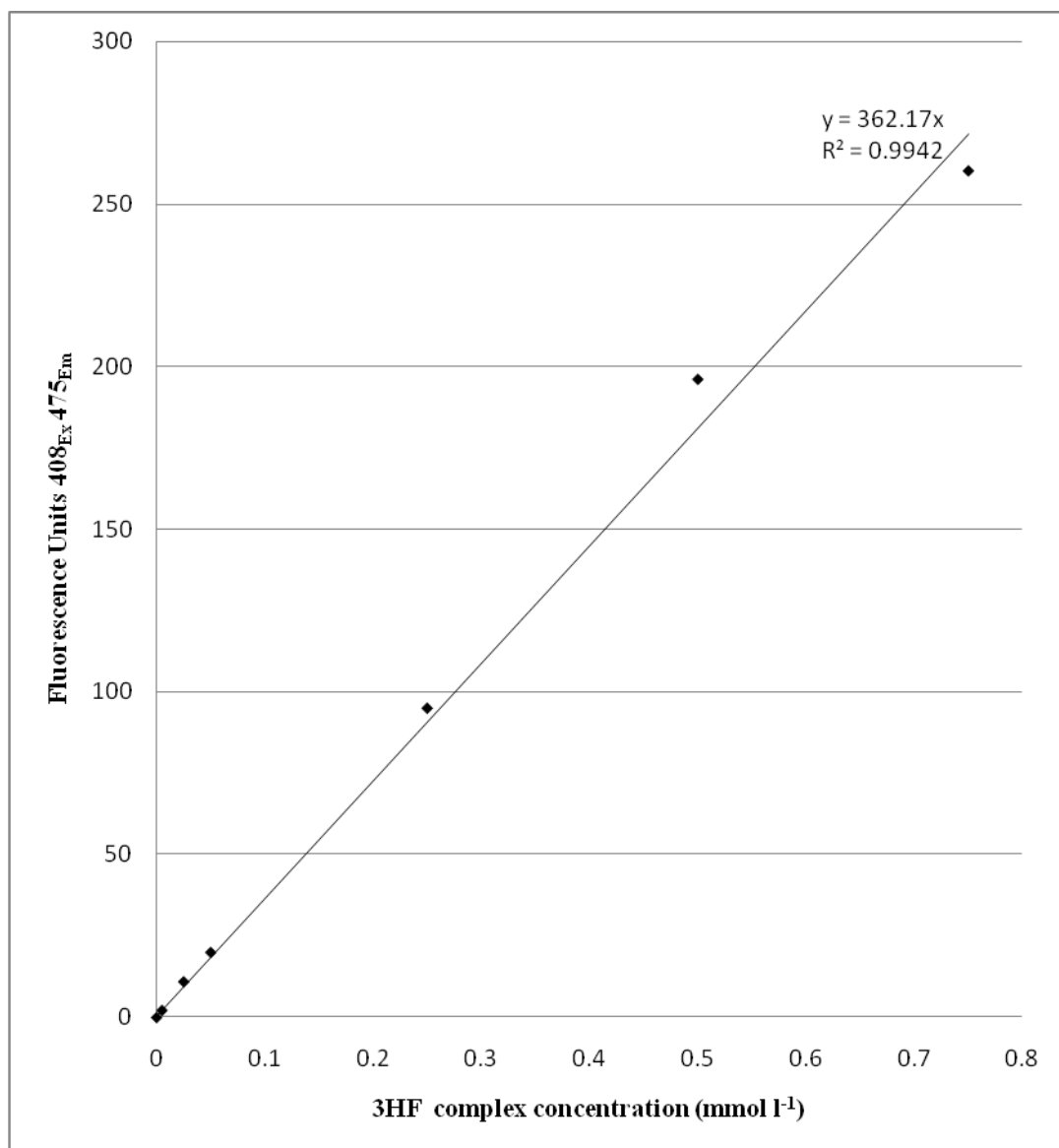


**Figure 4.27:** Linear standard curve for 3HF complex.

This, along with the results gained from varying the substrate concentration, can be used to calculate the following kinetics data (Figure 4.28).

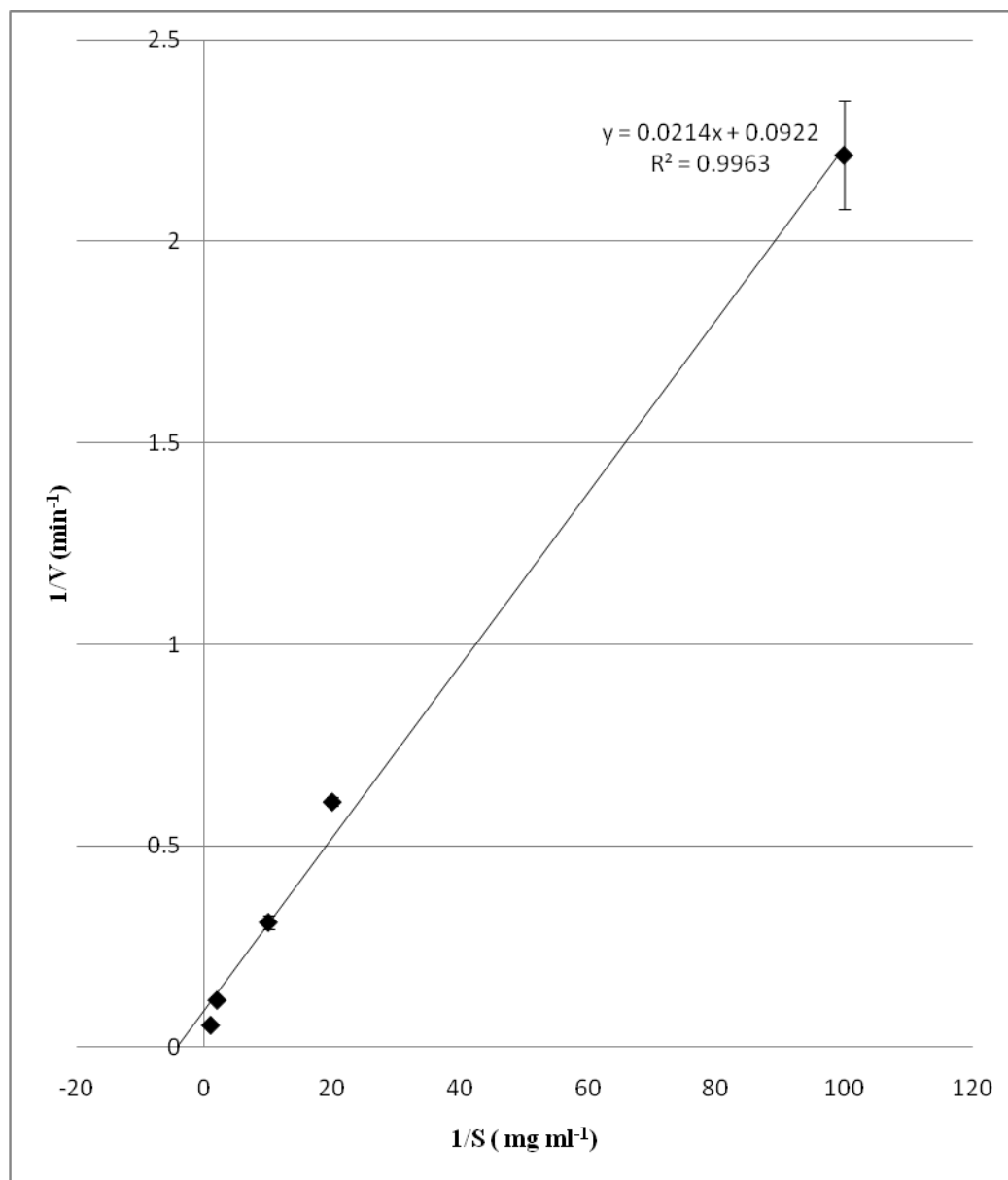


**Figure 4.28:** Lineweaver-Burk plot for 3HF-gluc.

A linear trendline was plotted from the Lineweaver-Burk data. Error bars represent the standard deviation from the mean. The correlation coefficient ( $r^2$ ) between

outcomes and their predicted values was calculated as 0.9963 (where values approaching 1 are desirable), therefore the data was acceptable.

$V_{\max} = 10.85$   $\mu\text{moles}$  of product released per minute, per  $\mu\text{mole}$  of enzyme

or  $0.18$   $k_{\text{cat}}$  ( $\mu\text{moles}$  of product released per second, per  $\mu\text{mole}$  of enzyme).

$K_M = 0.23$   $\text{mmol/L}$

The significance of these values are discussed later in chapter 6 when compared to those of the well documented artificial substrate 4-methylumbelliferyl- $\beta$ -D-glucopyranoside (MUD).

#### Confirmation of lipase activity with alizarin-2-octanoate

The detection of lipase activity has clinical significance, as it is produced by *Salmonella*, *Aeromonas* and *Acinetobacter* spp. One of the tests used for this purpose in Public Health, Pathological and Veterinary laboratories is the C8 esterase test, which employs 4-methylumbelliferyl caprilate (Freydiere and Gille, 1991).

To confirm that alizarin-2-octanoate could be used as a substrate to detect, or even quantify, lipase activity, the following initial investigations were performed.

Alizarin-2-octanoate (10 mg) was dissolved in 1-methyl-2-pyrrolidone (1 ml), then added to sodium acetate buffer (99 ml, 0.05 M) and adjusted to pH 8 with acetic acid (1 M) to give a stock solution with a concentration of 100 mg/L.

Lipase from *Candida cylindracea*, a lipase enzyme active with intermediate chain esters (Cambou and Klibanov, 1984), and lipase from *Rhizopus arrhizus*, active with long chain esters (Kim and Chung, 1989), both from Sigma, were prepared in the above buffer at a concentration of 1 mg/ml (equivalent to 10 U/ml).

To alizarin-2-ocatanoate (100  $\mu$ l), lipase from *Rhizopus arrhizus* (lipase R) was added (2.5  $\mu$ l) and the reaction monitored by recording the production of alizarin at 520 nm over time (Figure 4.29 and 4.30).



**Figure 4.29:** Alizarin-2-ocatanoate (left) and when reacted with lipase R (right).

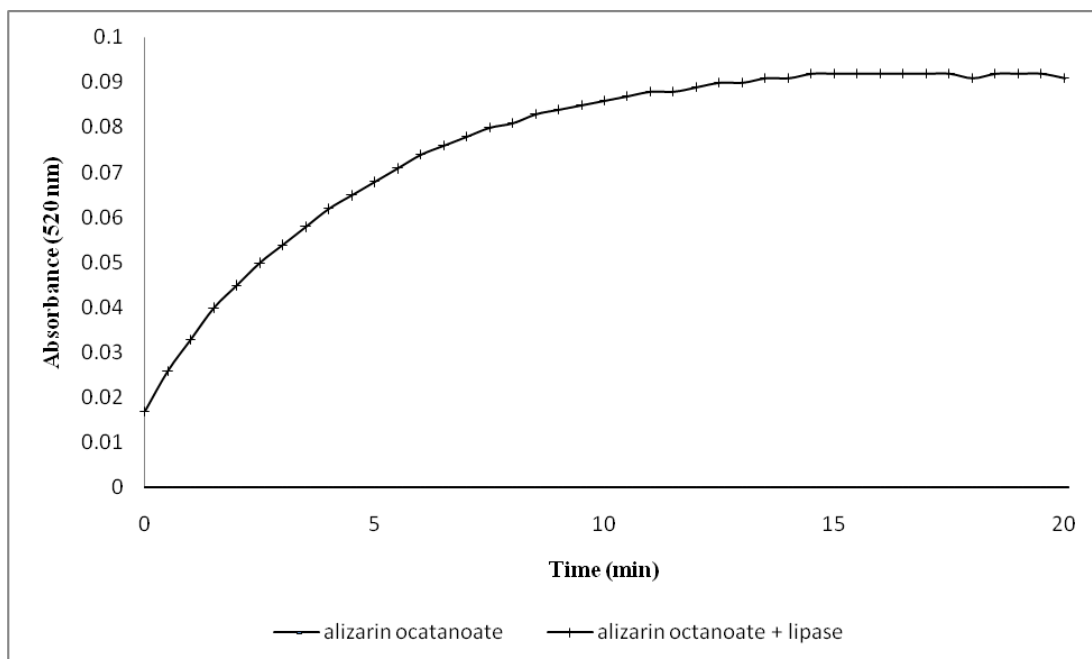


**Figure 4.30:** Production of alizarin when alizarin-2-octanoate is acted upon by lipase R.

From Figure 4.30 above it can be seen that the reaction reaches end point at approximately 15 min.

Dilutions of the substrate were prepared (0, 10, 20, 50 and 100 mg/L) and reacted with lipase from *Candida cylindracea* (lipase C) and lipase R. Readings were taken at 520 nm after incubation for 15 min (Figure 4.31 and 4.32).



**Figure 4.31:** Increasing concentrations of alizarin-2-octanoate (top row left to right) and then reacted with lipase C (centre) and lipase R (bottom).

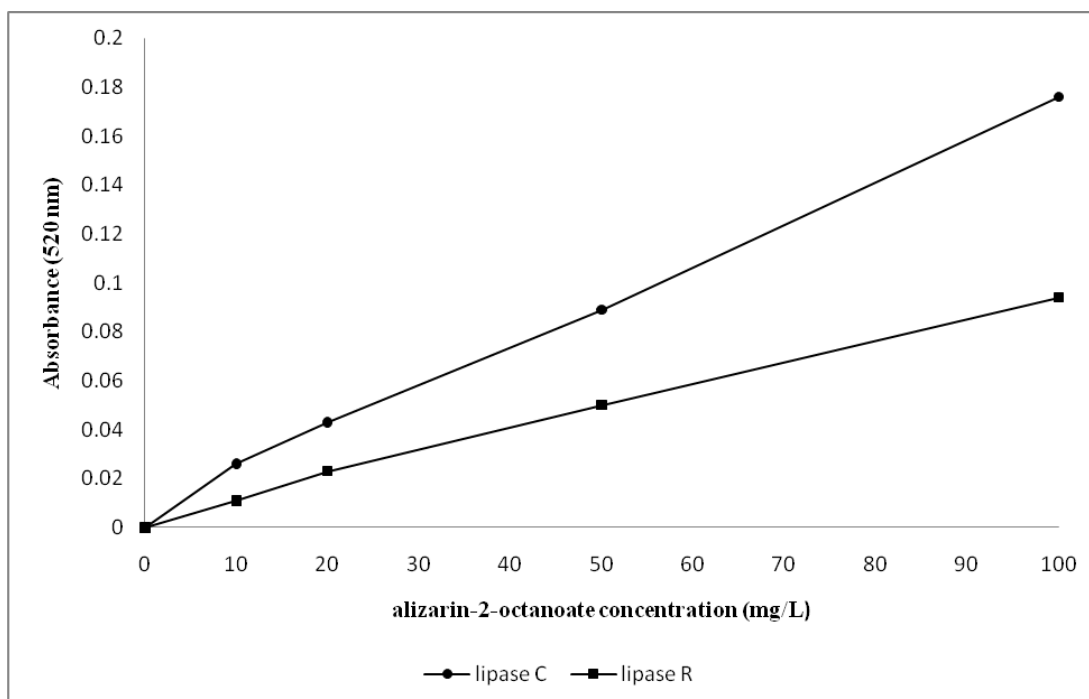


**Figure 4.32:** Variation of alizarin-2-octanoate concentration.

Both enzymes showed activity with alizarin-2-octanoate, although lipase C appeared to convert substrate to product faster than lipase R. This substrate may have value in detecting lipases.

Initial investigations were also made into the ability of alizarin-2-octanoates to identify a *Salmonella* spp. Alizarin-2-octanoate (100 mg) was dissolved in dimethyl sulfoxide (6 ml) and Tween 20 (7.5 ml), then incorporated into Columbia agar (40.6 g/986.5 ml) containing 500 mg/L ferric ammonium citrate, which had previously been sterilised, and then cooled to 50 °C. The agar plate was inoculated with *Salmonella typhimurium* NCTC 74 and incubated at 37 °C for 17 h.

After this time, the substrate had been hydrolysed by the *Salmonella* to produce diffuse, yet vivid, purple colonies (Figure 4.33).

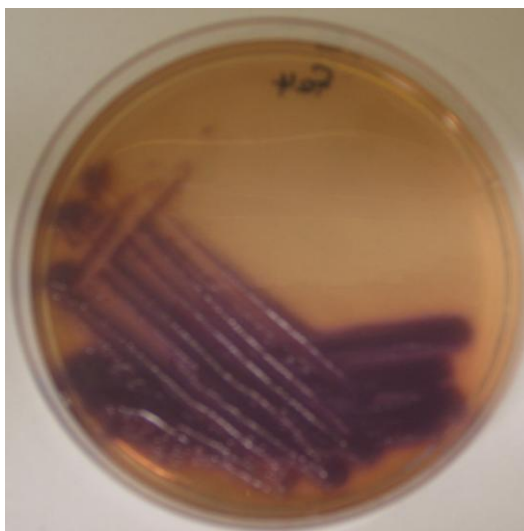


**Figure 4.33:** Hydrolysis of alizarin-2-octanoate by *Salmonella typhimurium* NCTC 74 to produce a purple iron chelate.

### 4.5.3 Molecular biology application

#### Alizarin-2-yl- $\beta$ -D-galactoside

The role of  $\beta$ -galactosides in the field of molecular biology, e.g. screening for recombinant and non-recombinant transformants of bacterial *E. coli* cells carrying the *lacZ* gene, was mentioned in the introduction. The need for a highly colourful contrast between the two types of cells, when grown on an agar plate medium, is of the utmost importance.

The most popular and well known substrate used for this purpose is X-gal. When released by  $\beta$ -galactosidase, the indoxyl group gives light blue colour in the presence of oxygen (Kodaka et al., 1995).

Similarly 3,4-cyclohexenoescluletin- $\beta$ -D-galactopyranoside (CHE-gal) is also commercially available (S-gal<sup>®</sup> from Sigma) and gives black colonies when chelated with ferrous iron (James et al., 1996).

Both of these substrates have certain draw backs. X-gal is expensive and time consuming to prepare, while the iron present with CHE-gal can also interact with deaminases to give coloured products (Carricajo et al., 1999).

Alizarin-2-yl- $\beta$ -D-galactoside (Aliz-gal) was selected as a possible alternative to these. Previous work with Aliz-gal involved testing the substrate against  $\beta$ -galactosidase from a range of Gram-negative bacteria. From this, it was shown Aliz-gal was a useful and highly sensitive substrate (James et al., 2000b), but no work was carried out to compare it to the other substrates for screening for recombinant and non-recombinant transformants of *E. coli* cells carrying the *lacZ* gene.

To optimise the colour produced and decrease the background colour of the agar medium, thus giving the greatest contrast between coloured and white (colourless) colonies, the following investigations were performed.

Both recombinant and non-recombinant transformed cells were prepared using a modified Cohen method (Cohen et al., 1972) (see preparation of chemically competent cells in Appendix C).

A pGEM-T plasmid (Promega) with an insert and a plasmid without an insert were chemically transformed into competent *E. coli* strain XL1 Blue cells. The plasmids were prepared via MIDAS® PlasmidSpin™ miniprep kit Protocol (Appendix C) and were kindly supplied by Ian E. Brown. Cells transformed with the plasmid without the insert can produce  $\beta$ -galactosidase and therefore cleave the substrate to give coloured colonies. In cells transformed with the plasmid with the insert present, the insert blocks production of  $\beta$ -galactosidase by interrupting the genetic sequence of the enzyme. As a result, there is no cleavage of substrate and colonies remain white. In further molecular work, white colonies are generally selected as they contain the insert to be studied.

When the transformation mixture was plated onto LB/ampicillin agar containing X-gal and incubated for 24 h at 37 °C both blue and white colonies were observed (Figure 4.34).

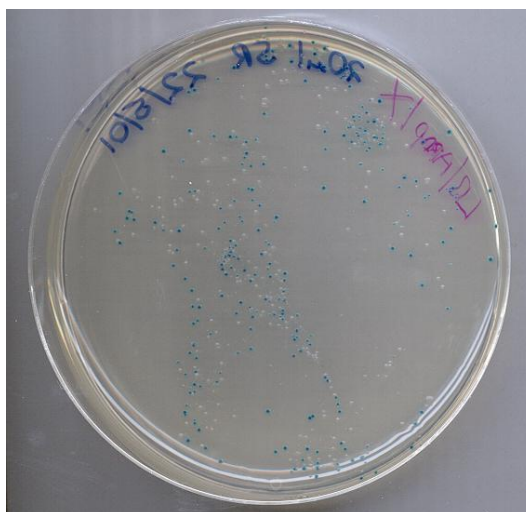


**Figure 4.34:** Transformed recombinant and non-recombinant XL1 Blue cells.

To ascertain the optimum amount of Aliz-gal needed to produce coloured colonies the following agar medium was prepared with varying concentrations of the substrate:

10 g Tryptone  
5 g Yeast extract  
10 g NaCl  
12 g Agar No. 1  
in 1 L of distilled water

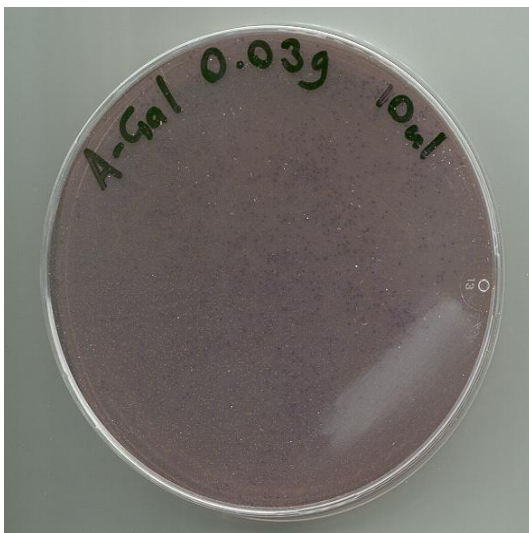
The medium was sterilised via autoclave, cooled to 55 °C before 100 mg ampicillin and 0.030 g IPTG (isopropyl- $\beta$ -D-thiogalactopyranoside) were added. Aliz-gal was then added in amounts varying from 0.01-0.3 g/L. 10  $\mu$ l of transformation mixture was spread on the surface of the plates and incubated for 24 h at 37 °C (Figure 4.35).



Insufficient Aliz-gal (little colouration).



Optimised Aliz-gal



Excess Aliz-gal (colour overloaded)

**Figure 4.35:** Aliz-gal concentration (0.001 - 0.03 g/100ml Agar).

The optimum concentration was 0.1 g/L. Below this, there was, not enough substrate to give sufficient colour for identification of non-recombinant transformants. Conversely, above 0.1 g/L the plate was overloaded and it was difficult to detect recombinant transformants.

Using the agar medium described previously with 0.1 g/L Aliz-gal, the chelating effect of different metals was investigated. To the agar, 10 mmol/L of the metals below were added (Table 4.4).

**Table 4.4:** Summary of the effects of various metal chelators with aliz-gal (the more pluses the greater the effect).

Metal salt	Colour	Intensity	Diffusion	Toxicity
Aluminium sulfate	red	+++	-	-
Bismuth ammonium citrate	purple	++	-	++
Ceric ammonium nitrate	purple	++	+++	-
Lanthanum chloride	red/purple	+	++	+
Tin chloride	red/purple	+	++	+

The most intense, non-toxic chelators, that did not spread through the agar came from aluminium sulfate (Figure 4.36).

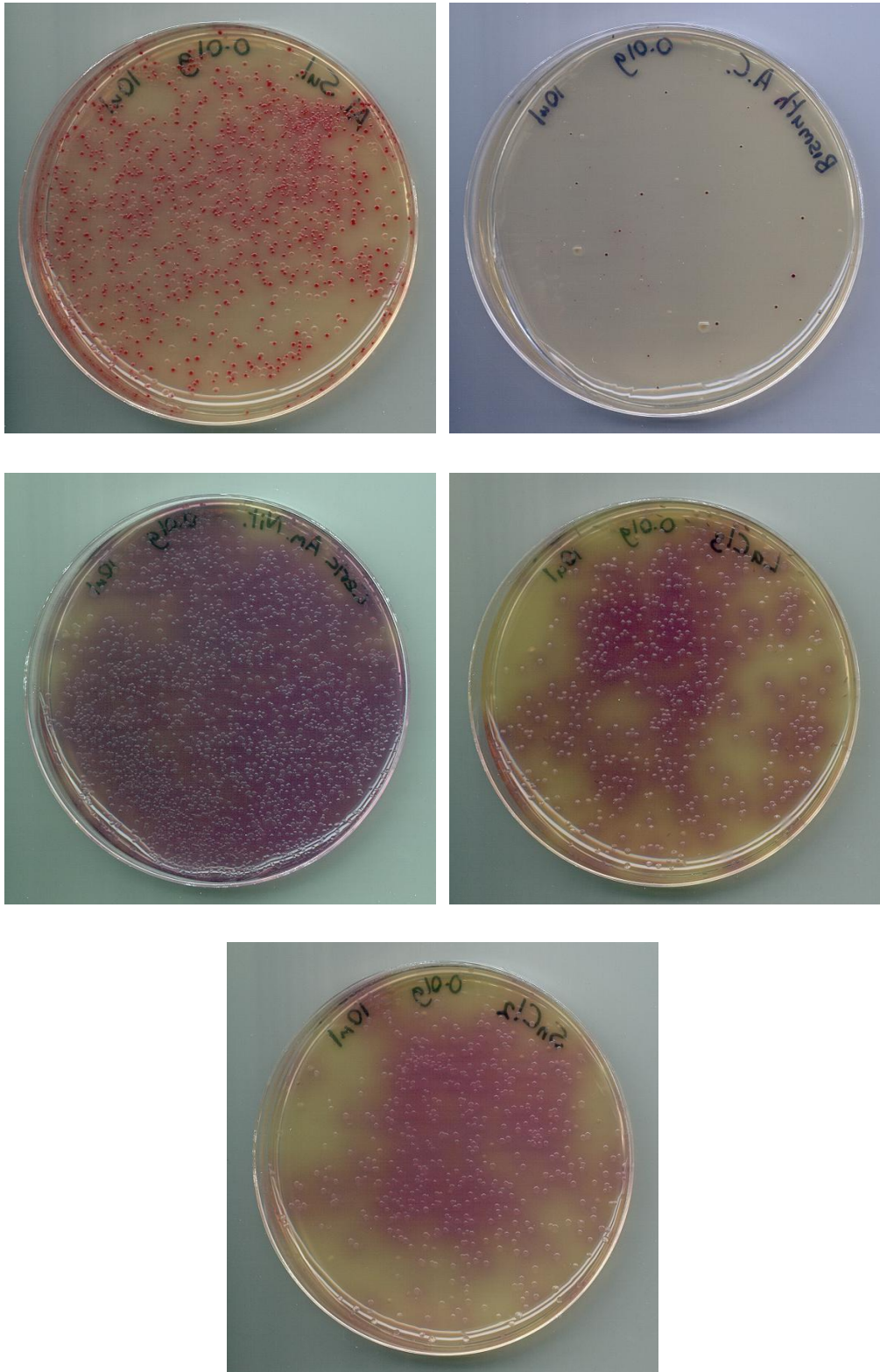


**Figure 4.36:** The effect of different metal chelators with Aliz-gal in LB/ampicillin agar. Starting from top right; aluminium sulfate, bismuth ammonium citrate, ceric ammonium nitrate, lanthanum chloride and tin chloride.

A range of aluminium salts (10 mmol/L) were then investigated (Table 4.5).

**Table 4.5:** Effects of various aluminium salts with aliz-gal (the more pluses the greater the effect).

Metal salt	Colour	Intensity	Diffusion
Aluminium ammonium sulfate	red	+++	-
Aluminium nitrate	red	++	-
Aluminium potassium sulfate	red	++	-
Aluminium sulfate	red	+++	-
Aluminium sulfate + ammonium ferric citrate	purple	+++	+

Only aluminium sulfate + ammonium ferric citrate showed undesirable diffusion through the agar medium. Aluminium sulfate and aluminium ammonium sulfate showed the most intense and vivid colours (Figure 4.37).

Results showed alizarin-2-yl- $\beta$ -D-galactoside, when optimised as in the conditions described above, could be used to identify recombinant and non-recombinant transformants. Comparisons between this and other screening substrates already commercially available are made later.

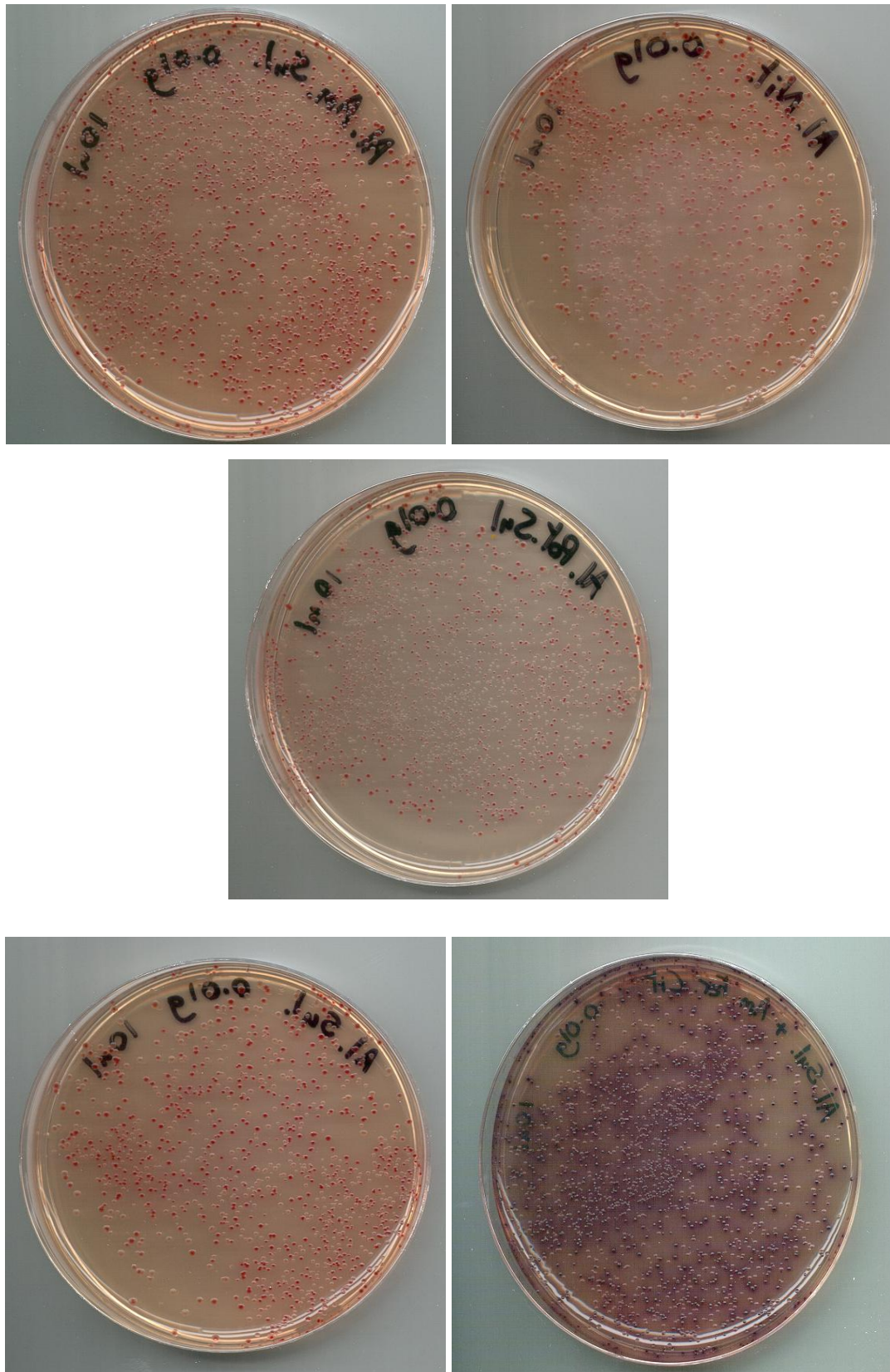


**Figure 4.37:** The effect of different aluminium salts with Aliz-gal in LB/ampicillin agar. Starting from top right; ammonium sulfate, nitrate, potassium sulfate, sulfate, sulfate + ammonium ferric citrate.

### *p*-Naphtholbenzein- $\beta$ -D-galactoside

Another galactoside which could be used as a similar molecular biological tool was *p*-naphtholbenzein- $\beta$ -D-galactoside (PNB-gal). LB agar plates were made in an identical manner to those described earlier with alizarin-2-yl- $\beta$ -D-galactoside, but using 0.1g/L *p*-naphtholbenzein- $\beta$ -D-galactoside, and the same transformed cells were used; the results can be seen in Figure 4.38.

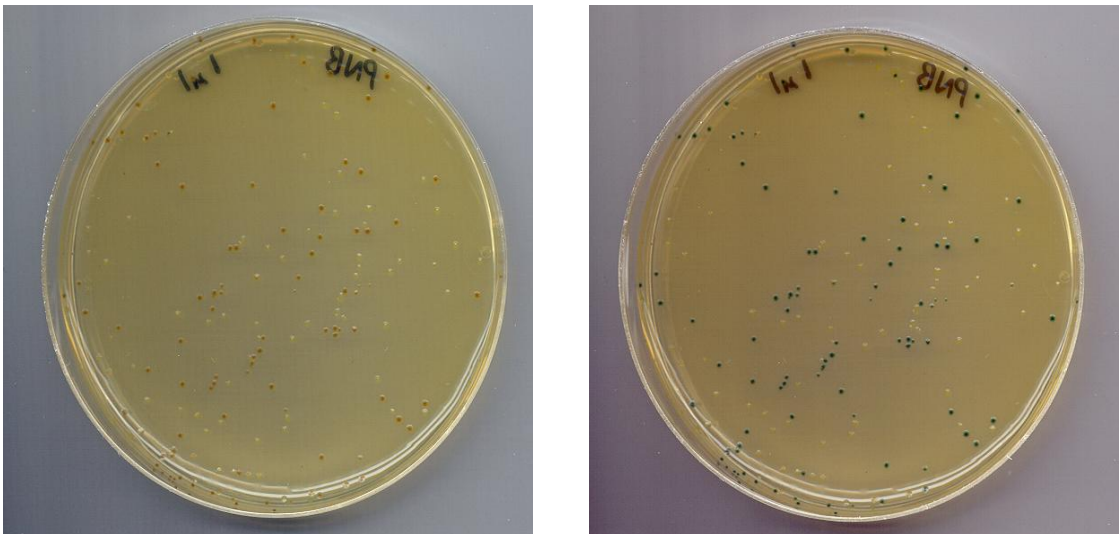


**Figure 4.38:** PNB-gal incorporated into solid agar media for use in the screening of recombinant and non-recombinant transformants (left) and after exposure to ammonia fumes (right).

Under normal physiological conditions yellow/pink colonies of non-recombinant cells were observed alongside white recombinant cells. Under alkali conditions, such as exposure to ammonia fumes or the addition of a drop of NaOH (1 M), the *p*-naphtholbenzein darkened to give the much more intense green/blue coloration of its ionised form (Figure 4.39).

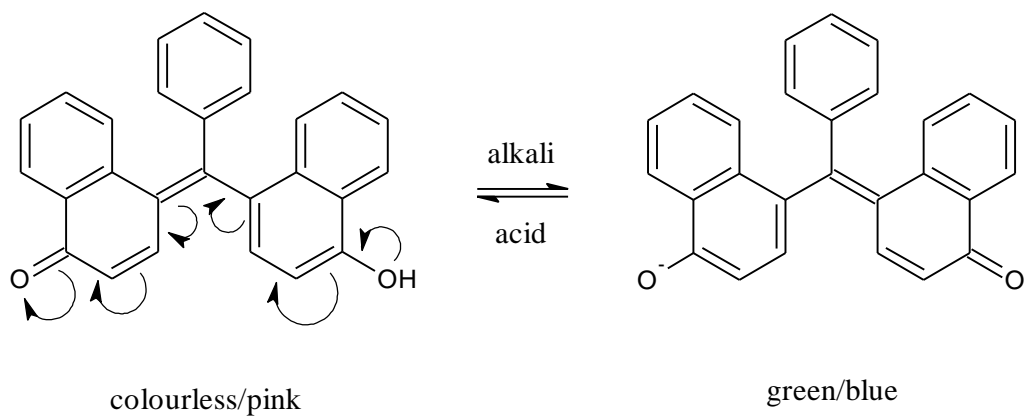


**Figure 4.39:** pH effect of *p*-naphtholbenzein.

## 4.6 Discussion

Various high points emerge from the work. These are largely related to the chelators, since the chelators showed the best localisation on colonies when incorporated into agar media or produced strong coloration or fluorescence in liquid assays when investigating enzyme kinetics. This is to be expected in view of the results obtained with alizarin and CHE based substrates (James et al., 2000b; James et al., 1996). The core molecules of particular interest were:

- alizarin (1,2-dihydroxyanthraquinone)
- 5-nitrosalicylaldehyde
- 3-hydroxyflavone

### 4.6.1 Alizarins

The synthesis of alizarin-2-yl- $\beta$ -D-glucoside (Figure 4.40) was first described by Robertson (Robertson, 1930; Robertson, 1933). This was part of an investigation into the structure of the naturally occurring alizarin which, in plants, is present as a complex glycoside termed ruberythric acid. The  $\beta$ -glucoside had been synthesised, but none of its biological properties had been investigated in detail. This was re-investigated in more recent years (James et al., 2000b). The scope of possibilities for these compounds is considerable and in the present work an attempt was made to re-examine the glycosides and other derivatives of this core molecule.

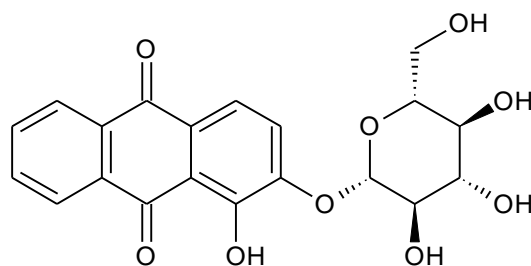


**Figure 4.40:** Structure of alizarin-2-yl- $\beta$ -D-glucoside.

The glycosides were synthesised by a conventional Koenigs-Knorr reaction. However, a modification was introduced which greatly simplified the work-up, taking advantage of the fact that free alizarin binds strongly to basic alumina, whilst glycosides and other derivatives do not since the vicinal dihydroxy system is no longer present. A column technique was employed and gave easily observable bands of the reaction components.

Deacetylation of the tetraacetyl derivatives proved to be relatively straightforward using aqueous methanolic alkali. This relatively drastic treatment could not be used with many protected glycosides, but, in the case of alizarin, the glycosidic link is considerably more stable. This is due to there being no powerful electron withdrawing groups present, such as those found in methylumbelliferone or resorufin, which can weaken the glycosidic link.

In an attempt to utilise these compounds in a practical situation in the field of molecular biology, alizarin-2-yl- $\beta$ -D-galactoside was compared with various other galactosides for demonstration of recombinant and non-recombinant transformants in bacterial cells carrying the *lacZ* gene, in conjunction with a range of salts, to provide the chelatable metal. The alizarin galactoside along with the *p*-naphtholbenzein galactoside also tested for this application, gave equal or better results as regards colour and definition than most of the other substrates chosen including the traditionally used X-gal.

Seen together X-gal, CHE-gal, Aliz-gal and PNB-gal are comparable (Figure 4.41). All give vivid colours with good contrast. Aliz-gal could be more cost and labour effective, as its core compound is already commercially available and less Aliz-gal is

needed in the agar medium (0.1 g/L compared to 0.3 g/L of CHE-gal found in pre-prepared screening media from Sigma).

PNB-gal is also of parity even with the necessity to expose the colonies to alkali conditions to get the maximum coloration, as each of the others requires an addition to enhance the visualised colour. X-gal requires exposure to oxygen to produce indigo dye, while CHE-gal and Aliz-gal benefit from a metal chelator.

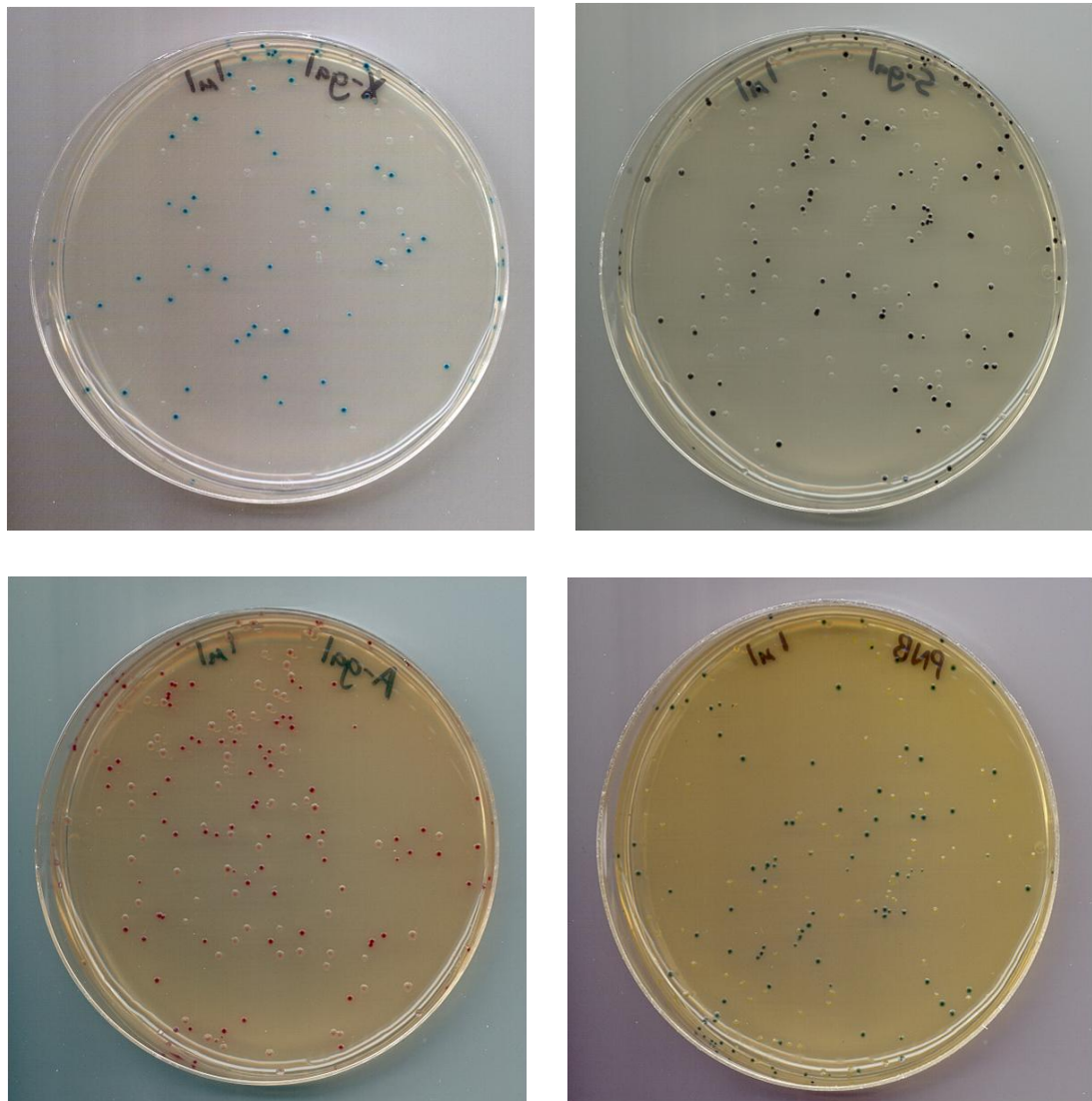


**Figure 4.41:** A comparison of four galactoside substrates separately incorporated into solid agar media for use in the screening of recombinant and non-recombinant transformants. Starting from top right; X-gal, CHE-gal, Aliz-gal, PNB-gal.

A main point of the value of the alizarin system in the present context is the use of alizarin-2-octanoate (Figure 4.42) as a substrate for visualisation of C8 esterase or lipase.

When employed in agar based medium positive colonies were readily recognised by formation of the purple coloured chelate. It is well known that organisms, such as *Salmonella*, *Aeromonas* and *Acinetobacter*, have a strong lipase activity (Kok et al., 1995; Lotrakul and Dharmsthiti, 1997; Cooke et al., 1999) and this is borne out in the present study.

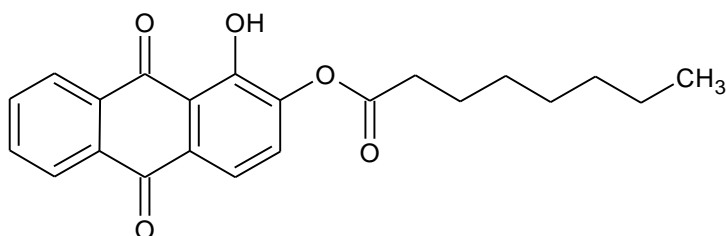


**Figure 4.42:** Structure of alizarin-2-octanoate.

To demonstrate the activity of alizarin-2-octanoate, the substrate was incubated with lipase enzymes of commercial origin (Sigma). Aqueous insolubility problems were evident but could be overcome by the addition of organic solvents or surfactants, such as initially dissolving the substrate in 1-methyl-2-pyrrolidone. The lipase enzymes selected were shown to be active with alizarin-2-octanoate and the substrate could therefore be used to quantify these enzymes. Microbial investigations would have to be carried out with a range of bacteria before its true value as method for detecting species such as *Salmonella*, could be commented upon.

#### 4.6.2 5-Nitrosalicylaldehyde- $\beta$ -D-galactoside

5-Nitrosalicylaldehyde was chosen as it has a nitrophenolic structure analogous with *p*-nitrophenol, a well established synthetic substrate core compound discussed in Chapter 1 (Figure 4.43). The presence of an aldehyde group adjacent to the phenolic hydroxyl gives the potential for chelation with metals, such as iron, which has the effect of darkening the coloration, therefore making it more intense.

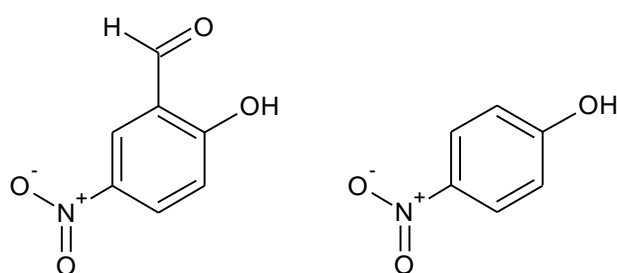


**Figure 4.43:** Structures of 5-nitrosalicylaldehyde (left) and *p*-nitrophenol.

Glycosidation of the core molecule using  $\alpha$ -acetobromogalactose gave, after deprotection, a reasonable yield of the  $\beta$ -galactoside. This compound, when incorporated into agar-based medium in the presence of ferric ammonium citrate, gave orange colonies with relevant  $\beta$ -galactosidase producing bacteria. It was theorized that a chelation complex would have the effect of restricting coloration to the colonies. However, it was noticed that there was a certain degree of spreading of colour away from the colony mass, as there is with *p*-nitrophenol substrates.

The results of the microbial investigations showed, that for Gram-negative bacteria, the 5-nitrosalicylaldehyde galactoside could detect the same species as its alizarin counterpart. Of the Gram-positive bacteria, no species were active with this substrate, a trait which could be exploited in the identification of Gram-negative bacterial species.

### 4.6.3 3-Hydroxyflavones and hydroxyquinolones

The compound 3-hydroxyflavone was chosen to study as some information was already available on the phosphate ester. This appears in a patent (Jackim, 1969) describing the synthesis of the compound and its use as a sensitive method for estimating phosphatase enzyme.

3-Hydroxyflavone (Figure 4.44) is only one of a number of hydroxyflavones which is capable of demonstrating fluorescence and also the property of chelation with appropriate metal ions. Both 3-hydroxyflavone and 5-hydroxyflavone derive these properties from the proximity of the hydroxyl group to the carbonyl function of the  $\gamma$ -pyrone ring. This allows for both intramolecular hydrogen bonding and metal chelation.

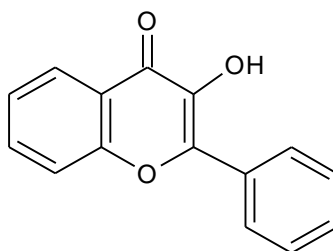


**Figure 4.44:** Structure of 3-hydroxyflavone.

Other hydroxyflavones, such as 3',4'-dihydroxyflavone, and 7,8-dihydroxyflavone exhibit these properties because of the vicinal dihydroxy system, which is similar to that observed with CHE. In fact 3',4'-dihydroxyflavone has been successfully glycosidated and is marketed by Glycosynth as a potential substrate for bacterial identification, such as  $\beta$ -glucosidase positive *Enterococcus faecalis* (Burton, 2004).

Initial studies showed that the 3-hydroxyflavone possessed better fluorescence and chelation properties than the corresponding 5-isomer. Additionally, the 3-isomer is readily available and considerably less expensive.

Accordingly, 3-hydroxyflavone was derivatised as the  $\beta$ -glucoside and  $\beta$ -galactoside using both Koenigs-Knorr methodologies and the tetraacetyl intermediates deprotected using sodium methoxide. Synthesis of the glucoside via the potassium hydroxide method gave a good yield of product while the 2,6-lutidine and silver carbonate method did not give as great a yield. This could be due to the formation of a silver complex owing to the strong chelating effect of 3-hydroxyflavone which would impair the progress of the glycosidation.

The compound was investigated both as a substrate for isolated  $\beta$ -glucosidase enzyme and for microbial identification in agar medium. This latter work carried out by Professor Perry (of the Freeman Hospital, Newcastle) showed that  $\beta$ -glucosidase containing strains gave strongly dark coloured colonies in the presence of iron, but only in the case of Gram-positive organisms (with the exception of one Gram-negative bacteria, *E. coli* NCTC 10418, which gave only a trace amount of coloration). The explanation for this is unclear but could be due to a membrane effect. This effect is interesting, since it gives a potential method for discriminating Gram-positive organisms from  $\beta$ -glucosidase producing Gram-negative organisms.

Of the bacteria that were active with this substrate, *Listeria monocytogenes* NCTC 11994 gave the most vivid colonies. The detection of this bacterium is of great interest due to it being a widely distributed food borne pathogen responsible for listeriosis and listeric meningitis (Becker et al., 2006). It is possible that, with further study, this substrate could be developed as part of protocol of the isolation of *Listeria* spp. as it has similar properties to substrates such as 3,4-cyclohexenoesuletin- $\beta$ -D-glucoside (James, 2001) which Lab M employs in its Harlequin™ *Listeria* Medium (Figure 4.45) (Smith et al., 2001).

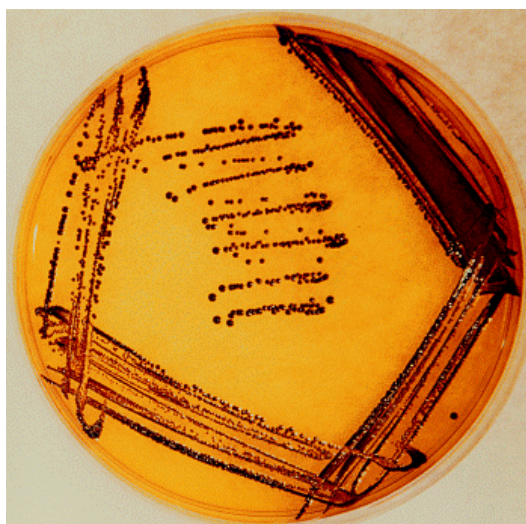


**Figure 4.45:** *Listeria* isolation with Harlequin™ *Listeria* Medium. Brown colouration of colonies result from the chelation of CHE, released from CHE- $\beta$ -D-glucoside, and ferrous gluconate.

It was also observed that incubation of selected organisms on a medium containing 3-hydroxyflavone- $\beta$ -D-glucoside in the presence of zinc ions produced bright yellow colonies with appropriate  $\beta$ -glucosidase containing Gram-positive organisms. This effect is interesting, since relatively few chromogenic substrates produce satisfactory yellow colonies. This particular effect had also been noted by Professor Perry (of the Freeman Hospital, Newcastle) with respect to 3,4-dihydroxyflavone- $\beta$ -D-galactoside (DHF-gal) synthesised by Dr M Burton of Glycosynth.

To further investigate the properties of the glucoside, the compound was incubated under various conditions with  $\beta$ -glucosidase enzyme and the enzymatic characteristics, including kinetic data, determined.

Compared to the commercially available and well documented artificial substrate 4-methylumbelliferyl- $\beta$ -D-glucopyranoside (MUD) (see Enzyme kinetics of 4-methylumbelliferyl- $\beta$ -D-glucopyranoside – in Appendix B), 3-hydroxyflavone- $\beta$ -D-glucoside (3HF-gluc) had a lower  $V_{\max}$  (Table 4.6).

**Table 4.6:** Comparison of Lineweaver-Burk enzyme kinetics data for MUD and 3HF-gluc.

Substrate	$V_{\max}$	$k_{\text{cat}}$	$K_M$
MUD	25.32	0.42	0.30
3HF-gluc	10.85	0.18	0.23

This means  $\beta$ -glucosidase cleaves 3HF-gluc at a slower rate than MUD. The Michaelis constants ( $K_M$ ) show this enzyme has a greater affinity for 3HF-gluc. This is beneficial in these sensitive fluorescent molecules, as a smaller amount of enzyme and substrate are required to increase the reaction rate to half of its maximum and therefore can therefore be detected at an earlier stage.

Another advantage 3HF-gluc has is that, unlike MU substrates, it adheres to bacterial colony cell mass and so does not spread through solid agar medium making the task of identification and isolation easier.

There is a similarity of structure between 3-hydroxyflavone and certain of the hydroxyquinolones. The compound 1-methyl-2-phenyl-3-hydroxy-4-quinolone, and certain of its derivatives, were synthesised and their fluorescence qualities were studied and recorded (Yushchenko et al., 2006a; Yushchenko et al., 2006b). The proximity of the hydroxyl group to the carbonyl function of the quinolone ring gives rise to intramolecular hydrogen bonding and should therefore give rise to chelation possibilities. Blocking the hydroxyl group by glycosidation, for example, would be expected to prevent this.

In this present study the hydroxyquinolone was synthesised by the method described (Yushchenko et al., 2006a) and the related compound, 1-methyl-2-(4'-fluorophenyl)-3-hydroxy-4(1*H*)-quinolone (Figure 4.46) was synthesised by a similar procedure. Examination of these compounds demonstrated the characteristic fluorescence properties and illustrated their capacity for chelation with a range of metal ions.

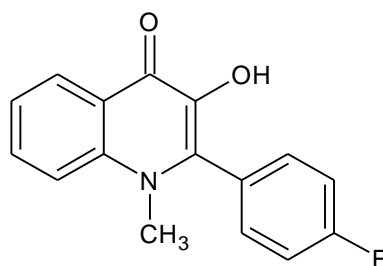


**Figure 4.46:** Structure of 1-methyl-2-(4'-fluorophenyl)-3-hydroxy-4(1*H*)-quinolone.

Several attempts at glycosidation were made using a variety of methods, but it was not possible to achieve satisfactory results. This may have been due to the very limited solubility of these particular quinolones.

## **CHAPTER FIVE**

### **Gene cloning and protein expression**

## 5.1 Introduction

This study was to include the synthesis of a range of aminopeptidase substrates, particularly those of leucine aminopeptidase. Due to the expense of the enzyme leucine aminopeptidase (£600/100 units, Sigma), it was not feasible to purchase the enzyme needed to test the effectiveness of the substrates. It was therefore decided to attempt to clone the enzyme in order to produce a more cost effective supply.

It has been documented that *E. coli* is a bacterial source of leucine aminopeptidase (Vogt, 1970; Murgier et al., 1976; Murgier et al., 1977; Lazdunski, 1989; Matsui et al., 2006).

To demonstrate this, *E. coli* K12 was grown on nutrient agar at 37 °C for 24 h. Colonies were transferred to 0.1 M Tris buffer pH 7.4 (10 ml) until it gave a cell suspension with an absorbance value of 0.350 at 500 nm. 0.5, 0.05 and 0.005 mg/ml dilutions of L-leucine-7-amido-4-methyl-coumarin hydrochloride (Sigma) were prepared by dissolving the substrate first in 2 drops of dimethyl sulphoxide (DMSO) then Tris buffer. To 1 ml of each dilution, 0.5 ml of the cell suspension was added then incubated at 37 °C for 1 h before being viewed under exposure to ultraviolet light. The substrate was cleaved to produce fluorescent 7-amino-4-methyl-coumarin showing that aminopeptidase was indeed present in the *E. coli* K12 cell suspension (Figure 5.1).

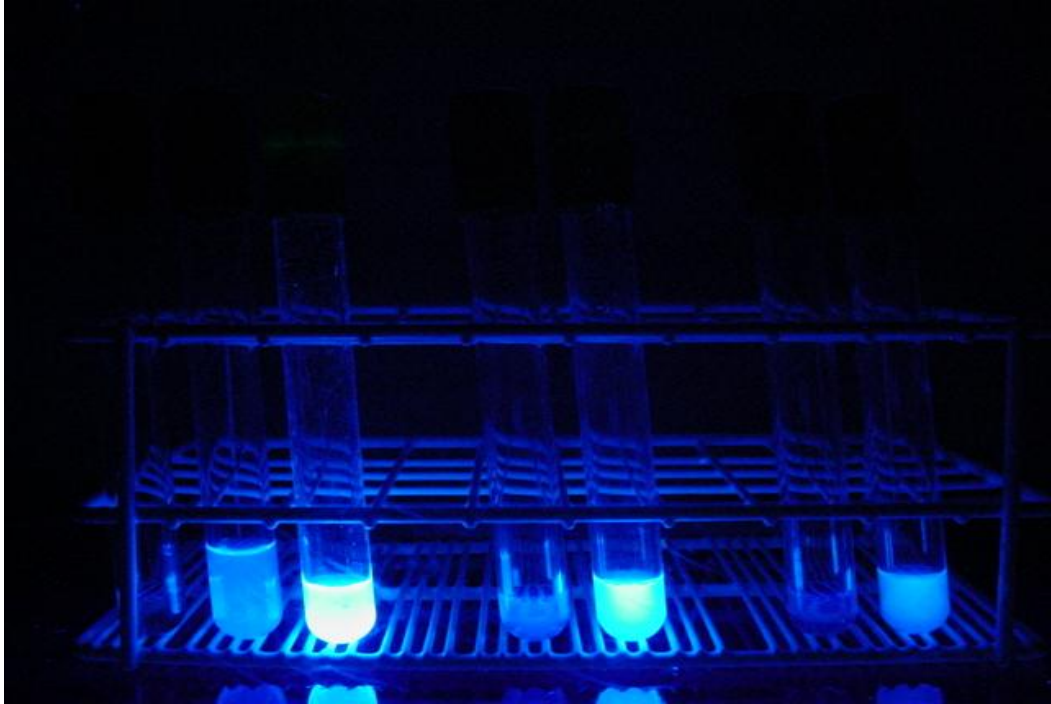


**Figure 5.1:** Action of *E. coli* K12 cell suspension on dilutions of L-leucine-7-amido-4-methyl-coumarin hydrochloride in 0.1 M tris buffer pH 7.4. Tubes contain (from left to right): *E. coli* + Buffer, 0.5 mg/ml substrate, 0.5 mg/ml substrate + *E. coli*, 0.05 mg/ml substrate, 0.05 mg/ml substrate + *E. coli*, 0.005 mg/ml substrate, 0.005 mg/ml substrate + *E. coli*.

A search performed on 27/4/07 of the National Center for Biotechnology Information's database (<http://www.ncbi.nlm.nih.gov/Genbank/>), an annotated collection of all publicly available DNA and protein sequences, found a gene sequence from *E. coli* K12 that was annotated as a putative leucyl aminopeptidase (protein i.d. NP\_418681, see protein and gene sequence in Appendix C).

Forward and reverse primers were designed for this gene (1.509 kb) using the Primer Design Programme, part of the *Saccharomyces* Genome Database (<http://www.yeastgenome.org/>). This design programme is a tool that can be used to design primers for genes other than those of *Saccharomyces* spp. The primers;

forward primer 5'-CAC CAC CAC CAC ATG GAG TTT AGT GTA AAA AGC-3' and reverse primer 5'-GAG GAG AAG GCG CGT TAC TCT TCG CCG TTA AAC CCA-3' were supplied in a lyophilised form by MWG Biotech (see MWG Oligo synthesis report in Appendix C). The primers were reconstituted with 18.2 MΩ/cm

H<sub>2</sub>O to give a stock concentration of 100 mM (100 pm/μl) and stored at -20 °C. This was further diluted to give a working concentration of 20 mM when required.

## 5.2 Experimental Methods

### 5.2.1 DNA extraction

DNA was extracted from *E. coli* K12 using a Qiagen DNeasy kit (see protocol in Appendix C). The purity of the four elutions from the DNeasy kit column were visualised (Figure 5.2) by running 5 μl on a 1% (w/v) agarose gel containing 5 μl 1 x Sybr® Safe (Invitrogen) at 120 mA for 45 min (see agarose gel electrophoresis in Appendix C).

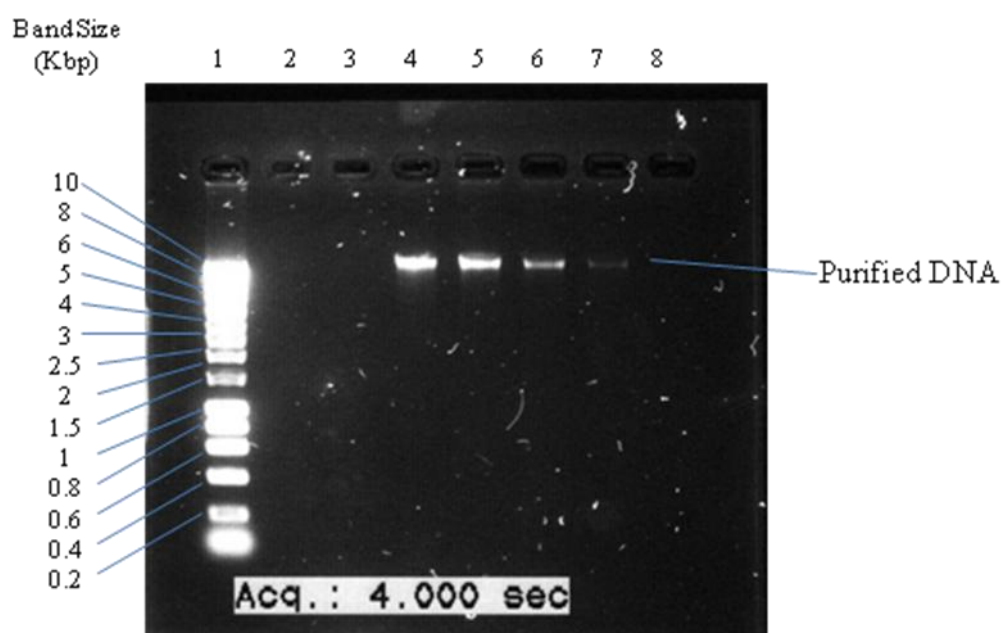


**Figure 5.2:** Elutions of purified genomic DNA from *E. coli* K12 (lanes 4-7). Each sequential elution being of a lower concentration. Lane 1 contains 'Bioline Hyperladder 1' size standards (10 Kbp top – 0.2 Kbp bottom).

### 5.2.2 Gene amplification

The putative gene for leucyl aminopeptidase was amplified from the purified genomic DNA. A polymerase chain reaction (PCR) (Takagi et al., 1997) was performed by preparing the reaction mix below (Table 5.1) and carried out with an Eppendorf Mastercycler Gradient thermocycler under the following conditions (Table 5.1).

**Table 5.1:** Contents of PCR reaction mixture.

\* For contents of 10 x KOD buffer see Appendix C.

Reagent	Amount ( $\mu$ l)
20 mM forward primer	1
20 mM reverse primer	1
2 mM dNTP's	5
25 mM MgSO <sub>4</sub>	2
10 x KOD buffer*	5
H <sub>2</sub> O	35.5
gDNA	0.5
KOD Hotstart Polymerase (1U/ $\mu$ l)	1

**Table 5.2:** Conditions of PCR reaction carried out with a Eppendorf Mastercycler Gradient thermocycler.

	Temperature (°C)	Duration (minutes)
Initial denature	95	2
Denature	95	0.25
Annealing 1	40	0.5
Extension	72	2.37
Denature	95	0.25
Annealing 2	63.2	0.5
Extension	72	2.37
Extension	72	10
Hold	10	∞

A 5 µl sample of the amplified product was visualised in a 1% (w/v) agarose gel as described above (Figure 5.3).

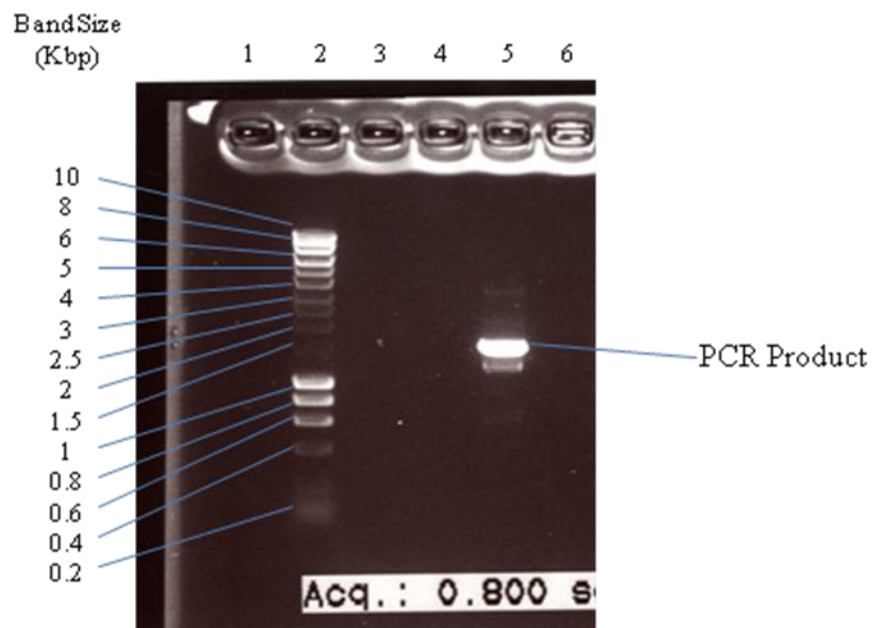


**Figure 5.3:** Amplified PCR product. Gene of interest is approximately 1.5 Kbp.

The amplified PCR product was the correct size for the gene encoding NP\_418681. To remove the smaller, fainter band, and also any unused nucleotides, the PCR product was cut out of the gel and purified using a QIAquick Gel Extraction kit (see protocol in Appendix C) to give a single band (Figure 5.4).

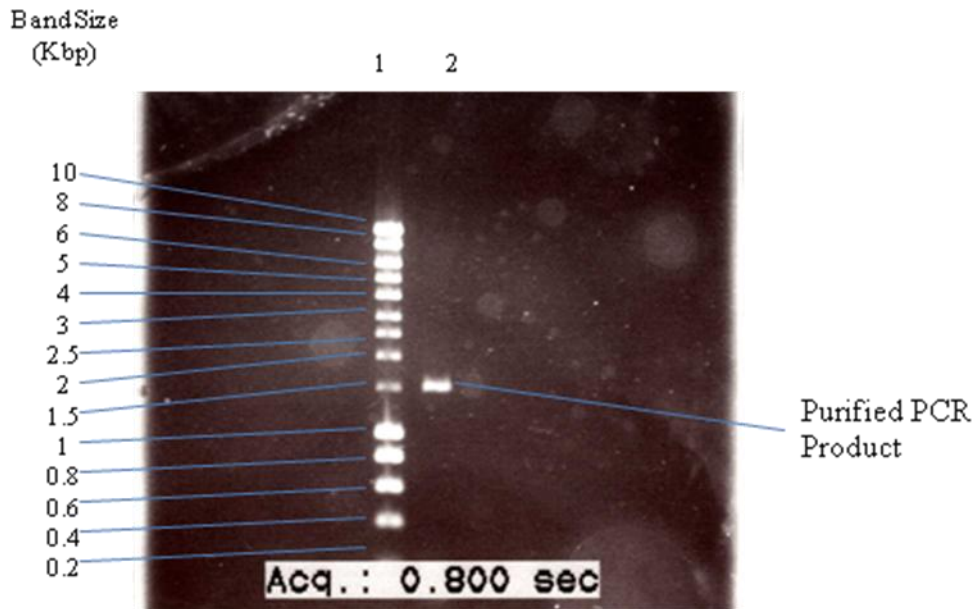


**Figure 5.4:** Extracted and purified PCR product.

The modified pET-28a vector, pET-YSBLIC, was provided Dr. Mark Fogg of the University of York (Bonsor et al., 2006; Fogg and Wilkinson, 2008) and prepared for use by Dr Meng Zhang (see pET-28a vector map and construction of pET-YSBLIC vector in Appendix C) (Figure 5.5).

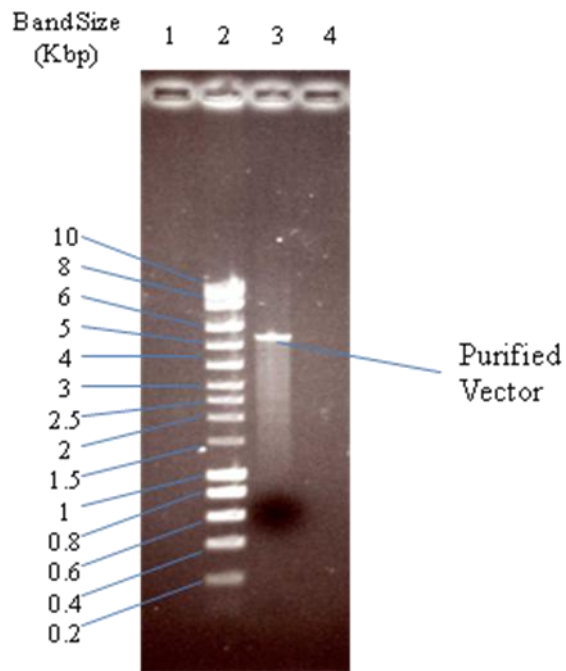


**Figure 5.5:** Purified pET-YSBLIC vector.

### 5.2.3 T4 DNA polymerase reaction

The *Bse* RI linearised vector was treated with T4 DNA polymerase (T4pol), in the presence of dTTP, to create single-stranded ends (Table 5.3). The PCR product was also treated with T4pol, in the presence of dATP, to create single-stranded ends that are complementary to the single-stranded ends of the vector (Table 5.4).

**Table 5.3.** T4pol reaction with vector and thymidine triphosphate (dTTP).

\* For contents of 10 x T4pol buffer see Appendix C.

Reagent	Amount ( $\mu$ l)
2 pM vector	146
10 x T4pol buffer*	20
25 mM dTTP	20
100 mM dithiothretol	10
T4pol (2.5 U/ $\mu$ l)	4

**Table 5.4:** T4pol reaction with PCR product and adenosine triphosphate (dATP).

Reagent	Amount ( $\mu$ l)
0.2 pM PCR product	14.6
10 x T4pol buffer	2
25 mM dATP	2
100 mM dithiothretol	1
T4pol (2.5 U/ $\mu$ l)	0.4

Both reactions were incubated at 22 °C for 30 min then stopped by incubating at 75 °C for 20 min. Excess nucleotides were removed using QIAquick Nucleotide Removing kit.

To anneal the product into the vector, a LIC (ligation independent cloning) annealing reaction was set up (Table 5.5).

**Table 5.5:** Annealing reaction.

Reagent	Amount ( $\mu$ l)
vector/T4pol reaction mix	1
PCR product/T4pol reaction mix	2
22 °C, 10 min	-
100 mM EDTA	1
22 °C, 10 min	-

The product of this reaction was a possible recombinant plasmid, which was then transformed into chemically competent *E. coli* XL1 Blue cells.

#### 5.2.4 Transformation of annealing products

Competent *E. coli* XL1 Blue cells (Stratagene) were prepared using a modified Cohen method (Cohen et al., 1972; Cohen et al., 1973) (see preparation of chemically competent cells in Appendix C).

To 50  $\mu$ l of competent *E. coli* XL1 Blue cells, 2  $\mu$ l of annealing product was added and mixed gently, then left on ice for 10 min. The mixture was heat shocked by incubating at 42°C for 90 s then placed back on ice for 2 min. LB medium (200  $\mu$ l) was added before incubation at 37 °C for 1 h.

Transformation mixture (200  $\mu$ l) was spread on a dried LB plate containing kanamycin (50  $\mu$ g/ml) which was then incubated at 37 °C overnight.

Of the 18 colonies that grew, ten were inoculated into 5 ml of LB broth containing kanamycin (50 µg/ml), incubated at 37 °C and shaken at 200 rpm overnight.

### 5.2.5 Isolation of plasmid

From each of the LB cultures, 4.5 ml was centrifuged at 4,000 x g for 10 min and the supernatant was then discarded. Plasmid samples of 50 µl were purified from the pellets using a QIAprep Spin **Miniprep** Kit (see protocol in Appendix C). Of each sample, 48 µl was stored at -20 °C for further use if successful. The remaining 2 µl were used in the following digest reactions.

## 5.2.6 Digest

To ascertain which plasmids had successfully taken up inserts, the plasmids were digested with the enzymes *Xho* I and *Xba* I which have respective restriction sites within the vector either side of the gene insertion site (see pET-28a vector map in Appendix C) therefore releasing the insert, if present (Table 5.6).

**Table 5.6:** Contents of Digest reaction mixture.

\* For contents of 10 x digest buffer 2 see Appendix C.

Reagent	Amount ( $\mu$ l)
Plasmid	2
<i>Xho</i> I (20 kU/ml)	1
<i>Xba</i> I (20 kU/ml)	1
10 x BSA (10mg/ml)	1
10 x digest buffer 2*	1
H <sub>2</sub> O	4

The digests were incubated at 37 °C for 2 h. The results were compared to their equivalent undigested plasmid by running them through a 1% (w/v) agarose gel (Figure 5.6 and 5.7).

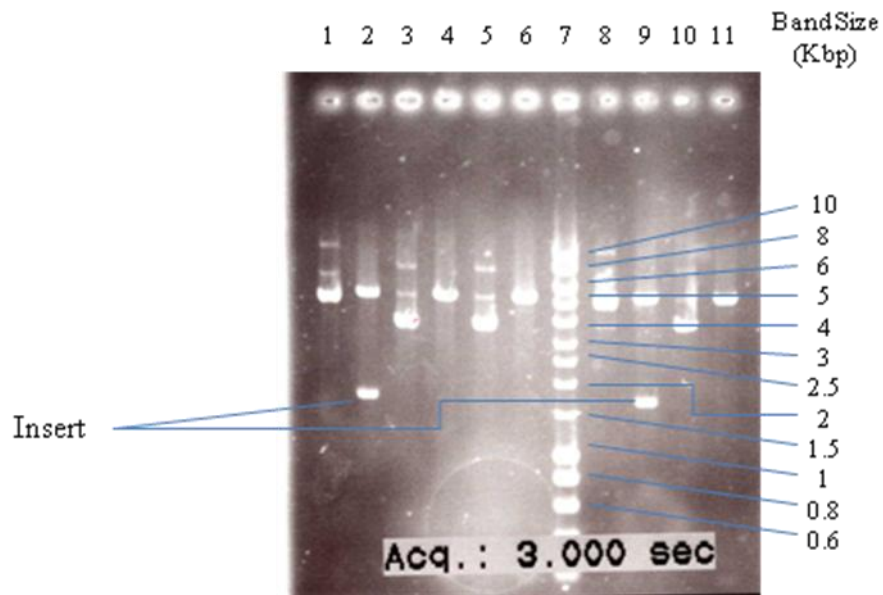


**Figure 5.6:** Undigested and digested plasmid. Lanes contain samples 1-5 (undigested then digested in the next lane); lane 7 contains hyperladder size standard.

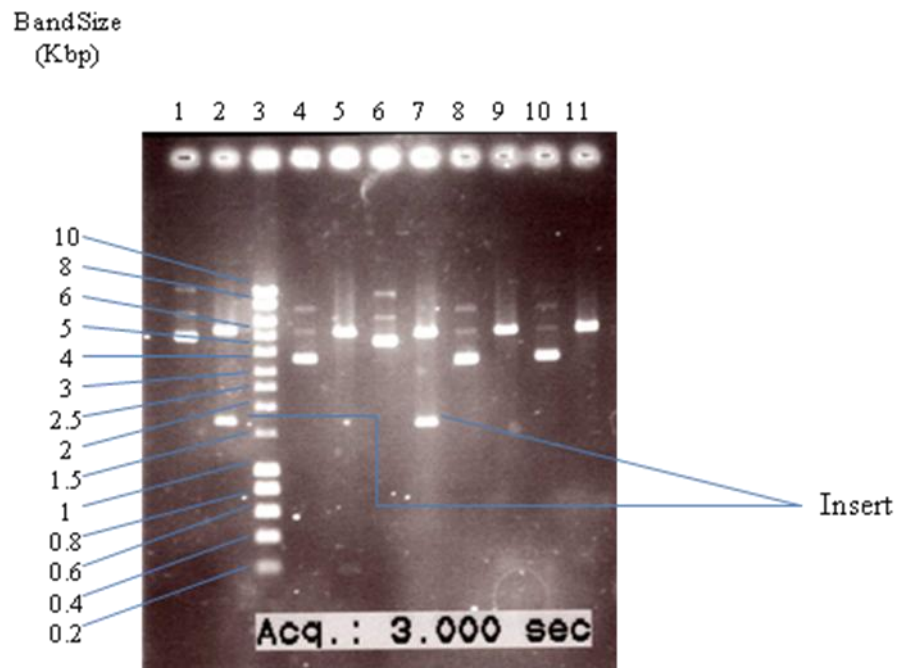


**Figure 5.7:** Undigested and digested plasmid. Lanes contain samples 6-10 (undigested then digested in the next lane); lane 3 contains hyperladder size standard.

Samples 1, 4, 6, and 8 contained the insert (40% success rate). From these 4, sample 8 was selected for transformation.

### 5.2.7 Transformation of recombinant plasmid

*E. coli* BL21 cells (Novagen) were transformed with undigested plasmid sample 8 (stored at -20 °C when plasmid was isolated above) via the same method used to transform the annealing products above. From this, a single colony was selected and inoculated into 5 ml of MDG medium (Studier, 2005) (see Appendix C), incubated at 37 °C and shaken at 200 rpm overnight.

MDG culture (0.5 ml) was added to 0.5 ml of 50% (v/v) glycerol, mixed and then stored at -80 °C for possible future work. The remaining 4.5 ml was added to 50 ml of ZYM medium (Studier, 2005) (see Appendix C), incubated at 30 °C and shaken at 100 rpm for 24 h. After this time, the optical density of the culture was measured at 600 nm as  $>4$  indicating sufficient growth had taken place to produce protein.

### 5.2.8 Determination of solubility of protein

ZYM culture (0.5 ml) was microcentrifuged at 18,000 x g for 2 min. The supernatant was discarded. To the pellet, 300 µl of solubilising buffer (see Appendix C) was added and then vortex mixed and boiled for two minutes. This process solubilises the total protein present.

The remaining 49.5 ml of ZYM culture was centrifuged at 4,000 x g for 15 min at 4 °C. The supernatant was discarded and the pellet resuspended in 5 ml of a buffer consisting of 50 mM Na<sub>2</sub>HPO<sub>4</sub> (pH 7.4); 10 mM imidazole; 0.5 M NaCl. The suspension was sonicated at an amplitude of 14 microns for two minutes (10 seconds on, 10 seconds off) on ice, to release the soluble proteins, before being centrifuged at 20,000 x g for 30 min at 4 °C and the pellet discarded. Supernatant (20 µl) was mixed with 5 µl SDS-PAGE loading buffer (see Appendix C), vortex mixed, then boiled for 2 min. The two samples (for total and soluble protein) were compared on a 12% (w/v) SDS-PAGE gel (200 V, 100 mA for 60 min) which was stained with

Coomassie blue stain (see Appendix C), for 10 min before being destained, until blue bands could be seen on a clear background (Figure 5.8 and 5.9).

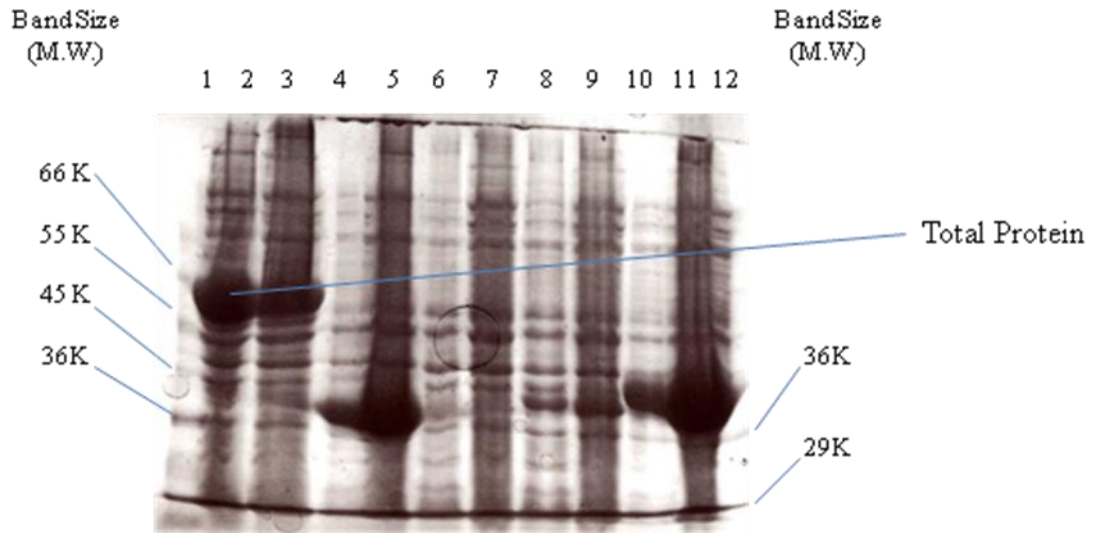


**Figure 5.8:** Total protein sample (lane 2); High (lane 1) and low (lane 12) molecular weight markers.

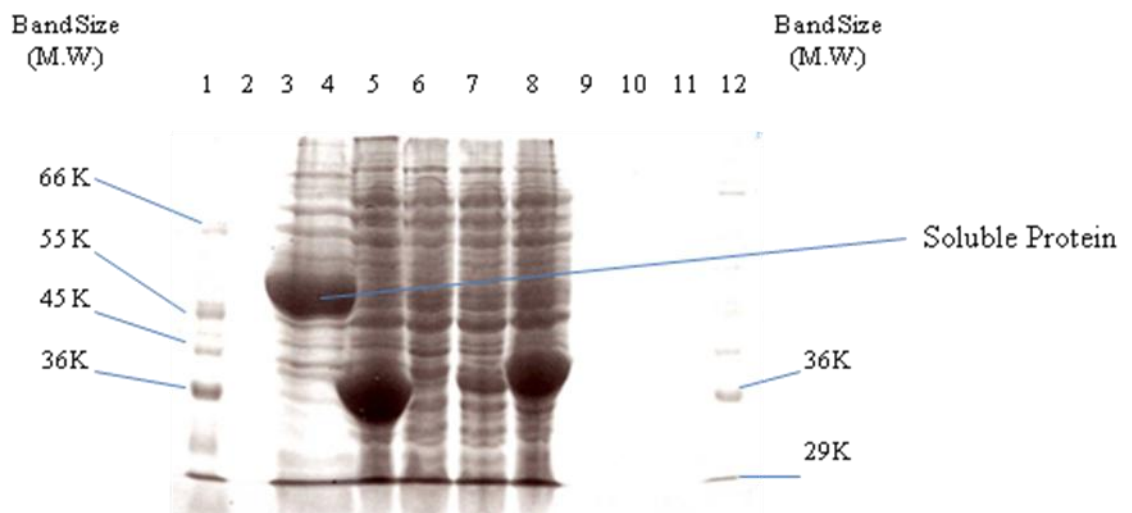


**Figure 5.9:** Soluble protein sample (lane 4); High (lane 1) and low (lane 12) molecular weight markers.

The gels above show a large band of hyper-expressed recombinant protein of an approximate relative molecular weight of 55,000. By entering the amino acid sequence for the putative enzyme (obtained earlier from the NCBI Genbank database) into the 'ProtParam' tool on the Expasy website (<http://www.expasy.ch/tools/protparam.html>) its predicted molecular weight was calculated as 54,879.8 Da. This corresponded to the size of the expressed protein. This protein was found to be soluble due to the appearance of a large band of protein, of the correct size, in the soluble protein sample.

### **5.2.9 Purification by nickel affinity chromatography**

Of the supernatant used to produce the soluble protein sample, 50  $\mu$ l was stored at 4 °C for later use when assaying for enzyme activity and the remaining 4.93 ml was processed through a nickel affinity column under the following conditions.

The column was equilibrated to the same conditions as that of the supernatant by applying 30ml of start buffer (20 mM HEPES; 500 mM NaCl; 10mM imidazole, pH 7.4) at a rate of 5 ml/min. The supernatant was then introduced to the column. The protein binds to the nickel of the column because of the hexahistadine (histag) on the N-terminus of the protein. Other proteins present will have less affinity for the nickel and will be eluted from the column. To elute the protein in a controlled manner, an elution buffer (500 mM imidazole; 20 mM HEPES, pH 7.4) was applied on a linear increasing gradient at a flow rate of 5 ml/min. Fractions were collected every minute. The results of this process are shown in the chromatogram below (Figure 5.10).

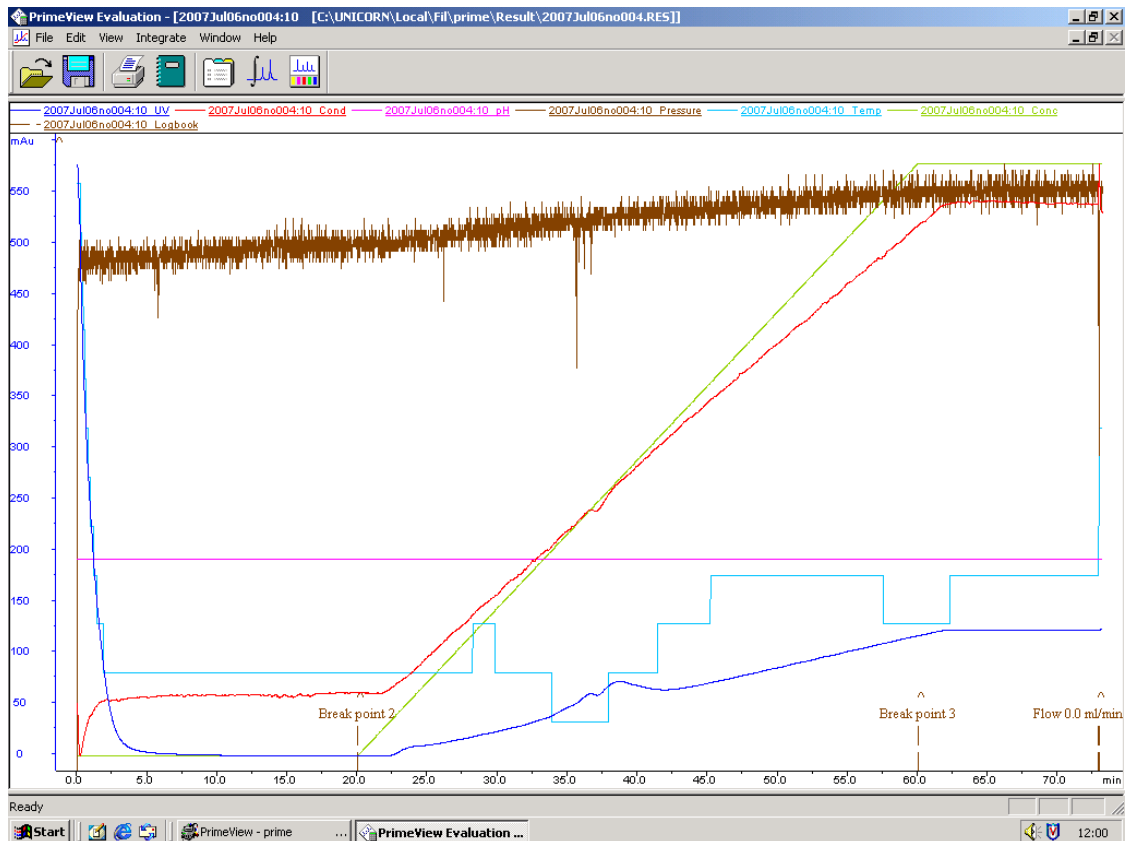


**Figure 5.10:** Purification of protein by nickel affinity chromatography. Chromatogram of absorbance at 280 nm against time in minutes. Green line shows the increasing gradient of elution buffer. Blue line shows changing absorbance at 280 nm.

An increase in absorbance at 36 - 45 mins indicated a large amount of protein had been eluted from the column. The fractions corresponding to those times were run on a 12% (w/v) SDS-PAGE gel under conditions described previously (Figure 5.11) which showed that contaminating proteins had been removed.

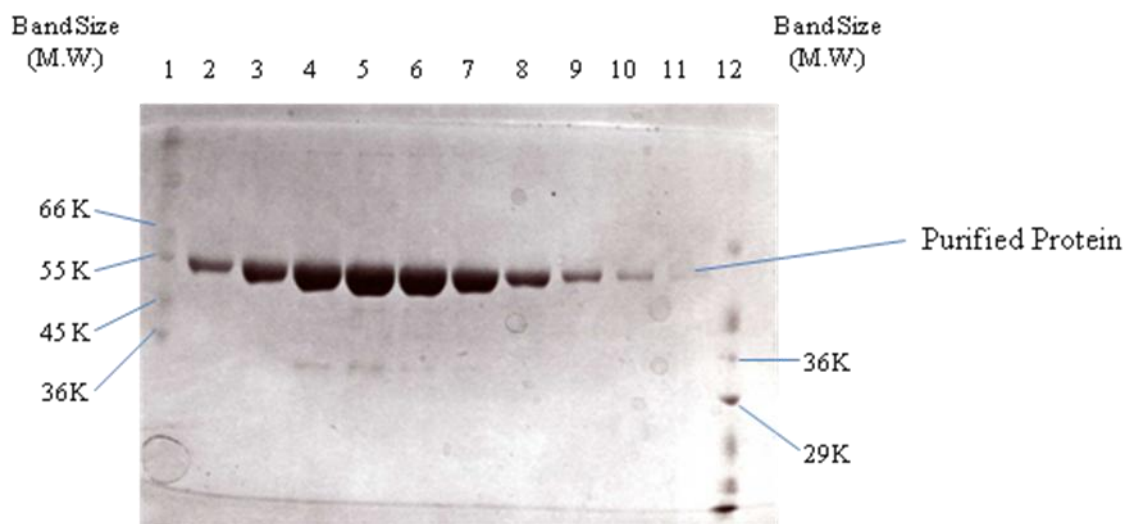


**Figure 5.11:** Purified protein. Samples 36 - 45 (lanes 2 - 11); High (lane 1) and low (lane 12) molecular weight markers.

### 5.2.10 Concentration of protein

The pure protein fractions 36 – 45 were pooled and concentrated using a Vivascience ‘vivaspin’ centrifuge tube with a 30,000 Da molecular weight cut-off. When centrifuged at 4,000 x g, anything with a MW below 30,000 Da is filtered from the pooled fractions, including buffer. The fractions were concentrated until the volume decreased from 50 ml to approximately 0.5 ml. The concentrate was washed 3 times with 5 mM HEPES buffer, pH 7.4 to remove imidazole, which can be inhibitory to enzymes, and again concentrated to a final volume of 0.5 ml. The protein solution was then stored at 4 °C in 3.2 M ammonium sulfate (0.5 g/l).

### 5.3 Results

To determine if the protein expressed has activity as a leucyl aminopeptidase the following assay was performed with the substrate L-leucine-7-amido-4-methyl-coumarin hydrochloride. Substrate (0.005 mg/ml) was dissolved in a drop of dimethyl sulfoxide (DMSO), then in 10 mM HEPES buffer, pH 7.4. To 1 ml of this was added either 50  $\mu$ l of distilled H<sub>2</sub>O (blank), protein solution, filtered washings from concentration process or cell free extract supernatant (stored just prior to purifying with nickel column). These reactions were then incubated at 37 °C for 1 h before being viewed under exposure to ultraviolet light (Figure 5.12).

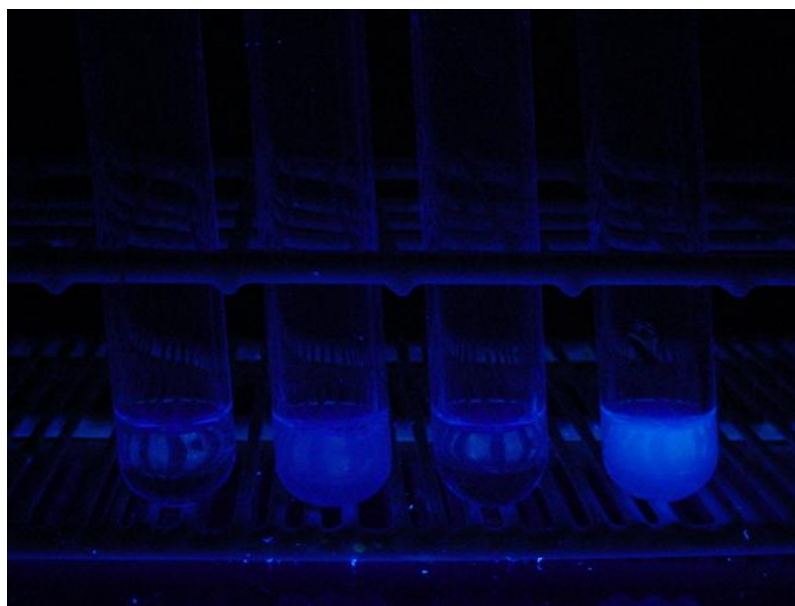


**Figure 5.12:** Leucyl aminopeptidase activity. Tubes (from left to right); blank, protein, washings and cell free extract supernatant.

Fluorescence showed enzyme activity against L-leucine-7-amido-4-methyl-coumarin hydrochloride in the purified protein sample and the cell free extract supernatant but none in the filtered washings from the concentration process. From these results, it can be concluded that the process has successfully produced an active leucyl aminopeptidase.

## 5.4 Discussion

Although time did not permit the synthesis or evaluation of any aminopeptidase substrates, the work done in this part of the study still had positive outcomes.

An active recombinant leucyl aminopeptidase was produced and the expression vector produced during this work has been taken up by Prozomix Ltd. (a U.K. biotechnology company that develops, produces and supplies a large, diverse and rapidly expanding range of highly purified recombinant enzymes and proteins of known sequence with associated biochemical reagents) as part of their commercial academic partnering programme. This programme offers royalty based commercialisation of enzyme and protein encoding recombinant plasmids from the global academic resource.

Once the specific activity of this enzyme has been determined, it may be used to measure kinetics and evaluate newly synthesised substrates at a fraction of the cost of purchasing aminopeptidase from a commercial source, not to mention produce royalties.

## **CHAPTER SIX**

### **Conclusions and future work**

## 6.1 Conclusions

The aim of this study was to produce novel enzyme substrates and apply them to uses in biomedical science. This has been achieved by synthesising a range of chromogenic and fluorogenic core compounds, then evaluating their suitability as chromophores, fluorophores and metal chelators. It was then attempted to glycosidate the promising compounds leading to the successful substrates being selected for evaluation with respect to applications in biomedical science.

Major findings include:-

- Novel core compounds synthesised:-

2-hydroxy-1-naphthaldehyde-4-nitrophenylhydrazone

4-acetoxy-3-methoxycinnamylidene-1,3-indandione

4-hydroxy-3-methoxycinnamylidene-3-phenyl-5-isoxazolone

3,4-dihydroxybenzylidene benzhydrazide

- Substrates applied and evaluated:-

alizarin-2-yl- $\beta$ -D-galactoside, used to identify recombinant and non-recombinant transformants in molecular biology

alizarin-2-octanoate, used to detect species such as *Salmonella* and

5-nitrosalicylaldehyde- $\beta$ -D-galactoside used to identify Gram-negative bacterial species in microbiology

3-hydroxyflavone- $\beta$ -D-glucoside used as a fluorogenic and chromogenic substrate for isolated  $\beta$ -glucosidase enzyme and for microbial identification of *Listeria* spp.

- The cloning and expression of a gene and the characterisation of its encoded product as an active recombinant leucyl aminopeptidase.

## 6.2 Future work

Apart from the uses already stated in this work, for example diagnostic microbiology, it may be possible to develop other roles for these chromogenic and fluorogenic substrates.

They may be employed in the field of microbial systematics, the classification, nomenclature and identification of microorganisms. If a range of substrates with different sugars was produced they could form the basis of a semi-automated rapid multiplate test, used to build taxonomic profiles. Another use of this system would be a faster method of determining the correct nutrient (sugar) content when developing new selective media.

Although highly specific, these substrates could be, for example, used as a more cost effective and less hazardous method of investigating bacterial cell wall development in pathogens such as *Mycobacterium tuberculosis*, with the hope of identifying new drug targets. Current experimental research uses a  $^{14}\text{C}$  radiolabelled sugar, to monitor uptake and function in the cell wall and is visualised by thin layer chromatography and autoradiography (Birch et al., 2008). A chromogenic substrate with the correct sugar moiety may be used instead of the radiolabelled sugar, reducing both the hazard and the amount of labour required to perform the method.

The use of alizarin based substrates has so far been limited to the incorporation of iron and aluminium salts, but, in this study, a variety of other metal ions have been used and compared and some show additional potential. Cobalt and zinc, for

example, gave a dark purple chelate, while magnesium gave a lighter purple coloration, and all of these precipitated to some degree.

An alternative, although more involved, method of creation of alizarin substrates having varied colours with added metal ions, is to substitute other groupings in the anthraquinone skeleton. Inspection of such works as the Handbook of the Society of Dyeists and Colourists describes various alizarinic molecules such as 3- and 4-nitroalizarins (Figure 6.1) and their reduction products, i.e. the aminoalizarins. The aminoalizarins, in particular, give rise to substantially different coloured metal complexes.

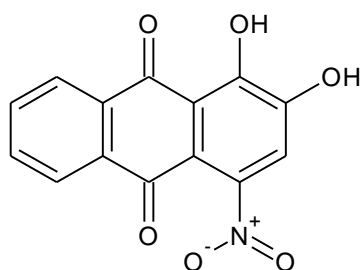


**Figure 6.1:** Structure of 4-nitroalizarin.

Furthermore, by subjecting the aminoalizarins to a Skraup reaction such as is commonly encountered in the synthesis of quinolines (Li, 2006), cyclisation occurs giving rise to, e.g., ‘Alizarin Green’ (Figure 6.2). This is reported to give a bright green metal complex with iron and could find value if derivatised as a glycoside.

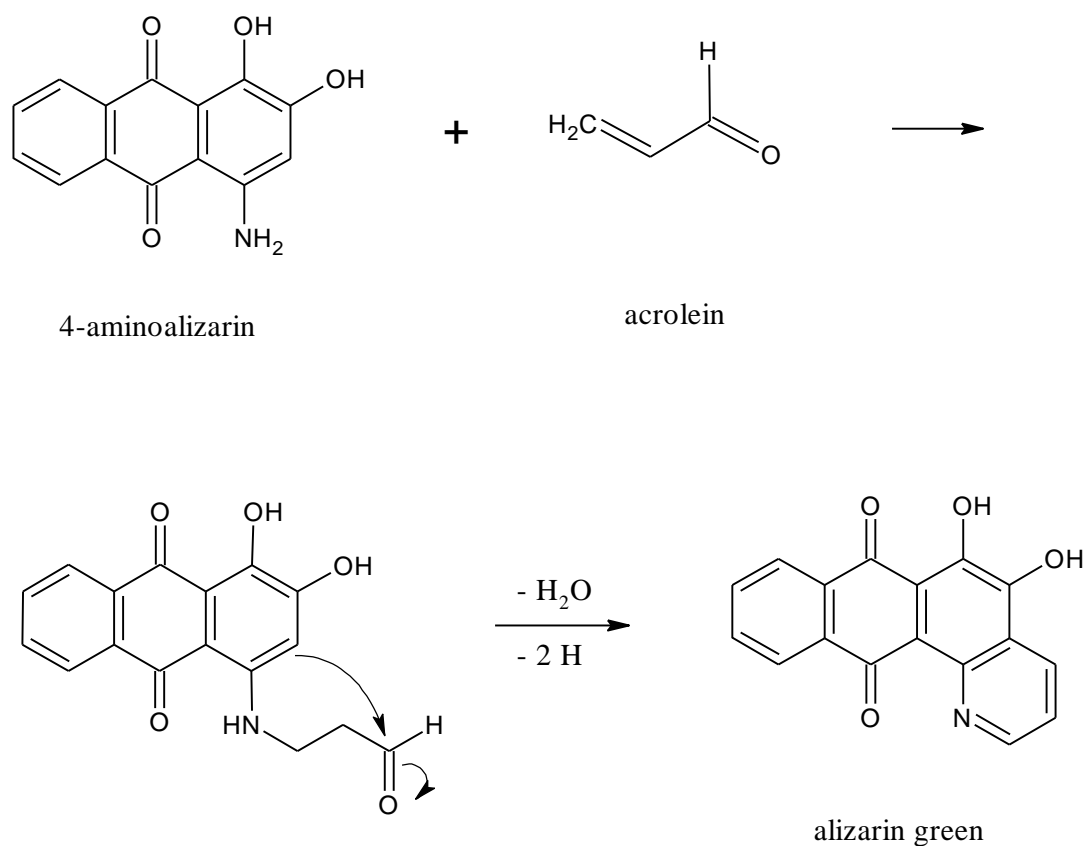


**Figure 6.2:** Possible cyclisation of 4-aminoalizarin to form alizarin green via the Skraup reaction.

In addition to the octanoate, several other esters of alizarin were synthesised, e.g. alizarin-2-palmitate. The disadvantage of such long chain esters is, however, the aqueous insolubility. One possible solution to the insolubility problems associated with the use of these alizarin esters would be to synthesise the corresponding Alizarin Red S compound (Figure 6.3). This is a 3-sulphonic acid derivative of alizarin and the sulphonic acid group would confer a high measure of water solubility to the otherwise highly non-polar substrate.

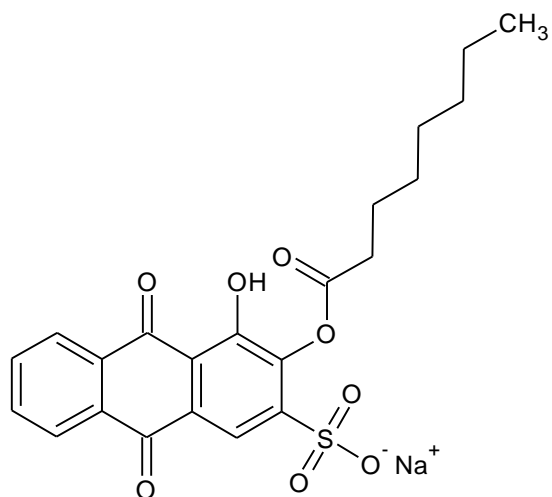
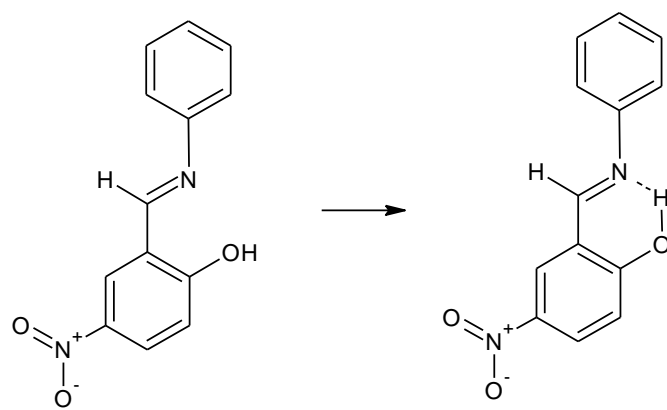
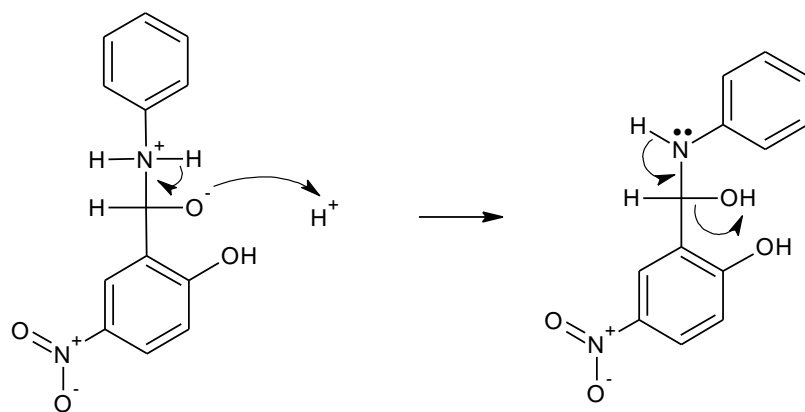
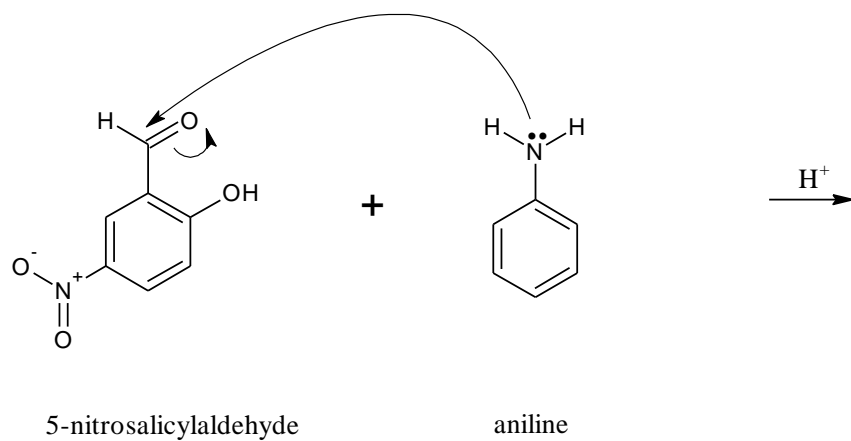


**Figure 6.3:** Structure of alizarin Red S-2-octanoate.

Regarding 5-nitrosalicylaldehyde substrates, the chelation depends on an interaction between the phenolic hydroxyl group and the adjacent aldehyde, it is conceivable that an extension of this work could be to create a Schiff's base or aldimine by reaction of either nitrosalicylaldehyde itself or the glycoside with an amine, e.g. aniline (Figure 6.4). Formation of these aldimines is usually straightforward, involving reaction of the components in acidic ethanol.



5-nitrosalicylidene-aniline

**Figure 6.4:** Possible synthesis of 5-nitrosalicylidene-aniline.

The chelation properties of such aldimines could be studied using appropriate metal ions and the glycosides evaluated accordingly (Figure 6.5).

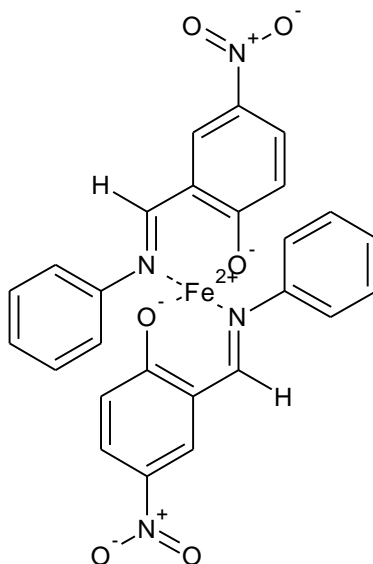
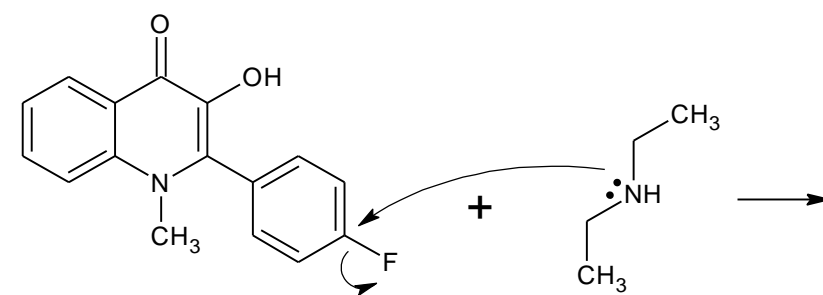


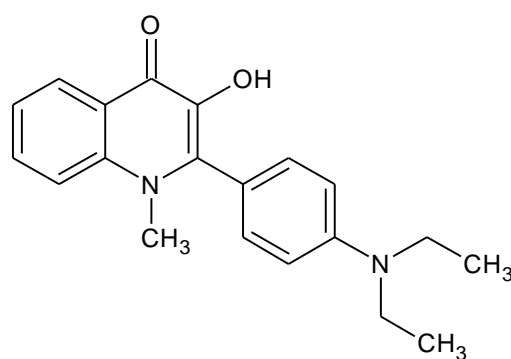
**Figure 6.5:** Chelation of 5-nitrosalicylidene-aniline with  $Fe^{2+}$ .

The attempts at glycosidating the quinolone compounds did not give satisfactory results, probably because of their limited solubility. One possible method of improving the situation with respect to solubility would be to react the fluorophenyl compound with a secondary amine such as diethylamine in dimethylformamide (Figure 6.6). This is described in the previously mentioned paper. The 4-dialkylaminophenyl compounds produced could have greater solubility and be more readily glycosidated.



1-methyl-2(4'-fluorophenyl)-3-hydroxy-4(1*H*)-quinolone

diethylamine



1-methyl-2(4'-diethylaminophenyl)-3-hydroxy-4(1*H*)-quinolone

**Figure 6.6:** Formation of 1-methyl-2(4'-diethylaminophenyl)-3-hydroxy-4(1*H*)-quinolone (Yushchenko et al., 2006a).

Finally, with the production of a more cost effective supply of recombinant leucyl aminopeptidase it will be possible (once the specific activity of the enzyme has been determined) to test the effectiveness of any leucyl aminopeptidase substrates synthesised in the future.

- AGBAN, A., OUNANIAN, M., LUUDUC, C. & MONGET, D. (1990) Synthesis of Indigogenic Substrates - Investigation of Salmonella Esterase-Activity. *European Journal of Medicinal Chemistry*, 25, 697-699.
- ALTMAN, F. P. (1976) Tetrazolium salts and formazans. *Prog Histochem Cytochem*, 9, 1-56.
- ANDERSON, F. B. & LEABACK, D. H. (1961) Substrates for the histochemical localization of some glycosidases. *Tetrahedron Letters*, 12, 236-239.
- APTE, S. C., DAVIES, C. M. & PETERSON, S. M. (1995) Rapid Detection of Fecal-Coliforms in Sewage Using a Colorimetric Assay of Beta-D-Galactosidase. *Water Research*, 29, 1803-1806.
- ARTICO, M., DI SANTO, R., COSTI, R., NOVELLINO, E., GRECO, G., MASSA, S., TRAMONTANO, E., MARONGIU, M. E., DE MONTIS, A. & LA COLLA, P. (1998) Geometrically and conformationally restrained cinnamoyl compounds as inhibitors of HIV-1 integrase: synthesis, biological evaluation, and molecular modeling. *J Med Chem*, 41, 3948-60.
- BABSON, A. L., GREELEY, S. J., COLEMAN, C. M. & PHILLIPS, G. E. (1966) Phenolphthalein monophosphate as a substrate for serum alkaline phosphatase. *Clin Chem*, 12, 482-90.
- BARTOS, J. & PESEZ, M. (1979) Colorimetric and Fluorimetric Determination of Aldehydes and Ketones. *Pure and Applied Chemistry*, 51, 1803-1814.
- BASCOMB, S. & MANAFI, M. (1998) Use of enzyme tests in characterization and identification of aerobic and facultatively anaerobic gram-positive cocci. *Clin Microbiol Rev*, 11, 318-40.
- BECKER, B., SCHULER, S., LOHNEIS, M., SABROWSKI, A., CURTIS, G. D. & HOLZAPFEL, W. H. (2006) Comparison of two chromogenic media for the detection of *Listeria monocytogenes* with the plating media recommended by EN/DIN 11290-1. *Int J Food Microbiol*, 109, 127-31.
- BERG, J. D. & FIKSDAL, L. (1988) Rapid detection of total and fecal coliforms in water by enzymatic hydrolysis of 4-methylumbelliferone-beta-D-galactoside. *Appl Environ Microbiol*, 54, 2118-22.
- BERLUTTI, F., DAINELLI, B., MARTINI, A. & THALLER, M. C. (1986) o-Nitrophenyl-beta-D-galactopyranoside-urease-indole broth, a new composite tube medium for *Salmonella* screening. *J Clin Microbiol*, 24, 650-1.
- BESSON, C., VESSILLIER, S., GONZALES, T., SAULNIER, J. & WALLACH, J. (1994) Conductimetric Assay of Pyroglutamyl Peptidase Activity. *Analytica Chimica Acta*, 294, 305-309.
- BIENIARZ, C., YOUNG, D. F. & CORNWELL, M. J. (1992) Chromogenic redox assay for beta-lactamases yielding water-insoluble products. I. Kinetic behavior and redox chemistry. *Anal Biochem*, 207, 321-8.
- BIRCH, H. L., ALDERWICK, L. J., BHATT, A., RITTMANN, D., KRUMBACH, K., SINGH, A., BAI, Y., LOWARY, T. L., EGGELING, L. & BESRA, G. S. (2008) Biosynthesis of mycobacterial arabinogalactan: identification of a novel alpha(1-->3) arabinofuranosyltransferase. *Mol Microbiol*, 69, 1191-206.

- BONSOR, D., BUTZ, S. F., SOLOMONS, J., GRANT, S., FAIRLAMB, I. J. S., FOGG, M. J. & GROGAN, G. (2006) Ligation independent cloning (LIC) as a rapid route to families of recombinant biocatalysts from sequenced prokaryotic genomes. *Organic & Biomolecular Chemistry*, 4, 1252-1260.
- BOUDET, A. C., CORNARD, J. P. & MERLIN, J. C. (2000) Conformational and spectroscopic investigation of 3-hydroxyflavone-aluminium chelates. *Spectrochim Acta A Mol Biomol Spectrosc*, 56, 829-39.
- BRETAUDIÈRE, J. P., VASSAULT, A., AMSELLEM, L., POURCI, M. L., THIEU-PHUNG, H. & BAILLY, M. (1977) Criteria for establishing a standardized method for determining alkaline phosphatase activity in human serum. *Clin Chem*, 23, 2263-74.
- BROWN, T. A. (2006) Gene cloning and dna analysis, an introduction. Wiley-Blackwell.
- BURESTEDT, E., NISTOR, C., SCHAGERLOF, U. & EMNEUS, J. (2000) An enzyme flow immunoassay that uses beta-galactosidase as the label and a cellobiose dehydrogenase biosensor as the label detector. *Analytical Chemistry*, 72, 4171-4177.
- BURKE, M. D., THOMPSON, S., ELCOMBE, C. R., HALPERT, J., HAAPARANTA, T. & MAYER, R. T. (1985) Ethoxy-, pentoxy- and benzyloxyphenoxazones and homologues: a series of substrates to distinguish between different induced cytochromes P-450. *Biochem Pharmacol*, 34, 3337-45.
- BUTTERWORTH, L. A., PERRY, J. D., DAVIES, G., BURTON, M., REED, R. H. & GOULD, F. K. (2004) Evaluation of novel beta-ribosidase substrates for the differentiation of Gram-negative bacteria. *Journal of Applied Microbiology*, 96, 170-176.
- CAMBOU, B. & KLIBANOV, A. M. (1984) Comparison of Different Strategies for the Lipase-Catalyzed Preparative Resolution of Racemic Acids and Alcohols - Asymmetric Hydrolysis, Esterification, and Trans-Esterification. *Biotechnology and Bioengineering*, 26, 1449-1454.
- CARRICAJÓ, A., BOISTE, S., THORE, J., AUBERT, G., GILLE, Y. & FREYDIÈRE, A. M. (1999) Comparative evaluation of five chromogenic media for detection, enumeration and identification of urinary tract pathogens. *European Journal of Clinical Microbiology & Infectious Diseases*, 18, 796-803.
- CASSAR, R. & CUSCHIERI, P. (2003) Comparison of Salmonella chromogenic medium with DCLS agar for isolation of Salmonella species from stool specimens. *J Clin Microbiol*, 41, 3229-32.
- CHEN, L., LI, J., LUO, C., LIU, H., XU, W., CHEN, G., LIEW, O. W., ZHU, W., PUAH, C. M., SHEN, X. & JIANG, H. (2006) Binding interaction of quercetin-3-beta-galactoside and its synthetic derivatives with SARS-CoV 3CL(pro): structure-activity relationship studies reveal salient pharmacophore features. *Bioorg Med Chem*, 14, 8295-306.
- CLARK, A. G. & MCLAUCHLIN, J. (1997) Simple color tests based on an alanyl peptidase reaction which differentiate *Listeria monocytogenes* from other *Listeria* species. *Journal of Clinical Microbiology*, 35, 2155-2156.

- COHEN, S. N., CHANG, A. C. Y., BOYER, H. W. & HELLING, R. B. (1973) Construction of Biologically Functional Bacterial Plasmids in-Vitro. *Proceedings of the National Academy of Sciences of the United States of America*, 70, 3240-3244.
- COHEN, S. N., CHANG, A. C. Y. & HSU, L. (1972) Nonchromosomal Antibiotic Resistance in Bacteria - Genetic Transformation of Escherichia-Coli by R-Factor DNA. *Proceedings of the National Academy of Sciences of the United States of America*, 69, 2110-&.
- COMFORT, D. & CAMPBELL, D. J. (1966) One-step automated alkaline phosphatase analysis. *Clin Chim Acta*, 14, 263-9.
- COOKE, V. M., MILES, R. J., PRICE, R. G. & RICHARDSON, A. C. (1999) A novel chromogenic ester agar medium for detection of Salmonellae. *Appl Environ Microbiol*, 65, 807-12.
- CORNARD, J. P. & MERLIN, J. C. (2003) Comparison of the chelating power of hydroxyflavones. *Journal of Molecular Structure*, 651, 381-387.
- DALAL, F. R., AKHTAR, M., SHIN, K. H. & WINSTEN, S. (1971) Beta-glycerophosphate and thymolphthalein monophosphate compared as substrates for determining alkaline phosphatase activity in serum. *Clin Chem*, 17, 323-5.
- DAUZONNE, D. & ROYER, R. (1984) A Convenient Synthesis of 2-(2-Nitroethyl)-Phenols. *Synthesis-Stuttgart*, 1054-1057.
- DE SILONIZ, M. I., VALDERRAMA, M. J. & PEINADO, J. M. (2000) A chromogenic medium for the detection of yeasts with beta-galactosidase and beta-glucosidase activities from intermediate moisture foods. *J Food Prot*, 63, 651-4.
- DE, S. K. & GIBBS, R. A. (2005) An efficient and practical procedure for the synthesis of 4-substituted coumarins. *Synthesis-Stuttgart*, 1231-1233.
- DEALLER, S. F. (1993) Chromogenic and fluorogenic indicators and substrates in diagnostic microbiology. *Rev. Med. Microbiol.*, 4, 198-206.
- DELISLE, G. J. & LEY, A. (1989) Rapid detection of Escherichia coli in urine samples by a new chromogenic beta-glucuronidase assay. *J Clin Microbiol*, 27, 778-9.
- DORONIN, C. Y., CHERNOVA, R. K. & GUSAKOVA, N. N. (2004) 4-dimethylaminocinnamaldehyde as a photometric reagent for primary aromatic amines. *Journal of Analytical Chemistry*, 59, 335-344.
- EDBERG, S. C., ALLEN, M. J. & SMITH, D. B. (1988) National field evaluation of a defined substrate method for the simultaneous enumeration of total coliforms and Escherichia coli from drinking water: comparison with the standard multiple tube fermentation method. *Appl Environ Microbiol*, 54, 1595-601.
- ENYEDY, E. J. & KOVACH, I. M. (2004) Proton inventory studies of alpha-thrombin-catalyzed reactions of substrates with selected P and P' sites. *Journal of the American Chemical Society*, 126, 6017-6024.
- FENSOM, A. H., BENSON, P. F., BLUNT, S., BROWN, S. P. & COLTART, T. M. (1976) Amniotic Cell 4-Methylumbelliferyl-Alpha-Glucosidase Activity for Prenatal Diagnosis of Pompe Disease. *Journal of Medical Genetics*, 13, 148-149.
- FISCHER, O., KOENIG, E. (1914) *Chemische Berichte*, 47, 1078.

- FISHMAN, W. H., NAKAJIMA, Y., ANSTISS, C., GREEN, S. (1964) Naphthol AS-BI  $\beta$ -D-Glucosiduronic acid; its synthesis and suitability as a substrate for  $\beta$ -Glucuronidase. *J. Histochem. Cytochem*, 12, 298-305.
- FISKE, C. H. & SUBBAROW, Y. (1925) The colorimetric determination of phosphorus. *J. Biol. Chem.*, 66, 375-400.
- FOGG, M. J. & WILKINSON, A. J. (2008) Higher-throughput approaches to crystallization and crystal structure determination. *Biochemical Society Transactions*, 36, 771-775.
- FRAMPTON, E. W., RESTAINO, L. & BLASZKO, N. (1988) Evaluation of the Beta-Glucuronidase Substrate 5-Bromo-4-Chloro-3-Indolyl-Beta-D-Glucuronide (X-Gluc) in a 24-Hour Direct Plating Method for Escherichia-Coli. *Journal of Food Protection*, 51, 402-404.
- FREYDIERE, A. M. & GILLE, Y. (1991) Detection of Salmonellae by Using Rambach Agar and by a C8-Esterase Spot-Test. *Journal of Clinical Microbiology*, 29, 2357-2359.
- GE, F. Y., CHEN, L. G., ZHOU, X. L., PAN, H. Y., YAN, F. Y., BAI, G. Y. & YAN, X. L. (2007) Synthesis and study on hydrolytic properties of fluorescein esters. *Dyes and Pigments*, 72, 322-326.
- GILBERT, C. R.-D. A. S. O. (2002) Substrate for beta-N-acetylglucosaminidase. *WO 02/40706*.
- GONG, P. (1996) Dehydrogenase activity in soil: A comparison between the TTC and INT assay under their optimum conditions. *Soil Biol. Biochem.*, 29, 211-214.
- GOODFELLOW, M. (1991 ) Identification of Some Mycolic Acid Containing Actinomycetes Using Fluorogenic Probes Based on 7-Amino-4-methylcoumarin and 4-Methylumbelliferone. . *Actinomycetologica*, 5, 21-27.
- GOODFELLOW, M., THOMAS, E. G. & JAMES, A. L. (1987) Characterization of Rhodococci Using Peptide-Hydrolase Substrates Based on 7-Amino-4-Methylcoumarin. *Fems Microbiology Letters*, 44, 349-355.
- GOODFELLOW, M., THOMAS, E. G., WARD, A. C. & JAMES, A. L. (1990) Classification and identification of rhodococci. *Zentralbl Bakteriol*, 274, 299-315.
- GORDEUK, V. R., CALEFFI, A., CORRADINI, E., FERRARA, F., JONES, R. A., CASTRO, O., ONYEKWERE, O., KITTLES, R., PIGNATTI, E., MONTOSI, G., GARUTI, C., GANGAIDZO, I. T., GOMO, Z. A. R., MOYO, V. M., ROUAULT, T. A., MACPHAIL, P. & PIETRANGELO, A. (2004) Iron overload in Africans and African-Americans and a common mutation in the SCL40A1 (ferroportin 1) gene (vol 31, pg 299, 2003). *Blood Cells Molecules and Diseases*, 33, 94-94.
- GOSSRAU, R. (1977) Microchemical Investigation of Alpha-D-Glucosidases Using 4-Methylumbelliferyl-Alpha-D-Glucoside and 2-Naphthyl-Alpha-D-Glucoside. *Histochemistry*, 52, 187-197.
- GRANGE, J. M. (1978) Fluorimetric Assay of Mycobacterial Group-Specific Hydrolase Enzymes. *Journal of Clinical Pathology*, 31, 378-381.
- GRANGE, J. M. & MCINTYRE, G. (1979) Fluorogenic Glycosidase Substrates - Their Use in the Identification of Some Slow Growing Mycobacteria. *Journal of Applied Bacteriology*, 47, 285-288.

- GREEN, J. (1927) *Journal of the Chemical Society*, 2931.
- GREEN, V. S., STOTT, D. E. & DIACK, M. (2006) Assay for fluorescein diacetate hydrolytic activity: Optimization for soil samples. *Soil Biology & Biochemistry*, 38, 693-701.
- GUILBAULT, G. G., KRAMER, D.N. (1966) Lipolysis of fluorescein and eosin esters. Kinetics of hydrolysis. *Anal Biochem*, 14, 28-40.
- HAUGHLAND, R. P. (2002) Handbook of Fluorescent Probes and Research Products (9th ed.), Molecular Probes.
- HAYASHI, M., NAKAJIMA, Y. & FISHMAN, W. H. (1964) The Cytologic Demonstration of Beta-Glucuronidase Employing Naphthol as-Bi Glucuronide and Hexazonium Pararosanilin; a Preliminary Report. *J Histochem Cytochem*, 12, 293-7.
- HAYS, W. S., WHEELER, D. E., EGHTESAD, B., GLEW, R. H. & JOHNSTON, D. E. (1998) Expression of cytosolic beta-glucosidase in guinea pig liver cells. *Hepatology*, 28, 156-63.
- HEANEY, S. I. & DAVISON, W. (1977) Determination of Ferrous Iron in Natural-Waters with 2,2' Bipyridyl. *Limnology and Oceanography*, 22, 753-760.
- HERZENBERG, L. A., PARKS, D., SAHAF, B., PEREZ, O., ROEDERER, M. & HERZENBERG, L. A. (2002) The history and future of the fluorescence activated cell sorter and flow cytometry: A view from Stanford. *Clinical Chemistry*, 48, 1819-1827.
- HUGH, R. & LEIFSON, E. (1953) The taxonomic significance of fermentative versus oxidative metabolism of carbohydrates by various gram negative bacteria. *J Bacteriol*, 66, 24-6.
- HUSSON, M. O., MIELCAREK, C., IZARD, D. & LECLERC, H. (1989) Alkaline phosphatase capture test for the rapid identification of *Escherichia coli* and *Shigella* species based on a specific monoclonal antibody. *J Clin Microbiol*, 27, 1518-21.
- IBANEZ, G. A., ESCANDAR, G. M. & OLIVIERI, A. C. (2002) Proton transfer and coordination properties of aromatic alpha-hydroxy hydrazones. *Journal of Molecular Structure*, 605, 17-26.
- INAYAMA, S., MAMOTO, K., SHIBATA, T. & HIROSE, T. (1976) Structure and Antitumor Activity Relationship of 2-Arylidene-4-Cyclopentene-1,3-Diones and 2-Arylideneindan-1,3-Diones. *Journal of Medicinal Chemistry*, 19, 433-436.
- JACKIM, E. H., LAND, DAVID B. (1969) PHOSPHATE DERIVATIVES OF 3-HYDROXYFLAVONE. United States, Navy US.
- JAMES, A. L. (1993) Enzymes in taxonomy and diagnostic bacteriology. In: *M. Goodfellow and A.G. O'Donell, Editors, Chemical Methods in Prokaryotic Systematics, John Wiley & Sons, Chichester (1993)*. 471-492.
- JAMES, A. L., ARMSTRONG, L. (2001) Esculetin derivatives. United States, IDG (UK) Limited (Manchester, GB).
- JAMES, A. L., CHILVERS, K. F., PERRY, J. D., ARMSTRONG, L. & GOULD, F. K. (2000a) Evaluation of p-naphtholbenzein-beta-D-galactoside as a substrate for bacterial beta-galactosidase. *Appl Environ Microbiol*, 66, 5521-3.
- JAMES, A. L., PERRY, J. D., CHILVERS, K., ROBSON, I. S., ARMSTRONG, L. & ORR, K. E. (2000b) Alizarin-beta-D-galactoside: a new substrate

- for the detection of bacterial beta-galactosidase. *Letters in Applied Microbiology*, 30, 336-340.
- JAMES, A. L., PERRY, J. D., FORD, M., ARMSTRONG, L. & GOULD, F. K. (1996) Evaluation of cyclohexenoescluletin-beta-D-galactoside and 8-hydroxyquinoline-beta-D-galactoside as substrates for the detection of beta-galactosidase. *Applied and Environmental Microbiology*, 62, 3868-3870.
- JAMES, A. L. & YEOMAN, P. (1987) Detection of specific bacterial enzymes by high contrast metal chelate formation. Part I. 8-Hydroxyquinoline-beta-D-glucoside, an alternative to aesculin in the differentiation of members of the family Enterobacteriaceae. *Zentralbl Bakteriol Mikrobiol Hyg [A]*, 267, 188-93.
- JAMES, A. L. & YEOMAN, P. (1988) Detection of Specific Bacterial Enzymes by High Contrast Metal Chelate Formation .2. Specific Detection of Escherichia-Coli on Multipoint-Inoculated Plates Using 8-Hydroxyquinoline-Beta-D-Glucuronide. *Zentralblatt Fur Bakteriologie Mikrobiologie Und Hygiene Series a-Medical Microbiology Infectious Diseases Virology Parasitology*, 267, 316-321.
- JERMYN, M. A. (1955) Fungal Cellulases IV: Production and purification of an extracellular B-glucosidase of *Stachybotrys atra*. *Aust J Biol Sci*, 8, 541-562.
- KILIAN, M. & BULOW, P. (1976) Rapid diagnosis of Enterobacteriaceae. I. Detection of bacterial glycosidases. *Acta Pathol Microbiol Scand [B]*, 84B, 245-51.
- KILIAN, M. & BULOW, P. (1979) Rapid Identification of Enterobacteriaceae .2. Use of a Beta-Glucuronidase Detecting Agar Medium (Pgua Agar) for the Identification of Escherichia-Coli in Primary Cultures of Urine Samples. *Acta Pathologica Et Microbiologica Scandinavica Section B-Microbiology*, 87, 271-276.
- KIM, T. G. & CHUNG, K. M. (1989) Some Characteristics of Palm Kernel Olein Hydrolysis by Rhizopus-Arrhizus Lipase in Reversed Micelle of Aot in Isooctane, and Additive Effects. *Enzyme and Microbial Technology*, 11, 528-532.
- KITAZAWA, M., OHIZUMI, Y., OIKE, Y., HISHINUMA, T. & HASHIMOTO, S. (2007) Angiopoietin-related growth factor suppresses gluconeogenesis through the akt/forkhead box class O1-Dependent pathway in Hepatocytes. *Journal of Pharmacology and Experimental Therapeutics*, 323, 787-793.
- KITSON, T. M. & KITSON, K. E. (1997) Studies of the esterase activity of cytosolic aldehyde dehydrogenase with resorufin acetate as substrate. *Biochem J*, 322 ( Pt 3), 701-8.
- KODAKA, H., ISHIKAWA, M., IWATA, M., KASHITANI, F., MIZUOCHI, S. & YAMAGUCHI, K. (1995) Evaluation of New Medium with Chromogenic Substrates for Members of the Family Enterobacteriaceae in Urine Samples. *Journal of Clinical Microbiology*, 33, 199-201.
- KOK, R. G., VAN THOR, J. J., NUGTEREN-ROODZANT, I. M., BROUWER, M. B., EGMOND, M. R., NUDEL, C. B., VOSMAN, B. & HELLINGWERF, K. J. (1995) Characterization of the extracellular

- lipase, LipA, of *Acinetobacter calcoaceticus* BD413 and sequence analysis of the cloned structural gene. *Mol Microbiol*, 15, 803-18.
- KROGER, L. & THIEM, J. (2007) Synthesis and evaluation of glycosyl donors with novel leaving groups for transglycosylations employing beta-galactosidase from bovine testes. *Carbohydr Res*, 342, 467-81.
- KUMAR, A., SINGH, B. K., TYAGI, R., JAIN, S. K., SHARMA, S. K., PRASAD, A. K., RAJ, H. G., RASTOGI, R. C., WATTERSON, A. C. & PARMAR, V. S. (2005) Mechanism of biochemical action of substituted 4-methylcoumarins. Part 11: Comparison of the specificities of acetoxy derivatives of 4-methylcoumarin and 4-phenylcoumarin to acetoxy coumarins: protein transacetylase. *Bioorganic & Medicinal Chemistry*, 13, 4300-4305.
- LAZDUNSKI, A. M. (1989) Peptidases and Proteases of *Escherichia-Coli* and *Salmonella-Typhimurium*. *Fems Microbiology Reviews*, 63, 265-276.
- LE MINOR, L. A. F. B. H. (1962) Advantages of detecting  $\beta$ -galactosidase activity without the fermentation of lactose in diagnostic microbiology for the *Enterobacteriaceae*. *Ann. Inst. Pasteur (Paris)* 1962; 102, 267-277. *Annals Microbiology*, 112, 713-731.
- LEDER, L. D. (1970) Diagnostic experiences with the naphthol AS-D chloroacetate esterase reaction. *Blut*, 21, 1-8.
- LEDERBERG, J. (1950) The beta-d-galactosidase of *Escherichia coli*, strain K-12. *J Bacteriol*, 60, 381-92.
- LEQUIN, R. M. (2005) Enzyme Immunoassay (EIA)/Enzyme-Linked Immunosorbent Assay (ELISA). *Clinical Chemistry*, 51, 2415-2418.
- LEY, A., BARR, S., FREDENBURGH, D., TAYLOR, M. & WALKER, N. (1993) Use of 5-bromo-4-chloro-3-indolyl-beta-D-galactopyranoside for the isolation of beta-galactosidase-positive bacteria from municipal water supplies. *Can J Microbiol*, 39, 821-5.
- LEY, A. N., BOWERS, R. J. & WOLFE, S. (1988) Indoxyl-beta-D-glucuronide, a novel chromogenic reagent for the specific detection and enumeration of *Escherichia coli* in environmental samples. *Can J Microbiol*, 34, 690-3.
- LEYTUS, S. P., MELHADO, L. L. & MANGEL, W. F. (1983a) Rhodamine-Based Compounds as Fluorogenic Substrates for Serine Proteinases. *Biochemical Journal*, 209, 299-307.
- LEYTUS, S. P., PATTERSON, W. L. & MANGEL, W. F. (1983b) New Class of Sensitive and Selective Fluorogenic Substrates for Serine Proteinases - Amino-Acid and Dipeptide Derivatives of Rhodamine. *Biochemical Journal*, 215, 253-260.
- LI, J. J. (2006) Name Reactions. A collection of detailed reaction mechanisms. 3rd Ed. Springer., 545.
- LITTEL, K. J. & HARTMAN, P. A. (1983) Fluorogenic selective and differential medium for isolation of fecal streptococci. *Appl Environ Microbiol*, 45, 622-7.
- LJUNGBERG, H., OHLSON, S. & NILSSON, S. (1998) Exploitation of a monoclonal antibody for weak affinity-based separation in capillary gel electrophoresis. *Electrophoresis*, 19, 461-4.
- LOTRAKUL, P. & DHARMSTHITI, S. (1997) Purification and characterization of lipase from *Aeromonas sobria* LP004. *J Biotechnol*, 54, 113-20.

- LOWRY, O. H. (1957) Micromethods for the assay of enzymes. *Methods in Enzymology*, 4, 366-381.
- LUEDY-TENGER, F. (1956) *Microchimica Acta*, 37, 104,112.
- MACFADDIN, J. F. (2000) *Biochemical Tests for Identification of Medical Bacteria*, third ed. . *Williams & Wilkins, Baltimore, MD, USA*.
- MANAFI, M. (1996) Fluorogenic and chromogenic enzyme substrates in culture media and identification tests. *International Journal of Food Microbiology*, 31, 45-58.
- MANAFI, M. & KNEIFEL, W. (1990) Rapid methods for differentiating gram-positive from gram-negative aerobic and facultative anaerobic bacteria. *J Appl Bacteriol*, 69, 822-7.
- MANAFI, M., KNEIFEL, W. & BASCOMB, S. (1991) Fluorogenic and Chromogenic Substrates Used in Bacterial Diagnostics. *Microbiological Reviews*, 55, 335-348.
- MANAFI, M. & ROTTER, M. L. (1991) A new plate medium for rapid presumptive identification and differentiation of Enterobacteriaceae. *Int J Food Microbiol*, 14, 127-34.
- MANAFI, M. & SOMMER, R. (1992) Comparison of 3 Rapid Screening Methods for Salmonella Spp - Mucap Test, Microscreen Latex and Rambach Agar. *Letters in Applied Microbiology*, 14, 163-166.
- MANAFI, M. & SOMMER, R. (1993) Rapid Identification of Enterococci with a New Fluorogenic-Chromogenic Assay. *Water Science and Technology*, 27, 271-274.
- MANAFI, M., WINDHAGER, K. (1997) Rapid identification of enterococci in water with a new chromogenic assay. *Abstracts of the 97th Meeting of the American Society for Microbiology*, 453.
- MANTLE, D., HARDY, M. F., LAUFFART, B., MCDERMOTT, J. R., SMITH, A. I. & PENNINGTON, R. J. (1983) Purification and characterization of the major aminopeptidase from human skeletal muscle. *Biochem J*, 211, 567-73.
- MARCINOWSKI, S. & GRISEBACH, H. (1978) Enzymology of lignification. Cell-wall bound beta-glucosidase for coniferin from spruce (*Picea abies*) seedlings. *Eur J Biochem*, 87, 37-44.
- MARSH, C. A. & REID, L. M. (1965) Chemical Synthesis of Phenolphthalein Beta-Glucuronide. *Biochim Biophys Acta*, 97, 597-9.
- MATSUI, M., FOWLER, J. H. & WALLING, L. L. (2006) Leucine aminopeptidases: diversity in structure and function. *Biological Chemistry*, 387, 1535-1544.
- MEEZAN, E., MEEZAN, J., MANZELLA, S. & RODEN, L. (1997) Alkylglycosides as artificial primers for glycogen biosynthesis. *Cell Mol Biol (Noisy-le-grand)*, 43, 369-81.
- MELLIDIS, A. S. & PAPAGEORGIOU, V. P. (1986) Novel Method for Selective Esterification of Polyhydroxy-Anthraquinones. *Tetrahedron Letters*, 27, 5881-5882.
- MICHAELIS, L., MENTEN, M. (1913) Die Kinetik der Intertinwirkung *Biochem. Z.* , 49, 333-369.
- MILHAZES, N., CALHEIROS, R., MARQUES, M. P., GARRIDO, J., CORDEIRO, M. N., RODRIGUES, C., QUINTEIRA, S., NOVAIS, C., PEIXE, L. & BORGES, F. (2006) Beta-nitrostyrene derivatives as

- potential antibacterial agents: a structure-property-activity relationship study. *Bioorg Med Chem*, 14, 4078-88.
- MILLER, M., PALOJARVI, A., RANGGER, A., REESLEV, M. & KJOLLER, A. (1998) The use of fluorogenic substrates to measure fungal presence and activity in soil. *Applied and Environmental Microbiology*, 64, 613-617.
- MIZUNO, K., AWAZU, N. & TACHIKI, T. (1998) Purification and some properties of p-nitrophenyl-beta-D-glucoside-hydrolyzing enzymes in culture filtrate of *Bacillus circulans* KA-304 grown on cell-wall preparation of *Schizophyllum commune*. *Bioscience Biotechnology and Biochemistry*, 62, 39-43.
- MOHLER, W. A. & BLAU, H. M. (1996) Gene expression and cell fusion analyzed by lacZ complementation in mammalian cells. *Proceedings of the National Academy of Sciences of the United States of America*, 93, 12423-12427.
- MOLONEY, W. C., MCPHERSON, K. & FLIEGELMAN, L. (1960) Esterase activity in leukocytes demonstrated by the use of naphthol AS-D chloroacetate substrate. *J Histochem Cytochem*, 8, 200-7.
- MURGIER, M., PELISSIER, C., LAZDUNSKI, A., BERNADAC, A. & LAZDUNSKI, C. (1977) Aminopeptidase-N from *Escherichia-Coli* - Unusual Interactions with Cell-Surface. *European Journal of Biochemistry*, 74, 425-433.
- MURGIER, M., PELISSIER, C., LAZDUNSKI, A. & LAZDUNSKI, C. (1976) Existence, Localization and Regulation of Biosynthesis of Aminoendopeptidase in Gram-Negative Bacteria. *European Journal of Biochemistry*, 65, 517-520.
- ODA, Y., KINOSHITA, M. & KAKEHI, K. (1997) Fluorometric assay of binding specificity of plant lectins to yeast cells by biotin-avidin system and its application to the classification of yeast cells. *Anal Biochem*, 254, 41-8.
- OGDEN, I. D. & WATT, A. J. (1991) An Evaluation of Fluorogenic and Chromogenic Assays for the Direct Enumeration of *Escherichia-Coli*. *Letters in Applied Microbiology*, 13, 212-215.
- ORENGA, S. N. S. A., (FR), ROGER-DALBERT, CELINE (CHAZEY SUR AIN, FR), JAMES, ARTHUR (COCKERMOUTH, GB), PERRY, JOHN (NEWCASTLE-UPON-TYNE, GB) (2009) Method For Identifying at Least Two Groups of Microorganisms. United States, BIOMERIEUX (MARCY L'ETOILE, FR).
- PARK, S. J., LEE, E. J., LEE, D. H., LEE, S. H. & KIM, S. J. (1995) Spectrofluorometric Assay for Rapid Detection of Total and Fecal-Coliforms from Surface-Water. *Applied and Environmental Microbiology*, 61, 2027-2029.
- PEARSON, B., DEFENDI, V. (1957) A comparison between the histochemical demonstration of non-specific esterase activity by 5-bromo-indoxyl acetate, alpha-naphthyl acetate and naphthol AS acetate. *Journal of Histochemistry & Cytochemistry*, 5, 72-83.
- PECHMANN, H., DUISBERG, C. (1883) Ueber die Verbindungen der Phenole mit Acetessigather. *Berichte Der Deutschen Chemischen Gesellschaft*, 16, 2119-2128.

- PEMBERTON, R. M., HART, J. P., STODDARD, P. & FOULKES, J. A. (1999) A comparison of 1-naphthyl phosphate and 4 aminophenyl phosphate as enzyme substrates for use with a screen-printed amperometric immunosensor for progesterone in cows' milk. *Biosensors & Bioelectronics*, **14**, 495-503.
- PEREZ, J. M., CAVALLI, P., ROURE, C., RENAC, R., GILLE, Y. & FREYDIERE, A. M. (2003) Comparison of four chromogenic media and Hektoen agar for detection and presumptive identification of Salmonella strains in human stools. *J Clin Microbiol*, **41**, 1130-4.
- PERRY, J. D., FORD, M., TAYLOR, J., JONES, A. L., FREEMAN, R. & GOULD, F. K. (1999) ABC medium, a new chromogenic agar for selective isolation of Salmonella spp. *J Clin Microbiol*, **37**, 766-8.
- PETTIPHER, G. L., MANSELL, R., MCKINNON, C. H. & COUSINS, C. M. (1980) Rapid Membrane Filtration-Epifluorescent Microscopy Technique for Direct Enumeration of Bacteria in Raw-Milk. *Applied and Environmental Microbiology*, **39**, 423-429.
- PROTTI, S., MEZZETTI, A., LAPOUGE, C. & CORNARD, J. P. (2008) Photochemistry of metal complexes of 3-hydroxyflavone: towards a better understanding of the influence of solar light on the metal-soil organic matter interactions. *Photochem Photobiol Sci*, **7**, 109-19.
- PRUSAK, E., SIEWINSKI, M. & SZEWCZUK, A. (1980) A new fluorimetric method for the determination of gamma-glutamyltransferase activity in blood serum. *Clin Chim Acta*, **107**, 21-6.
- RABINOVITCH, P. S., TORRES, R. M. & ENGEL, D. (1986) Simultaneous cell cycle analysis and two-color surface immunofluorescence using 7-amino-actinomycin D and single laser excitation: applications to study of cell activation and the cell cycle of murine Ly-1 B cells. *J Immunol*, **136**, 2769-75.
- RAIFORD, L. C., FOX, D. E. (1944) Condensation of vanillin substitution products with nitromethane. *Journal of Organic Chemistry*, **09**, 170-174.
- RAMBACH, A., BOULEVARD MONTPARNASSE, 75006 PARIS, FR) (2007) Vibrio bacteria detection and differentiation. United States.
- RAYMOND, K. N., DERTZ, E. A. & KIM, S. S. (2003) Enterobactin: An archetype for microbial iron transport. *Proceedings of the National Academy of Sciences of the United States of America*, **100**, 3584-3588.
- REDONDO, F. L., PASCUAL, T., BERGON, E. & MIRAVALLS, E. (1986) L-Alanine-4-Nitroanilide as a Substrate for Microsomal Aminopeptidase. *Clinical Chemistry*, **32**, 912-913.
- RIGGS, J. L., SEIWALD, R. J., BURCKHALTER, J. H., DOWNS, C. M. & METCALF, T. G. (1958) Isothiocyanate compounds as fluorescent labeling agents for immune serum. *Am J Pathol*, **34**, 1081-97.
- ROBERTSON, A. (1930) The synthesis of glucosides. Part IV. Alizarin glucoside. *J. Chem. Soc.*, 1136 - 1141.
- ROBERTSON, A., JONES, E.T. (1933) Natural Glycosides. Part V. Ruberythric Acid. *J. Chem. Soc.*, 1167-1169.
- ROTMAN, B., ZDERIC, J. A. & EDELSTEIN, M. (1963) Fluorogenic substrates for beta-D-galactosidases and phosphatases derived from fluorescein (3,6-dihydroxyfluoran) and its monomethylether. *Proc Natl Acad Sci U S A*, **50**, 1-6.

- SAMBROOK, J. (1989) *Molecular Cloning: A Laboratory Manual*, Cold Spring Harbor Laboratory. 186.
- SARTORY, D. P. & HOWARD, L. (1992) A Medium Detecting Beta-Glucuronidase for the Simultaneous Membrane Filtration Enumeration of Escherichia-Coli and Coliforms from Drinking-Water. *Letters in Applied Microbiology*, 15, 273-276.
- SCHRAM, A. W., BROUWERKELDER, B., DONKERKOOPTMAN, W. E., LOONEN, C., HAMERS, M. N. & TAGER, J. M. (1979) Use of Immobilized Antibodies in Investigating Acid Alpha-Glucosidase in Urine in Relation to Pompe Disease. *Biochimica Et Biophysica Acta*, 567, 370-383.
- SCHRECKER, A. W. & CHIRIGOS, M. A. (1978) Improved determination of beta-glucuronidase in serum. *Clin Chim Acta*, 88, 413-5.
- SEIDERMAN, M. & LINK, K. (1950) New compounds, substituted salicylaldehydes and derivatives. *J. Am. Chem. Soc.*, 72, 4324-4324.
- SHIMOMURA, O., INOUE, S., MUSICKI, B. & KISHI, Y. (1990) Recombinant Aequorin and Recombinant Semisynthetic Aequorins - Cellular Ca<sup>2+</sup> Ion Indicators. *Biochemical Journal*, 270, 309-312.
- SMITH, M. L., CARSKI, T. R. & GRIFFIN, C. W. (1962) Modification of fluorescent-antibody procedures employing crystalline tetramethylrhodamine isothiocyanate. *J Bacteriol*, 83, 1358-9.
- SMITH, P. A., MELLORS, D., HOLROYD, A. & GRAY, C. (2001) A new chromogenic medium for the isolation of Listeria spp. *Lett Appl Microbiol*, 32, 78-82.
- SNYDER, C. (2005) Solution interaction with the ocular surface: The significance of making the grade. *Clinical and Refractive Optometry*, 16, 134-140.
- STUDIER, F. W. (2005) Protein production by auto-induction in high-density shaking cultures. *Protein Expression and Purification*, 41, 207-234.
- SZABO, R. A., TODD, E. C. D. & JEAN, A. (1986) Method to Isolate Escherichia-Coli O157-H7 from Food. *Journal of Food Protection*, 49, 768-772.
- TAKAGI, M., NISHIOKA, M., KAKIHARA, H., KITABAYASHI, M., INOUE, H., KAWAKAMI, B., OKA, M. & IMANAKA, T. (1997) Characterization of DNA polymerase from Pyrococcus sp. strain KOD1 and its application to PCR. *Applied and Environmental Microbiology*, 63, 4504-4510.
- TOBE, S. S., WATSON, N. & NIC DAEID, N. (2007) Evaluation of six presumptive tests for blood, their specificity, sensitivity, and effect on high molecular-weight DNA. *Journal of Forensic Sciences*, 52, 102-109.
- TODD, M. J. & GOMEZ, J. (2001) Enzyme kinetics determined using calorimetry: a general assay for enzyme activity? *Anal Biochem*, 296, 179-87.
- TSUKADA, T. & YOSHINO, M. (1987) Beta-Glucuronidase from Ampullaria Purification and Kinetic-Properties. *Comparative Biochemistry and Physiology B-Biochemistry & Molecular Biology*, 86, 565-569.
- VALENTE, J. V., BUNTINE, M. A., LINCOLN, S. F. & WARD, A. D. (2007) UV-Vis and fluorimetric Al<sup>3+</sup>, Zn<sup>2+</sup>, Cd<sup>2+</sup> and Pb<sup>2+</sup> complexation

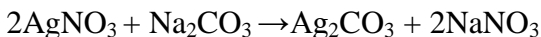
- studies of two 3-hydroxyflavones and a 3-hydroxythioflavone. *Inorganica Chimica Acta*, 360, 3380-3386.
- VILLARI, P., IANNUZZO, M. & TORRE, I. (1997) An evaluation of the use of 4-methylumbelliferyl-beta-D-glucuronide (MUG) in different solid media for the detection and enumeration of *Escherichia coli* in foods. *Letters in Applied Microbiology*, 24, 286-290.
- VOGT, V. M. (1970) Purification and Properties of an Aminopeptidase from *Escherichia-Coli*. *Journal of Biological Chemistry*, 245, 4760-&.
- WANG, C. S. (1981) Human milk bile salt-activated lipase. Further characterization and kinetic studies. *J Biol Chem*, 256, 10198-202.
- WARD, T. R., LUTZ, A., PAREL, S. P., ENSLING, J., GUTLICH, P., BUGLYO, P. & ORVIG, C. (1999) An iron-based molecular redox switch as a model for iron release from enterobactin via the salicylate binding mode. *Inorganic Chemistry*, 38, 5007-5017.
- WEIS, J., FINE, S. M., DAVID, C., SAVARIRAYAN, S. & SANES, J. R. (1991) Integration site-dependent expression of a transgene reveals specialized features of cells associated with neuromuscular junctions. *J Cell Biol*, 113, 1385-97.
- WITTRUP, K. D. & BAILEY, J. E. (1988) A single-cell assay of beta-galactosidase activity in *Saccharomyces cerevisiae*. *Cytometry*, 9, 394-404.
- WOLF, P. L., HORWITZ, J. P., VAZQUEZ, J., CHUA, J. & DAROOGUE, M. A. (1965) The Utilization of the Indigogenic Reaction for the Demonstration of N-Acetyl-Beta-Glucosaminidase. A New and Improved Method. *Am J Clin Pathol*, 44, 307-14.
- WRIGHT, R. C. (1983) A Simplified 1,10-Phenanthroline Technique Suitable for the Determination of Dissolved Iron in Remote Sources of Water. *Freshwater Biology*, 13, 293-296.
- YALOW, R. S. & BERSON, S. A. (1995) Immunoassay of Endogenous Plasma-Insulin in Man (Reprinted from the *Endocrinologist*, Pg 1157-1175, 1960). *Endocrinologist*, 5, 4-22.
- YUSHCHENKO, D. A., BILOKIN', M. D., PYVOVARENKO, O. V., DUPORTAIL, G., MELY, Y. & PIVOARENKO, V. G. (2006a) Synthesis and fluorescence properties of 2-aryl-3-hydroxyquinolones, a new class of dyes displaying dual fluorescence. *Tetrahedron Letters*, 47, 905-908.
- YUSHCHENKO, D. A., SHVADCHAK, V. V., KLYMCHENKO, A. S., DUPORTAIL, G., MELY, Y. & PIVOARENKO, V. G. (2006b) 2-Aryl-3-hydroxyquinolones, a new class of dyes with solvent dependent dual emission due to excited state intramolecular proton transfer. *New Journal of Chemistry*, 30, 774-781.
- ZHOU, M., DIWU, Z., PANCHUK-VOLOSHINA, N. & HAUGLAND, R. P. (1997) A stable nonfluorescent derivative of resorufin for the fluorometric determination of trace hydrogen peroxide: applications in detecting the activity of phagocyte NADPH oxidase and other oxidases. *Anal Biochem*, 253, 162-8.
- ZHU, R. H. & KOK, W. T. (1998) Determination of trace metal ions by capillary electrophoresis with fluorescence detection based on post-column complexation with 8-hydroxyquinoline-5-sulphonic acid. *Analytica Chimica Acta*, 371, 269-277.

**ZUBKOV, M. V. & SLEIGH, M. A. (1998) Heterotrophic nanoplankton biomass measured by a glucosaminidase assay. *Fems Microbiology Ecology*, 25, 97-106.**

## 8 Appendices

### 8.1 Appendix A: Chemistry

#### Active silver carbonate



This reaction is light sensitive and was therefore performed in the dark or subdued lighting. Distilled water (200 ml) was placed in a 1 litre beaker and silver nitrate (34 g, 5 M) was added and stirred until dissolved.

A slight excess of sodium carbonate (17 g, 6 M) was dissolved in distilled water (100 ml) then slowly poured into the continually stirred silver nitrate solution.

A white/yellow precipitate was formed. If the precipitate was brown in colour more silver nitrate was added. After 5 min stirring the suspension was allowed to settle then the water was decanted. More distilled water (400 ml) was added to the solid material which was stirred for a further 5 min to dissolve any unreacted sodium carbonate and sodium nitrate. The suspension was then filtered. Distilled water (100 ml) was filtered through the solid, then ethanol (100 ml), then diethyl ether (100 ml) to remove any unreacted material and to extract water to assist the drying process. The silver carbonate was dried in a vacuum desiccator (29 g yield).

#### Brady's reagent

Dissolve 40 g of 2,4 dinitrophenylhydrazine in 80 ml concentrated sulphuric acid (80 ml). Cool and add methanol (900 ml) and water (100ml). Filter if necessary.

#### Charring reagent

Methanol (33 ml) was added to distilled water (33 ml) and stirred. Concentrated sulphuric acid (33 ml) was then cautiously added and stirred.

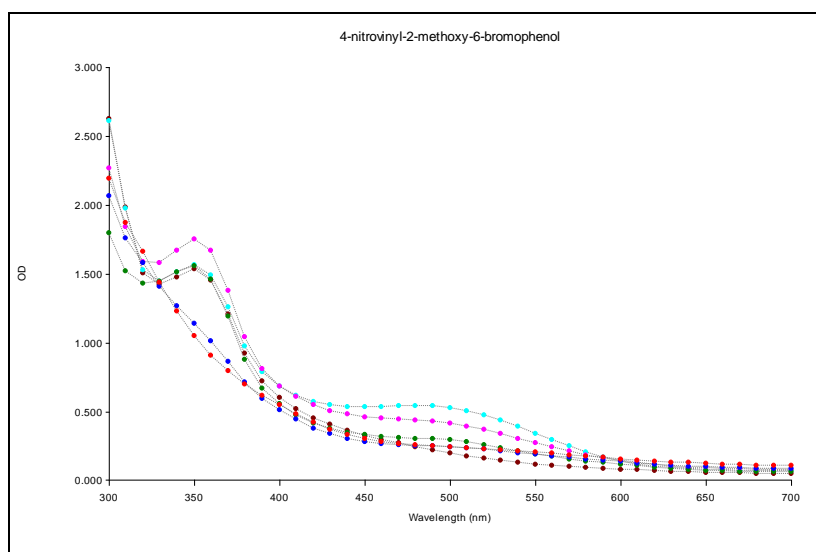
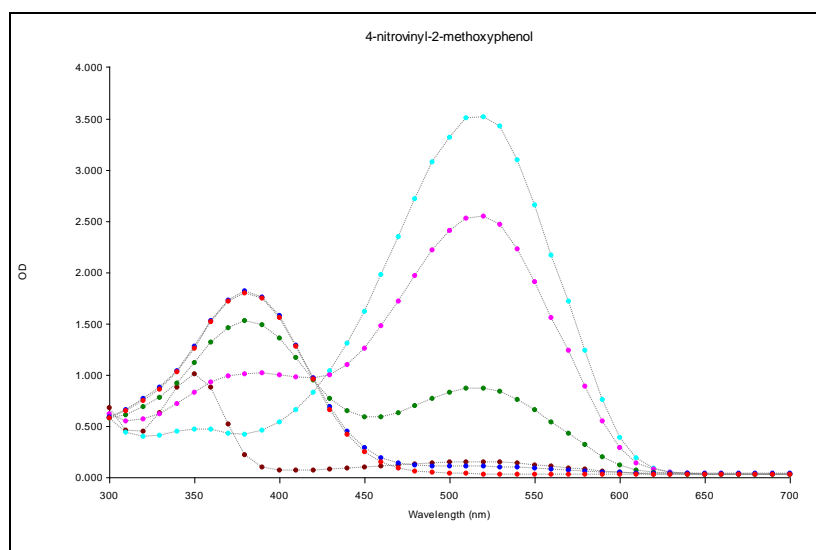
### **Sodium methoxide**

200 mmol Sodium methoxide was prepared by adding freshly cut sodium metal (0.47 g) to HPLC grade methanol (100 ml).

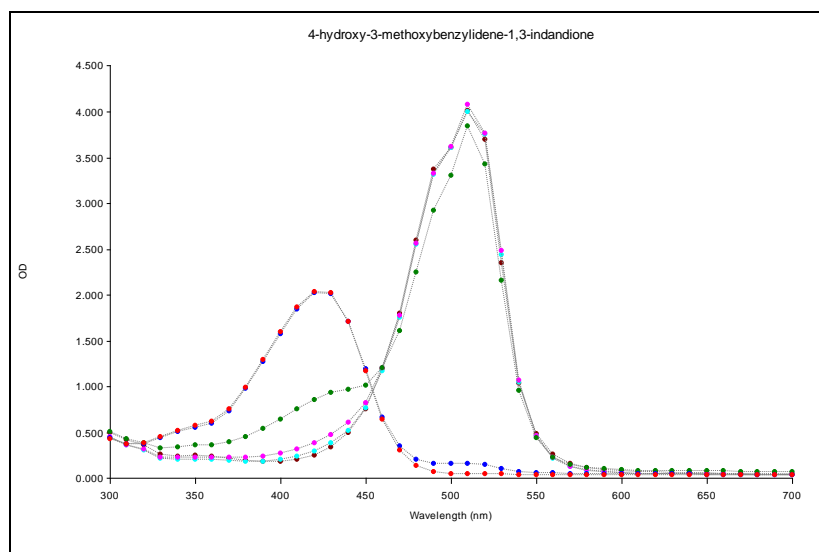
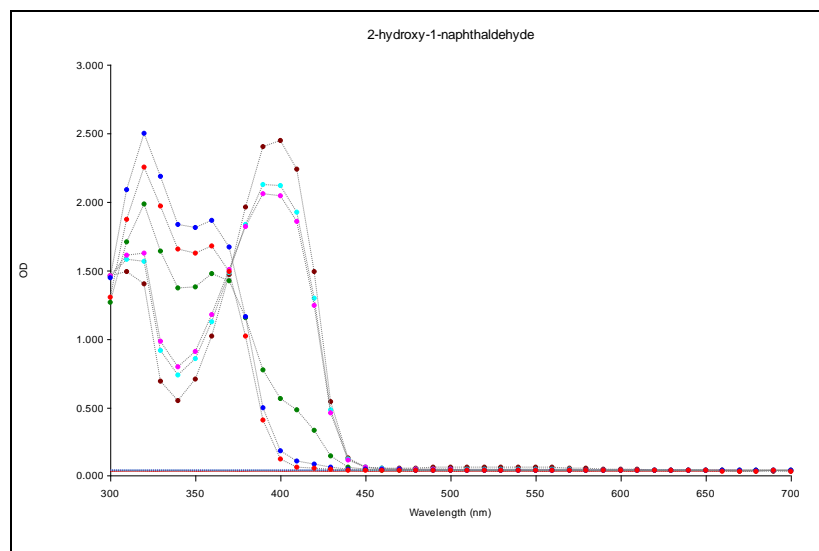
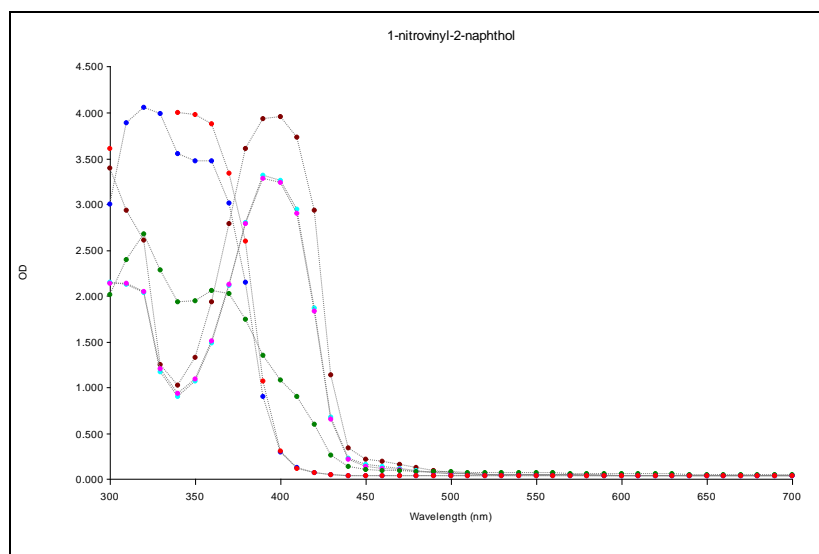
## 8.2 Appendix B: Biochemistry

### Synthesised compound spectrum scans

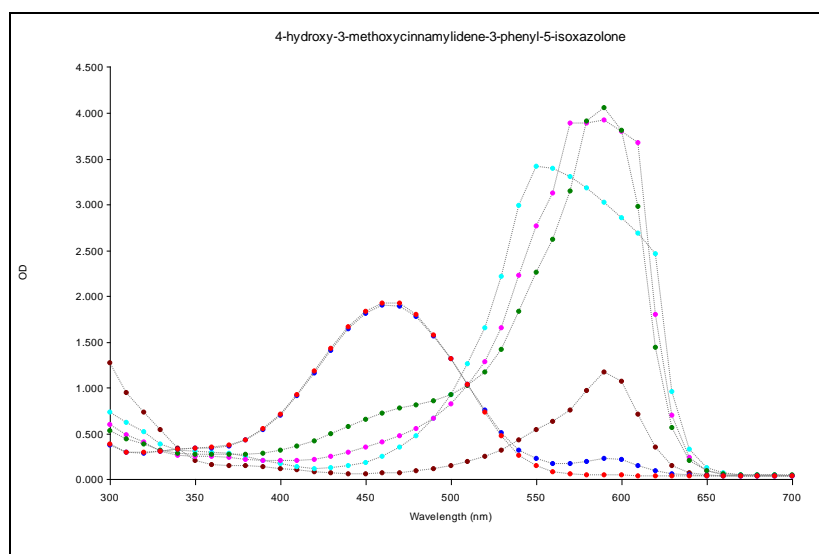
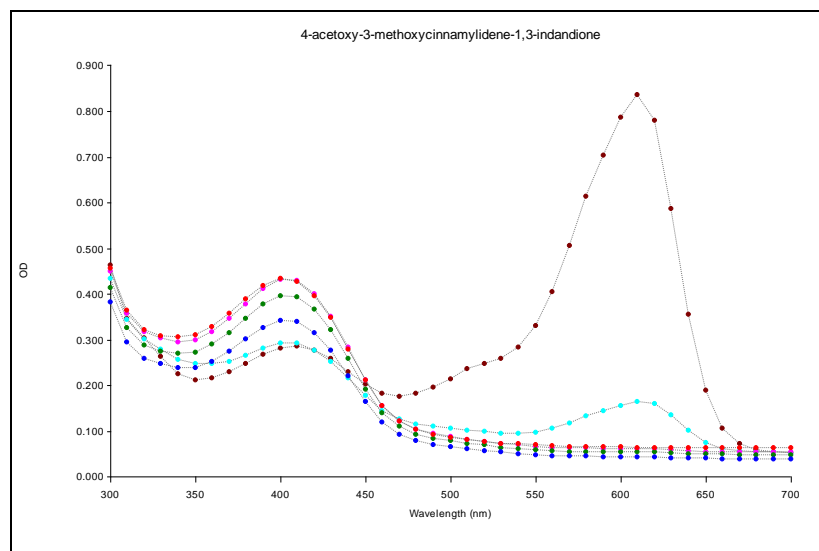
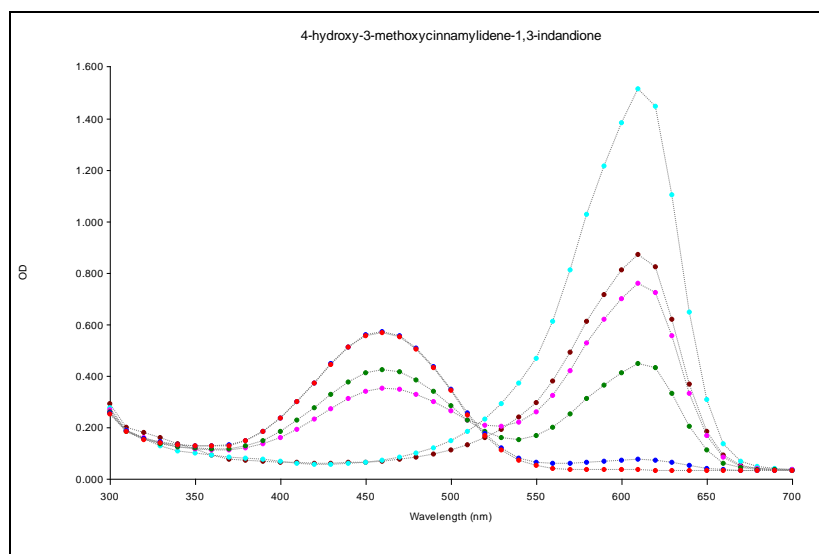
Spectra are colour coded as pH: **3** **5** **7** **9** **11** **13**



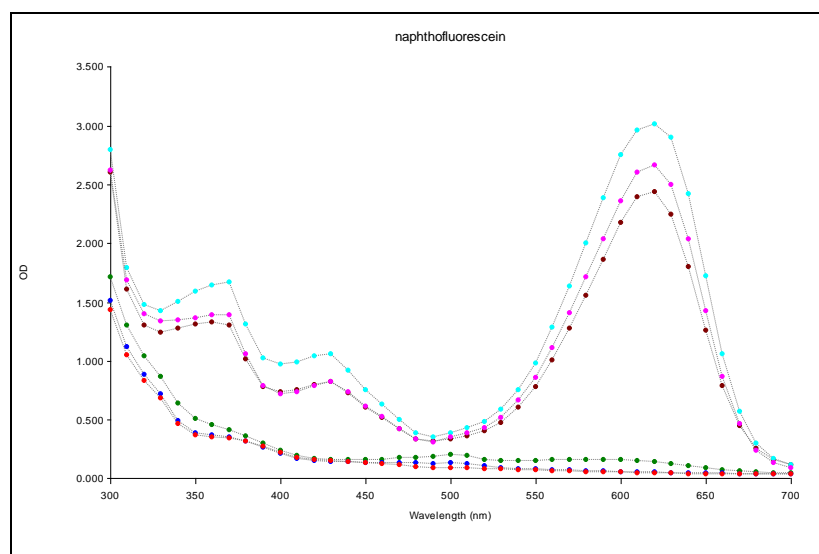
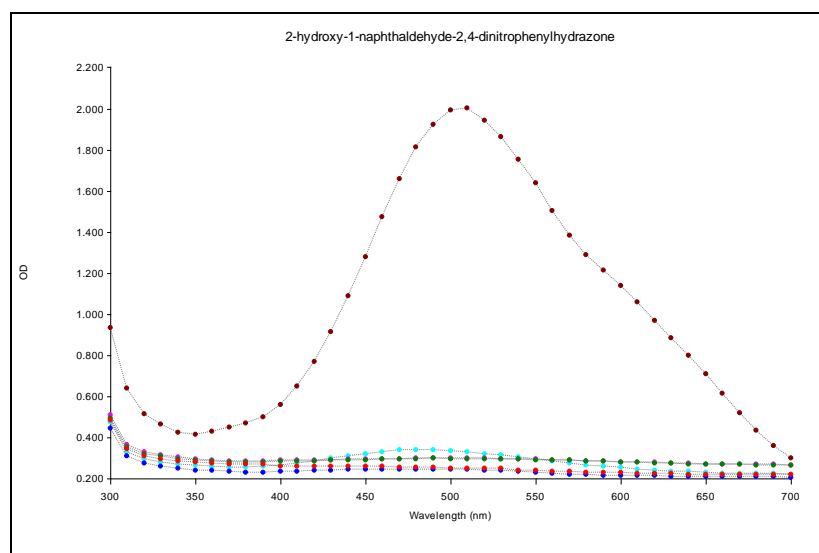
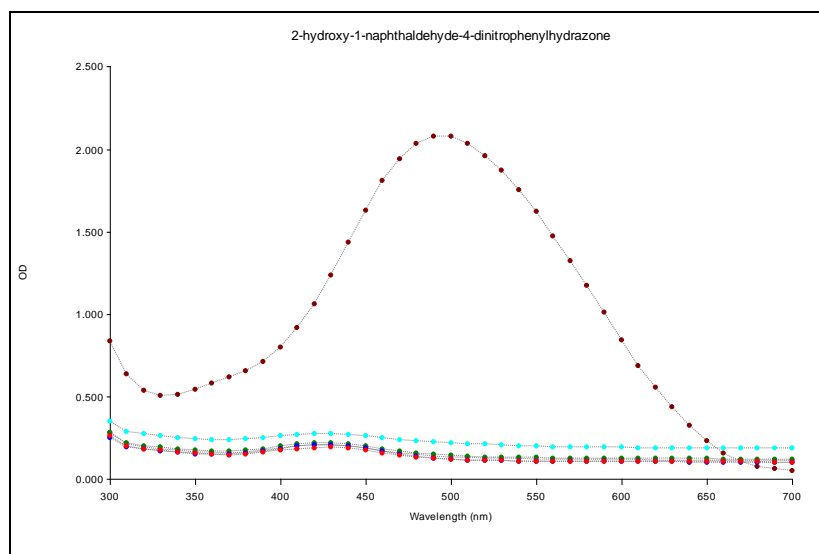
Spectra are colour coded as pH: **3** **5** **7** **9** **11** **13**



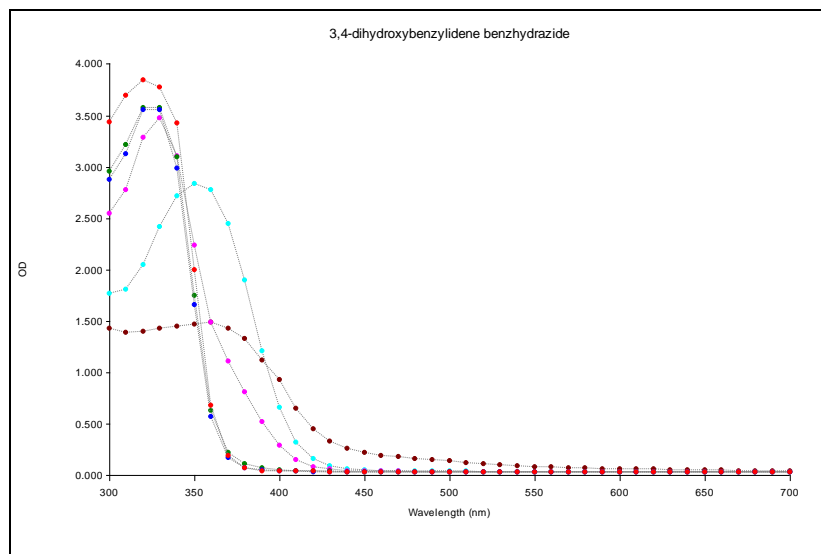
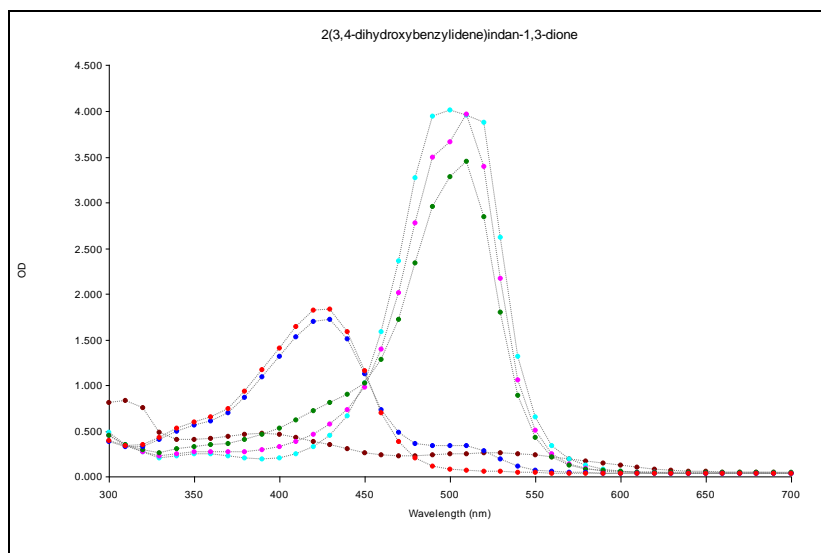
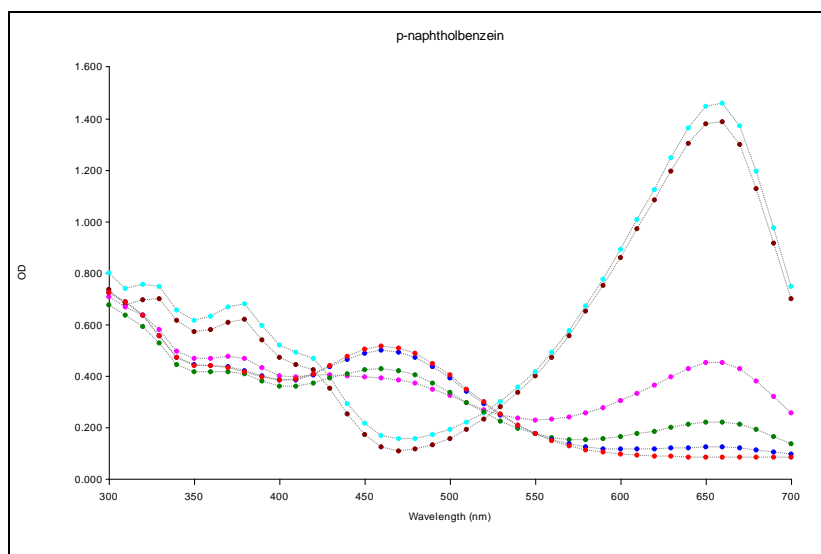
Spectra are colour coded as pH: **3** **5** **7** **9** **11** **13**



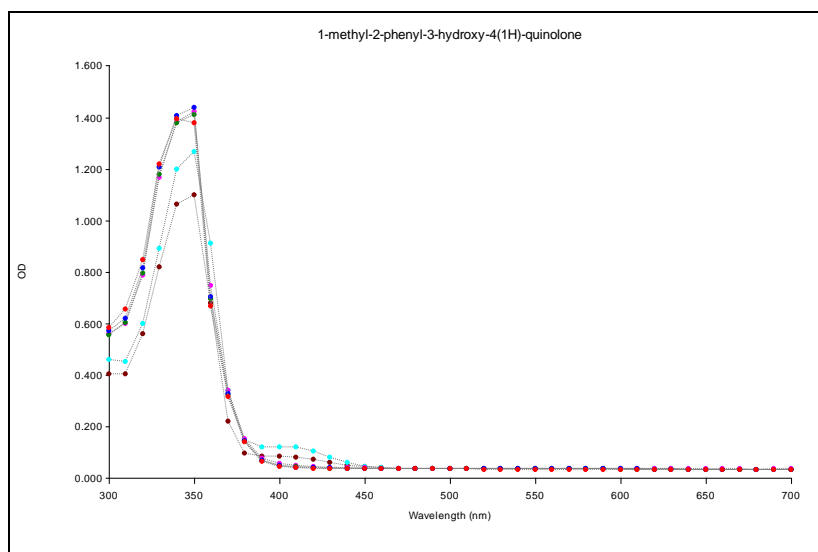
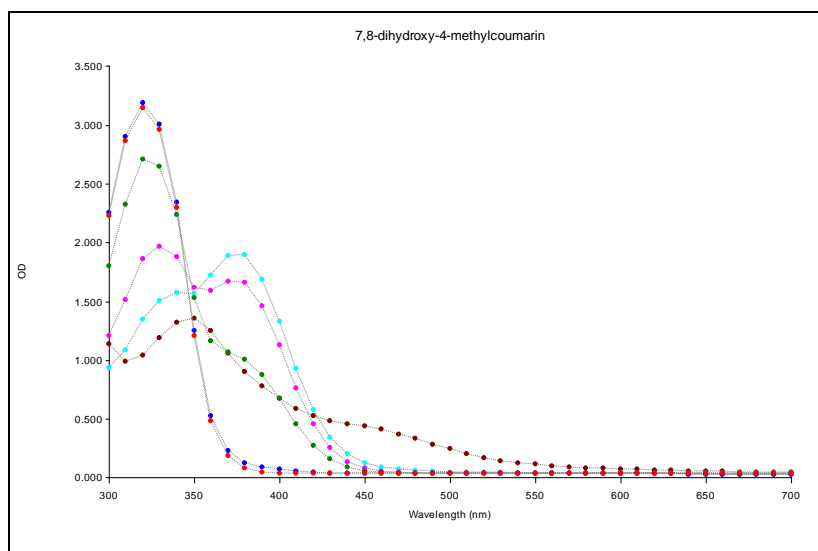
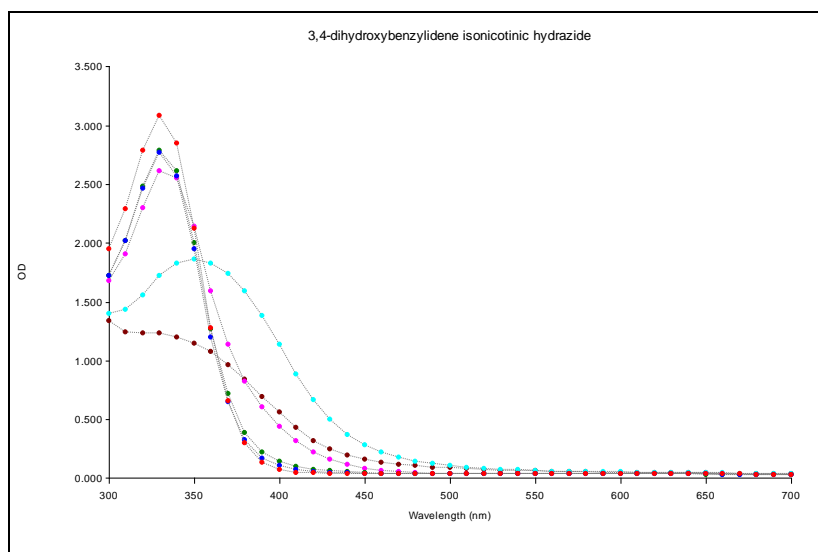
Spectra are colour coded as pH: **3** **5** **7** **9** **11** **13**



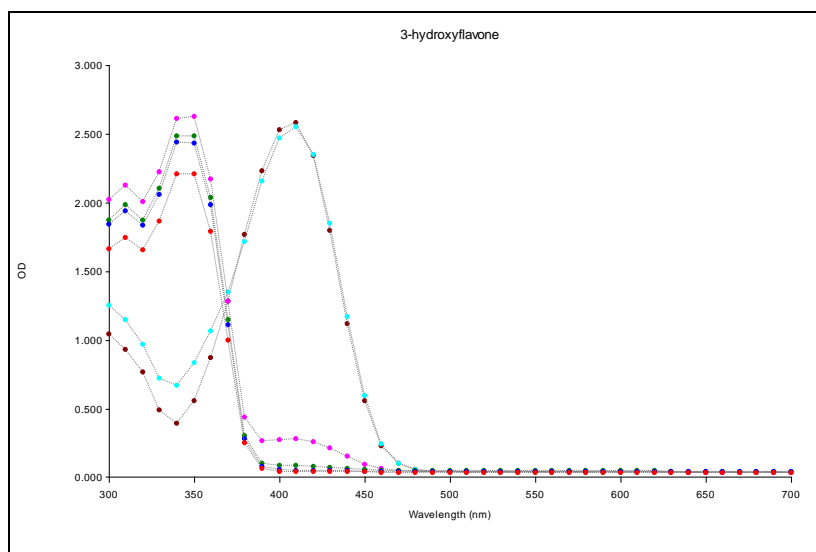
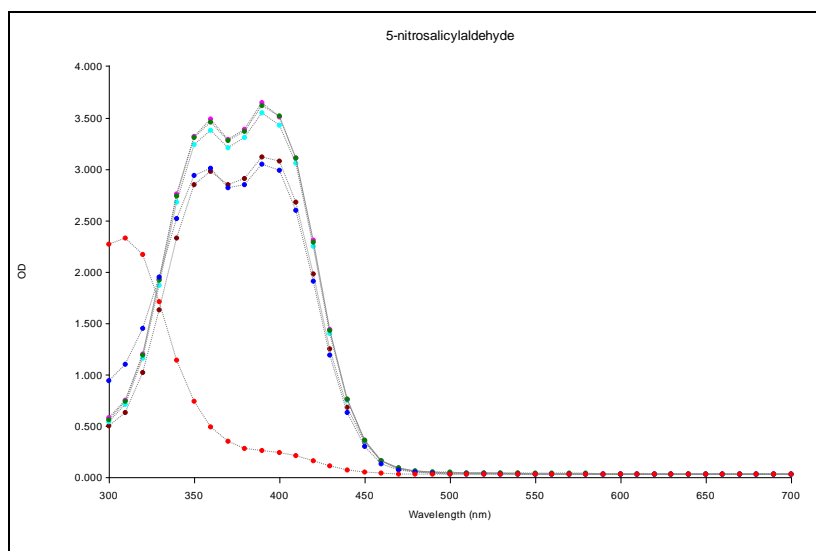
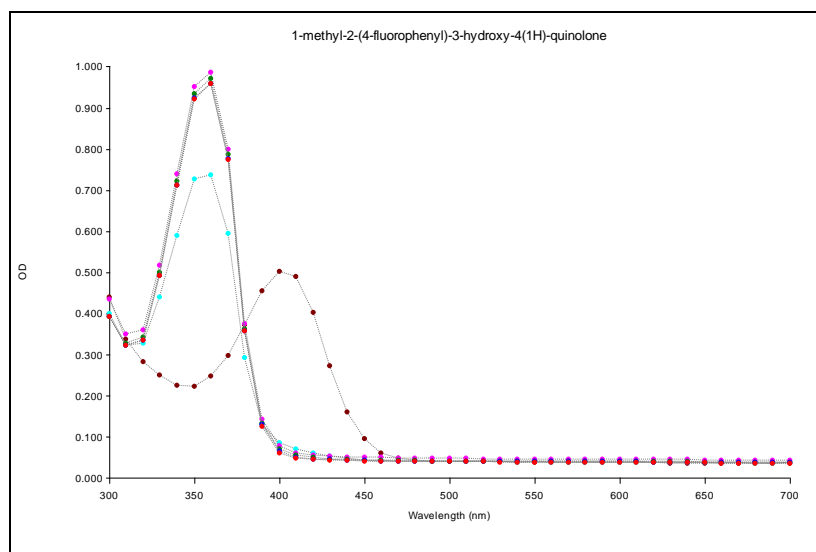
Spectra are colour coded as pH: **3** **5** **7** **9** **11** **13**



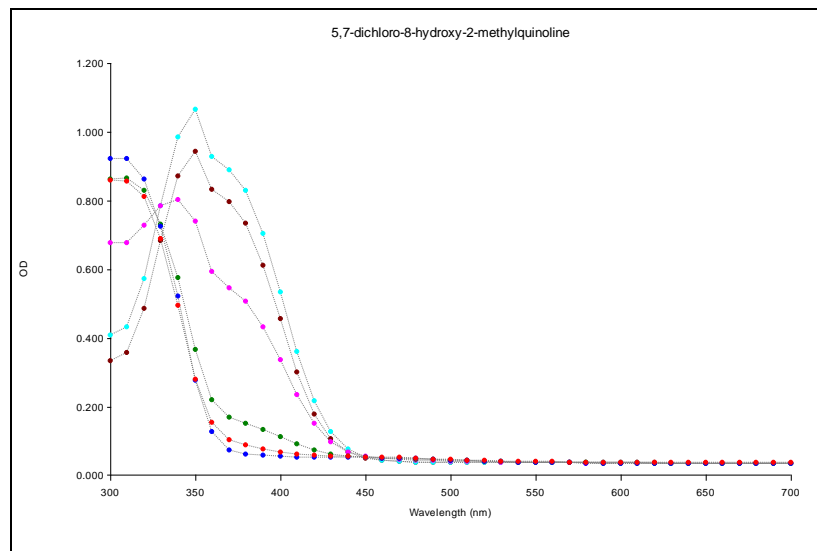
Spectra are colour coded as pH: **3** **5** **7** **9** **11** **13**



Spectra are colour coded as pH: **3** **5** **7** **9** **11** **13**



Spectra are colour coded as pH: **3** **5** **7** **9** **11** **13**



## Enzyme kinetics of 4-methylumbelliferyl- $\beta$ -D-glucopyranoside

4-Methylumbelliferyl- $\beta$ -D-glucopyranoside (MUD) (Figure B1) is a commercially available and well documented artificial fluorescence substrate (Grange and McIntyre, 1979; Park et al., 1995; Villari et al., 1997). The enzyme kinetics of MUD were investigated in order to have a point of reference when comparing the kinetics of the novel fluorescence glucosides synthesised in this study.

0.3mmol of 4-methylumbelliferone (4-MU) (Sigma) was dissolved in one litre of distilled water. The fluorescence maximum ( $\lambda_F$ ) of this core compound was determined using a Biotek Synergy multi-detection microplate reader and found to be Ex 360, Em 460 nm (Figure B2).

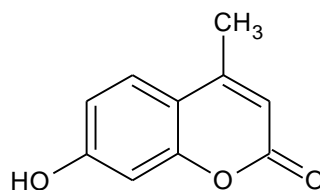


**Figure B1:** Structure of 4-methylumbelliferone.

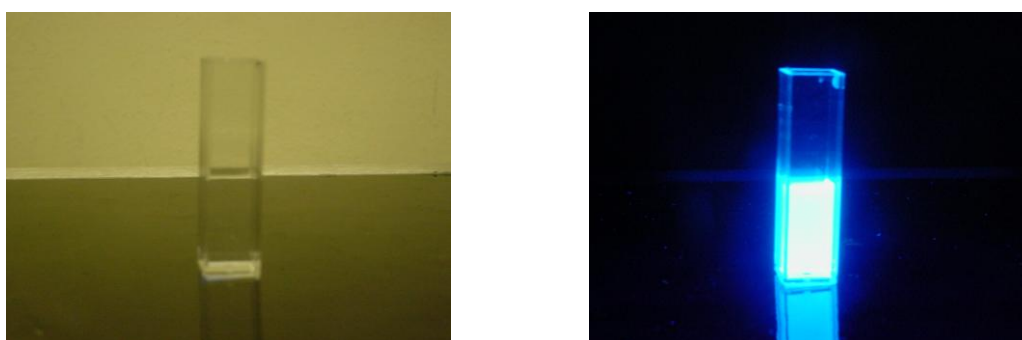


**Figure B2:** Fluorescence of 4-MU.

The glucoside of 4-MU (Sigma) was then reacted with  $\beta$ -glucosidase enzyme (Sigma) at varying pH using the following reaction mixture.

200  $\mu$ l 0.05M/L sodium acetate/acetic acid buffer containing:-

0.3 mmol/L MUD

5  $\mu$ l 1.5 g/L  $\beta$ -glucosidase

The reactions were monitored for 30 minutes, at 37 °C, at pH 5-9 and the rates of the reaction are shown (Figure B3).

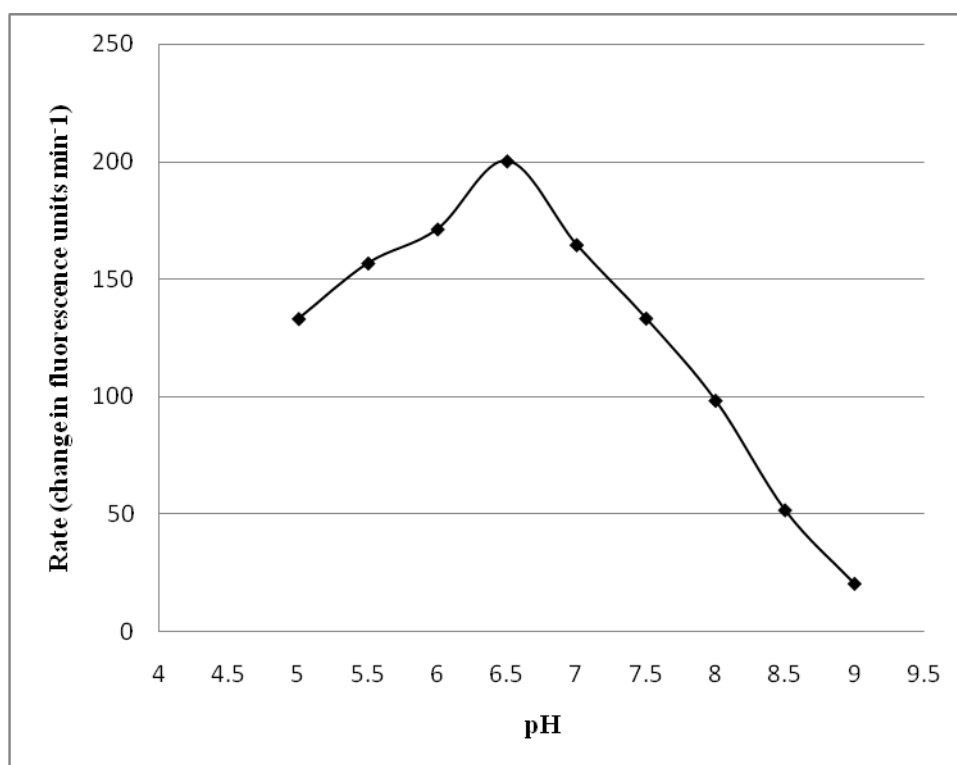


**Figure B3:** Rate of reactions of MUD and  $\beta$ -glucosidase at pH 4-9.

The pH optimum for this enzyme system was determined to be pH 6.5.

Using the same reaction mixture at pH 6.5, the substrate concentration was varied (Figure B4).

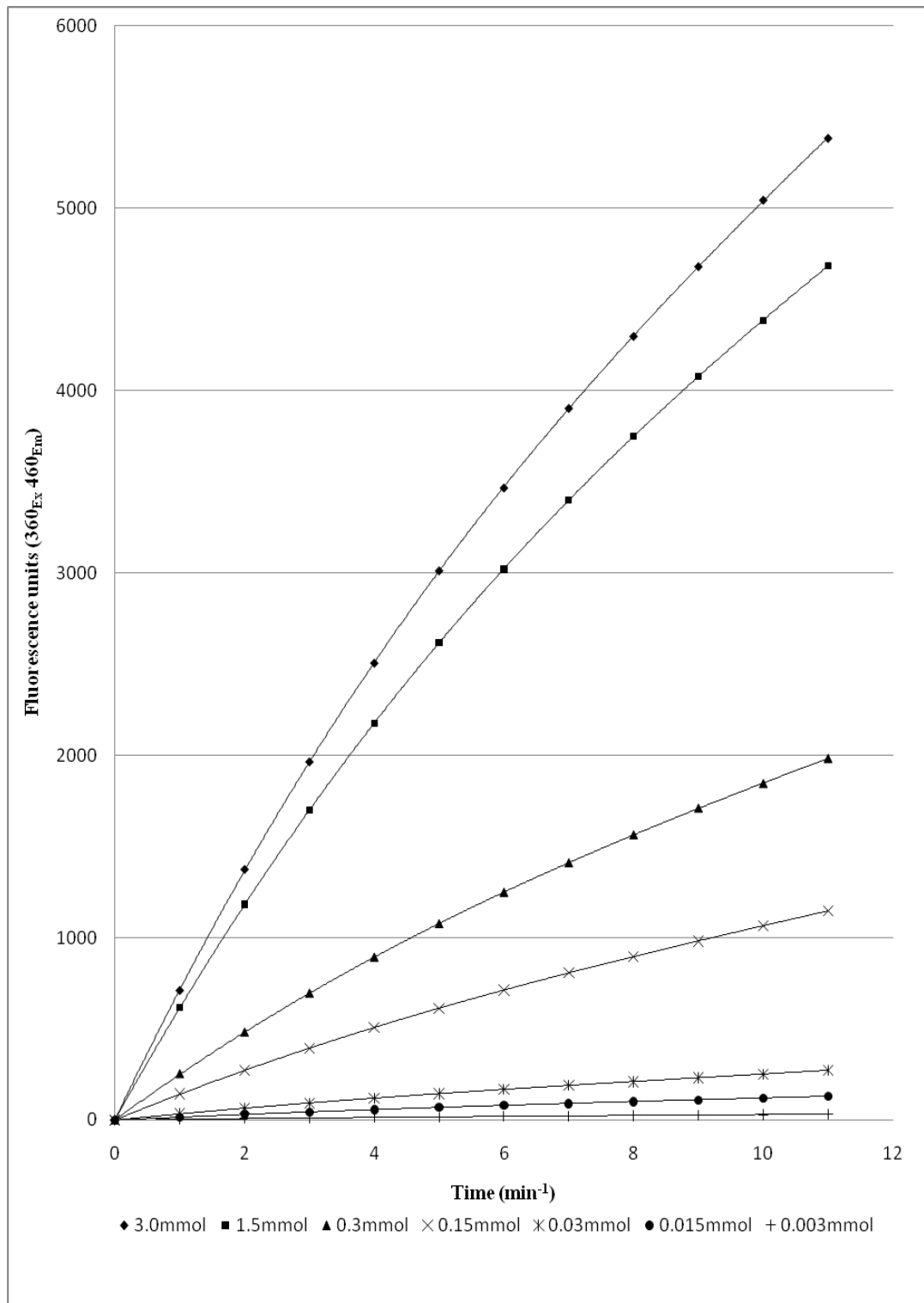


**Figure B4:** Rate of reactions of MUD and  $\beta$ -glucosidase at substrate concentrations 0.003-3 mmol/L.

To convert FU into concentrations (mmol/L) of 4-MU a standard curve was prepared and measured. A linear relationship between FU and 4-MU concentration was found to exist up to 0.2 mmol/L (Figure B5).

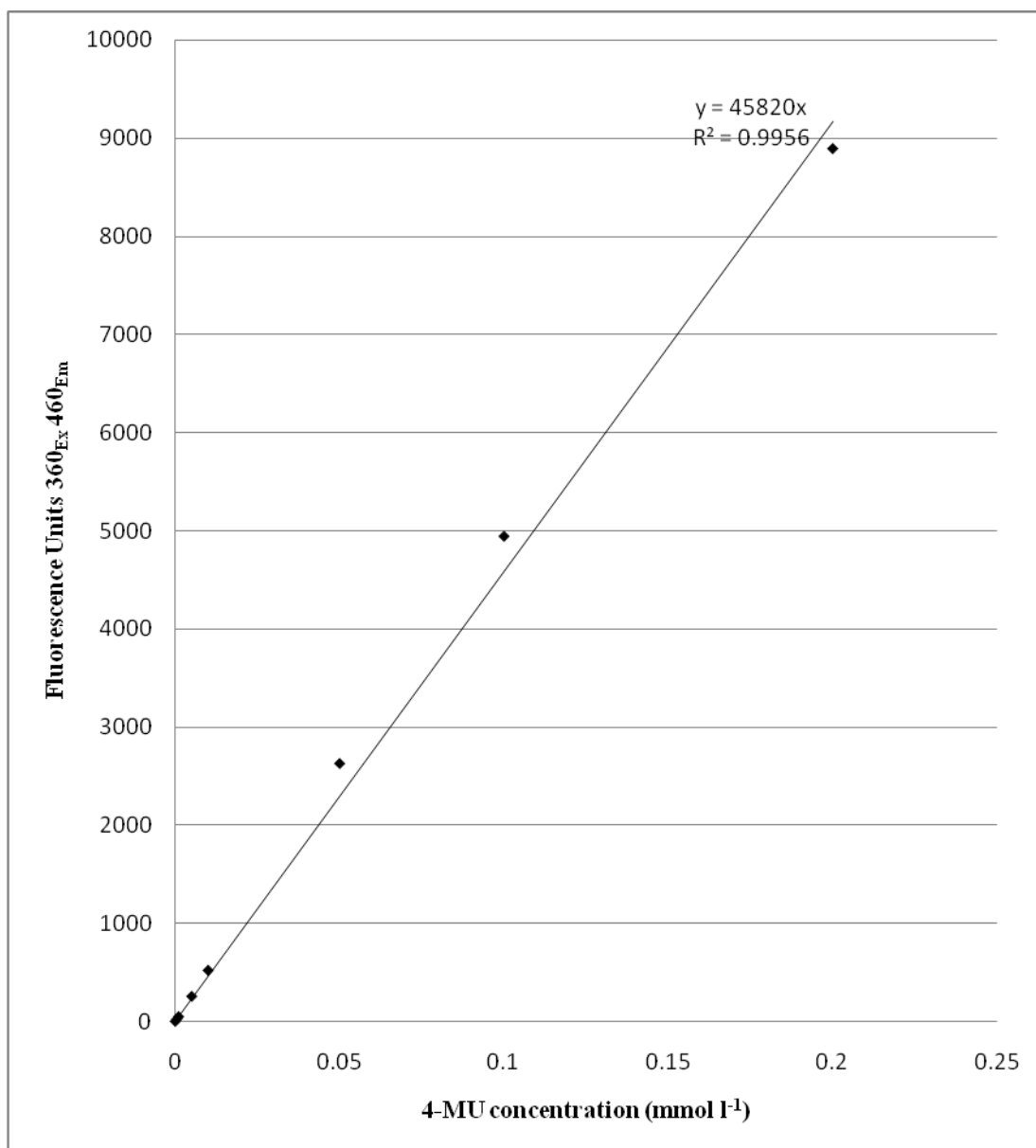


**Figure B5:** Linear standard curve for 4-MU.

This, along with the results gained from varying the substrate concentration, was used to calculate the following kinetics data (Figure B6).

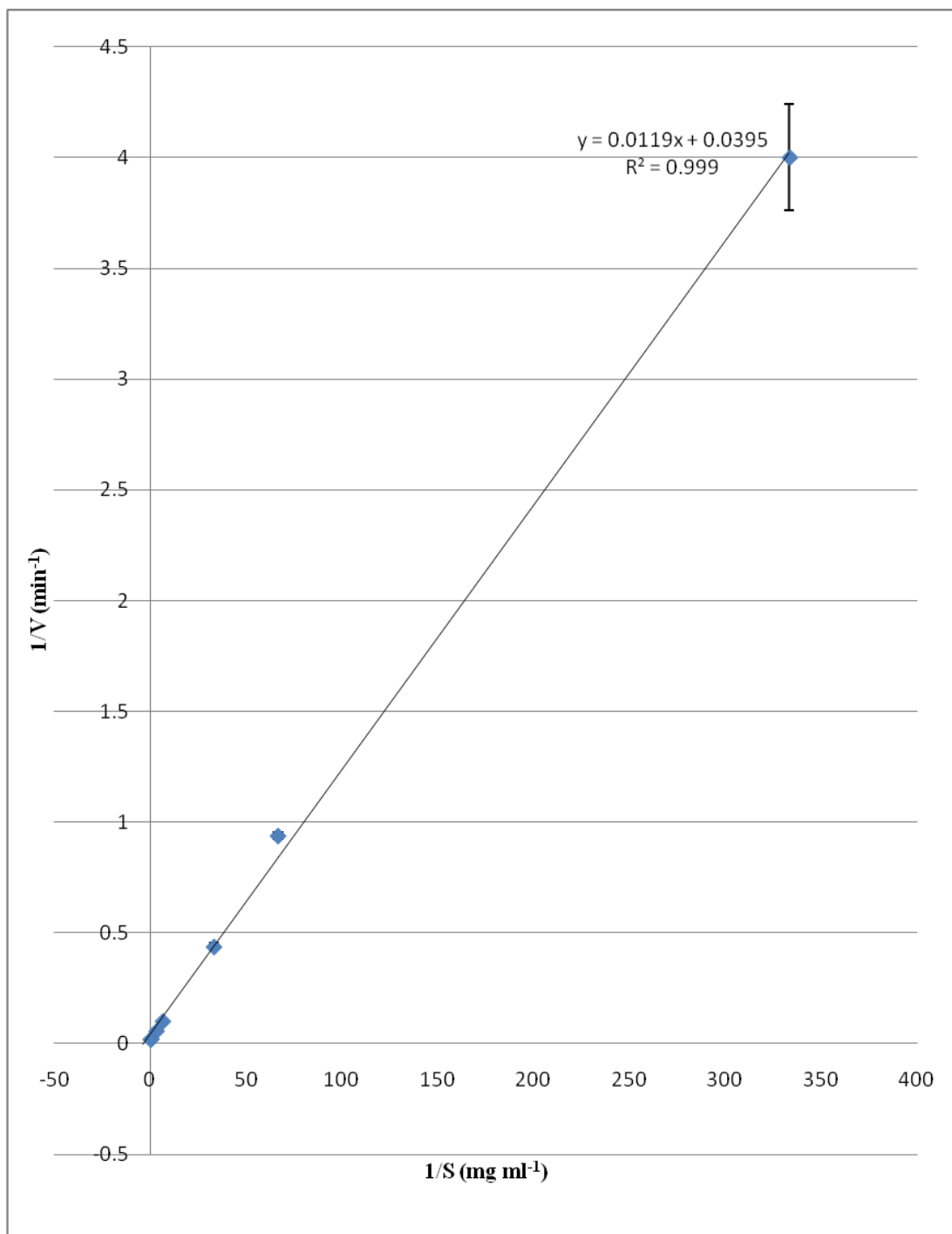


**Figure B6:** Lineweaver-Burk plot for MUD.

A linear trendline was plotted from the Lineweaver-Burk data. Error bars represent the standard deviation from the mean. The correlation coefficient ( $r^2$ ) between outcomes and their predicted values was calculated as 0.999 (where values approaching 1 are desirable), therefore the data was acceptable.

$V_{\max} = 25.32 \mu\text{moles of product released per minute, per } \mu\text{mole of enzyme.}$

or  $0.42 k_{\text{cat}}$  ( $\mu\text{moles of product released per second, per } \mu\text{mole of enzyme}$ ).

$K_M = 0.30 \text{ mmol/L.}$

### 8.3 Appendix C: Microbiology/molecular biology

#### Protein sequence

MEFSVKSGSPEKQRSACIVVGVFEPRLSPIAEQLDKISDGYISALLRRGELEGKPGQTLHHPNVLS  
 ERILLIGCGKERELDERQYKQVIQKTINTLNDTGSMEAVCFLELHVKGRNNYWKVRQAVETAKETLYSF  
 DQLKTNKSEPRRPLRKMVFNVPTRRELTSGERAIQHGLAIAAGIKAAKDLGNMPPNICNAAAYLASQARQL  
 ADSYSKNVITRVIQEQQMKELGMHSYLAVGQGSQNESLMSVIEYKGNASEDARPIVLVKGKGLTFDSSGIS  
 IKPSEGMDKMDMCGAAAVYGVMRMVAELQLPINVIGVLGACENMPGGRAYRPGDVLTTMSGQTVEVLN  
 TDAEGRVLVCDVLTYYVERFEPEAVIDVATLTGACVIALGHHTGLMANHNPLAHELIAASEQSGDRAWRL  
 PLGDEYQEQLSDFADMANIGGRPGGAITAGCFLSRFTRKYNWAHLDIAGTAWRSKGKAKGATGRPVALLA  
 QFLLNRAGFNSEE

#### Gene sequence

ATGGAGTTTAGTGTAATAAAGCGGTAGCCCGGAGAAACAGCGGAGTGCCTGCATCGTCGTGGGCGTCTTCGAACCACGTGCGCTTT  
 CTCCGATTGCAGAACAGCTCGATAAAAATCAGCGATGGGTACATCAGCGCCCTGCTACGTCGGGGCGAACTGGAAGGAAAACCGGG  
 GCAGACATTGTTGCTGCACCATGTTCCGAATGTACTTTCCGAGCGAATTCTCCTTATTGGTTGCGGCAAAGAACGTGAGCTGGAT  
 GAGCGTCAGTACAAGCAGGTTATTCAGAAAACCATTAATACGCTGAATGATACTGGCTCAATGGAAGCGGTCTGCTTTCTGACTG  
 AGCTGCACGTTAAAGGCCGTAACAACACTACTGGAAAGTGCCTGAGGCTGTCGAGACGGCAAAGAGACGCTCTACAGTTTCGATCA  
 GCTGAAAACGAACAAGAGCGAACCAGCGTCCGCTGCGTAAGATGGTGTCAACGTGCCGACCCCGCTGAACTGACCAGCGGT  
 GAGCGCGGATCCAGCAGGCTCTGGCGATTGCCGCCGGATTAAGCAGCAAAGATCTCGGCAATATGCCGCCGAATATCTGTA  
 ACGCCGCTTACCTCGCTTACAAGCGCGCAGCTGGCTGACAGCTACAGCAAGAATGTCAATCACCCGCTTATCGGCGAACAGCA  
 GATGAAAGAGCTGGGGATGCATTCCTATCTGGCGGTCCGTCAGGTTTCGCAAACGAATCGCTGATGTCGGTGATTGAGTACAAA  
 GGCAACCGCTCGGAAGATGCACGCCCAATCGTGCTGGTGGGTAAAGTTTAACTTCGACTCCGCGGTATCTCGATCAAGCCTT  
 CAGAAGGCATGGATGAGATGAAGTACGATATGTGCGGTGCGGCAGCGGTTTACGGCGTGATGCGGATGGTCGGGAGCTACAAC  
 GCCGATTAACGTTATCGGCGTGTGGCAGGCTGCGAAAACATGCCTGCGGACGAGCCTATCGTCCGGCGATGTGTTAACACC  
 ATGTCCGGTCAAACCGTTGAAGTGTGAACACCGACGCTGAAGGCCCGCTGGTACTGTGCGACGTGTTAACTTACGTTGAGCGTT  
 TTGAGCCGAAGCGGTGATTGACGTGGCGACGCTGACCGGTGCCTGCGTGATCGCGCTGGGTATCATATTAATGCTGATGGC  
 GAACCATAATCCGCTGGCCATGAAGTATTGCCGCTGTAACAATCCGGTGACCGCGCATGGCGCTTACCGCTGGGTGACGAG  
 TATCAGGAACAACCTGGAGTCCAATTTGCGGATATGGCGAATTTGGCGGTGCTCCTGGTGGGGCGATTACCGCAGGTTGCTTCC  
 TGTCACGCTTTACCCGTAAGTACAACCTGGGCGCACCTGGATATCGCCGTTACCGCTGGCGTTCTGGTAAAGCAAAGGCCAC  
 CGGTCGTCGGTAGCGTTGCTGGCACAGTTCTGTTAAACCGCGTGGGTTTAAACGGCGAAGAGTAA

#### MWG Oligo synthesis report

NP_418681.1FP		64/67	
5'-CAC CAC CAC CAC ATG GAG TTT AGT GTA AAA AGC-3'			
Amount	Concentration (Volume 1 ml)	89 pmol/μl	Length 33-mer
33.6 OD	Volume for 100 pmol/μl <i>m</i>	890 μl	GC Content 45.5 %
898 μg	Molecular Weight	10100 g/mol	Scale 0.01 μmol
89.0 nmol	T <sub>m</sub>	68.2 °C	Purification HPSF

NP_418681.1RP		65/67	
5'-GAG GAG AAG GCG CGT TAC TCT TCG CCG TTA AAC CCA-3'			
Amount	Concentration (Volume 1 ml)	52 pmol/μl	Length 36-mer
20.5 OD	Volume for 100 pmol/μl	519 μl	GC Content 55.6 %
575 μg	Molecular Weight	11070 g/mol	Scale 0.01 μmol
51.9 nmol	T <sub>m</sub>	74.0 °C	Purification HPSF

## Qiagen DNeasy kit protocol

### Appendix D: Purification of Genomic DNA from Gram-Negative Bacteria

The DNeasy procedure has been successfully used to purify DNA from Gram-negative bacteria such as *E. coli*. See "Quantification of starting material" on page 12 for details of how to collect and store samples, and how to determine the number of cells in a bacterial culture.

#### Procedure

*0.5 ml of culture*

- D1. Harvest cells (maximum  $2 \times 10^9$  cells) in a microcentrifuge tube by centrifuging for 10 min at 5000 x g (7500 rpm). Discard supernatant.
  
- D2. Resuspend pellet in 180  $\mu$ l Buffer ATL.
- D3. Continue with the "Protocol: Purification of Total DNA from Animal Tissues" (from step 2, page 19).

- 2. Add 20  $\mu$ l proteinase K, mix by vortexing, and incubate at 55°C until the tissue is completely lysed. Vortex occasionally during incubation to disperse the sample, or place in a shaking water bath or on a rocking platform.**

Lysis time varies depending on the type of tissue processed. Lysis is usually complete in 1–3 h. If it is more convenient, samples can be lysed overnight; this will not affect them adversely.

After incubation the lysate may appear viscous, but should not be gelatinous as it may clog the DNeasy Mini spin column. If the lysate appears very gelatinous, please see the “Troubleshooting Guide” on page 26 for recommendations.

**Optional:** RNase treatment of the sample. Add 4  $\mu$ l of RNase A (100 mg/ml), mix by vortexing, and incubate for 2 min at room temperature (15–20°C).

Transcriptionally active tissues such as liver and kidney contain high levels of RNA, which will copurify with genomic DNA. If RNA-free genomic DNA is required, carry out this optional step. If residual RNA is not a concern, omit this step and continue with step 3.

- 3. Vortex for 15 s. Add 200  $\mu$ l Buffer AL to the sample, mix thoroughly by vortexing, and incubate at 70°C for 10 min.**

It is essential that the sample and Buffer AL are mixed immediately and thoroughly by vortexing or pipetting to yield a homogeneous solution.

A white precipitate may form on addition of Buffer AL, which in most cases will dissolve during the incubation at 70°C. The precipitate does not interfere with the DNeasy procedure. Some tissue types (e.g., spleen, lung) may form a gelatinous lysate after addition of Buffer AL. In this case, vigorously shaking or vortexing the preparation before addition of ethanol in step 4 is recommended.

- 4. Add 200  $\mu$ l ethanol (96–100%) to the sample, and mix thoroughly by vortexing.**

It is important that the sample and the ethanol are mixed thoroughly to yield a homogeneous solution.

A white precipitate may form on addition of ethanol. It is essential to apply all of the precipitate to the DNeasy Mini spin column.

- 5. Pipet the mixture from step 4 into the DNeasy Mini spin column placed in a 2 ml collection tube (provided). Centrifuge at  $\geq 6000 \times g$  (8000 rpm) for 1 min. Discard flow-through and collection tube.\***
- 6. Place the DNeasy Mini spin column in a new 2 ml collection tube (provided), add 500  $\mu$ l Buffer AW1, and centrifuge for 1 min at  $\geq 6000 \times g$  (8000 rpm). Discard flow-through and collection tube.\***

\* Flow-through contains Buffer AL or Buffer AW1 and is therefore not compatible with bleach. See page 7 for safety information.

7. Place the DNeasy Mini spin column in a 2 ml collection tube (provided), add 500  $\mu$ l Buffer AW2, and centrifuge for 3 min at 20,000  $\times$  g (14,000 rpm) to dry the DNeasy membrane. Discard flow-through and collection tube.

This centrifugation step ensures that no residual ethanol is carried over during the following elution.

Following the centrifugation step, remove the DNeasy Mini spin column carefully so that the column does not come into contact with the flow-through, since this will result in carryover of ethanol. If carryover of ethanol occurs, empty the collection tube and reuse it in another centrifugation step for 1 min at 20,000  $\times$  g (14,000 rpm).

8. Place the DNeasy Mini spin column in a clean 1.5 ml or 2 ml microcentrifuge tube (not provided), and pipet 200  $\mu$ l Buffer AE directly onto the DNeasy membrane. Incubate at room temperature for 1 min, and then centrifuge for 1 min at  $\geq$ 6000  $\times$  g (8000 rpm) to elute.

*2  $\times$  100  $\mu$ l*  
Elution with 100  $\mu$ l (instead of 200  $\mu$ l) increases the final DNA concentration in the eluate, but also decreases the overall DNA yield (see Figure 2, page 14).

9. Repeat elution once as described in step 8.

A new microcentrifuge tube can be used for the second elution step to prevent dilution of the first eluate. Alternatively, to combine the eluates, the microcentrifuge tube from step 8 can be reused for the second elution step.

**Note:** More than 200  $\mu$ l should not be eluted into a 1.5 ml microcentrifuge tube because the DNeasy Mini spin column will come into contact with the eluate.

## **Agarose gel electrophoresis**

Agarose gels were prepared by heating agarose in 1 x TAE buffer until the solid had completely dissolved. All gels in this study were 1 % (w/v) agarose in a total volume of 50 ml.

Once dissolved, the solution was allowed to cool to ~ 60 °C, 5 µl of 1 x Sybr® Safe (Invitrogen) was added, and the solution poured into a mini gel casting tray avoiding the introduction of air bubbles. The appropriate sized comb was then inserted into the solution (for analytical purposes, a 12-toothed comb able to hold 15 µl in each well was used) and the gel allowed to set for > 20 min.

After the gel had set, the gel tray was placed horizontally in an agarose gel electrophoresis tank, submerged in 1 x TAE buffer. The comb was then carefully removed and samples were prepared by the addition of sample buffer, and added to the wells. A 5 µl volume of Hyperladder 1 size standard was also added to an unoccupied well in order to determine the size of electrophorised DNA fragments. The samples were then electrophoresed at 120 mA (200 V) for approximately 45 min to ensure good separation of DNA fragments.

## **Visualisation of DNA and photography of agarose gels**

After electrophoresis, the gel was visualised using a gel documentation system (Bio-Rad Gel Doc 2000 using Quantity One™ software). Hard copies of the gel picture were produced using a Mitsubishi Video Copy Processor (Model P91 attached to the gel doc system), with Mitsubishi thermal paper (K65HM-CE / High density type, 110 mm x 21 m).

**TAE buffer (50 x stock)**

Per L

Tris Base (ultra-pure) (MelforD)	242.0 g
17.51 M Glacial acetic acid (Fisher)	57.1 ml
0.5 M EDTA pH 8.0 (Duchefa)	100.0 ml

This buffer was diluted to 1 x by a 1:50 dilution prior to use in the preparation of agarose gels and use as reservoir buffer in gel tanks.

**Bromophenol blue (6 x) sample loading buffer**

Per 10 ml

Bromophenol blue (BDH Laboratory Supplies)	0.025 g
Glycerol (Fisher)	3.000 g

This buffer was diluted to 1 x with the sample prior to loading on an agarose gel.

## Size Standards

Bioline Hyperladder I agarose gel size standard was diluted to a concentration of 1 µg/12 µl prior to loading on a gel (Figure C1)

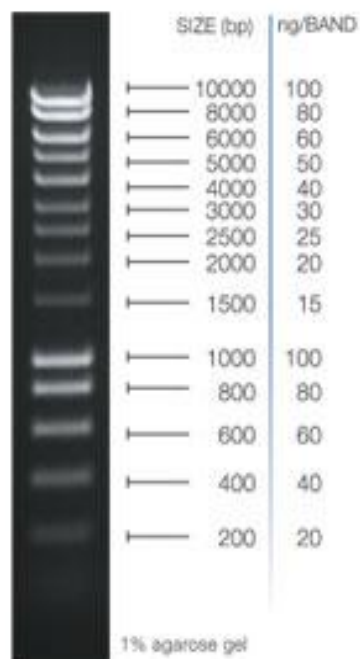


**Figure C1:** Agarose gel size standards. Bioline Hyperladder I.

## 10 x KOD buffer

1.2 M Tris-HCl; 100 mM KCl; 60 mM (NH<sub>4</sub>)<sub>2</sub> SO<sub>4</sub>; 1% (v/v) Triton X-100; 0.01% (w/v) bovine serum albumin, pH 8.0.

## QIAquick Gel Extraction Kit Protocol

### using a microcentrifuge

This protocol is designed to extract and purify DNA of 70 bp to 10 kb from standard or low-melt agarose gels in TAE or TBE buffer. Up to 400 mg agarose can be processed per spin column. This kit can also be used for DNA cleanup from enzymatic reactions (see page 8). For DNA cleanup from enzymatic reactions using this protocol, add 3 volumes of Buffer QG and 1 volume of isopropanol to the reaction, mix, and proceed with step 6 of the protocol. Alternatively, use the MinElute Reaction Cleanup Kit.

#### Important points before starting

- The yellow color of Buffer QG indicates a pH  $\delta$ 7.5.
- Add ethanol (96–100%) to Buffer PE before use (see bottle label for volume).
- All centrifugation steps are carried out at 17,900 x g (13,000 rpm) in a conventional table-top microcentrifuge at room temperature.

#### Procedure

##### 1. Excise the DNA fragment from the agarose gel with a clean, sharp scalpel.

Minimize the size of the gel slice by removing extra agarose.

##### 2. Weigh the gel slice in a colorless tube. Add 3 volumes of Buffer QG to 1 volume of gel (100 mg ~ 100 $\mu$ l).

For example, add 300  $\mu$ l of Buffer QG to each 100 mg of gel. For >2% agarose gels, add 6 volumes of Buffer QG. The maximum amount of gel slice per QIAquick column is 400 mg; for gel slices >400 mg use more than one QIAquick column.

##### 3. Incubate at 50°C for 10 min (or until the gel slice has completely dissolved). To help dissolve gel, mix by vortexing the tube every 2–3 min during the incubation.

**IMPORTANT:** Solubilize agarose completely. For >2% gels, increase incubation time.

##### 4. After the gel slice has dissolved completely, check that the color of the mixture is yellow (similar to Buffer QG without dissolved agarose).

If the color of the mixture is orange or violet, add 10  $\mu$ l of 3 M sodium acetate, pH 5.0, and mix. The color of the mixture will turn to yellow.

The adsorption of DNA to the QIAquick membrane is efficient only at pH  $\delta$ 7.5.

Buffer QG contains a pH indicator which is yellow at pH  $\delta$ 7.5 and orange or violet at higher pH, allowing easy determination of the optimal pH for DNA binding.

##### 5. Add 1 gel volume of isopropanol to the sample and mix.

For example, if the agarose gel slice is 100 mg, add 100  $\mu$ l isopropanol. This step increases the yield of DNA fragments <500 bp and >4 kb. For DNA fragments between 500 bp and 4 kb, addition of isopropanol has no effect on yield. Do not centrifuge the sample at this stage.

##### 6. Place a QIAquick spin column in a provided 2 ml collection tube.

##### 7. To bind DNA, apply the sample to the QIAquick column, and centrifuge for 1 min.

The maximum volume of the column reservoir is 800  $\mu$ l. For sample volumes of more than 800  $\mu$ l, simply load and spin again.

##### 8. Discard flow-through and place QIAquick column back in the same collection tube.

Collection tubes are reused to reduce plastic waste.

##### 9. Recommended: Add 0.5 ml of Buffer QG to QIAquick column and centrifuge for 1 min.

This step will remove all traces of agarose. It is only required when the DNA will subsequently be used for direct sequencing, in vitro transcription, or microinjection.

##### 10. To wash, add 0.75 ml of Buffer PE to QIAquick column and centrifuge for 1 min.

**Note:** If the DNA will be used for salt-sensitive applications, such as blunt-end ligation and direct sequencing, let the column stand 2–5 min after addition of Buffer PE, before centrifuging.

##### 11. Discard the flow-through and centrifuge the QIAquick column for an additional 1 min at 17,900 x g (13,000 rpm).

**IMPORTANT:** Residual ethanol from Buffer PE will not be completely removed unless the flow-through is discarded before this additional centrifugation.

##### 12. Place QIAquick column into a clean 1.5 ml microcentrifuge tube.

##### 13. To elute DNA, add 50 $\mu$ l of Buffer EB (10 mM Tris·Cl, pH 8.5) or water (pH 7.0–8.5) to the center of the QIAquick membrane and centrifuge the column for 1 min. Alternatively, for increased DNA concentration, add 30 $\mu$ l elution buffer to the center of the QIAquick membrane, let the column stand for 1 min, and then centrifuge for 1 min.

**IMPORTANT:** Ensure that the elution buffer is dispensed directly onto the QIAquick membrane for complete elution of bound DNA. The average eluate volume is 48  $\mu$ l

from 50  $\mu$ l elution buffer volume, and 28  $\mu$ l from 30  $\mu$ l.

Elution efficiency is dependent on pH. The maximum elution efficiency is achieved between pH 7.0 and 8.5. When using water, make sure that the pH value is within this range, and store DNA at  $-20^{\circ}\text{C}$  as DNA may degrade in the absence of a buffering agent. The purified DNA can also be eluted in TE (10 mM Tris-Cl, 1 mM EDTA, pH 8.0), but the EDTA may inhibit subsequent enzymatic reactions.

**14. If the purified DNA is to be analyzed on a gel, add 1 volume of Loading Dye to 5 volumes of purified DNA. Mix the solution by pipetting up and down before loading the gel.**

Loading dye contains 3 marker dyes (bromophenol blue, xylene cyanol, and orange G) that facilitate estimation of DNA migration distance and optimization of agarose gel run time. Refer to Table2 (page 15) to identify the dyes according to migration distance and agarose gel percentage and type.

# pET-28a vector map



## pET-28a-c(+) Vectors

TB074 12/98

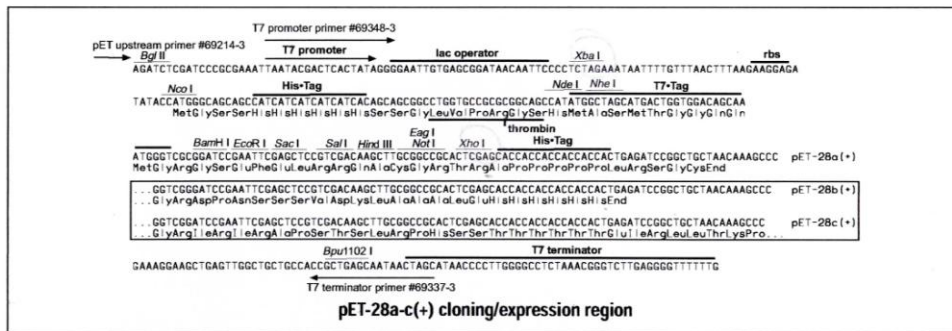
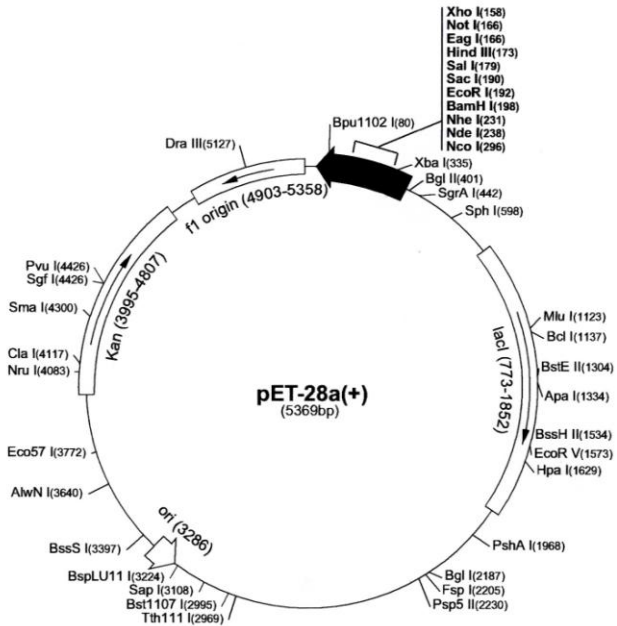
	Cat. No.
pET-28a DNA	69864-3
pET-28b DNA	69865-3
pET-28c DNA	69866-3

The pET-28a-c(+) vectors carry an N-terminal His<sup>6</sup> Tag<sup>®</sup>/thrombin/T7<sup>®</sup> Tag<sup>®</sup> configuration plus an optional C-terminal His<sup>6</sup> Tag sequence. Unique sites are shown on the circle map. Note that the sequence is numbered by the pBR322 convention, so the T7 expression region is reversed on the circular map. The cloning/expression region of the coding strand transcribed by T7 RNA polymerase is shown below. The f1 origin is oriented so that infection with helper phage will produce virions containing single-stranded DNA that corresponds to the coding strand. Therefore, single-stranded sequencing should be performed using the T7 terminator primer (Cat. No. 69337-3).

### pET-28a(+) sequence landmarks

T7 promoter	370-386
T7 transcription start	369
His <sup>6</sup> Tag coding sequence	270-287
T7 <sup>®</sup> Tag coding sequence	207-239
Multiple cloning sites ( <i>Bam</i> H I - <i>Xho</i> I)	158-203
His <sup>6</sup> Tag coding sequence	140-157
T7 terminator	26-72
<i>lac</i> I coding sequence	773-1852
pBR322 origin	3286
Kan coding sequence	3995-4807
f1 origin	4903-5358

The maps for pET-28b(+) and pET-28c(+) are the same as pET-28a(+) (shown) with the following exceptions: pET-28b(+) is a 5368bp plasmid; subtract 1bp from each site beyond *Bam*H I at 198. pET-28c(+) is a 5367bp plasmid; subtract 2bp from each site beyond *Bam*H I at 198.



Novagen · ORDERING 800-526-7319 · TECHNICAL SUPPORT 800-207-0144



# Construction of pET-YSBLIC vector

Construct = pET-YSBLIC

GAGGAG BseRI      PreScission (3C) Protease  
 GCGCGCC AscI      CTGGAAGTCTGTCCAGGGGCC  
 CATATG NdeI

Parent vector, Pet-28a containing 3C protease site

5'-AGATATACCATGGGCAGCAGCCATCATCATCATCATCACAGCAGCGGCCTGGAAGTCTGTCCAGGGGCCCATATGGCTAGCATGACTGGTGGACAGCAAATG-3'  
 3'-TCTATATGGTACCCGTCGTCGGTAGTAGTAGTAGTAGTGTGTCGTCGCCGACCTCAAGACAAGGTCCCGGGGTATACCGATCGTACTGACCACCTGTCGTTTAC-5'  
 ArgArgTyrMetGlySerSerHisHisHisHisHisHisSerSerGlyLeuGluValLeuPheGlnGlyProHisMetAlaSerMetThrGlyGlyGlnGlnMet

YSBL pET-28a LIC

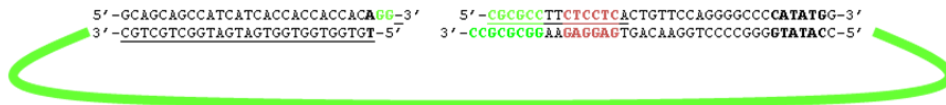
5'-AGATATACCATGGGCAGCAGCCATCATCACACCACCACAGCGCGCCCTTCTCCTCACTGTTCCAGGGGCCCATATGGCTAGCATGACTGGTGGACAGCAAATG-3'  
 3'-TCTATATGGTACCCGTCGTCGGTAGTAGTAGTAGTGTCCGCGCGGAAGAGGAGTGACAAGGTCCCGGGGTATACCGATCGTACTGACCACCTGTCGTTTAC-5'  
 ArgArgTyrMetGlySerSerHisHisHisHisHisHis

▲  
Non Cleavable Tag

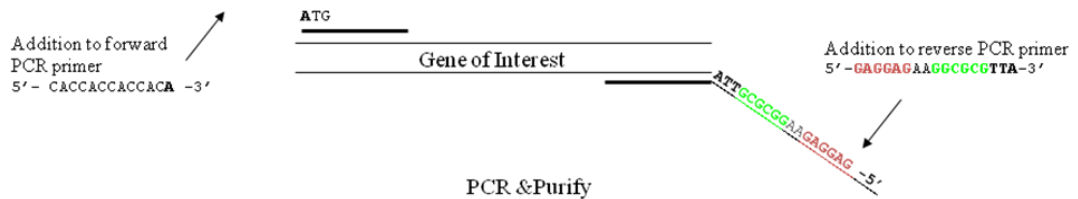
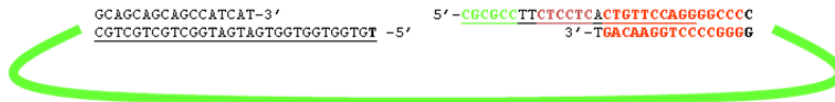
↑  
LIC site

9/10 additional N-terminal amino acids

BseRI digest



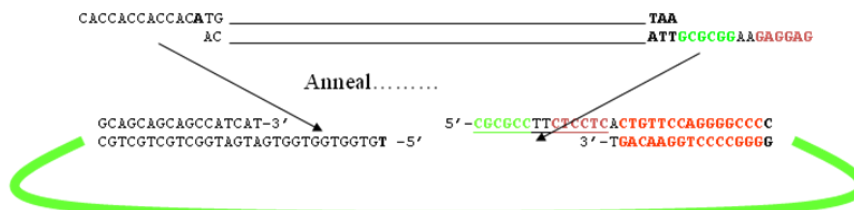
T4 pol/dTTP Treatment



PCR & Purify

CACCACCACCATG TAA GCGCCTTCTCCTC  
 GTGGTGGTGTAC ATTGCGCGGAAGAGGAG

Treat with T4 pol and dATP



... then transform

### **10 x T4pol buffer**

500 mM Tris-HCl pH 7.5, 100 mM MgCl<sub>2</sub>, 100 mM DTT, 10 mM ATP, 250 µg/ml BSA.

### **Preparation of chemically competent cells**

For all strains of *E. coli*, chemically competent cells were freshly prepared using the procedure described below and was essentially by the method of (Cohen et al., 1972). Firstly, an agar plate of the glycerol stock of the required cell type was prepared and incubated overnight at 37 °C. After overnight growth, 50 ml of prewarmed LB media in a 500 ml conical flask was inoculated using a wire loop. The culture was then allowed to grow at 37 °C with shaking at 200 rpm up to an optical density at 600 nm of 0.35~0.4. At this point the culture was placed on ice for 30 min. After incubation on ice, the culture was centrifuged at 4000 x g for 10 min at 4 °C and the supernatant discarded. The cell pellet was then re-suspended (by gentle vortex never more than 3 sec at a time off ice) in 15 ml of ice-cold 80 mM MgCl<sub>2</sub>, 20 mM CaCl<sub>2</sub> solution, and the cells were then re-centrifuged at 4000 x g for 10 min at 4 °C and the supernatant removed. The cell pellet was re-suspended (by gentle vortex never more than 3 sec at a time off ice) in 1 ml of ice- cold 100 mM CaCl<sub>2</sub>. The cells were then retained on ice for 1 h and were then used immediately or snap frozen (in liquid N<sub>2</sub>) and stored at -85 °C subsequent to the addition of 50 % (v/v) glycerol to a final concentration of 15 % (v/v).

### Protocol: Plasmid DNA Purification Using the QIAprep Spin Miniprep Kit and a Microcentrifuge

This protocol is designed for purification of up to 20 µg of high-copy plasmid DNA from 1–5 ml overnight cultures of *E. coli* in LB (Luria-Bertani) medium. For purification of low-copy plasmids and cosmids, large plasmids (>10 kb), and DNA prepared using other methods, refer to the recommendations on page 44.

Please read "Important Notes" on pages 15–21 before starting.

Note: All protocol steps should be carried out at room temperature.

#### Procedure

1. Resuspend pelleted bacterial cells in 250 µl Buffer P1 and transfer to a microcentrifuge tube.

Ensure that RNase A has been added to Buffer P1. No cell clumps should be visible after resuspension of the pellet.

If LyseBlue reagent has been added to Buffer P1, vigorously shake the buffer bottle to ensure LyseBlue particles are completely dissolved. The bacteria should be resuspended completely by vortexing or pipetting up and down until no cell clumps remain.

2. Add 250 µl Buffer P2 and mix thoroughly by inverting the tube 4–6 times.

Mix gently by inverting the tube. Do not vortex, as this will result in shearing of genomic DNA. If necessary, continue inverting the tube until the solution becomes viscous and slightly clear. Do not allow the lysis reaction to proceed for more than 5 min.

If LyseBlue has been added to Buffer P1 the cell suspension will turn blue after addition of Buffer P2. Mixing should result in a homogeneously colored suspension. If the suspension contains localized colorless regions or if brownish cell clumps are still visible, continue mixing the solution until a homogeneously colored suspension is achieved.

3. Add 350 µl Buffer N3 and mix immediately and thoroughly by inverting the tube 4–6 times.

To avoid localized precipitation, mix the solution thoroughly, immediately after addition of Buffer N3. Large culture volumes (e.g. ≥5 ml) may require inverting up to 10 times. The solution should become cloudy.

If LyseBlue reagent has been used, the suspension should be mixed until all trace of blue has gone and the suspension is colorless. A homogeneous colorless suspension indicates that the SDS has been effectively precipitated.

4. Centrifuge for 10 min at 13,000 rpm (~17,900 x g) in a table-top microcentrifuge. A compact white pellet will form.

5. Apply the supernatants from step 4 to the QIAprep spin column by decanting or pipetting.
6. Centrifuge for 30–60 s. Discard the flow-through.
7. **Recommended:** Wash the QIAprep spin column by adding 0.5 ml Buffer PB and centrifuging for 30–60 s. Discard the flow-through.  
 This step is necessary to remove trace nuclease activity when using endA<sup>+</sup> strains such as the JM series, HB101 and its derivatives, or any wild-type strain, which have high levels of nuclease activity or high carbohydrate content. Host strains such as XL-1 Blue and DH5α™ do not require this additional wash step.
8. Wash QIAprep spin column by adding 0.75 ml Buffer PE and centrifuging for 30–60 s.
9. Discard the flow-through, and centrifuge for an additional 1 min to remove residual wash buffer.  
**Important:** Residual wash buffer will not be completely removed unless the flow-through is discarded before this additional centrifugation. Residual ethanol from Buffer PE may inhibit subsequent enzymatic reactions.
10. Place the QIAprep column in a clean 1.5 ml microcentrifuge tube. To elute DNA, add 50 µl Buffer EB (10 mM Tris-Cl, pH 8.5) or water to the center of each QIAprep spin column, let stand for 1 min, and centrifuge for 1 min.

## 10 x digest buffer 2

500 mM NaCl; 100 mM Tris-HCl; 100 mM MgCl<sub>2</sub>; 10 mM Dithiothreitol, pH 7.9

## MDG media

MDG non-induction media for growing glycerol stocks and starter cultures

Inoculate starter cultures directly from glycerol stocks (by scraping up a small amount of frozen glycerol stock with a sterile plastic tip without thawing the rest of the stock and inoculating into MDG)

	<u>10 mL total</u>
- Water	9.55 mL
- 1M MgSO <sub>4</sub>	20 µL
- 1000 x metals (for metal containing protein)	2 µL
- 40 % glucose	125 µL
- 25 % aspartate	100 µL
- 50 x M	200 µL
- antibiotic	

## Stock solutions

- 1M MgSO<sub>4</sub> (100mL) (autoclave and reautoclave everytime it is used)
  
- 40 % (w/v) glucose (20 mL) (autoclave and reautoclave everytime it is used, make up fresh when it caramelizes)
  
- 50 x M (100 mL) (autoclave)
  - o dissolve sequentially in water
  - o 3.6 g Na<sub>2</sub>SO<sub>4</sub> anhydrous
  - o 13.4 g NH<sub>4</sub>Cl anhydrous
  - o 17.0 g KH<sub>2</sub>PO<sub>4</sub> anhydrous
  - o 17.7 g Na<sub>2</sub>HPO<sub>4</sub> anhydrous
  
- 1000 x metal (100mL) (autoclave separate solutions and mix aseptically)
  - o 36 mL water
  - o 50 mL 0.1M FeCl<sub>3</sub>-6H<sub>2</sub>O (dissolved in 100-fold dilution of HCl, ~0.12 M HCl and filter sterilize using 0.2 µm filters)
  - o 2 mL 1M CaCl<sub>2</sub> anhydrous
  - o 1 mL 1M MnCl<sub>2</sub>-4H<sub>2</sub>O
  - o 1 mL 1M ZnSO<sub>4</sub>-7H<sub>2</sub>O
  - o 1 mL 0.2M CoCl<sub>2</sub>-6H<sub>2</sub>O
  - o 2 mL 0.1M CuCl<sub>2</sub>-2H<sub>2</sub>O
  - o 1 mL 0.2M NiCl<sub>2</sub>-6H<sub>2</sub>O
  - o 2 mL 0.1M Na<sub>2</sub>MoO<sub>4</sub>-5H<sub>2</sub>O
  - o 2 mL 0.1M Na<sub>2</sub>SeO<sub>3</sub>-5H<sub>2</sub>O
  - o 2 mL 0.1M H<sub>3</sub>BO<sub>3</sub> anhydrous
  
- 25 % (w/v) aspartate (20 ml) (check pH is 7, if not neutralise with NaOH) (autoclave)

## ZYM media

ZYM-5052 auto-induction media  
Inoculate from MDG starter culture

	<u>10 mL total</u>	<u>1 L total</u>
		<u>(max vol for 2 L baffled flask)</u>
- ZY	9.77 mL	947 mL
- 1M MgSO <sub>4</sub>	20 µL	2 mL
- 1000 x metals		
- (for metal containing protein)	10 µL	1 mL
- 50 x 5052	200 µL	20 mL
- 50 x M	200 µL	20 mL
- antibiotic		

## Stock solutions

- 1M MgSO<sub>4</sub> (100mL) (autoclave and reautoclave everytime it is used)
- 50 x 5052 (100 mL) (autoclave and reautoclave everytime it is used)
  - o dissolve sequentially in water
  - o 25 g glycerol
  - o 2.5 g glucose
  - o 10 g α-lactose
- 50 x M (100 mL) (autoclave and reautoclave everytime it is used)
  - o dissolve sequentially in water
  - o 3.6 g Na<sub>2</sub>SO<sub>4</sub> anhydrous
  - o 13.4 g NH<sub>4</sub>Cl anhydrous
  - o 17.0 g KH<sub>2</sub>PO<sub>4</sub> anhydrous
  - o 17.7 g Na<sub>2</sub>HPO<sub>4</sub> anhydrous
- ZY (1 L) (autoclave)
  - o dissolve sequentially in water
  - o 10 g Tryptone
  - o 5 g Yeast extract

- 1000 x metal (100mL) (autoclave separate solutions and mix aseptically)
  - o 36 mL water
  - o 50 mL 0.1M FeCl<sub>3</sub>-6H<sub>2</sub>O (dissolved in 100-fold dilution of HCl, ~0.12 M HCl and filter sterilize using 0.2 µm filters)
  - o 2 mL 1M CaCl<sub>2</sub> anhydrous
  - o 1 mL 1M MnCl<sub>2</sub>-4H<sub>2</sub>O
  - o 1 mL 1M ZnSO<sub>4</sub>-7H<sub>2</sub>O
  - o 1 mL 0.2M CoCl<sub>2</sub>-6H<sub>2</sub>O
  - o 2 mL 0.1M CuCl<sub>2</sub>-2H<sub>2</sub>O
  - o 1 mL 0.2M NiCl<sub>2</sub>-6H<sub>2</sub>O
  - o 2 mL 0.1M Na<sub>2</sub>MoO<sub>4</sub>-5H<sub>2</sub>O
  - o 2 mL 0.1M Na<sub>2</sub>SeO<sub>3</sub>-5H<sub>2</sub>O
  - o 2 mL 0.1M H<sub>3</sub>BO<sub>3</sub> anhydrous

### **SDS-PAGE chemicals**

#### **12 % (w/v) Acrylamide resolving gel components**

40 % (w/v) solution (37.5:1 acrylamide: bisacrylamide) (Fisher)	3.0 ml
Solution B*	2.5 ml
18.2 MΩ/cm H <sub>2</sub> O	
10 % (w/v) Ammonium persulphate (Fisher)	50.0 µl
Tetramethylethylenediamine (TEMED) (Fisher)	10.0 µl

#### \*Solution B

Per 100 ml

2 M Tris Base (Melford) pH 8.8	75.0 ml
10 % (w/v) Sodium dodecyl sulphate (SDS) (Melford)	4.0 ml

#### **4% (w/v) Acrylamide stacking gel components**

40 % (w/v) solution (37.5:1 acrylamide: bisacrylamide) (Fisher)	0.5 ml
Solution C*	1.0 ml
18.2 MΩ/cm H <sub>2</sub> O	2.5 ml
10 % (w/v) Ammonium persulphate (Fisher)	30.0 μl
TEMED (Fisher)	10.0 μl

#### \*Solution C

Per 100 ml

1 M Tris Base (Melford) pH 6.8	50.0 ml
10 % (w/v) SDS (Melford)	

#### **SDS-PAGE running buffer 10 x (Stock)**

Running buffer was made up at 10 x stock concentration and diluted 1:10 before use.

Per L

Tris Base (Melford)	30.3 g
Glycine (Melford)	144.0 g
SDS (Melford)	10.0 g

The pH of the Tris Base and glycine was adjusted to 8.8 in a volume of ~900 ml prior to the addition of SDS.

### **SDS-PAGE sample buffer**

Per 10 ml

60 mM Tris Base (Melford) pH 6.8	0.6 ml
50 % (v/v) Glycerol (Fisher)	5.0 ml
10 % (w/v) SDS (Melford)	2.0 ml
14.4 mM $\beta$ -Mercaptoethanol (Sigma)	0.5 ml
1 % (w/v) Bromophenol blue (BDH)	1.0 ml

Stored at  $-20\text{ }^{\circ}\text{C}$  in 0.5 ml aliquots.

### **Solubilising SDS-PAGE sample buffer**

Per 10 ml

SDS - PAGE sample buffer	7.6 ml
Urea (Melford)	2.4 g

Stored at  $4\text{ }^{\circ}\text{C}$ .

### **Protein size standard**

High molecular weight range (M.W. 36, 45, 55, 66, 84, 97, 116 and 205 kDa)

Low molecular weight range (M.W. 20, 24, 29, 36, 45 and 66 kDa)

Lyophilised standards were reconstituted with 100  $\mu\text{l}$  of 18.2 M  $\Omega$   $\text{H}_2\text{O}$  to give a final concentration of  $\sim 2.0\text{-}3.5\text{ mg/ml}$ , which was aliquoted into 4  $\mu\text{l}$  amounts and stored at  $-20\text{ }^{\circ}\text{C}$ .

### **Coomassie blue gel stain solution**

Per L

Coomassie Blue R-250 (Fisher)	1.0 g
Glacial Acetic acid (Fisher)	100.0 ml
Methanol (Fisher)	450.0 ml

Coomassie blue gel stain solution is recycled for re-use by filtering through filter paper to remove any small pieces of gel.

### **Coomassie gel destain solution**

Per L

Glacial Acetic acid (Fisher)	100.0 ml
Methanol (Fisher)	100.0 ml

Coomassie gel destain solution is recycled for re-use by filtering through activated charcoal on a filter paper funnel to remove the Coomassie blue stain.

### **MIDAS® PlasmidSpin™ miniprep Protocol**

1. Inoculate 5 ml LB/ampicillin (50 µg/ml) medium placed in a 10-20 ml culture tube with *E. coli* carrying desired plasmid and grow at 37°C with agitation for 12-16 h. It is strongly recommended that an *endA* negative strain of *E. coli* be used for routine plasmid isolation.

2. Pellet 1.5-5 ml bacteria by centrifugation at 10,000 x g for 1 min at room temperature.

3. Decant or aspirate medium and discard. To the bacterial pellet add 250  $\mu$ l Solution I/RNase A. Resuspend cells completely by vortexing. Complete resuspension of cell pellet is vital for obtaining good yields.

4. Add 250  $\mu$ l Solution II and gently mix by inverting and rotating tube 4-6 times to obtain a cleared lysate. A 2 min incubation at room temperature may be necessary. Avoid vigorous mixing as this will shear chromosomal DNA and lower plasmid purity. (Store Solution II tightly capped when not in use.)

5. Add 350  $\mu$ l Solution III and gently mix by inverting several times until a flocculent white precipitate forms. Centrifuge at 10,000 x g for 10 minutes at room temperature.

6. CAREFULLY aspirate and add the clear supernatant to a clean BioBind™ mini column (blue) assembled in a 2 ml collection tube (provided). Ensure that the pellet is not disturbed and that no cellular debris is carried over into the column. Centrifuge 1 min at 10,000 x g at room temperature to completely pass lysate through column.

7. Discard liquid and wash column with 500  $\mu$ l Buffer HB and Centrifuge 1 min at 10,000 x g. This step ensures that residual protein contamination is removed and must be included for downstream applications requiring high quality DNA. This step can be skipped if the downstream applications don't require high quality plasmid, such as enzyme digestion or other screening methods.

8 Discard flow-through liquid and wash the column by adding 750  $\mu$ l of Wash Buffer diluted with ethanol. Centrifuge 1 min at 10,000 x g as above and discard flow-through.

Note: Wash Buffer Concentrate must be diluted with absolute ethanol before use. See label for directions. If refrigerated, Wash Buffer must be brought to room temperature before use.

9. Optional step: repeat wash step with another 750  $\mu$ l Wash Buffer.

10 Centrifuge the empty column for 1 min at 10,000 x g to dry the column matrix. Do not skip this step - it is critical for removing ethanol from the column.

11. Place column into a clean 1.5 ml microcentrifuge tube. Add 50 µl to 100 µl (depending on desired concentration of final product) sterile deionised water (or TE buffer) directly onto the column matrix and centrifuge 1 min at 10,000 x g to elute DNA. This represents approximately 75-80% of bound DNA. Further, optional, elutions will yield any residual DNA, though at a lower concentrations.

### **Chemical Transformation**

1. Equilibrate a water bath or heat block to 42°C. Remove the appropriate number of tubes of frozen XL1 Blue chemically competent cells (50 µl each) and thaw on ice.
2. Add 1 µl of each ligation reaction (if the cell competency is  $<1 \times 10^8$  cfu/µg, you may need to use more of the ligation mixture) to a separate tube of competent cells. Mix gently with the pipette tip. DO NOT PIPETTE UP AND DOWN. Repeat for all ligations.
3. For control reactions, add 1µl (10ng) of each supercoiled plasmid (e.g. pUC18 to a separate tube of cells.
4. Incubate all tubes on ice 20 minutes.
5. Transfer all tubes to 42°C heat block or water bath and incubate for 1 minute, then place on ice for 1 minute.
6. Add 450 µl of room temperature NZY+ medium to each tube and shake at 225 rpm for 60 minutes at 37°C. Place on ice.
7. Plate 25 and 100 µl of each transformation mix on LB/ampicilin agar plates. (If the cell competency is  $<1 \times 10^8$  cfu/µg, you may need to plate more of each transformation mix). Let all the liquid absorb, invert, and incubate at 37°C, 18-24 hours.

**LB broth**

10 g Tryptone

5 g Yeast extract

10 g NaCl

in 1 L distilled H<sub>2</sub>O and adjusted to pH 7.4.